SOMMAIRE

REMERCIEMENTS

Tout d'abord, je tiens à remercier Pascal Conan et Jean-François Ghiglione de m'avoir permis de réaliser cette thèse. Merci à vous deux de m'avoir donné l'occasion de réaliser des campagnes océanographiques et de m'avoir initié à l'océanographie et à la microbiologie marine.

Je tiens aussi à remercier Mireille, Mme DOC, et Pierre Galand pour sa patience et son naturel, deux qualités qui ont permis de faire passer les mystères de la phylogénie et des réseaux beaucoup plus facilement. I would like to thanks Matt Oliver and PhD Matt, I just spent one week with you in Delaware but I really appreciated to work with you and I love the room with all these big screens!

Je tiens très sincèrement à remercier les membres de mon jury d'avoir accepté d'évaluer mon travail. Merci à Josep Gasol et Richard Sempéré qui ont accepté de rapporter cette thèse, et merci à Stéphan Jacquet et Damien Cardinal pour avoir accepté de l'examiner. Mes prochains remerciements vont vers les membres de mon comité de thèse : Xavier Durrieu de Madron et France Van Wambeke, j'ai eu un immense plaisir à travailler avec vous aussi bien en mer que sur terre. Encore merci Xavier pour ta patience et ton acharnement à me faire comprendre tous ces processus physiques qui régissent le processus de convection.

Merci à vous Louise et Jocelyne, vous m'avez beaucoup appris scientifiquement et aussi humainement. Jocelyne, tu m'as formé en mer, tu m'as appris à arrimer tout un labo (chose vraiment pas facile surtout avec des rafales à 104 nœuds !), et tu as su me remettre à ma place quand j'en avais besoin (oui oui elle a réussi !). Louise (Mme sel nut.), ta gentillesse, ta patience et tous tes conseils m'ont été vraiment très précieux. Vous allez me manquer.

Je n'oublie pas toutes les autres personnes qui ont contribué de près ou de loin à l'élaboration de cette thèse. Merci aux teams CASCADE et DeWEX ! Merci à toi Caroline, j'ai appris à te connaitre sur CASCADE (le 4 mars 2011 !), mais ce n'était qu'une toute petite facette de ta personnalité. Merci à Chloé, Marina, Loïc, Mathieu, Faycal, Denisse et puis tous mes autres compagnons qui mon (difficilement) supporté en mer (en même temps qu'est-ce que tu faisais toujours dans mes pattes Mathieu ?!).

Un énorme merci à tous mes collègues et amis de labo : Marine B (je relisais la thèse de Marion et c'est vrai que tu miaules bien !), Sabrina, Crecre, Yann, Solveig, Margot, Sandrine, Mareike, Hugo B, Romain, Audrey, Hugo L… Et tous ceux que j'oublie de citer. Les pauses café (cafétito ?!), les déjeuners au soleil, les sorties, les sushis, les bières et mojito, top pizza (mama), les descentes en chaise de bureau… Bref merci pour tous ces moments de détentes qui font que la pilule passe beaucoup mieux ! Et merci aussi à mes coupines « externes » pour ces longues conversations téléphoniques qui vous

rappellent qu'il y a une vie en dehors du labo ! Ivia (j'ai fait plein de rhum arrangé pour la soirée !!), Jenna et Émilie, je vous nème !

Merci à la Familia !!! T'as vu papa je vais être docteur de la mer ! Même si vous étiez loin Maman, Papa, Louisa, Stan et mon bébé chien Gégé, c'est grâce à vous que j'en suis arrivée là et que j'ai tenu. Vous m'avez remis les pieds sur terre, vous m'avez redonné confiance et vous m'avez remonté le moral, je vous aime les Severin !! Et je t'aime aussi Rémy ♥ Pour le coup, toi tu t'es vraiment tout pris en pleine face ! (et ça fait BOUM dans ta face !) ! C'est un peu bateau, mais il n'y a pas de mots assez forts pour te remercier de tout ce que tu fais pour moi au quotidien, alors je vais juste te crier MERCI ! Peut-être qu'en le criant le mot sera assez fort ?! Très mauvais je sais, mais c'est pour sécher ma larme à l'œil.

Sur ces bonnes paroles, je vous souhaite une Bonne Lecture !

PREFACE

Les travaux présentés dans le présent manuscrit de thèse consistent en une approche pluridisciplinaire qui m'a amené à acquérir des compétences dans des domaines aussi variés que la biogéochimie, l'océanographie physique, l'écologie microbienne, la biologie moléculaire, la bio-informatique. Mes travaux ont été menés à la fois au laboratoire mais également sur le terrain, par des participations actives à des campagnes océanographiques côtières et hauturières. Les résultats présentés dans ce manuscrit sont le produit de multiples collaborations et d'efforts de différentes personnes que je tiens à associer à ce travail.

Une grande partie de mon travail fait partie des programmes scientifiques CASCADE (HERMIONE-Europe) et DeWEX (MISTRALS). Mon travail a tout d'abord consisté en la préparation des campagnes océanographiques CASCADE et DeWEX, qui m'ont conduit à passer 63 jours en mer. A bord, je m'occupais des prélèvements, des filtrations et du conditionnement des échantillons pour plusieurs paramètres (les sels nutritifs dont l'ammonium, la matière organique dissoute et particulaire pour les éléments C, N, P, la diversité procaryotique, et les pigments chlorophylliens), grâce à l'aide de Jocelyne Caparros (IR CNRS), Louise Oriol (IR CNRS), Caroline Sauret (doctorante), Mathieu Rembauville (master), Denisse Sanchez (doctorante) et Fayçal Kessouri (doctorant). Au laboratoire, j'ai réalisé les dosages de chlorophylle et de phaeopigments, ainsi que toutes les analyses de cytométrie en flux pour les bactéries, le phytoplancton et les hétéro nanoflagellés de la campagne CASCADE. J'ai aussi fait les extractions d'ADN ainsi que tous les traitements moléculaires et bio-informatiques pour l'analyse de la diversité procaryotique avec J.F. Ghiglione (CR CNRS) et Pierre Galand (CR CNRS). Pour la campagne DeWEX, j'ai réalisé à bord les mesures de production primaire, ainsi que des mesures en continues des concentrations en nitrate et silicate avec le CHEMINI (CHEmical MINIaturised analyser), un analyseur chimique miniaturisé développé par l'IFREMER de Brest. J'ai encadré une étudiante de M2 (Sandra Boban) pour les extractions d'ADN et d'ARN et le traitement bio-informatique des données de séquences de la campagne DeWEX avec JF Ghiglione (CR CNRS). J'ai également co-encadrée le stage de M2 de Mathieu Rembauville en assurant sa formation à la mer au cours du Leg1 de DeWEX.

Les analyses des sels nutritifs et de matière organique dissoute et particulaire pour les éléments azote et phosphore ont été réalisées par Louise Oriol (IR CNRS). Mireille Pujo-Pay (CR CNRS)

a analysé les échantillons de carbone organique dissous (HTCO). Jocelyne Caparros (IR CNRS) a mesuré les concentrations en carbone et azote organique particulaire (CHN).

Comme cette préface le prouve, ce travail n'aurait pu être réalisé sans la participation active de nombreux acteurs du Laboratoire d'Océanographie Microbienne (LOMIC – UMR7621).

J'ai aussi eu l'occasion de participer à d'autres projets en cours au sein du LOMIC, comme le projet Vermeillecotox (Europe) pour lequel j'ai filtré et conditionné les échantillons de carbone organique particulaire, et je réalisais les mesures de production primaire et bactérienne pour plus de 100 échantillons. J'ai pris la suite de Caroline Sauret (doctorante) pour l'optimisation de la technique de Stable Isotope Probing, ainsi que le développement de cultures phytoplanctoniques axéniques en milieu artificiel pauvre en carbone organique dissous et enrichi en bicarbonate marqués en carbone 13. Cette technique est désormais au point et disponible pour les membres du LOMIC

ABBREVIATIONS

AABW	Antarctic Bottom Water
AdDW	Adriatic Deep Water
ADN	Acide DésoxyriboNucléique
ADNr	Acide DésoxyriboNucléique ribosomal
AeDW	Aegean Deep Water
ARN	Acide RiboNucléique
ARNr	Acide RiboNucléique ribosomal
AW	Atlantic Water
CCA	Canonical Correspondence Analysis
Chla	Chlorophylle a
CNM	Courant Nord Méditerranéen
COD	Carbone Organique Dissous
COP	Carbone Organique Particulaire
COT	Carbone Organique Total
DIC	Dissolved Inorganic Carbon
GdL	Golfe du Lion
HMW	High Molecular Weight
Lip	Lipase activity
LIW	Levantine Intermediate Water
LL	Aminopetidase activity
LMW	Low Molecular Weight
MGI	Marine Group I *Thaumarchaeota*
MGII	Marine Group II *Euryarchaeota*
MIC	Maximal Information Coefficient
MLD	Mixed Layer Depth
MNO	Méditerranée Nord Occidentale
MO	Matière Organique
MOD	Matière Organique Dissoute
MOP	Matière Organique Particulaire
NADH	North Atlantic Deep Water
NH_4	Ammonium
NO_2	Nitrite
NO_3	Nitrate
nWMDW	New Western Mediterranean Deep Water
$nWMDW_{fev}$	New Western Mediterranean Deep Water formed by convection event of February 2011
$nWMDW_{mar}$	New Western Mediterranean Deep Water formed by convection event of March 2011
OTU	Operational Taxon Unit
PCA	Principal Correspondence Analysis
Pho	Phosphatase activity
PHP	Prokaryotic Heterotrophic Production
PO_4	Phosphate
$Si(OH)_4$	Silicate
TDW	Tyrrhenian Dense Water
WIW	Winter Intermediate Water
WMDW	Western Mediterranean Deep Water
β-Glc	Glucosidase activity

Chapitre I

INTRODUCTION GÉNÉRALE

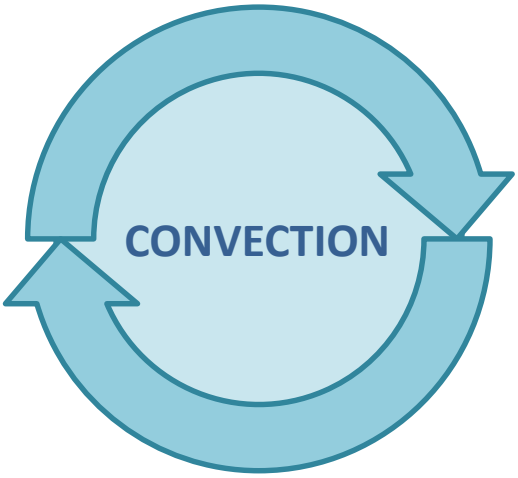

I. INTRODUCTION GÉNÉRALE

I.1. Le processus de convection profonde dans les océans du monde

I.1.1. Les sites de convection connus et leur rôle dans la circulation thermohaline

Relativement peu de sites de convection sont répertoriés à travers le monde malgré leur rôle crucial (Killworth, 1983 ; Figure I-1). En effet, les processus de convection en océan hauturier sont à l'origine de la formation et du renouvellement des masses d'eaux profondes. Ces eaux se propagent ensuite dans tous les océans, participant activement à la circulation thermohaline de l'océan global (Figure I-2).

Ce processus complexe a été observé au nord de l'océan Atlantique, et plus précisément dans les mers d'Irminger, du Groenland et en mer du Labrador (Marshall and Schott, 1999). Alors que les eaux profondes formées en mer du Groenland restent confinées à la circulation de l'océan Arctique et autour de l'Islande, les eaux Profondes Nord Atlantique (NADW, North Atlantic Deep Water) formées en mer du Labrador réapprovisionnent en eaux profondes tout l'océan Atlantique, puis se divisent à la pointe africaine pour alimenter l'océan Indien puis l'océan Pacifique (Mauritzen, 1996). Dans l'hémisphère sud, les mers de Weddell et de Ross (Marshall and Schott, 1999) sont des sites de convections en océan ouvert à l'origine de la formation des eaux profondes Antarctique (AABW, Antarctic Bottom Water). Les AABW sont les eaux les plus denses de l'océan global, et comme les NADW, elles pénètrent dans les 3 océans principaux : l'océan Atlantique, puis l'océan Indien et enfin le Pacifique (Orsi et al., 1999). Un dernier site de convection existe dans l'hémisphère nord, la mer Méditerranée (Medoc Group, 1970; Thetis Group, 1994). Ce site est notre zone d'étude et sera détaillé dans la section I.2.4.

Figure I-1 : Cartes des sites majeurs de convection en océan hauturier ; tirées de http://puddle.mit.edu/~helen/oodc.html.

Figure I-2 : Carte de la circulation thermohaline de l'océan globale répertoriant les sites majeurs de plongées et de remontées convectives, moteurs de la circulation ; tirée de http://amap.no/acia/

I.1.2. Structuration des épisodes de convection

La convection en océan hauturier est un processus physique hivernal complexe, dont le déclenchement des épisodes est réalisé en 3 étapes pouvant se chevaucher (Send & Marshall, 1995; Marshall & Schott, 1999; Figure I-3).

Des eaux denses sont formées en surface lors de la phase de préconditionnement (Figure I-3A) grâce aux forçages atmosphériques. Ces forçages consistent en l'action combinée de la diminution de température saisonnière et de l'action de forts vents, ce qui entraine une perte de chaleur de la couche de surface (diminution de la température) ainsi qu'une évaporation (augmentation de la salinité). Ceci se traduit par une augmentation de l'anomalie de masse volumique des eaux de surface, dépendant des conditions atmosphériques hivernales, mais également de l'état de stratification de la colonne d'eau. Toutes les zones connues de convection en océan hauturier se situent au centre d'un tourbillon cyclonique. Cette circulation particulière a pour effet de remonter localement les différentes masses d'eaux (pompage d'Ekman), formant un dôme isopycnal qui affaiblie la stratification de la colonne d'eau (Killworth, 1983; Marshall and Schott, 1999). Les forçages atmosphériques hivernaux déstabilisent d'autant plus facilement les couches stratifiées, formant ainsi une cheminée de convection parfois large de plus de 100km de diamètre.

La phase de mélange intense (Figure I-3B) consiste en l'approfondissement de la cheminée de convection par la propagation de cellules de convectives, larges d'environ 1km de

diamètre chacune. Au sein de ces cellules, des vitesses verticales descendantes parfois supérieur à 10 $cm.s^{-1}$ ont été enregistrées (Mertens and Schott, 1998). Plusieurs cellules convectives coexistent au sein de la cheminée de convection, des cellules dynamiques entre lesquelles des courants ascendants permettent de remonter des eaux profondes à des vitesses inférieures que les courants descendants (Send and Marshall, 1995).

Lors de la phase de propagation (Figure I-3C), la diminution des forçages atmosphériques ralentie puis stoppe le mélange vertical permettant aux eaux environnantes de progressivement recouvrir l'ancienne zone de convection. Les eaux denses sont exportées par gravité à leur pression hydrostatique, puis se propagent progressivement vers les autres bassins en fonction de la circulation générale.

Figure I-3 : Diagrammes schématiques des 3 phases de formation des processus de convection : (A) préconditionnement, (B) mélange vertical profond, (C) propagation des eaux profondes nouvellement formées. Adaptés de Send & Marshall (1995) et Marshall & Schott (1999).

I.1.3. Impact du changement climatique sur le processus de convection

La fréquence et l'intensité des épisodes de convection sont susceptibles d'être altérées avec le changement climatique, puisque la convection en océan hauturier est un processus dépendant du forçage atmosphérique (cf. section I.1.2). En effet, les échanges de chaleur entre l'atmosphère et l'océan jouent un rôle essentiel dans la déstabilisation d'une colonne d'eau

(Marshall and Schott, 1999). Ces 50 dernières années, une augmentation de température des eaux de surface de ~0.64°C a été enregistrée dans l'océan global (Reid et al., 2009), avec notamment une élévation de plus de 1°C en mer Australe depuis les années 1950 (Meredith, 2005). Les prédictions actuelles tendent donc à voir le processus de convection diminuer du fait de l'augmentation de température de l'océan et de la stratification, ce qui pourrait conduire à une diminution de la circulation thermohaline Atlantique de 50% au 21ème siècle (Reid et al., 2009).

Toutefois en Méditerranée Nord Occidentale, une augmentation de la fréquence des épisodes de convection profonde a été observée ces dernières décennies. La diminution du taux de précipitation et l'augmentation de la fréquence des évènements de vents froids et intenses auraient conduit à une élévation du taux d'évaporation des eaux de surface (Marty and Chiavérini, 2010), contrebalançant l'augmentation de température des eaux de surface par l'augmentation de salinité. Au début des années 90, la génération massive d'eaux denses dans la mer d'Égée a conduit à une importante modification des caractéristiques des eaux profondes dans le bassin oriental. Ce processus a été appelé « Eastern Mediterranean Transient » (EMT) (Roether et al., 1995) et a entrainé un changement de la circulation thermohaline profonde dans tout le bassin oriental, ainsi que sur les caractéristiques des eaux passant dans le bassin occidental par le seuil de Sicile (Vilibić et al., 2012). Suite à cela, des modifications des eaux profondes ont aussi été observées dans le bassin occidental (eaux profondes plus chaudes, plus salées et plus dense) engendrant ainsi le « Western Mediterranean Transient » (WMT) (Schröder et al., 2006).

L'exemple de la Méditerranée indique que l'impact du changement climatique sur les processus de convection n'est pas homogène dans tous les océans du monde. Ces observations montrent la nécessité d'étudier davantage ces processus, afin d'alimenter les modèles existants et d'améliorer leur prédiction.

I.2. La Mer Méditerranée

I.2.1. La Mer Méditerranée – un océan miniature

La Méditerranée est une mer semi-fermée séparée en 2 sous-bassins oriental et occidental, connectée à l'océan Atlantique par le détroit de Gibraltar et à la mer Rouge par le canal de Suez. Il s'agit d'un bassin de concentration où le taux d'évaporation est supérieur au taux de précipitation, ce qui induit un déficit hydrique naturel d'environ 1 m.a^{-1} (Béthoux et al., 1999). Un équilibre est toutefois atteint via les eaux atlantiques entrantes qui compensent 21

fois ce déficit hydrique, et les eaux méditerranéennes sortantes excédant le déficit en eau douce de 20 fois. Mais ces bilan hydriques ne sont pas fixes et font encore sujet de nombreux travaux de recherche, notamment par le programme HYMEX (HYdrological cycle in Mediterranean EXperiment).

La mer Méditerranée représente 0.7% de la surface des océans mondiaux et 0.3% de leur volume. Ces caractéristiques favorisent un temps de résidence des eaux court, de l'ordre de 70 ans contre ~2000 ans dans l'océan global (Mermex group, 2011). Quatre sites de convection y sont répertoriés (Figure I-4) : 3 dans le bassin oriental, en mer Adriatique et en mer Égée et en mer de Rhodes, et un site dans le bassin occidental, au niveau du golfe du Lion. La Méditerranée est une des mers les plus sensibles au changement climatique avec l'océan Arctique (IPCC, 2007). Pour toutes ces raisons, elle est considérée comme un « océan miniature » (Béthoux et al., 1999) permettant de surveiller des changements climatiques et environnementaux similaires à l'océan global, mais sur des échelles de temps et d'espace beaucoup plus courtes.

Figure I-4 : Carte de la mer Méditerranée répertoriant en bleu les sites de convection en océan hauturier (de gauche à droite) dans le golfe du Lion, en mer Adriatique, en mer Égée et en mer de Rhodes.

I.2.2. Influence du changement climatique sur la mer Méditerranée

Les premières observations et mesures du changement climatique ont été réalisées en mer Méditerranée, grâce à une surveillance du climat et de ses conséquences depuis les années 40 (Béthoux et al., 1998a). Depuis 1995, une diminution de 2% des pertes de chaleur et une augmentation de 10% du déficit en eau douce aurait contribué à une augmentation du déficit hydrique par évaporation de 2 $cm.a^{-1}$ (Béthoux et al., 1999).

Dans les eaux de surface de la mer Méditerranée, une augmentation de 0.03-0.15°$C.a^{-1}$ de la température a été enregistrée de 1957 à 1997 (Béthoux et al., 1998a). Une augmentation

aussi observée dans les eaux de fond avec une élévation de la température de 0.0034°C.a^{-1} et de la salinité de 1.05 10^{-3} a^{-1} entre 1993 et 2000 (Bethoux et al., 2002). Ces tendances sont également observées à la station de surveillance du canal de Gibraltar, avec à la fois une augmentation de température et de salinité des 3 masses d'eau sortantes de la Méditerranée (Tableau I-1).

Figure I-5 : Diagrammes θ/S collectés à 270 m de la station de surveillance de Gibraltar, de 1985 à 1986 (noir), en 1994 (jaune), en 1996 (vert) et entre Janvier 2003 et Avril 2004 (rouge). La figure montre que les masses d'eau à la sortie de la Méditerranée sont aujourd'hui plus chaudes et plus salées qu'il y a deux décennies (Millot et al., 2006).

L'augmentation de la salinité de la mer Méditerranée s'expliquerait par un déficit en eau douce naturel, lié à une diminution du taux de précipitation, mais aussi anthropique. La construction du haut barrage d'Assouan sur le Nil, achevée en 1970, a conduit à la diminution du débit du Nil, annihilant le contre-courant existant à l'embouchure du canal de Suez qui limitait les échanges d'eaux et de faunes entre la mer Méditerranée et la mer Rouge. Les chantiers d'approfondissement et d'agrandissement du Canal de Suez contribuent encore aujourd'hui à accentuer les entrées d'eau de la mer Rouge en Méditerranée. Les eaux de la mer Rouge de salinité d'environ 42, ont un effet de salinisation de la mer Méditerranée.

I.2.3. Masses d'eaux et circulation de la mer Méditerranée

Trois couches de circulation coexistent en mer Méditerranée (Figure I-6 et Figure I-7) (Millot and Taupier-Letage, 2005). La couche de surface est formée par l'eau d'origine Atlantique (AW, Atlantic Water) entrant par le canal de Gibraltar (Figure I-7A). Ces eaux suivent les côtes africaines pour se diviser au niveau du détroit de Sicile en 2 branches. L'une

continue dans le bassin oriental y formant un tourbillon cyclonique, la 2ème remonte la côte ouest italienne pour se diriger vers le golfe du Lion.

La couche intermédiaire est formée de l'Eau Levantine Intermédiaire (LIW, Levantine Intermediate Water) qui trouvent leur origine dans le bassin Levantin (Figure I-7B). Ces eaux, les plus salées et les plus chaudes de la Méditerranée, suivent les côtes de la Turquie, de la Grèce, puis de l'Italie pour finalement passer le détroit de Sicile et se déverser dans le bassin occidental.

La couche la plus profonde de la Méditerranée est formée de plusieurs masses d'eau (Figure I-7C). Les eaux profondes égéennes (AeDW, Aegean Deep Water) et adriatiques (AdDW, Adriatic Deep Water) sont formées dans le bassin oriental et sont principalement restreintes à la circulation profonde de ce bassin. Ces eaux forment un tourbillon cyclonique, n'interagissant pas ou peu avec celui formé par les LIW puisque ces dernières sont situées à des profondeurs moins importantes. Une partie des AeDW et AdDW les moins denses, et donc les moins profondes, franchit le détroit de Sicile (Figure I-6 et Figure I-7). Ces eaux se mélangent au niveau du bassin tyrrhénien et forment les eaux profondes tyrrhéniennes (TDW, Tyrrhenian Dense Water) qui à leur tour, circulent dans le bassin ouest. Une 4ème masse d'eau profonde est formée dans le golfe du Lion, les eaux profondes méditerranéennes occidentales (WMDW, Western Mediterranean deep Water). Ces dernières forment une circulation cyclonique dans le bassin ouest, se mélangeant au passage avec les TDW, pour qu'au final une partie de ces eaux se déverse dans l'océan Atlantique par le détroit de Gibraltar (Figure I-6 et Figure I-7).

Figure I-6 : Schéma simplifié de la circulation en 3 couches de la Méditerranée, le long d'une radiale du canal de Gibraltar, au bassin oriental. Adapté de Zavattarelli et Mellor (1995).

Figure I-7 : Schémas de la circulation en Méditerranée des (A) AW (Atlantic Water), (B) LIW (Levantine Intermediate Water) and (C) and the deep waters (AeDW, Aegean Deep Water; AdDW, Adriatic Deep Water; TDW, Tyrrhenian Dense Water; WMDW, Western Mediterranean Deep Water). Illustrations tirées de Millot et Taupier-Letage (2005).

Figure I-8 : Schémas de la circulation du bassin ouest méditerranéen, avec (A) en surface les AW et WIW (Winter Intermediate Water), (B) dans la couche intermédiaire, les LIW et TDW, et (C) les WMDW dans la circulation profonde. Schémas tirés de Millot (Millot, 1999).

Si l'on s'intéresse plus spécifiquement à la circulation du bassin ouest méditerranéen (Millot, 1999 ; Figure I-8), la circulation de surface générée par les AW (Figure I-8A) forment de nombreux tourbillons anticycloniques au large des côtes africaines. Dans le bassin ouest, les AW se situent entre 0 et de 200m de profondeur pour une salinité moyenne d'environ 36.5 (Millot, 1999; La Violette, 1994 ; Figure I-9). Après avoir longé les côtes italiennes, les AW circulent le long des côtes françaises pour former le Courant Nord Méditerranéen (CNM). La circulation générale du bassin nord occidental est cyclonique avec comme limite nord le CNM et comme limite sud le front nord Baléares (Millot, 1999; Testor and Gascard, 2006). Cette circulation forme un dôme isopycnal au centre de la zone MEDOC (Medoc Group, 1970), un phénomène qui fragilise la stratification de la colonne d'eau et favorise le processus de convection dans le golfe du Lion (cf. section I.1.2). En hiver, l'action modérée de la tramontane et du mistral peut conduire au refroidissement des AW, sans provoquer de mélange intense avec les masses d'eaux sous-jacentes. Cela forme une nouvelle masse d'eau, l'eau intermédiaire hivernale (WIW, Winter Intermediate Water), plus froide et plus dense que l'AW, dont la température varie entre 12.5 et 13.0°C et se situent entre 200 et 400 m de profondeur (Millot, 1999).

Les LIW, plus chaudes (~13.2°C) et plus salées que les AW (Figure I-9), puisque formées dans le bassin oriental, suivent globalement la circulation des AW, mais à des profondeurs plus importantes (entre 400 et 700m).

Au niveau de la zone MEDOC, les épisodes intenses de convection hivernale forment les WMDW. Une fois formées et exportées, les WMDW se mélangent aux TDW pour circuler de manière cyclonique dans tout le bassin ouest.

Figure I-9 : (A) Caractéristiques des masses d'eau du bassin oriental méditerranéen tiré de La Violette (1994) et (B) diagramme Théta-S caractéristique de ces masses d'eau.

I.2.4. La convection dans le golfe du Lion

En Méditerranée Nord Occidentale (MNO) deux processus sont à l'origine de la formation des eaux profondes Méditerranéennes: la convection et le cascading (Durrieu de Madron et al., 2005, 2013) (Figure I-10A-B). Ces 2 processus reposent sur la formation d'eaux denses hivernales (cf. section I.1.2), un mécanisme favorisé par la tramontane et le mistral, de forts vents froids et secs. Le front nord Baléares et le CNM forment une circulation cyclonique dans le golfe du lion (voire section I.2.3) qui favorise les épisodes convectifs en affaiblissant la stratification de la colonne d'eau (cf. section I.1.3). La convection en MNO suit les 3 phases décrites dans Marshall et Schott (1999) et dans la section I.1.2. La phase de préconditionnement a généralement lieu entre décembre et janvier. De janvier à mars a lieu la phase de mélange intense. Quant à la phase de propagation, sa durée et son étendue spatiale dépendent du volume d'eau profonde formé. En 2010, les eaux denses nouvellement formées ont mis environ un mois pour se propager de la zone MEDOC (Medoc Group, 1970) jusqu'à la station d'observation ANTARES (Astronomy with a Neutrino Telescope and Abyss environmentam REsearch ; 42°48.200' N - 06°04.500' E) située au large de la Seyne sur Mer (Tamburini et al., 2013).

Figure I-10 : (A) Schéma de la co-localisation des processus de cascading et de convection, tiré de Pusceddu et al. (2010). (B) Reconstitution des processus de cascading (Ca) et de convection (Co) dans le golfe du Lion sous l'action de la tramontane (T), du mistral (M) et de la circulation cyclonique initiée en partie par le Courant Nord Méditerranéen (CNM). (C) Classique diagramme Θ/S d'une masse d'eau convective (campagne CASCADE, mars 2011).

Les épisodes de convection profonde en MNO conduisent au mélange de toute la colonne d'eau jusqu'au sédiment, ne formant alors qu'une seule masse d'eau homogène dite « convective » (Figure I-10C). En MNO, l'intense mélange remet en suspension du sédiment, formant une couche néphéloïde capable de remonter plus ou moins haut dans la colonne d'eau selon l'intensité du mélange convectif (Canals et al., 2006; Puig et al., 2013). Ce processus est aussi à l'origine de la formation de nouvelles WMDW (nWMDW, new Western Mediterranean Deep Water). Durant la phase de propagation, les nWMDW plongent par gravité pour progressivement tapisser tout le fond du bassin oriental (cf. section I.2.3). Lorsque les forçages atmosphériques ne sont pas assez intenses (faible perte de chaleur par exemple), le mélange convectif n'atteindra que des profondeurs intermédiaires. Dans ce cas, les eaux formées sont généralement moins denses que les nWMDW formées et exportées par le précédent épisode profond de convection. Ces WMDW moins denses s'équilibrent à des profondeurs moins importantes que les nWMDW, reposant par-dessus ces dernières. Ce phénomène n'est pas exceptionnel en MNO, il a généralement lieu à la fin de l'hiver vers le mois de mars, suite à la diminution des forçages atmosphériques.

Bien que le processus de convection soit un phénomène hivernal récurrent, la variabilité des forçages atmosphériques a pour conséquence une inégalité de l'intensité, la fréquence et le volume d'eau dense formé d'un hiver à l'autre (Tableau I-1). Entre 1980 et 2012, 22 épisodes de convection profonds ont été observé en Méditerranée nord occidental, dont 6 entre 2005 et 2012 (Houpert, 2013). Les hivers 2005, 2009, 2010 et 2012 étaient les plus intenses en termes de pertes de chaleur et de flottabilité des eaux de surface. Cela a eu pour conséquences d'important renouvellement et formation de volumes d'eaux profondes en MNO (Schroeder et al., 2008; Zunino et al., 2012; Houpert, 2013). Les répercussions d'un faible épisode de convection, comme celui de l'hiver 2008 (Tableau I-1), sont à la fois physiques, avec un faible renouvellement des eaux profondes, mais aussi biogéochimiques avec une réduction des échanges entre les couches de surface et de fond (voir section I.3.3), ainsi qu'une diminution de la ventilation des eaux profondes, et biologiques, les microorganismes étant dépendant de ces échanges de matière (voir section I.4.2). Dans ce contexte, la nécessité d'étudier et de récolter davantage de données sur ces processus de convection en MNO devient nécessaire afin d'alimenter et d'améliorer les modèles physiques et biogéochimiques, dans le but d'affiner les prédictions de l'évolution de ces écosystèmes.

Tableau I-1 : Caractéristiques des évènements de convection profonde en Méditerranée nord occidental, à partir des données de la ligne de mouillage LION. Tiré de Houpert (2013).

I.3. Les cycles biogéochimiques dans les océans et l'influence des phénomènes de convection

I.3.1. Les sels nutritifs dans les océans

La Méditerranée est une mer globalement oligotrophe (milieu caractérisé par de faibles concentrations en sel nutritifs et par de faibles biomasses de producteurs primaires), avec un gradient d'oligotrophie croissant du bassin oriental vers le bassin occidental (Pujo-Pay et al., 2011). Néanmoins, des efflorescences printanières récurrentes excédant 2 $\mu g.L^{-1}$ de chlorophylles ont été enregistrées dans le bassin nord occidental (D'ortenzio and Ribera d'Alcalà, 2009 ; Figure I-11). La Méditerranée est reconnue comme particulièrement pauvre en phosphate (PO_4) (Béthoux et al., 1998b). Le phosphate serait le principal élément limitant la croissance des microorganismes en Méditerranée.

Cette limitation en phosphate se traduit par un rapport nitrate (NO_3) sur PO_4 variant entre ~22 et 25 dans le compartiment minéral des 2 sous bassins (Pujo-Pay et al., 2011), au lieu

du classique rapport NO_3:PO_4 de 16 (voire de 15 pour l'océan profond) connu sous l'appellation de "rapport de Redfield" (Redfield et al., 1963). Les rapports de Redfield sont les rapports atomiques moyens entre le carbone, l'azote, et le phosphore que l'on mesure dans phase minérale dissoute et dans la matière organique vivante dans l'océan global (Redfield, 1934). Cette observation empirique faisait suite à l'analyse de milliers d'échantillons marins à travers les 3 océans principaux, l'Atlantique, le Pacifique et l'océan Indien, ainsi que dans la mer de Barents. Suite à ces analyses, Redfield a conclu que globalement la stœchiométrie des éléments C, N et P tendait toujours vers ce même ratio de 106:16:1 respectivement, en raison de l'équilibre entre processus de synthèse et de minéralisation (i.e. photosynthèse / respiration). Entre 400 et 4000m de profondeur, Anderson et Sarmiento (1994) après correction de l'effet de la dénitrification, ont obtenu un rapport de 117(±14):16(±1):1. Il est toutefois à noter que dès la publication originelle, Redfield signalait l'existence de possibles variations autour de ces valeurs, préfigurant ainsi la notion de "plasticité cellulaire". La notion de stœchiométrie a ensuite été étendue à l'ensemble des éléments biogènes (« rapports de Redfield étendus ») dont l'oxygène, la silice (Brzezinski, 1985) et le fer résultant en un rapport des éléments O:C:Si:N:P:Fe de 276:106:15:16:1:0.01. Depuis, le rapport de Redfield a été remis de nombreuses fois en question, sa variabilité étant trop importante à l'échelle locale (Anderson et al., 2005; Banse, 1994; Geider and La Roche, 2002; Sterner et al., 2008). Toutefois, Arrigo (2005) a démontré que bien que le rapport de Redfield ne soit pas une valeur universelle, il représente tout de même une moyenne pour un assemblage phytoplanctonique marin divers, évoluant sous une variété de différentes conditions environnementales. Ce rapport aurait donc une signification à l'échelle écologique, même si Geider et La Roche (2002) indiquent que *"None of our analyses have suggested that the average elemental composition of phytoplankton is fixed, or should have remained invariant over past geological time"*.

En biogéochimie, ces rapports restent utiles et pertinents pour l'étude de la dynamique des communautés phytoplanctoniques naturelles grâce à leur « signification écologique à large échelle ». Les variations de ces rapports sont couramment utilisées pour détecter des anomalies liées à des activités biologiques particulières. Elles font également de la Méditerranée un modèle à part et un laboratoire géant d'expérimentation, puisque la matière organique particulaire suit les rapports de Redfield malgré l'important déséquilibre au sein de la matière minérale (Pujo-Pay et al., 2011).

Figure I-11 : Distribution spatiale des catégories d'efflorescence en Méditerranée obtenues par l'accumulation de 10 ans de données SeaWifs (D'ortenzio and Ribera d'Alcalà, 2009).

Les sources de sels nutritifs généralement considérées en mer Méditerranée sont les apports par l'océan Atlantique, les fleuves et rivières, ainsi que les dépôts atmosphériques dont les poussières sahariennes (Tableau I-2). A ces processus, nous pouvons ajouter la diazotrophie, c'est-à-dire la capacité de certains organismes marins à fixer le diazote (N_2) atmosphérique en ammonium, source d'azote plus accessible par le phytoplancton et les bactéries marines (Krom, 2011; Yogev et al., 2011). Notons que la variabilité spatiale et temporelle de la fixation de N_2 et les facteurs physiques et chimiques qui contrôlent ce processus sont encore mal appréhendés, surtout en Méditerranée (Sachs and Repeta, 1999).

Tableau I-2 : Compilation des stocks de sels nutritifs (silicate, $Si(OH)_4$; nitrate + nitrite, NO_3+NO_2 ; phosphate, PO_4) introduits dans les eaux de surface du bassin nord occidental méditerranée par différents processus physiques.

Processus apportant des nutriments	Date	$Si(OH)_4$ mol	$NO_3 + NO_2$ mol	PO_4 mol	Références
Flux annuel du bassin oriental	1945-1993	-	$142\ 10^9$	$4.4\ 10^9$	Krom et al., 2004
Décharge annuelle par le Rhône	June 94-May 95	$1.4\ 10^9$	$1.5\text{-}1.6\ 10^9$	$2.8\text{-}3.1\ 10^7$	Moutin et al., 1998
Décharge annuelle des rivières	1989-1993	$3.4\ 10^9$	$5.7\ 10^9$	$2.5\ 10^8$	Ludwig et al., 2009
Décharge annuelle des rivières	1994-1998	$3.8\ 10^9$	$5.9\ 10^9$	$1.8\ 10^8$	Ludwig et al., 2009
Apports annuels par les pluies sahariennes	1999	-	-	$3.0\text{-}4.0\ 10^9$	Ridame and Guieu, 2002
Flux annuel Atlantique	2008	-	$91\ 10^8$	$9.8\ 10^8$	Ramirez-Romero et al., 2014

L'activité humaine est aussi non négligeable en termes d'apports de phosphate et de nitrate rejetés dans les eaux usées et par ruissellement à travers les terres agricoles. Depuis les années 60, une augmentation des phosphates et des nitrates d'environ 3% par an a été enregistrée (Béthoux et al., 1998), alors que les quantités de silicate restaient constantes, voire diminuaient légèrement. En 1990, une interdiction en France d'introduire des phosphates dans les lessives, a conduit à un retour des concentrations en PO_4 tel que dans les années 60 après une augmentation de plus de 30% entre 1980 et 1990 (Ludwig et al., 2009). Cela se traduit par une importante modification des rapports stœchiométriques élémentaires dans les rejets fluviaux. Par exemple, le rapport NO_3:PO_4 dans les principaux fleuves méditerranéens est passé d'environ 20 à plus de 50 au début des années 2000 et atteint de nos jours, près de 80 dans les eaux du Rhône (Ludwig et al., 2009 ; Figure I-12).

Figure I-12 : Evolution des (A) nitrate, (B) phosphate, et (C) du rapport nitrate sur phosphate dans les principaux fleuves méditerranéens et de la Mer Noire. Tiré de Ludwig et al. (2009).

De telles modifications des rapports stœchiométriques mènent à une diminution du rapport $Si(OH)_4$:NO_3, ce qui pourrait conduire à un changement d'un écosystème dominé par des organismes siliceux (les diatomées) vers un écosystème dominé par des organismes non siliceux (flagellés et dinoflagellés) (Officer and Ryther, 1980; Jickells, 1998; Béthoux et al., 2002). Ce processus, déjà observé en mer Noire (Moncheva et al., 2001; Yunev et al., 2007), a conduit à une modification drastique de la chaine trophique marine, amenant de nouveaux équilibres dans les flux d'export et de stockage de la matière dans les écosystèmes.

I.3.2. La matière organique dans les océans

La matière organique marine (MO) est produite principalement par le réseau trophique marin (Figure I-15), via notamment l'exsudation des cellules phytoplanctoniques, le « sloppy feeding » du zooplancton, la lyse cellulaire naturelle ou virale. En milieu plus côtier, des sources allochtones telles que les apports terrigènes s'ajoutent aux sources autochtones. La MO existe sous forme particulaire (MOP), l'une des formes dégradables par les organismes hétérotrophes. L'autre forme de la MO est la matière organique dissoute (MOD), composée de molécules organiques de haut poids moléculaire >1000 Da (HMW, High Molecular Weight) et de faible poids moléculaire <1000 Da (LMW, Low Molecular Weight) (Carlson, 2002). L'activité des microorganismes hétérotrophes assure la transformation de la MOP en MOD HMW puis en LMW au cours des processus de reminéralisation, mais une fraction plus ou moins importante de cette matière finie par s'accumuler sous forme "réfractaire".

La MOD (HMW+LMW) forme le principal réservoir marin de carbone organique dissous (COD), qui est équivalent aux 700 Gt de carbone contenus dans le CO_2 atmosphérique (Nagata, 2008). Plus de 70% de ce stock de carbone (Benner, 2002) est composée de MOD réfractaire (Figure I-13A), dominée par des molécules LMW (Carlson, 2002) diagénétiquement altérées, donc peu accessibles pour les hétérotrophes marins. La composition exacte de la MOD réfractaire reste jusqu'à présent inconnue en raison de la grande diversité et de la complexité des molécules qui la compose (Figure I-13B). Son caractère récalcitrant pour la reminéralisation par les organismes marins permet à cette MOD de s'accumuler sur toute la colonne d'eau, sur une échelle de temps de 4000-6000 ans (Benner, 2002) (Figure I-13A), largement supérieur au taux de renouvellement de l'océan global qui est d'environ 2000 ans (Mermex group, 2011). Le taux de dégradation de la MOD semi-labile est de quelques mois à plusieurs années, lui permettant ainsi de s'accumuler en surface et d'être exportée vers les zones méso- et bathypélagique (~200-1000m et >1000m respectivement) par diverses processus physiques (sédimentation, downwelling, convection…) (Santinelli et al., 2013). La MOD semi-labile est composée de molécules LMW et HMW, qui sont principalement des polysaccharides, mais on y détecte aussi des acides aminés, des sucres aminés et des sucres neutres (Figure I-13B). La MOD labile est le pool de MO ayant le taux de renouvellement le plus rapide, allant de la minute à l'heure. Elle représente une infime portion de la MO marine (0-6%, Figure I-13A), et elle est composée en partie de molécules LMW, c'est-à-dire des sucres neutres ainsi que des acides aminés dissous libres (Carlson, 2002) (Figure I-13B).

Figure I-13 : (A) Schéma conceptuel des différents stocks de COD réfractaire, semi-labile et labile en océan hauturier, avec une représentation du pool de DOC ayant un taux de renouvellement supérieur à celui de l'océan global (rectangle blanc A) et le pool de COD au taux de renouvellement équivalent à celui de l'océan global ; tiré de (Carlson, 2002). (B) Représentation des biomolécules spécifiques et non caractérisées des fractions marines de COD et NOD (azote organique dissous) de surface (<100 m) et de fond (>1000 m) ; tirée de (Benner, 2002).

I.3.3. Impact des épisodes de convection sur les cycles biogéochimiques

Alors que la physique et l'hydrologie des processus de convection sont relativement bien connues, peu d'études du compartiment biologique existent (biogéochimie et microbiologie). Les difficultés d'échantillonnage durant les évènements intenses de convection en MNO sont certainement à l'origine de cette lacune. L'utilisation des lignes de mouillage et des pièges à particules a permis de quantifier les exports de MOP lors des épisodes de convection (Heimbürger et al., 2013; Stabholz et al., 2013; Gogou et al., 2014). En effet, les masses d'eaux denses en convection entrainent avec elles la MO de surface accumulée, séquestrant ainsi des quantités importantes de carbone, mais surtout apportant en profondeur de la matière organique "fraiche" et relativement labile. Grâce à ces pièges à particules, un export de carbone organique particulaire (COP) de ~10 mg C. m^{-2}. d^{-1} a été enregistré durant la convection hivernale de 2008-2009 en MNO (Stabholz et al., 2013). Outre l'utilisation de la modélisation, la plupart des calculs d'export de matière disponibles dans la littérature sont effectués à partir de vitesses verticales enregistrées par des lignes de mouillage et de concentrations potentielles de matière organique accumulée avant le mélange convectif. De cette manière, l'intense phénomène de convection observé en 2005 aurait exporté environ 3000 mg C. m^{-2}. d^{-1} en considérant une aire de convection d'un diamètre de 100 km (Santinelli et al., 2010).

La qualité de la MO exportée reste une question fondamentale pour le fonctionnement des écosystèmes mésopélagique et bathypélagique (Boutrif et al., 2011), mais aussi benthique (Pusceddu et al., 2010). Des études en mer de Sargasse ont montré que le processus de convection atteignant ~300 m de profondeur dans cette zone, pouvait exporter de 0.3 à 0.6 µM.C (soit 0.04-0.08 µg $C.L^{-1}.d^{-1}$) de sucres neutres dissous combinés (Goldberg et al., 2009), des molécules appartenant aux fractions labiles et semi-labiles du pool de MO. En MNO, Stabholtz et al. (2013) ont montré que la resuspension du sédiment associée à l'intense mélange vertical physique (cf. section I.2.4) était capable par simple effet mécanique d'introduire également de la MO réfractaire jusque-là piégée dans les premiers centimètres des sédiments de fond situés à 2500 m, jusqu'à ~1200 m en 2009, soit une couche de plus de 1000 m d'épaisseur impactée par cet apport de matière réfractaire. La simple mesure des excès de concentrations de MOD dans les couches profondes ne suffit donc pas à comprendre la dynamique et l'accessibilité du matériel dissous par les procaryotes suite au mélange convectif.

La convection profonde participe également activement à la séquestration du carbone en stimulant la pompe biologique. Les courants ascendants existant entre les cellules convectives (cf. section I.1.2) permettent la remontée d'eaux profondes riches en sels nutritifs. La quantité de sels nutritifs apportée conditionne directement l'intensité du bloom printanier. Grâce à ce processus, de fortes concentrations en chlorophylle *a* sont régulièrement observées en MNO (Figure I-11). En 2007, l'absence de convection en mer Adriatique a conduit à une forte réduction de l'efflorescence printanière (Gačić et al., 2002). Outre l'apport de sels nutritifs, la profondeur de mélange de la convection conditionnerait la phénologie du bloom, avec un pas de temps estimé à 30 jours entre la profondeur de mélange maximale et le pic de concentration en chlorophylle *a* (Lavigne et al., 2013). Ceci a conduit à supposer que la géométrie de la convection influence le déclenchement du bloom.

La théorie de « Phyto-Convection » a été proposée la première fois par Backhaus et al. (1999) et a été reprise par Behrenfeld (2010) sous le nom de « dilution-recoupling hypothesis ». Cette hypothèse propose que les courants descendants et ascendants au sein de la cheminée de convection, permettent aux cellules phytoplanctoniques d'être maintenues en vie par leur transport régulier dans la couche euphotique, la cheminée de convection se comportant alors comme une « couche euphotique virtuelle » (Figure I-14). A la fin du mélange convectif, la profondeur de la couche de mélange (MLD, Mixed Layer Depth) s'amoindrie, permettant de concentrer physiquement le stock hivernal de phytoplancton dans la couche euphotique. Cette hypothèse, associée à d'autres facteurs biologiques, expliquerait la régularité du pas de temps entre l'approfondissement de la MLD et le bloom phytoplanctonique.

Figure I-14 : Schéma représentant le cycle annuel du phytoplancton (points noirs) en relation avec l'approfondissement de la couche de mélange convective (trait noir foncé) et de la couche euphotique (zone hachurée). Tiré de Backhaus et al. (2003).

I.4. Le compartiment microbien

I.4.1. La boucle microbienne et la relation diversité/fonction

Invisible à l'œil humain, les procaryotes hétérotrophes marins (bactéries et archées) sont pourtant présents partout sur Terre. Leur abondance est estimée à 10^{29} cellules dans les océans (Whitman et al., 1998), excédant ainsi la biomasse combinée du zooplancton et des poissons (Pomeroy et al., 2007). Ignorés en milieu marin jusque dans les années 70, les avancées technologiques ont permis de mettre en évidence leur importance quantitative, leur ubiquité, ainsi que leur rôle clé dans la productivité de l'océan (Pomeroy, 1974). Ce n'est que dans les années 80 que l'importance biogéochimique des procaryotes à plus grande échelle fut découverte. En mettant au point une technique basée sur l'incorporation de leucine radioactive, Kirchman et al. (1985) ont permis d'estimer l'importance de l'activité de reminéralisation de la matière organique par les procaryotes hétérotrophes. En découvrant que 20 à 50% de la matière organique était reminéralisée par les bactéries, ces auteurs démontraient que le compartiment microbien était un maillon essentiel dans le cycle biogéochimique du carbone des océans, jusqu'alors complètement ignoré. Ils permettaient du même coup de montrer l'importance de la « boucle microbienne » énoncée quelques années plus tôt (Azam et al., 1983) en relation à la chaîne trophique linéaire classique (« boucle macrobienne ») pour la compréhension des cycles biogéochimiques dans les océans (Figure I-15).

Les microorganismes peuvent soit assimiler et minéraliser directement la MOD labile et semi-labile, soit dégrader la MOP en MOD HMW (cf. section I.3.2) via l'action d'enzymes extracellulaires. La reminéralisation de la MO est limitée à la fois par les autres éléments nutritifs nécessaires à la croissance des bactéries hétérotrophes (contrôle de type "bottom-up" par l'azote et/ou le phosphore, par exemple), ainsi que par la prédation par les protistes hétérotrophes (flagellés et ciliés) et la lyse virale (contrôle de type "top-down"). Les protistes permettent également un transfert de matière et d'énergie vers les maillons trophiques supérieurs, la quantité et la stœchiométrie conditionnant les flux trophiques (Figure I-15).

Figure I-15 : Schéma de la boucle microbienne tirée d'Azam et Malfatti (2007).

Afin de pouvoir dégrader et assimiler l'importante complexité des composés de la MOD (Benner, 2002; Repeta et al., 2002; cf. section I.3.2), chaque groupe taxonomique a développé une gamme toute aussi importante de fonctions impliquées dans le processus de dégradation. Dans ce contexte, la diversité et la composition des communautés procaryotiques devient un élément crucial pour la transformation de la MOD et le cycle du carbone en général. La question de la relation entre diversité et fonction est encore de nos jours une question essentielle de l'écologie microbienne marine (Yokokawa and Nagata, 2010). Du fait de leur petite taille, l'étude des microorganismes a toujours été dépendante de la levée de verrous méthodologiques. La compréhension de la relation diversité/fonction des microorganismes est également soumise à ces évolutions.

Certains travaux ont mis en évidence des groupes taxonomiques associés à des environnements contrastés où la composition de la matière organique est différente. C'est le cas par exemple de la diversité très différente observée entre les eaux de mers (dominées par les *Alphaproteobacteria* et les *Roseobacter*) (Morris et al., 2002; Selje et al., 2004) et les eaux douces (dominées par les *Betaproteobacteria*) (Glöckner et al., 1999), deux systèmes très différents en terme de qualité et de composition de la MO (Cauwet, 2002; Repeta et al., 2002). Mais d'autres paramètres environnementaux peuvent expliquer ces différences (salinité, turbidité, teneur en éléments nutritifs, lumière, etc.). D'autres travaux ont démontré plus précisément que différentes compositions de la MOD influençaient l'abondance, l'activité, mais aussi la structuration des communautés procaryotiques (Cottrell and Kirchman, 2000; Carlson et al., 2004; Sarmento and Gasol, 2012; Landa et al., 2013, 2014). La relation entre diversité bactérienne et diversité phytoplanctonique a été également observée statistiquement en milieu marin (Ghiglione et al., 2009). Or, il a été démontré que différentes lignées phytoplanctoniques exsudaient une MOD de composition distincte (Becker et al., 2014). Les variations spatiales et temporelles des communautés phytoplanctoniques pourraient donc être accompagnées de variations prédictibles de la composition en MOD et par conséquent, des variations de communautés procaryotiques. En 2005, Kirchman et al. (2005) ont proposé que : « la présence systématique de motifs biogéographiques pour certains groupes taxonomiques […] indique qu'ils pourraient fonctionner comme des unités écologiques, ayant des rôles définis dans la régulation des processus biogéochimiques ». Une structuration verticale et saisonnière des communautés procaryotiques est aujourd'hui bien connue en Méditerranée (La Ferla and Azzaro, 2001; Ghiglione et al., 2007, 2009; Galand et al., 2010; Díez-Vives et al., 2014), mais la relation de cette structuration avec le cycle du carbone doit être approfondie dans cette région (Pulido-Villena et al., 2012), mais aussi à une échelle plus globale (Yokokawa and Nagata, 2010).

Une révolution de la vision de la diversité microbienne et du monde vivant en général est apparue avec les travaux de Woese (1987) qui, par une analyse comparative des séquences des gènes ARNr 16S et 18S, décrivit 3 domaines du vivant: *Bacteria, Eucarya* et *Archaea* (Figure I-16). Actuellement, les archées constituent l'un des domaines le moins connu : taxonomiquement, avec la découverte du troisième phylum *Thaumarchaeota* en 2008 (Brochier-Armanet and Boussau, 2008), mais aussi physiologiquement. Les Archaea sont majoritairement hétérotrophes, mais outre l'assimilation démontrée d'acides aminés (Ouverney and Fuhrman, 2000; Teira et al., 2006), certains groupes seraient capables de fixer le CO_2

dissous dans l'eau de mer (Herndl et al., 2005; Ingalls et al., 2006; Wuchter et al., 2003), d'oxyder l'ammonium en nitrite via le gène amoA (Francis et al., 2005; Spang and Hatzenpichler, 2010), tandis que d'autres possèdent le gène de la protéorhodopsine (Frigaard et al., 2006) qui leur permet d'augmenter leur efficacité métabolique via le rayonnement solaire.

La large gamme des fonctions présentes chez les Archaea permet aujourd'hui de les considérer comme des acteurs de la régulation des cycles biogéochimiques. Comme pour les bactéries, une structuration spatiale et saisonnière a été mise en évidence en MNO (Galand et al., 2010), avec notamment, en surface, une prédominance des Marines Groupe II *Euryarchaeota* en période stratifiée (printemps, été), qui bascule vers une prédominance des Marines Groupe I *Thaumarchaeota* en période hivernale (automne, hiver).

Figure I-16 : Arbre phylogénétique du vivant montrant les relations entre les espèces dont les génomes ont été séquencés jusqu'en 2006. Chaque couleur représente un des trois domaines du vivant : en rose les *Eucarya* (animaux, plates et champignons), en bleu les *Bacteria* et en vert les *Archaea*. Les bandes claires et foncées du pourtour représentent les clades (Letunic and Bork, 2011, 2007).

I.4.2. Impact des épisodes de convection sur le compartiment microbien

Très peu d'études se sont intéressées à l'impact de la convection sur le compartiment bactérien, si ce n'est celle réalisée en mer de Sargasse par Morris et al. (2005). Suite à un mélange convectif atteignant ~300 m de profondeur, ces auteurs ont montré que différentes communautés bactériennes étaient stimulées dans la zone euphotique et mésopélagique par cet événement convectif. Ces différents développements seraient liés au découplage du cycle du carbone entre la zone euphotique et la zone mésopélagique (Hansell and Carlson, 2001). Dans cette zone, une convection profonde semble accentuer l'export de carbone organique total (COT) accumulé en surface, principalement constituée de molécules semi-labile. Des bactéries capables de dégrader cette qualité de MO et adaptées aux conditions de la zone mésopélagique sont donc favorisées, en l'occurrence les OCS116, SAR11 et *Actinobacteria*. En surface, une convection profonde stimule une production importante de COT par le développement du bloom phytoplanctonique, donc une MO fraiche et de qualité plus labile qui stimulerait des clades opportunistes tels que les SAR11, SAR86 et SAR116. Dans ces conditions, le développement de communautés différentes en zones euphotique et mésopélagique serait dû à différentes qualités de la MO, rejoignant le concept de diversité/fonction développé précédemment en section I.4.1.

A notre connaissance, un tel suivi de la diversité procaryotique et de la qualité de la MO n'existe pas en MNO. Cependant, Azzaro et al. (2012) ont suivi pendant presque 2 ans l'abondance et l'activité des procaryotes dans la zone de convection de la mer Adriatique (Figure I-4). Tout comme Morris et al. (2005), ces auteurs concluent que le mélange convectif favoriserait l'export de MO polymérique disponible pour les organismes marins (labile et/ou semi-labile) et par conséquent, stimulerait la pompe biologique microbienne profonde en piégeant la MO exportée dans les eaux profondes nouvellement formées.

I.5. Objectifs de la thèse

Les phénomènes de convection sont des processus physiques ayant de fortes répercutions sur les écosystèmes pélagiques, à la fois dans le domaine biogéochimique (oxygénation des eaux profondes, export de matière organique, apport de sels nutritifs), et dans le domaine biologique (conditionnement de l'efflorescence printanière, modifications de l'activité et de la diversité des procaryotes). Alors que la physique des évènements intenses de convection dans le golfe du Lion (GdL) est étudiée depuis 1969 avec les premières expériences

du groupe MEDOC (Medoc Group, 1970), les études biogéochimiques et biologiques restent sporadiques en raison des difficultés d'échantillonnage de cette zone en période hivernale.

Le principal objectif de ma thèse a donc été d'améliorer les connaissances de l'impact des processus de convection dans le GdL sur ces deux domaines que sont la **biogéochimie et la microbiologie** ; des domaines étroitement liés dans l'écosystème pélagique et pourtant diamétralement opposés en terme de méthodologie, de technique d'analyses et d'outils de traitement. Pour ces raisons, j'ai ajouté à mon manuscrit de thèse un glossaire des techniques que j'ai apprises et utilisées tout au long de mon doctorat (voir § PREFACE).

Je me suis particulièrement intéressée aux stocks et à la stœchiométrie des sels nutritifs pendant et après la convection, ainsi qu'à leur influence sur le conditionnement de l'efflorescence printanière. Le processus de convection influençant largement les cycles biogéochimiques, son influence directe (mélange physique) et indirecte (modification des stocks de MO et sels nutritifs) sur la diversité et l'activité du compartiment procaryotique a été étudiée. Mon manuscrit de thèse a donc été élaboré autour de 3 questions principales :

- Quels sont les impacts d'un évènement de convection en MNO sur les stocks et la stœchiométrie biogéochimique ? Et comment conditionne-t-il l'efflorescence printanière ?
- Quels sont les impacts d'un évènement de convection en MNO sur la diversité et l'activité des procaryotes ?
- Quels sont les impacts d'un évènement de convection en MNO sur les écotypes de SAR11, Marine Group I et Marine Group II ?

Pour cela, j'ai disposé d'un cadre programmatique très favorable avec le chantier Méditerranéen MISTRALS[1] et d'un cadre logistique comprenant deux campagnes océanographiques hauturières ayant permis un échantillonnage adaptée de la zone de convection ; la campagne CASCADE[2] en mars 2011 (Cascading, Surge, Convection, Advection and Downwelling Events) et les campagnes DeWEX[3] 1&2 en février et avril 2013 (Deep Water formation EXperiment), s'inscrivant respectivement dans les plans d'implémentation des WP1 et WP3 du programme MermEX[4].

[1] http://www.mistrals-home.org/spip/?lang=fr
[2] http://cefrem.univ-perp.fr/index.php/20-campagne-cascade/cascade/24-campagne-cascade
[3] http://lomic.obs-banyuls.fr/fr/test/campagne_dewex2.html
[4] http://mermex.pytheas.univ-amu.fr/

Ce manuscrit rend principalement compte des résultats obtenus lors de la campagne CASCADE, avec de premiers résultats de la campagne DeWEX discutés dans le chapitre IV. Son organisation, après cette introduction générale correspondant au chapitre I, suit le schéma ci-dessous (Figure I-17) :

- Le **chapitre II** discute de l'impact des processus de convection sur les cycles biogéochimiques. Un premier article intitulé « Impact of open-ocean convection on nutrient, phytoplankton biomass and activity » par Severin et al. (en correction) décrit les stocks en sels nutritifs et l'évolution de leur stœchiométrie pendant et après l'épisode convectif échantillonné lors de la campagne CASCADE.
- Dans le **chapitre III**, j'évalue l'impact de la convection sur l'abondance, la diversité et l'activité des procaryotes marins. Tout d'abord, je propose le deuxième article « Impact of an open-ocean convection event (0-1500m) on prokaryotic diversity and activity in the NW Mediterranean Sea » par Severin et al. (en préparation) qui aborde la question plus large de l'impact de la convection sur les communautés de bactéries et d'archées dans leur totalité. L'étude sur les activités procaryotiques menée dans cet article permet de faire le lien entre l'influence de la diversité et de l'activité des procaryotes sur les cycles biogéochimiques. Je me suis également intéressée à l'écologie des écotypes des procaryotes en utilisant la convection comme un modèle perturbant dans le troisième article intitulé « Vertical niche partitioning along marine bacterial (SAR11) and archaeal (Marine group I and II) ecotypes in response to physical turbulence » par Severin et al. (en préparation).
- Dans le **chapitre IV**, une discussion générale de l'impact de la convection sur l'écosystème pélagique est abordée grâce à une synthèse des résultats des différents compartiments.

Des travaux complémentaires tentant de mieux comprendre les liens entre la diversité et l'activité des procaryotes sont également exposés. Ces travaux sont relatifs à la fois à la campagne DeWEX, mais également à un programme d'optimisation de la technique de DNA-stable isotope probing (voir quatrième article en annexe intitulé « 'Rare biosphere' bacteria as key phenanthrene degraders in coastal seawaters » par Sauret et al. sous presse).

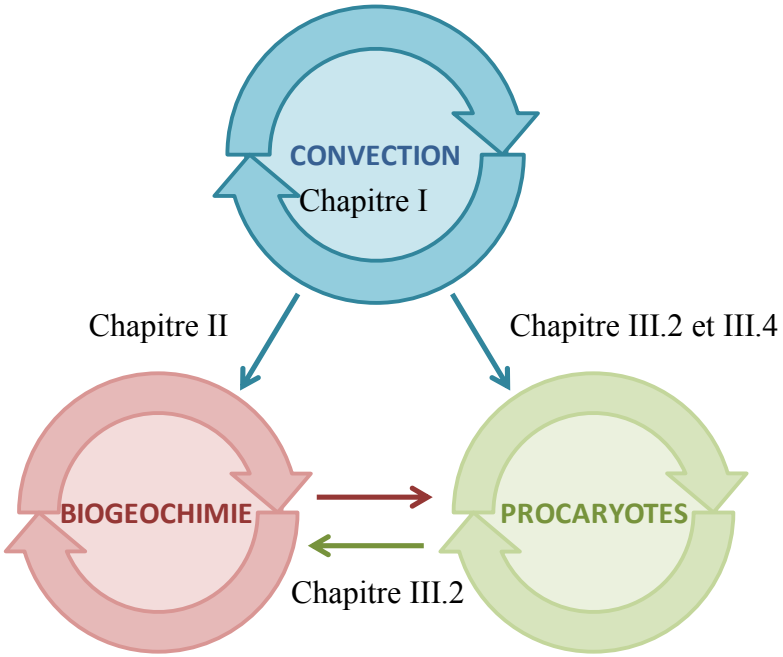

Figure I-17 : Schéma organisationnel de mon manuscrit de thèse.

Chapitre II

IMPACT DE LA CONVECTION SUR LA BIOGÉOCHIMIE DE LA MÉDITERRANÉE NORD OCCIDENTALE (MNO)

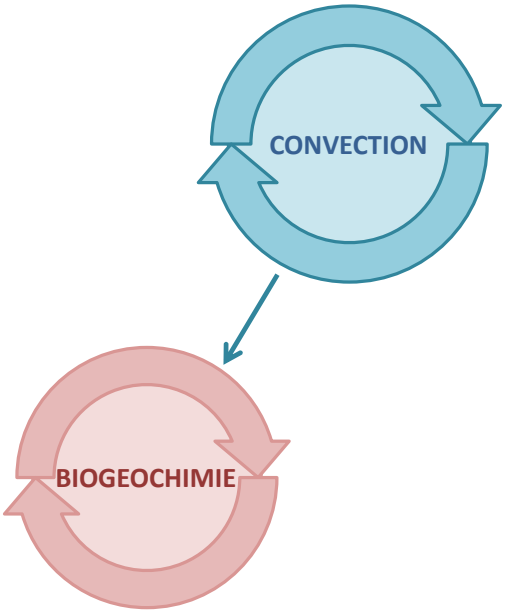

II. IMPACT DE LA CONVECTION SUR LA BIOGÉOCHIMIE DE LA MNO

II.1. Préambule

Nous avons évoqué dans l'introduction générale l'impact du processus de convection sur les stocks de sels nutritifs (cf. section I.3.3). La remontée des eaux profondes riches en sels nutritifs est provoquée par la plongée des eaux denses (cf. section I.1.2). Ce processus apporte en surface une importante quantité de nutriments qui conditionnent ensuite l'efflorescence printanière. À notre connaissance, aucune mesure biogéochimique n'a encore été réalisée lors des évènements convectifs en MNO. Actuellement, la relation entre l'hydrodynamisme de la zone et la phénologie du bloom printanier n'est étudiée qu'à travers les tendances à moyen-long terme des stations d'observations généralement situées en dehors de la zone de mélange intense (Marty and Chiavérini, 2002; Marty et al., 2002).

Ce premier chapitre de résultats décrit l'influence du dernier épisode de convection de l'année 2011 en MNO (campagne CASCADE) sur les stocks et les rapports stœchiométriques des nitrate (NO_3), nitrite (NO_2), phosphate (PO_4) et silicate ($Si(OH)_4$), ainsi que sur l'activité et la biomasse phytoplanctonique à l'échelle de la zone de convection. Pour cette étude, les stations ont été classées en 3 groupes en fonction de leurs caractéristiques hydrologiques (Figure II-1) :

- CONVg (pour CONVection group) est composé de 3 stations avec prélèvement mélangées par convection jusqu'à 1500 m de profondeur.
- STABg (pour STABilized group), échantillonné 4 jours plus tard, est composé de 3 stations avec prélèvement stratifiées sur toute la colonne d'eau, dont SC2400 échantillonnée pour la deuxième fois.
- R-STABg (pour Recently-STABilized group) correspond à la même station SC2400 échantillonnée une troisième fois, 12 jours après CONVg juste après un mélange superficiel de la colonne d'eau.

Le résultat majeur issu de cet échantillonnage a été de montrer que les apports de $Si(OH)_4$, NO_3+NO_2 et PO_4 lors de la convection étaient au moins équivalent à l'apport annuel des rivières et des dépôts atmosphériques dans le golfe du Lion. Cette nouvelle source de sels nutritifs s'avère potentiellement suffisante pour soutenir la production primaire nouvelle de l'océan hauturier de la MNO. L'évolution des rapports Si:N:P avant, pendant et après l'épisode de convection suggère que la diminution du rapport Si:N associée à l'activité anthropique (cf.

section I.3.1) pourrait être atténuée par le processus de convection, sauf si celui-ci était amené à disparaitre suite au changement climatique (cf. section I.1.3). A l'issue de l'analyse des données, le couplage des mesures *in situ* et satellitaires de la biomasse et de l'activité phytoplanctonique a permis de proposer trois scénarii quant à l'origine de l'efflorescence printanière liées au processus de convection. En fonction des conditions environnementales, l'importance relative de chacune des origines influencerait la diversité et la variabilité interannuelle des communautés rencontrées dans la zone convective.

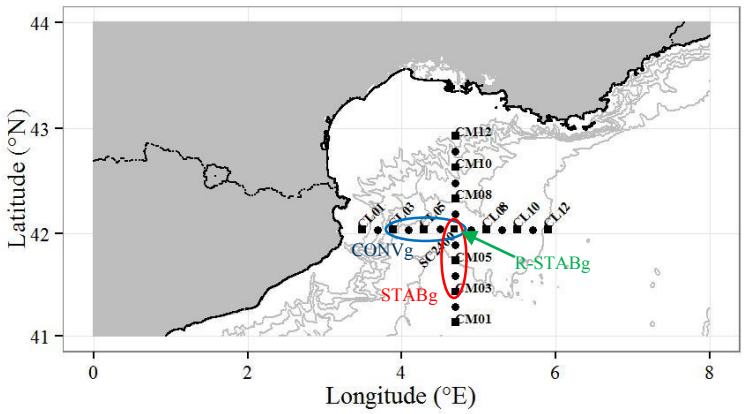

Figure II-1 : Carte d'échantillonnage de la campagne CASCADE (1-23 mars 2011). Les stations hydrologiques sans (notées ●) et avec (notées ■) prélèvements biogéochimiques sont indiquées, ainsi que les 3 groupes de stations CONVg (bleu), STABg (rouge) et R-STABg (vert) étudiés dans le 1er article.

II.2. Article 1: Impact of open-ocean convection on nutrients, phytoplankton biomass and activity

T. Severin[a,b,*], P. Conan[a,b], X. Durrieu de Madron[c], L. Houpert[c], M. J. Oliver[d], L. Oriol[a,b], J. Caparros[a,b], J. F. Ghiglione[a,b], and M. Pujo-Pay[a,b,*].

[a]Sorbonne Universités, UPMC Univ Paris 06, UMR 7621, Laboratoire d'Océanographie Microbienne, Observatoire Océanologique, F-66650 Banyuls/mer, France
[b]CNRS, UMR 7621, Laboratoire d'Océanographie Microbienne, Observatoire Océanologique, F-66650 Banyuls/mer, France
[c]CEFREM, UMR 5110, CNRS-UPVD, F-66860, Perpignan, France
[d]School of Marine Science and Policy, University of Delaware, Lewes, DE 19958, USA

[*]**Corresponding authors**:
T. Severin, Laboratoire d'Océanographie Microbienne, Observatoire Océanologique, Avenue du Fontaulé, F-66650 Banyuls/mer, France. Tel.: + 33 (0) 4 68 88 73 77. E-mail address: tatiana.severin@obs-banyuls.fr
M. Pujo-Pay, Laboratoire d'Océanographie Microbienne, Observatoire Océanologique, Avenue du Fontaulé, F-66650 Banyuls/mer, France. Tel.: + 33 (0) 4 68 88 73 51. E-mail address: mireille.pujo-pay@obs-banyuls.fr

Abstract

We describe the impact of an open-ocean convection event on nutrient budgets, carbon budget, elemental stoichiometry, phytoplankton biomass and activity in the Northwestern Mediterranean Sea (NWM). In the convective episode examined here we estimated an input of nutrients to the surface layer of 7.0, 8.0 and 0.4 10^8 mol of silicate, nitrate and phosphate, respectively. These quantities correspond to the annual nutrient input by river discharges and atmospheric depositions in the Gulf of Lion. Such nutrient input is sufficient to sustain new primary production from 46 to 63 g $C.m^{-2}.y^{-1}$, which is the same order of magnitude found in the NWM open waters. Our results together with satellite data analysis, propose new scenarios that explain the origin of the spring phytoplankton bloom occurring in NWM.

Keywords: Open-ocean convection, Northwestern Mediterranean Sea, nutrient budgets, nutrient stoichiometry, phytoplankton bloom, remote sensing

Introduction

Open-ocean convection is a fundamental process for the formation and the renewal of deep and intermediate waters (Medoc Group, 1970; Thetis Group, 1994; Marshall and Schott, 1999). In the Northwestern Mediterranean Sea (NWM), cyclonic circulation induces a doming of the isopycnals in the center of the basin that weaken the stratified waters (Millot, 1999; Robinson et al., 2001; Millot and Taupier-Letage, 2005) generally characterized by a three layer water column (AW: Surface water of Atlantic origin, LIW: Levantine Intermediate Water, and WMDW: Western Mediterranean Deep Water). The convection process is initiated by the combination of the geographic configuration of the area (Hogg, 1973; Madec et al., 1996) and by strong winds; the Mistral in the Rhone valley and the Tramontane bypassing the Pyrenees (Mertens and Schott, 1998; Jacq et al., 2005). The convection area generally centered on 42°N latitude and 5°E longitude (Medoc Group, 1970; Leaman and Schott, 1991; Thetis Group, 1994), and delimited to the South by the position of the Balearic front (Millot, 1999; Testor and Gascard, 2006).

Convection is an annual event in the Gulf of Lion, but there is a high degree of interannual variability associated with its lifetime and spatial extent (Mertens and Schott, 1998; L'Hévéder et al., 2013). The main factor controlling the onset and the termination of the convection event is the atmospheric forcing (cooling and evaporation) of water column density. The frequency and the intensity of the convection process are susceptible to being altered by processes associated with the climate change, but the method of change is not clear. Marty and Chiavérini (2010) observed an increase of the frequency of extreme convection events as a result of a substantial decrease of precipitation and an increase of evaporation, raising the surface water salinity. This would compensate for the already observed sea surface temperature (SST) increase of 0.03-0.15 °C.a^{-1} from 1957 to 1997 (Béthoux et al., 1998) as well as a slow warming (0.0034°C.a^{-1}) and increases in salinity (1.05 10^{-3} a^{-1}) of the WDMW during the 1993-2000 period (Béthoux et al., 2002a). Long-term warming and salinization trends in the deep layers have been confirmed by several studies (Leaman and Schott, 1991; Vargas-Yáñez et al., 2010).

Convection processes have important repercussions for carbon sequestration. The convective vertical mixing exports particulate organic matter, estimated to 10 mg C.m^{-2}.d^{-1} during the winter 2008-2009 in the NWM (Stabholz et al., 2013) and dissolved organic carbon estimated to 3000 mg C. m^{-2}.d^{-1} during the intense NWM open-ocean convection event of 2005 (e.g. considering a convection area of 100 km of diameter, Santinelli et al., 2010). But the quality of the organic matter present in the bathypelagic zone depends on the intensity of the

convective mixing (Turchetto et al., 2012; Stabholz et al., 2013). A bottom-reaching convection episode resuspends sediment, introducing refractory organic matter few meters above the sea floor (Stabholz et al., 2013). In contrast, a deep convection event that does not reach the sea floor might export only organic matter coming from the surface layer; theoretically more labile than the one from the sediment. The quantity and quality of organic matter exported have important consequences on the productivity and the diversity of bathy-pelagic microorganisms (Boutrif, 2011) and benthic fauna (Pusceddu et al., 2010).

The Mediterranean Sea is an oligotrophic region, with the eastern basin being more oligotrophic than the western basin (Mermex Group, 2011). The nutrient sources that could explain the observed primary production rates in the NWM are the Atlantic influx, riverine discharge, atmospheric deposition and deep ocean convection. However, the importance of deep ocean convections is rarely taken into account because of the lack of knowledge due to the difficulties of sampling a convection episode. Some authors have suggested that the nutrient input from deep to euphotic layers by the convection process directly determine the intensity of the spring bloom (Gacic et al., 2002, Gogou et al., 2014). In the Adriatic Sea, winter 1997 was marked by the absence of a convection event. It resulted in a reduced spring bloom. In the NWM, phytoplankton blooms following convection episodes generally exceed 2 $mg.m^{-3}$ of chlorophyll a concentration (D'Ortenzio and Ribera d'Alcala, 2009). Some studies based on remote sensing or modeling estimated a primary production of this NWM bloom ranging from 106 to 213 g C. $m^{-2}.y^{-1}$ (Morel and André, 1991; Lévy et al., 1999, 2000; Bosc et al., 2004). Hence, it contributes actively to the sequestration of carbon in the deep sea. A better estimate of the nutrient input by the convection process is necessary to improve the existing models and to propose a realistic scenario of the ecosystem functioning during and after winter convection.

In this study, we evaluated the impact of a convection event on the nutrient stoichiometry and the resulting phytoplankton bloom in the NWM during the winter 2010-2011. We analyzed (i) the relative importance of the spatial scale of the open-ocean convective event encountered during the cruise, (ii) the associated nutrient budget, (iii) the evolution of the nutrient stoichiometry during and after the convection event, and (iv) phytoplankton biomass, activity and carbon budget with respect to the biogeochemical fluxes initiated by the convection episode. We propose three mechanisms that initiate the NWM spring bloom: lateral advections, nutrient enrichment, and the ‘phyto-convection theory’.

2. Materials and methods

2.1 Study area and sampling

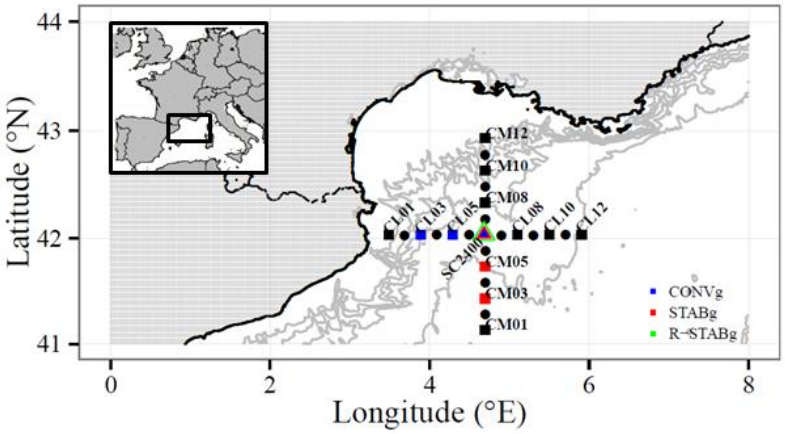

Fig. 1. Sampling map of the CASCADE cruise Leg 1 (1-23 March 2011) in the Gulf of Lion (Northwestern Mediterranean Sea). (•) indicates stations with CTD profiles only, (■ and ▲) indicate stations with CTD profiles and water sampling. Stations are aligned along 2 transects (West-East for L and South-North for M) arranged in a cross whose centre corresponds to the SC2400 station (▲) sampled 3 times during the cruise. The colors correspond to the 3 groups of stations determined in section 3.1.

The "CASCADE" cruise (Cascading, Surge, Convection, Advection and Downwelling Events) took place in the Gulf of Lion from the 01 to 23 March 2011 on the R/V *L'Atalante.* Two transects (CL and CM) of 13 stations each, crossed the 'known' dense water formation area of the NWM (Medoc Group, 1970; Leaman and Schott, 1991; Thetis Group, 1994) (Fig. 1). At each station, a profile was conducted from the surface to a few meters above the seafloor using a Seabird 911Plus CTD probe with SBE 32 Carousel water sampler. 13 data channels were measured: pressure, dual temperature (SBE3) and conductivity (SBE 4) with pump, dissolved oxygen (SBE 43), light transmission (WET Labs C-Star), turbidity (Seapoint), fluorescence (Chelsea Aquatracka III), photosynthetically active radiation (QSP-2300), Colored Dissolved Organic Matter (WET Labs ECO CDOM), and altimetry (Tritech PA500). At every other station, water samples were collected at 10 levels with 12L Niskin bottles. Note that the SC2400 central station had been sampled at three different dates (4, 9, and 16 March 2011). Moreover, this station was next to a subsurface mooring line (42° 02.4'N, 4° 41.0'E) maintained by the CEFREM and LOCEAN since 2007. This line was installed from 150 m deep to a few tens of meters above the bottom at 2350 m. The line is equipped with 10 RBR TR-1050 (temperature recorders), 11 SeaBird 39SMP (CTD recorders), and 5 Nortek Aquadopp acoustic current meters measuring horizontal and vertical currents (Durrieu de Madron et al., 2013). Data from the upper layer (2-200 m) came from the Meteo-France weather buoy LION (5 miles north of the mooring line) equipped with NKE SP2T temperature sensors at several levels between

depths of 2 m and 200 m since November 2009. Daily-averaged data from both the buoy and the mooring line were used to calculate the mixed layer depth (MLD), because of the lower accuracy of the buoy temperature sensors. The MLD was first estimated using the buoy sensors and a temperature difference < 0.1°C with respect to the uppermost sensor at 10 m depth. When the MLD was at depths greater than 200 m, the estimation was based on the mooring line sensors and considered a temperature difference of 0.01°C with respect to the uppermost sensor ~170 m deep.

2.2 Nutrients

Samples for silicate ($Si(OH)_4$ ± 0.05µM), nitrate (NO_3 ± 0.02µM), nitrite (NO_2 ± 0.01µM) and phosphate (PO_4 ± 0.01µM) were immediately filtered on board (using 0.45µm cellulose acetate filters) and stored in 20 ml polyethylene vials at -20°C until analysis. In the laboratory, samples were analyzed by colorimetry on a Seal-Bran-Luebbe autoanalyzer AA3 HR, according to Aminot and Kérouel (2007). Ammonium concentrations (NH_4 ± 2nM) were determined on board by nanomolar fluorometric method according to Holmes et al. (1999) on a fluorometer Jasco FP-2020.

2.3 Total chlorophyll a and phaeopigment a

250 ml of seawater were filtered on Whatman GF/F 25mm glass fiber filters. Filters were stored at -80°C. After extraction by 90% acetone, total chlorophyll a (CHL) and phaeopigment a (pigment of CHL degradation; PHAEO) concentrations were measured by fluorometry on a Turner Design 10-AU fluorometer, according to the method proposed by Strickland and Parson (1997).

2.4 Primary production and photosynthetic parameters

Water samples were collected at 5, 50 and 100 m depth to assess primary production and photosynthetic parameters with the use of radioactive ^{14}C-tracer technique (Steemann-Nielson, 1951) modified by Fitzwater et al. (1982).

For primary production measurements, 300 mL of water were dispensed into acid cleaned (0.5 N HCl) polycarbonate bottles (in triplicate for light measurements and once for dark fixation) and supplemented with 150µl of $Na_2H^{14}CO_3$ working solution (final activity of ~0.1µCi. ml^{-1}). 250 µL were then immediately sampled in 3 randomly selected bottles, mixed with 200µl of ethanolamine and placed in a 20 mL polyethylene scintillation vial in order to determine the level of radioactivity introduced. Samples were incubated under simulated *in situ*

conditions (52% of surface irradiance for 5m samples, 23% for 50 m samples and 1% for 100m samples) for 24 h on a deck incubator continuously cooled by surface seawater. Dark bottles were incubated in the dark. At the end of incubation, samples were filtered on Whatman GF/F 25 mm filters, rinsed with 10% HCl, dried at 50°C for 12 h, and placed into scintillation vials to be stored at room temperature until analysis.

The photosynthetic-irradiance parameters (α, P^b_m and I_k) were determined on the same samples (10 light levels in an irradiance gradient from 0 to 1327W.m^{-2}). For this purpose, ten 60mL Nunc culture vials were inoculated with $Na_2H^{14}CO_3$ (final activity of ~0.2µCi. ml^{-1}) and incubated for 45 min in a specifically designed incubator cooled to sea surface temperature. For each depth, triplicate of 250 µL were immediately sampled in 3 randomly selected bottles after the inoculation of $Na_2H^{14}CO_3$, mixed with 250µl of ethanolamine and placed into a 20 mL polyethylene scintillation vial in order to determine the level of radioactivity introduced. At the end of incubation, the 10 vials were simultaneously filtered on Whatman GF/F 25 mm filters. These filters received the same protocol as for primary production.

At the laboratory, 10 ml of a liquid scintillation cocktail (Ultima Gold uLLT) were added to the set of scintillation vials 6h before processing in a Beckman Scintillation Counter.

The photosynthetic parameters were determined by fitting the hyperbolic tangent model without photoinhibition proposed by Jassby and Platt (1976).

2.5 Remote sensing

Ocean color level 1b data from the MODIS-Aqua satellite were downloaded from NASA's Ocean Color website (http://oceancolor.gsfc.nasa.gov/, reprocessing 1.1) and processed with the Naval Research Lab Automated Processing System v. 4.2.5. Data was processed at 1 km resolution for daily and 8-day composite images of chlorophyll (mg.m^{-3} and sea surface temperature (°C) from November 2010 to April 2011.

3. Results

3.1 Hydrography

The convective cell sampled on 4 March (CONVg) was observed by the homogeneous vertical profiles of potential temperature (12.9 °C) and potential density anomaly (σ_0 = 29.116 kg.m^{-3}) down to 1500m (Fig. 2A). The presence of a thermocline and a pycnocline on 9 and 16 March 2011 (Fig. 2B and 2C respectively), illustrated a rapid restratification of the water column after the cessation of the convection episode (Fig. 2B, C). This early March convective cell was found in the western part of the basin between stations CL03 and CL07 (Fig. 3A). The

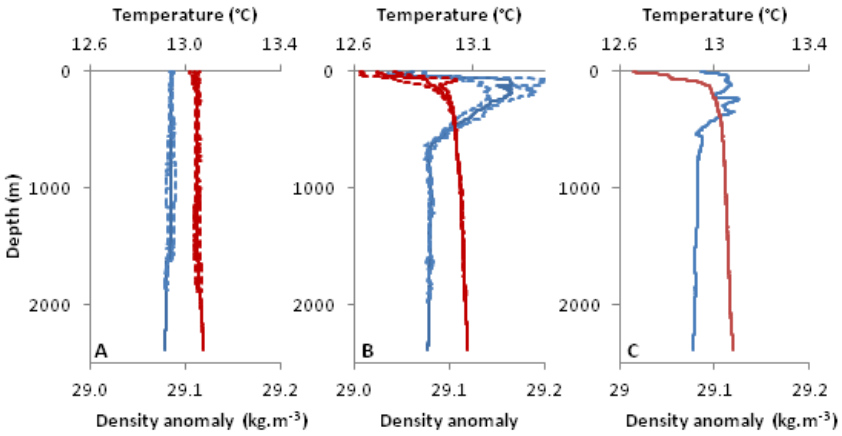

Fig. 2. Vertical profiles of the potential temperature (blue line) and density anomaly (red line) at (A) stations of CONVg, (B) STABg, and (C) R-STABg (refer to section 3.1). The solid lines are the potential temperature and density anomaly at SC2400 (see Fig. 1) and the dashed lines are the standard deviation of the potential temperature and density anomaly of each group.

mixed layer had a maximum potential density anomaly of 29.116 down to depths of ~1500m. Conversely, stratified conditions were along the eastern part of the L transect (stations CL08-CL12 conducted on 6-7 March 2011) and along the M transect conducted on 7-11 March 2011 (Fig. 3) with the presence of warmer and more saline LIW between 100 and 500 m of depth. The hydrological conditions for the stations around SC2400, next to the mooring line, allowed us to consider three groups of stations. The convective regime group (noted CONVg) consists of CL03, CL05 and SC2400_1 which had been sampled on 4 March 2011. Stations CM03, CM05 and SC2400_7, sampled on 9 March 2011 formed the stabilized regime group (noted STABg). Station SC2400_9 was sampled after an E-SE wind event from 12 to 16 March 2011 (Martin et al., 2012) that led to a homogenization of the surface layer (0-50 m) but without initiating a noteworthy deepening of the MLD (Fig. 4B). SC2400_9 is the single station sampled on 16 March 2011 in the MEDOC area. Hence it constitutes the third group characterized by recently stabilized conditions (noted R-STABg).

To assess the temporal changes of the biogeochemical process in the convection area, and to take into account the small spatial variability, we examined the changes of selected parameters at the central station SC2400, and used the neighboring stations within each group (CONVg, STABg) to calculate the standard deviation; with the exception of R-STABg for which only the central station was sampled.

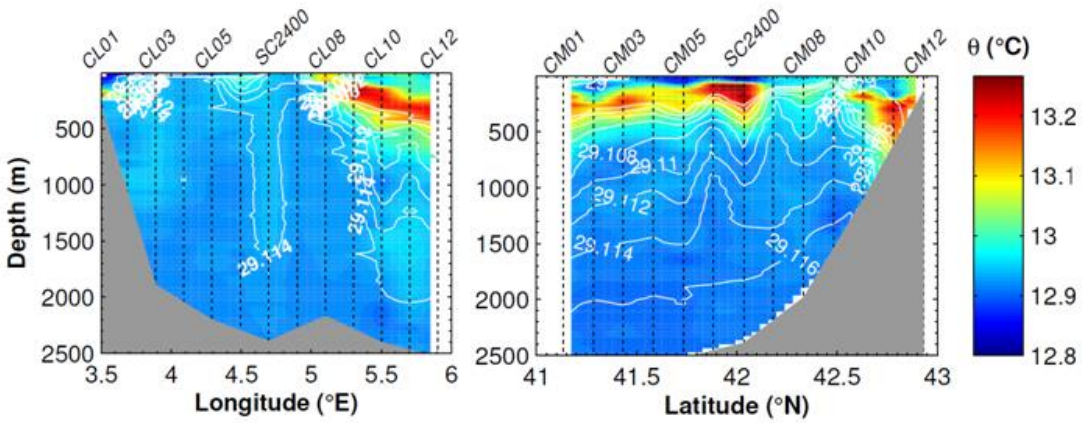

Fig. 3. Vertical sections of the potential temperature (°C) along the radial L (left) and the radial M (right). The white lines are the potential density anomaly (kg.m^{-3}) isolines.

When we monitored the convection episode sampling in March, the winter 2010-2011 was characterized by a progressive decrease of the SST (Sea Surface Temperature) between November 2010 (~16°C) and the end of March 2011 (12.9 °C) and then by a sharp increase in April 2011 (Fig. 4A). As for the SST, the water column temperature (Fig. 4B) illustrated a clear seasonal cycle by a deepening of MLD between November and December 2010 with the progressive mixing of AW and warmer and more saline LIW, a discontinuous homogenization of the water column from February to March 2011, and the restoration of the seasonal stratification in April 2011. The period between late January and early February 2011 was marked by a complete homogenization of the water column down to the seabed at 2300 m deep. It was followed by a period of re-stratification interrupted by a short episode of mixing with a MLD reaching a depth of 1500 m in early March 2011 (Fig. 4B). Thus, it is worth noting that an episode of intense event of bottom-reaching convection occurred about one month before the CASCADE cruise in March 2011. The period of the cruise was characterized by a secondary mixing episode during the first days (2-5 March 2011), yielding an homogeneous layer of 1500 m depth, and subsequently a long-lasting restratification associated with the reappearance of AW and LIW in the upper 800 m of the water column.

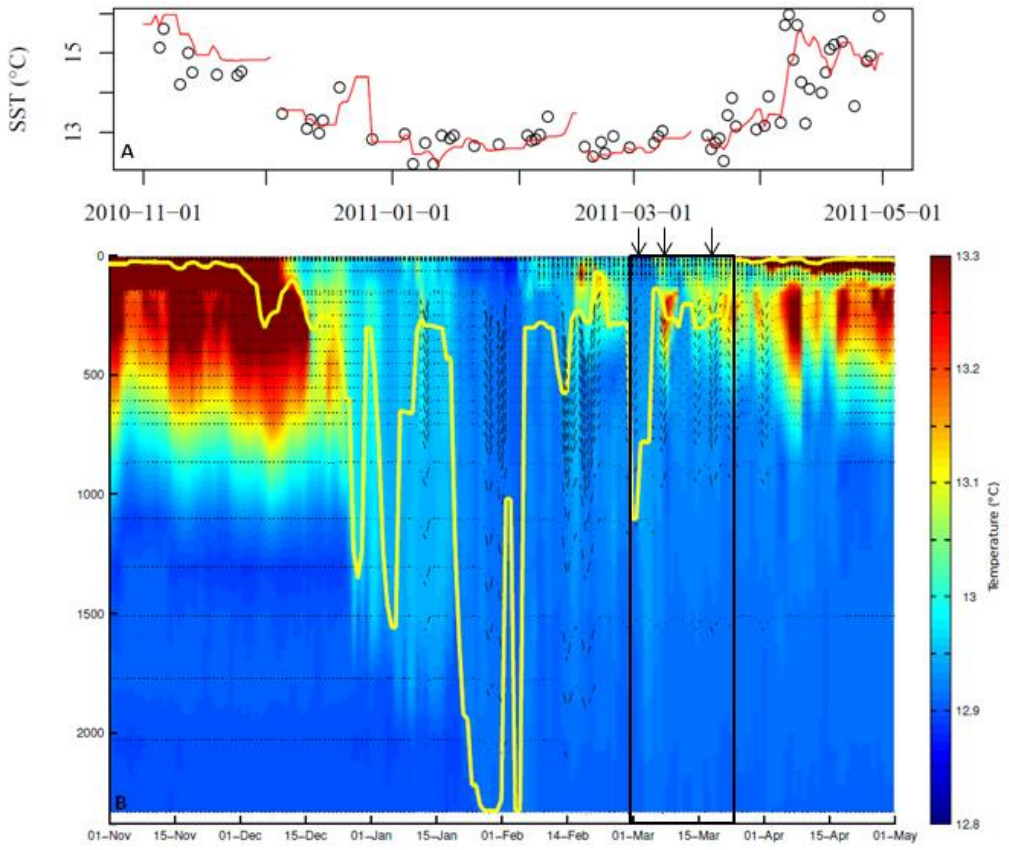

Fig. 4. Time series (A) of the SST extracted at 45°N 5°E from remote sensing data (MODIS satellite), and of (B) the potential temperature at the LION mooring line from November 02, 2010 to April 30, 2011. In (A) points are the SST meaning on 1 day, and the red line represents the 8-days running mean. In (B) the yellow line corresponds to the mixed layer depth. The black square is the CASCADE cruise period and the arrows correspond to the three sampling of station SC2400.

3.2 Biogeochemistry

	CONVg	STABg	R-STABg
NO_3+NO_2	800 ± 10	631 ± 207	694
PO_4	35.7 ± 0.8	24.9 ± 10	23.2
$Si(OH)_4$	697 ± 10	418 ± 113	520
Si:P	19.6 ± 0.2	16.8 ±5.7	22.4
N:P	22.5 ±0.3	25.4 ±5.2	30.1
Si:N	0.87 ± 0.00	0.66 ± 0.01	0.75
CHL	15.2 ± 2.5	56.7 ± 18	76.1
PHAEO	6.12± 1.2	9.03 ± 6.2	4.57
CHL:PHAEO	2.45± 0.6	6.28 ± 81	16.7
PP	319± 43	989 ± 365	1217

Table 1. Integrated (0-100m) quantities of NO_3+NO_2, PO_4 and $Si(OH)_4$ in mmol.m^{-2}, their molar ratios (noted Si for $Si(OH)_4$, N for NO_3+NO_2+NH_4 and P for PO_4, dimensionless), CHL and PHAEO in mg.m^{-2} and PP (Primary Production) in mgC.m^{-2}.d^{-1} for the 3 hydrological regimes, CONVg, STABg, R-STABg (refer to section 3.1).

During the convective event (CONVg), nutrients were homogenous between 0 and 1500 m and very close to the concentrations of the deep layer usually observed (8.94 ± 0.25 µM, 0.40 ± 0.02 µM, 7.74 ± 0.24 µM for NO_3+NO_2, PO_4 and $Si(OH)_4$ respectively; Fig. 5). Concentrations were slightly higher between 1500 and 2500 m than in the overlying homogenous layer. The stoichiometry was very similar in these two layers with a Si:N:P ratio around 20:22:1 over the entire water column.

Profiles after the stabilization of the water column (STABg; Fig. 5) exhibited a classical pattern with low concentrations in the surface layer of NO_3+NO_2 (4.19 ± 1.46 µM), PO_4 (0.13 ± 0.05 µM) and $Si(OH)_4$ (2.86 ± 0.56 µM), and high concentrations in the deeper layers for all these nutrients. Between 500 and 2500 m, nutrient concentrations were the same during the STABg period than during the convection event (CONVg). The stoichiometry remained unchanged between 500 and 2500 m, but the water column stabilization modified the surface stoichiometry to a Si:N:P ratio of 21:35:1.

Seven days after the sampling of the stabilized water column (R-STABg), nutrient concentrations were still very low at the surface. In water masses deeper than 350 m, NO_3+NO_2 were 0.30 µM higher and PO_4 concentrations decreased 0.04 µM compared to CONVg and STABg. This strongly affected the deep stoichiometry by an increase of the Si:N:P ratio from 20:22:1 to 21:25:1.

When only the first 100m are considered (Table 1), the same changes are found than on the vertical profils: NO_3+NO_2, PO_4 and $Si(OH)_4$ decreased ~1.3-1.6 fold from CONVg to STABg. The dissolved inorganic matter (DIM) budget of NO_3 + NO_2 and $Si(OH)_4$, and the molar ratio, slightly increased from STABg (17:25:1) to R-STABg (22:30:1).

3.3 Chlorophyll biomass and phytoplankton activity

In this study, CHL concentrations were used as a proxy of phytoplankton biomass. In the convective cell (CONVg), CHL concentrations were low and homogenous from the surface to 1000 m deep (~0.17 ± 0.04 µg.L^{-1}) and non-detectible at deeper levels (Fig. 5F). The stabilized water column (STABg) was characterized by a 90% increase of CHL concentrations in the 0-100 m layer, while it remained non-detectible below. CHL concentrations decreased in the surface layer at R-STABg compared to STABg (from 1.95 ± 0.31µg.L^{-1} at STABg to 1.20 µg.L^{-1} at R-STABg). However, CHL concentrations were detectable down to 500 m at R-STABg, but not detectable in STABg below 100m. Then integrated values of CHL were 1.3 times higher at R-STABg than at STABg (Table 1).

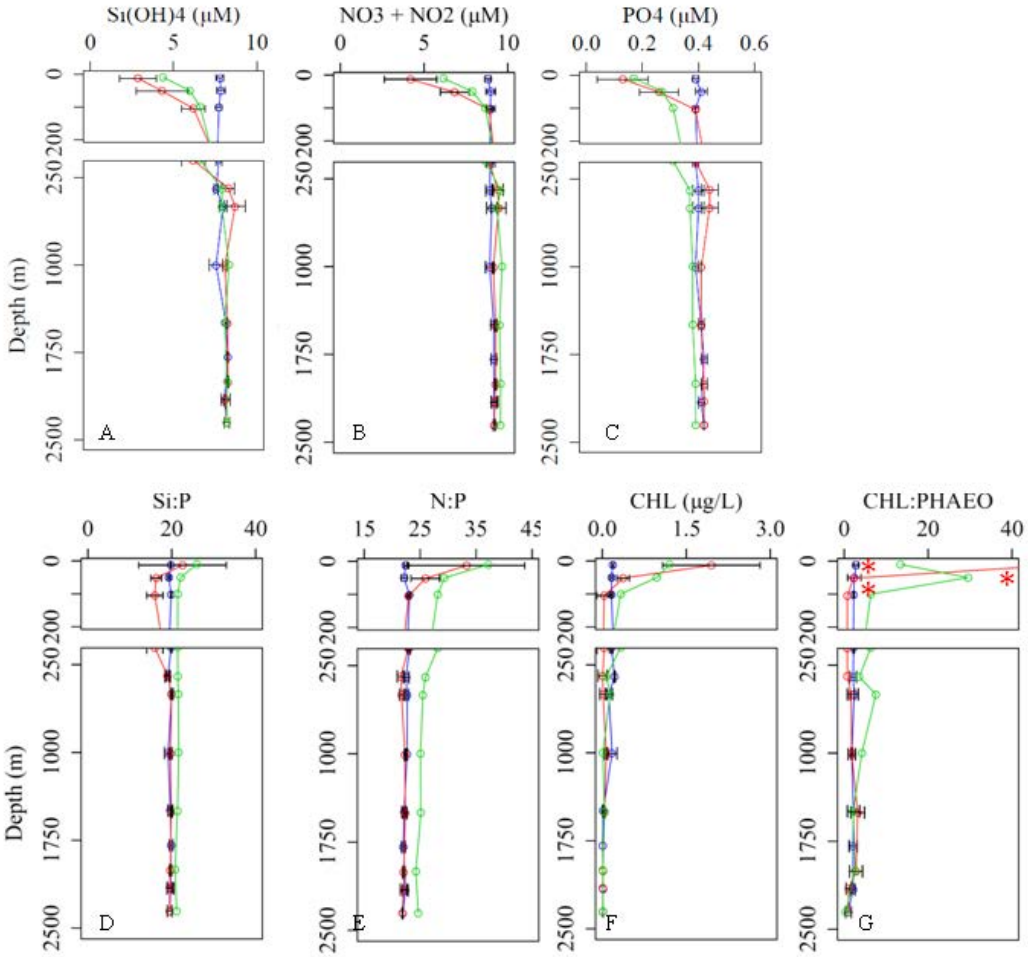

Fig. 5. Profiles of (A) silicate, (B) nitrate + nitrite, (C) phosphate, (D) silicate to phosphate ratio (noted Si:P), (E) total nitrogen to phosphate ratio (noted N:P), (F) chlorophyll a and (G) chlorophyll to phaeopigment ratio at CONVg (blue line), STABg (red line) and R-STABg (green line) (refer to section 3.1). The solid lines are the parameters at SC2400 (see Fig. 1) and the error bars are the standard deviation of the parameter for each group. In (G) the first three points of STABg (marked *) do not have error bars because of the concentration of phaeopigment under the limit of detection.

The ratio of CHL:PHAEO can be used as an indicator of the phytoplankton physiology (Barlow et al., 1993; Cuny et al., 2002), with senescent population being characterized by a ratio <1. It has been underlined that phaeopigments concentrations can be overestimated by the fluorometric method, thus underestimating the CHL:PHAEO ratio. Here we used an elevated CHL:PHAEO ratio of more than 1 to encompass this limitation. During our study, ratios were generally >1 (Fig. 5G), even in the convective cell (CONVg) which was deeper than the euphotic layer (ratio of ~2.5 from 0 to 2000m). Ratios increased with the stratification and were maximal at the surface for STABg conditions. This trend was also observed for the integrated ratio of CHL:PHAEO (x2.5 at STABg, x7 at R-STABg; Table 1).

Primary production followed CHL and CHL:PHAEO ratio patterns in the surface layer (Table 1) with a 3 to 4 fold increase at STABg and R-STABg respectively, with regard to CONVg.

3.4 Remote sensing

The dynamic of the chlorophyll bloom in relation to the convection process was monitored by remote sensing (Fig. 6). An upper threshold of 0.12 $mg.m^{-3}$ of the surface CHL was taken to determine the convection area during winter 2010-2011. Likewise, a bottom threshold of 1 $mg.m^{-3}$ for the surface CHL was used to compute the bloom area. From January to early March 2011, convection was the single process observed in the Gulf of Lion. Its area extended from 42.5°N / 6.5°E to the north of Majorca (~41°N / 3°E). From early March to mid-March 2011, the convection region diminished and phytoplankton biomass developed at the southern edge of the convective cell (41°N / 4°-7°N). Bloom intensified and progressively moved toward the center of the convection region while the vertical mixing decreased (19 March2011). In April 2011, when the convection process stopped and the water column stratified, the bloom covered the entire convection area.

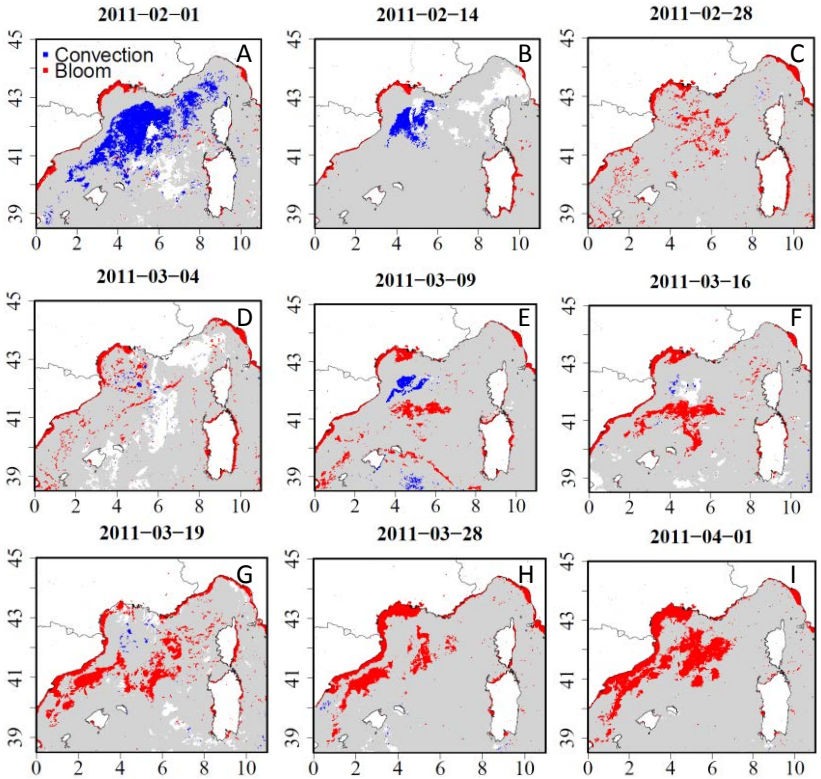

Fig. 6. MODIS-aqua satellite data of the convection area (blue; CHL < 0.12 $mg.m^{-3}$) and the phytoplankton bloom area (red; CHL > 1 $mg.m^{-3}$). Satellite data are averaged on 8 days at different time (A to I) during winter 2010-2011. Grey zone indicated satellite data available, while non-available data are in white because of the cloud cover.

4.1 Discussion

4.1 Importance of the convection episode of March 2011

The late convection event sampled during the cruise corresponded to 5% of the previous convection area of winter 2010-2011. While the bottom reaching convection episode of February 2011 covered an area of ~17000 km² during about 20 days, the convective cell in March 2011 reached a depth of 1500 m, extended an additional ~1000 km² during 8 days (Figs. 4 and 6). The convection episode of March 2011 was then a small episode more confined in space, shallower and shorter than the previous convective mixings of winter 2010-2011.

Winter 2010-2011 was less intense compared to other winters (2008-2009, 2009-2010, 2011-2012) in terms of mean surface net heat flux, and mean surface buoyancy losses (Houpert, 2013). Winters 2009, 2010 and 2012 were three of the nine coldest winters of the 1980-2012 period, while winter 2011 was the 22nd coldest winter.

4.2 Open-ocean convection impact on nutrient budget

In the Mediterranean Sea, few quantitative studies have dealt with the DIM replenishment by the convection process (Yılmaz and Tugrul, 1998; Gacic et al., 2002; Santinelli et al., 2012). To our knowledge, none of them concern the NWM, an area characterized by a recurrent and intense spring bloom (D'Ortenzio and Ribera d'Alcala, 2009). In our study, nitrate and phosphate surface concentrations (8.9 and 0.4 µM respectively) resulting from the small convection episode of March 2011 in the NWM were higher than the input related to convection events in the eastern basin. In the Adriatic Sea in January 2008, Santinelli et al. (2012) measured a nitrate and phosphate input of >3 and >0.1 µM respectively, while Gacic et al. (2002) observed a nitrate concentration of 4 µM introduced by the convection event of March 1998. Likewise in the Rhodes region, Yilmaz and Tugrul (1998) determined that the convection episodes of March 1992 and February 1993, introduced 3.8-4.7 µM of nitrate and 0.14-0.16 µM phosphate. We determined that similar silicate concentrations (7.7 µM) were introduced by convection episode in the NWM and in the eastern basin, with 7.3 to 7.8 µM observed during a convection event in the Rhodes region (Yılmaz and Tugrul, 1998). Such occurrence could be explained by the biogeochemical West-East Mediterranean gradient, which is positive for nitrate and phosphate concentrations in the deep layer, but weak and negative for silicate (Pujo-Pay et al., 2011). Thus, for a same order of magnitude, the convection process upwelled similar silicate quantity, but higher nitrate and phosphate concentrations in the western than in the eastern basin.

Table 2. Compilation of nutrient budget introduced into the surface layer of the NWM by different physical processes.

Nutrient input processes	Date	$Si(OH)_4$ mol	$NO_3 + NO_2$ mol	PO_4 mol	References
Annual fluxes from the Eastern basin	1945-1993	-	$142\ 10^9$	$4.4\ 10^9$	Krom et al., 2004
Annual Rhône river discharge	June 94-may 95	$1.4\ 10^9$	$1.5\text{-}1.6\ 10^9$	$2.8\text{-}3.1\ 10^7$	Moutin et al., 1998
Annual riverine discharge	1989-1993	$3.4\ 10^9$	$5.7\ 10^9$	$2.5\ 10^8$	Ludwig et al., 2009
Annual riverine discharge	1994-1998	$3.8\ 10^9$	$5.9\ 10^9$	$1.8\ 10^8$	Ludwig et al., 2009
Annual Saharan rains input	1999	-	-	$3.0\text{-}4.0\ 10^9$	Ridame and Guieu, 2002
Annual Atlantic influx	2008	-	$9.1\ 10^8$	$9.8\ 10^8$	Ramirez-Romero et al., 2014
Deep open-ocean convection	February 2011	$*1.2 \pm 0.02\ 10^{10}$	$*1.4 \pm 0.02\ 10^{10}$	$*6.1 \pm 0.1\ 10^8$	This study
Intermediate open ocean convection	March 2011	$7.0 \pm 0.1\ 10^8$	$8.0 \pm 0.1\ 10^8$	$0.36 \pm 0.01\ 10^8$	This study

* indicates values obtain by an assumption made in this study (refer to section 4.2).

Considering the DIM concentrations in the euphotic layer of the convective cell (Table 1), and the 1000 km² of convective area in March 2011, this single small convection event brought to the surface $8.0 \pm 0.1\ 10^8$ mol of NO_3+NO_2, $0.36 \pm 0.01\ 10^8$ mol of PO_4 and $7.0 \pm 0.1\ 10^8$ mol of $Si(OH)_4$ (Table 2). As several convection events occurred during winter 2011 (Fig. 4), the total nutrient input during an entire winter was obviously much larger. The nutricline is generally located in the first 200 m (Conan et al., 1999; Diaz et al., 2000), and nutrient concentrations are relatively homogeneous below 500 m in the NWM (Pujo-Pay et al., 2011). Thus, any vertical mixing below this depth will introduce similar nutrient concentrations into the euphotic layer. So the deep convection event of February 2011 (Fig. 2B) may contribute to the same nutrient concentration input than the convection event of March (Table1). Taking into account the 17000 km² of the convection area in February 2011, this led to a higher DIM budget of $1.3 \pm 0.02\ 10^{10}$ mol of NO_3+NO_2, $6.1 \pm 0.1\ 10^8$ mol of PO_4 and $1.2 \pm 0.02\ 10^{10}$ mol of $Si(OH)_4$ (Table 2). These estimations for a single convection episode are much more important than the annual nutrient discharge of all the Gulf of Lion rivers. Thus, if we make a generalization, the first convection episode of winter (February 2011 in this study) introduces a large amount of nutrient in a depleted surface layer. The stabilization of the water column (Fig. 4) allows the development of primary producers (Fig. 6) which by deduction consumed a part of these nutrients recently introduced. The last convection event of winter (March 2011 in this study) is the process which determines the nutrient quantity available for the ensuing spring

bloom. Further investigations covering an entire winter are necessary to confirm our hypothesis and to calculate the total DIM budget introduced by the global convection process in the NWM. Finally, our results suggest that such events could be considered as one of the major processes for nutrient input at the NWM basin scale (Table2), comparing to annual river discharges (Moutin et al., 1998; Ludwig et al., 2009), annual Saharan rains (Ridame and Guieu, 2002), eastern basin fluxes per year (Krom et al., 2004), and also annual Atlantic influx (Ramírez-Romero et al., 2014) whose nutrient supply firstly enrich the Algerian basin because of the general Mediterranean circulation (Millot, 1999; Millot and Taupier-Letage, 2005).

4.3 Open-ocean convection impact on nutrient elemental stoichiometry

We saw previously that the nutrient replenishment was mainly determined by the convection area extension rather than the depth reached by the convective mixing. However, the observation of higher surface Si:N and Si:P in the convective conditions compared to the stratified conditions (0.9 vs 0.7 for Si:N and 20 vs 17 for Si:P) suggested that the MLD deeply influenced the nutrient stoichiometry. Our results imply that the depth reached by winter convections controlled the ensuing spring bloom, not only in terms of phytoplankton biomass because nutrients are introduced in the surface layer, but also in terms of phytoplankton diversity because of the resulting stoichiometry of the mineral compartment. Because of anthropogenic pressure, an increase of phosphate and nitrate concentrations in the coastal margin of the western basin is currently observed, which causes a decrease of the Si:N and Si:P ratios (Ludwig et al., 2009; Mermex Group, 2011). Many authors suggested that such a trend could shift the phytoplankton population from diatom- dominated assemblages to non-siliceous species (flagellates and dinoflagellates) (Officer and Ryther, 1980; Jickells, 1998; Moncheva et al., 2001; Béthoux et al., 2002b; Yunev et al., 2007; Jiang et al., 2014). In the Black Sea, a decrease in the Si:N ratio by a factor of 15 led to a shift in phytoplankton populations from diatoms to coccolithophorids and flagellates that likely impacted the food web structure (Humborg, 1997). Thus, the NWM open-ocean convection could be a process that would delay or limit this Si:N and Si:P decrease and its consequences by introducing more silicate compared to nitrate and phosphate in the western basin.

Nutrient stoichiometry variations were observed over the entire water column after the stratification. This could be inferred from a microbial activity, autotrophs and also heterotrophs. The N:P nutrient ratio was 22:1 over the entire water column during the convection event (Table 1). With the stratification, the surface N:P ratio increased to 25:1, and then to 30:1 seven days later (Table 1), concomitantly to a chlorophyll development (Fig. 5). This increase was then a

consequence of autotroph consumptions confirming the 'known' phosphate depletion in the Mediterranean Sea (Béthoux and Copin-Montégut, 1988; Thingstad et al., 1998; Mermex Group, 2011; Pujo-Pay et al., 2011). Twelve days after the convection episode, the higher N:P ratio observed all over the water column resulted from a nitrate increase and a phosphate depletion (Fig. 5B and D). Mineralization processes may have led to this nitrate regeneration while phosphate would be consumed by heterotrophs to metabolize the fresh organic matter exported during the convective vertical mixing (Kirchman, 1994). In the eastern basin, Santinelli et al. (2010) inferred an increase of oxygen consumption rate in the deep waters after the sinking of dense waters rich in semi-labile dissolved organic matter to mineralization processes. This biological process may potentially be a mechanism at the origin of the Mediterranean phosphate depletion, but further investigations are necessary to confirm this hypothesis.

4.4 Open-ocean convection impact on phytoplankton and carbon budget

In March 2011, the water column was marked by successive periods of mixing and stratification, modifying the phytoplankton distribution through the water column and their biomass. The convective mixing of early March 2011 diluted a healthy phytoplankton community (CHL:PHAEO = 2) to 1000 m, far below the euphotic layer (Fig. 5). Phytoplankton biomass increased 2 days later with the water column stratification (Fig. 5F and Table 1), but the destabilization of the surface layer before the third sampling resulted in an export of this community to 350 m (Fig. 5). This process led to a redistribution of the phytoplankton biomass into a thicker layer, resulting in an increase of chlorophyll a (CHL) and phytoplankton production (PP) integrated over the first 100 m of the water column (Table 1). Thus, the successive vertical mixings stimulated the phytoplankton development and activity by many DIM inputs.

Assuming that all of the nutrients present in the euphotic zone at the end of the convective period (Table 1) will be used by primary producers during the spring bloom, and without taking into account the possible mineralization in the euphotic layer, the potential new primary production ranges from 46 to 63 $gC.m^{-2}.y^{-1}$ according to the classical C:Si:N:P Redfield ratio (1963). The use of this ratio has been questionable for a long time (Anderson et al., 2005; Sterner et al., 2008). But since it represents an average for a diverse oceanic phytoplankton assemblage (Arrigo, 2005), its use is still valid in biogeochemistry, and it has been justified at large scale in the Mediterranean Sea (Pujo-Pay et al., 2011). New primary production rates had been estimated to be 45 $gC.m^{-2}.y^{-1}$ in the open margin of the Gulf of Lion (Tusseau-Vuillemin

et al., 1998). The influence of the river discharges on primary production may be more limited to the coastal zone, whereas the open sea new primary production could be entirely supported by the nutrients introduced by the convective mixing.

Our study, coupled with satellite data analysis, shows that different processes in relation to the convection process act together to produce the recurrent and intense spring bloom of the NWM (D'Ortenzio and Ribera d'Alcala, 2009). With the cessation of the convection process, the first origin of the bloom is the advection of the surrounding waters (AW and LIW). These water masses have not been influenced by the vertical mixing, so they act as an inoculum via their own biological properties, i.e. winter phytoplankton populations, bacteria and grazers. By remote sensing observations, the extension of the convection area in February 2011 appeared to be limited to the south by the Balearic front (Fig. 6A). With the shrinking of the convection area, the bloom began to develop on the south edge of the convection area (Fig. 6E) in waters still marked by the SST signature of the convection process (SST<12.9°C; Fig. 2A), while the center of the studying region still mixed.

Secondly, an autochthonous development may be favored through the nutrient replenishment by the convection process, associated with the seasonal increase of light and temperature. The input of nutrients may also control the spatial distribution of the bloom (Fig. 2A). An elevated surface CHL:PHAEO ratio in stratified conditions during the sampling period (Fig. 5G and Table 1) confirmed the development of fresh phytoplankton cells. The satellite data showed the propagation of the bloom from the Balearic front to the center of the convection area in early April. A spatial relation between the DIM input by the convection process and the spring bloom does exist (Lévy et al., 1999; D'Ortenzio and Ribera d'Alcala, 2009). Recently, Lavigne et al. (2013) explored the role of MLD variations in shaping the phytoplankton phenology in the Mediterranean Sea. They also concluded that the intense spring bloom was triggered about one month after the deepening of the MLD, when both the light and nutrients were no longer limiting.

The third origin of the bloom may be a physical-biological coupling process depending on the geometry of the convection cell when vertical mixing stopped. This refers to the 'Phyto-Convection theory' first proposed by Backhaus et al. (Backhaus et al., 1999; Wehde et al., 2001; Backhaus et al., 2003) and detailed as ''dilution–recoupling hypothesis" by Behrenfeld (2010). This theory focuses on the balance between phytoplankton growth and grazing, and the seasonally varying physical processes influencing this balance (open ocean convection here). Phytoplankton cells are diluted by the convective cells over the water column, as during the sampled convection event (Fig. 5F). However, the upward motion in the convective mixed layer

(CML) allows the phytoplankton cells to be regularly transported into the euphotic zone, before being exported again to the deep layer. This process (~100 days from the preconditioning phase to the stratification onset according to the model) (Backhaus et al., 1999) could be sufficient to maintain the viability of some cells. The entire CML is then considered as a productive region ("virtual euphotic layer"), and consists of a large winter phytoplankton stock. At the end of the convective period, the CML geometry changes, inducing a gradual rise of the MLD. The winter cells stock diluted in a deep water column is physically concentrated into the euphotic layer. Our measurements of photosynthetic parameters are in agreement with this hypothesis. The homogeneous P^b_m of 3 mgC.mgCHL^{-1}.h^{-2} from 10 to 100 m during the convection process confirmed that phytoplankton cells were still alive and active even below the euphotic depth of 70 m. In addition, the high Ek of 67 W.m^{-2} measured at 100 m in the convective cell is consistent with an adaptation of phytoplankton to low irradiance. Furthermore, phytoplankton development began in waters still marked by the SST signature of the convection process (SST<12.9°C; Fig. 2A) as said above. This involves that phytoplankton responded to convection relaxation, and not to the seasonal warming induced stratification.

Finally, the contribution of these processes to the spring bloom depends on the length of time and the area of the convection process. An extended convection episode in time and space should favor the autochtonous bloom (mostly diatoms) by several nutrient input, while the succession of short convection events should maintain phytoplankton cells alive in the CML (phyto-convection hypothesis). Years with atmospheric conditions not suitable to trigger the convection process should be characterized by a weak spring bloom originated mostly from the advected waters, and so be less favorable to diatoms because of the Si:N:P ratio decrease currently observed in the Mediterranean Sea (Mermex Group, 2011).

Acknowledgments

We are grateful to the crew and officials of R/V *L'Atalante* and to all the scientific and technical staff involved in the CASCADE cruise for their support during sea operations. This work was funded by the HERMIONE Project (N° 226354) under the European Commission's Seventh Framework Program and the French Program MERMEX under the MISTRALS framework.

References

Aminot, A., Kérouel, R., 2007. Dosage automatique des nutriments dans les eaux marines : méthodes en flux continu, Ifremer ed. Ifremer, Méthodes d'analyse en milieu marin, 188p.

Anderson, Thomas R., Hessen, Dag O., Elser, James J., and Urabe, J., 2005. Metabolic Stoichiometry and the Fate of Excess Carbon and Nutrients in Consumers. Am. Nat. 165, 1-15.

Arrigo, K. R., 2005. Marine microorganisms and global nutrient cycles. Nature. 437, 349-355.

Backhaus, J.O., Wehde, H., Hegseth, E.N., Kämpf, J., 1999. 'Phyto-convection': the role of oceanic convection in primary production. Mar. Ecol-Prog. Ser. 189, 77-92.

Banse, K., 1994. Uptake of inorganic carbon and nitrate by marine plankton and the Redfield Ratio. Global Biogeochem. Cycles. 8, 81-84.

Barlow, R.G., Mantoura, R.F.C., Gough, M.A., Fileman, T.W., 1993. Phaeopigment distribution during the 1990 spring bloom in the northeastern Atlantic. Deep Sea Res. Part I. 40, 2229-2242.

Béthoux, J.-P., Copin-Montégut, G., 1988. Phosphorus and nitrogen in the Mediterranean Sea: specificities and forecastings. Oceanol. Acta, 9, 75-78.

Béthoux, J.-P., Gentili, B., Tailliez, D., 1998. Warming and freshwater budget change in the Mediterranean since the 1940s, their possible relation to the greenhouse effect. Geophys. Res. Lett. 25, 1023-1026.

Béthoux, J.-P., Durieu de Madron, X., Nyffeler, F., Tailliez, D., 2002a. Deep water in the western Mediterranean: peculiar 1999 and 2000 characteristics, shelf formation hypothesis variability since 1970 and geochemical inferences. J. Marine Syst. 33–34, 117-131.

Béthoux, J.-P., Morin, P., Ruiz-Pino, D.P., 2002b. Temporal trends in nutrient ratios: chemical evidence of Mediterranean ecosystem changes driven by human activity. Deep Sea Res. Part II. 49, 2007-2016.

Behrenfeld, M.J., 2010. Abandoning Sverdrup's Critical Depth Hypothesis on phytoplankton blooms. Ecology. 91(4): 977–989.

Bosc, E., Bricaud, A., Antoine, D., 2004. Seasonal and interannual variability in algal biomass and primary production in the Mediterranean Sea, as derived from 4 years of SeaWiFS observations. Global Biogeochem. Cycles. 18, GB1005.

Boutrif, M., 2011. Dégradation de la matière organique dissoute de haut poids moléculaire par les communautés procaryotiques des zones méso- et bathypélagiques. University of Aix-Marseille.

Conan, P., Turley, C., Stutt, E., Pujo-Pay, M., Wambeke, F.V., 1999. Relationship between phytoplankton efficiency and the proportion of bacterial production to primary production in the Mediterranean Sea. Aquat. Microb. Ecol. 17, 131-144.

D'Ortenzio, F., Ribera d'Alcala, M., 2009. On the trophic regimes of the Mediterranean Sea: a satellite analysis. Biogeoscience. 6, 139-148.

Diaz, F., Raimbault, P., Conan, P., 2000. Small-scale study of primary productivity during spring in a Mediterranean coastal area (Gulf of Lions). Cont. Shelf Res. 20, 975-996.

Durrieu de Madron X., Houpert, L., Puig, P., Sanchez-Vidal, A., Testor, P., Bosse, A., Estournel, C., Somot, S., Bourrin, F., Bouin, M.N., Beauverger, M., Beguery, L., Calafat, A., Canals, M., Coppola, L., Dausse, D., D'Ortenzio, F., Font, J., Heussner, S., Kunesch, S., Lefevre, D., Le Goff, H., Martín, J., Mortier, L., Palanques, A., Raimbault, P., 2013. Interaction of dense shelf water cascading and open-sea convection in the northwestern Mediterranean during winter 2012. Geophys. Res. Lett. 40, 1379-1385.

Fitzwater, S.E., Knauer, G.A., Martin, J.H., 1982. Metal contamination and its effect on primary production measurements. Limnol. Oceanogr. 27, 544-551.

Gacic, M., Civitarese, G., Miserocchi, S., Cardin, V., Crise, A., Mauri, E., 2002. The open-ocean convection in the Southern Adriatic: a controlling mechanism of the spring phytoplankton bloom. Cont. Shelf Res. 22, 1897-1908.

Gogou, A., Sanchez-Vidal, A., Durrieu de Madron, X., Stavrakakis, S., Calafat, A.M., Stabholz, M., Psarra, S., Canals, M., Heussner, S., Stavrakaki, I., Papathanassiou, E., 2014. Carbon flux to the deep in three open sites of the Southern European Seas (SES). J. Mar. Syst. 129, 224-233.

Hogg, N.G., 1973. The preconditioning phase of MEDOC 1969-II. Topographic effects. Deep Sea Res. 20, 449-459.

Holmes, R.M., Aminot, A., Kérouel, R., Hooker, B.A., Peterson, B.J., 1999: A simple and precise method for measuring ammonium in marine and freshwater ecosystems. Can. J. Fish. Aquat.Sci. 56, 1801-1808.

Houpert, L., 2013. Contribution to the Study of Transfer Processes from the Surface to the Deep Ocean in the Mediterranean Sea using in-situ Measurements. Université de Perpignan via Domitia.

Humborg, C.V., 1997. Effect of Danube River dam on Black Sea biogeochemistry and ecosystem structure. Nat. 386, 385.

Jacq, V., Albert, P., Delome, R., 2005. Le mistral -Quelques aspects des connaissances actuelles. La Météorologie. 50, 30-38.

Jassby, R.M., Platt, T., 1976. Mathematical formulation of the relationship between photosynthesis and light for phytoplankton. Limnol. Oceanogr. 21, 540-547.

Jiang, Z., Liu, J., Chen, J., Chen, Q., Yan, X., Xuan, J., and Zeng, J., 2014. Responses of summer phytoplankton community to drastic environmental changes in the Changjiang (Yangtze River) estuary during the past 50 years. Water Res. 54, 1-11.

Jickells, T. D., 1998. Nutrient Biogeochemistry of the Coastal Zone. Science. 281, 217-222.

Kirchman, D.L., 1994. The uptake of inorganic nutrients by heterotrophic bacteria. Microb. Ecol. 28, 255-271.

Krom, M.D., Herut, B., Mantoura, R.F.C., 2004. Nutrient budget for the Eastern Mediterranean: implications for phosphorus limitation. Limnol. Oceanogr. 49, 1582-1592.

L'Hévéder, B., Li, L., Sevault, F., Somot, S., 2013. Interannual variability of deep convection in the Northwestern Mediterranean simulated with a coupled AORCM. Clim. Dyn. 41, 937-960.

Lavigne, H., D'Ortenzio, F., Migon, C., Claustre, H., Testor, P., d'Alcalà, M.R., Lavezza, R., Houpert, L., Prieur, L., 2013. Enhancing the comprehension of mixed layer depth control on the Mediterranean phytoplankton phenology. J. Geophys. Res. Oceans. 118, 3416-3430.

Leaman, K.D., Schott, F.A., 1991. Hydrographic Structure of the Convection Regime in the Gulf of Lions: Winter 1987. J. Phys. Oceanogr. 21, 575-598.

Lévy, M., Mémery, L., Madec, G., 1999 The onset of the Spring Bloom in the MEDOC area: mesoscale spatial variability. Deep Sea Res. Part I. 46, 1137-1160.

Lévy, M., Mémery, L., Madec, G., 2000. Combined effects of mesoscale processes and atmospheric high-frequency variability on the spring bloom in the MEDOC area. Deep Sea Res. Part I. 47, 27-53.

Ludwig, W., Dumont, E., Meybeck, M., Heussner, S., 2009. River discharges of water and nutrients to the Mediterranean and Black Sea: Major drivers for ecosystem changes during past and future decades? Prog. Oceanogr. 80, 199-217.

Madec, G., Delecluse, P., Crépon, M., Lott, F., 1996. Large-scale preconditioning of deep-water formation in the northwestern Mediterranean Sea. J. Phys. Oceanogr. 26, 1393-1408.

Marshall, J., Schott, F., 1999. Open-ocean convection: Observations, theory, and models. Rev. Geophys. 37, 1-64.

Martin, J., Durrieu de Madron, X., Puig, P., Bourrin, F., Palanques, A., Houpert, L., Higueras, M., Sanchez-Vidal, A., Calafat, A.M., Canals, M., Heussner, S., 2012. Sediment transport along the Cap de Creus Canyon flank during a mild, wet winter. Biogeoscience. 9, 18211-12252.

Marty, J.C., Chiavérini, J., 2010. Hydrological changes in the Ligurian Sea (NW Mediterranean, DYFAMED site) during 1995-2007 and biogeochemical consequences. Biogeoscience. 7, 1377-1406.

Medoc Group, 1970. Observation of formation of deep water in the mediterranean sea, 1969; Nat. 227, 1937-1040.

Mermex Group, 2011. Marine ecosystems' responses to climatic and anthropogenic forcings in the Mediterranean. Prog. Oceanogr. 91, 97-166.

Mertens, C., Schott, F., 1998. Interannual variability of deep-water formation in the Northwestern Mediterranean. J. Phys. Oceanogr. 28, 1410-1424.

Millot, C., 1999. Circulation in the Western Mediterranean Sea. J. Mar. Syst. 20, 423-442.

Millot, C., Taupier-Letage, I., 2005. Circulation in the Mediterranean Sea, in: Saliot, A. (Eds.), The Mediterranean Sea. Springer Berlin Heidelberg, pp. 29-66.

Moncheva, S., Gotsis-Skretas, O., Pagou, K., and Krastev, A., 2001. Phytoplankton Blooms in Black Sea and Mediterranean Coastal Ecosystems Subjected to Anthropogenic Eutrophication: Similarities and Differences. Estuar. Coast. Shelf. S. 53, 281-295.

Morel, A., André, J.-M., 1991. Pigment distribution and primary production in the western Mediterranean as derived and modeled from coastal zone scanner observations. J. Geophys. Res. 96, 12685-12698.

Moutin, T., Raimbault, P., Golterman, H.L., Coste, B., 1998. The input of nutrients by the Rhône river into the Mediterranean Sea: recent observations and comparison with earlier data. Hydrobiologia. 373-374, 237-246.

Officer, C. B., and Ryther, J. H., 1980. The possible importance of silicon in marine eutrophication. Mar. Ecol.-Prog. Ser. 3, 83-91.

Pujo-Pay, M., Conan, P., Oriol, L., Cornet-Barthaux, V., Falco, C., Ghiglione, J.-F., Goyet, C., Moutin, T., Prieur, L., 2011. Integrated survey of elemental stoichiometry (C, N, P) from the western to eastern Mediterranean Sea. Biogeoscience. 8, 883–899.

Pusceddu, A., Mea, M., Gambi, C., Bianchelli, S., Canals, M., Sanchez-Vidal, A., Calafat, A., Heussner, S., Durrieu De Madron, X., Avril, J., Thomsen, L., Garcìa, R., Danovaro, R., 2010. Ecosystem effects of dense water formation on deep Mediterranean Sea ecosystems: an overview. Adv. Oceanogr. Limnol. 1, 67-83.

Ramírez-Romero, E., Macías, D., García, C. M., and Bruno, M., 2014. Biogeochemical patterns in the Atlantic Inflow through the Strait of Gibraltar. Deep Sea Res. Part I. 85, 88-100.

Redfield, A.C., Ketchum, B.H., Richards, F.A., 1963. The influence of organisms on the composition of sea water, in: Hill, M. N. (Eds.), The sea. Wiley Interscience, Hoboken, N. J., pp 26-77.

Ridame, C., Guieu, C., 2002. Saharan input of phosphate to the oligotrophic water of the ope ocean western Mediterranean Sea. Limnol. Oceanogr. 47, 856-869.

Robinson, A.R., Leslie, W.G., Theocharis, A., Lascaratos, A., 2001. Mediterranean Sea Circulation, Ocean Currents. 376, 1-19.

Santinelli, C., Nannicini, L., Seritti, A., 2010. DOC dynamics in the meso and bathypelagic layers of the Mediterranean Sea. Deep Sea Res. Part II. 57, 1446-1459.

Santinelli, C., Ibello, V., Lavezza, R., Civitarese, G., Seritti, A., 2012. New insights into C, N and P stoichiometry in the Mediterranean Sea: The Adriatic Sea case. Cont. Shelf Res. 44, 83-93.

Stabholz, M., Durrieu de Madron, X., Canals, M., Khripounoff, A., Taupier-Letage, I., Testor, P., Heussner, S., Kerhervé, P., Delsaut, N., Houpert, L., Lastras, G., Dennielou, B., 2013. Impact of open-ocean convection on particle fluxes and sediment dynamics in the deep margin of the Gulf of Lions. Biogeoscience. 10, 1097-1116.

Steemann-Nielson, E., 1951. Measurement of the production of organic matter in the sea by means of carbon-14. Nat. 167, 684-685.

Sterner, R. W., Anderson, T., Elser, J. J., Hessen, D. O., Hood, J. M., McCauley, E., and Urabe, J., 2008. Scale-dependent carbon : nitrogen : phosphorous seston stoichiometry in marine and freshwaters. Limnol. Oceanogr. 53, 1169-1180.

Strickland, J.D.H., Parsons, T.R., 1997: A Practical Hanbook of Seawater Analysis. Bulletin of the Fisheries Research Board of Canada, Bulletin 167.

Testor, P., Gascard, J.C., 2006. Post-convection spreading phase in the Northwestern Mediterranean Sea. Deep Sea Res. Part I. 53, 869-893.

Thetis Group, 1994. Open-ocean deep convection explored in the Mediterranean. Eos Transactions. 75 (19), 217-224.

Thingstad, T.F., Zweifel, U.L., Rassoulzadegan, F., 1998. P limitation of heterotrophic bacteria and phytoplankton in the northwest Mediterranean. Limnol. Oceanogr. 43, 88-94.

Turchetto, M., Boldrin, A., Langone, L., Miserocchi, S., 2012. Physical and biogeochemical processes controlling particle fluxes variability and carbon export in the Southern Adriatic. Cont. Shelf Res. 44, 72-82.

Tusseau-Vuillemin, M.-H., Mortier, L., Herbaut, C., 1998. Modeling nitrate fluxes in an open coastal environment (Gulf of Lions): Transport versus biogeochemical processes. J. Geophys. Res. Oceans. 103, 7693-7708.

Vargas-Yáñez, M., Zunino, P., Benali, A., Delpy, M., Pastre, F., Moya, F., García-Martínez, M.d.C., Tel, E., 2010. How much is the western Mediterranean really warming and salting? J. Geophys. Res. Oceans. 115, C04001.

Yilmaz, A., Tugrul, S., 1998. The effect of cold- and warm-core eddies on the distribution and stoichiometry of dissolved nutrients in the northeastern Mediterranean. J. Mar. Syst. 16, 253-268.

Yunev, O. A., Carstensen, J., Moncheva, S., Khaliulin, A., Ærtebjerg, G., and Nixon, S., 2007. Nutrient and phytoplankton trends on the western Black Sea shelf in response to cultural eutrophication and climate changes. Estuar. Coast. Shelf. S. 74, 63-76.

Chapitre III

IMPACT DE LA CONVECTION SUR LES PROCARYOTES MARINS EN MÉDITERRANÉE NORD OCCIDENTALE (MNO)

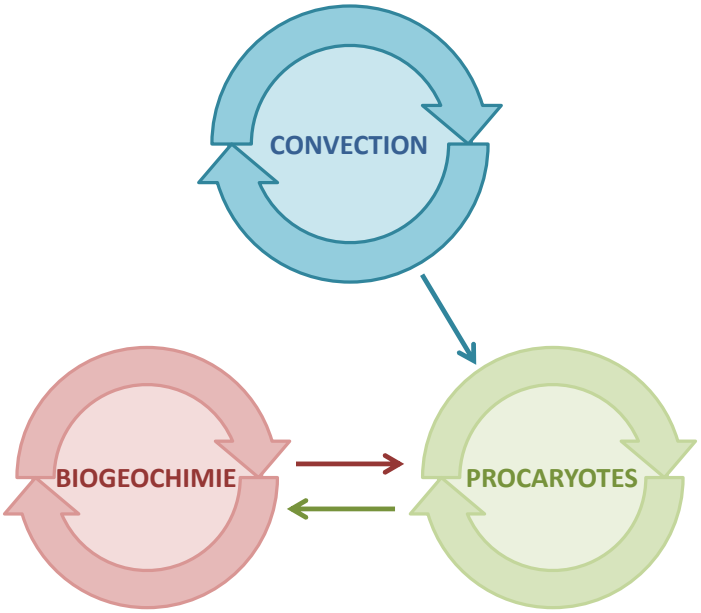

III. IMPACT DE LA CONVECTION SUR LES PROCARYOTES MARINS EN MNO

III.1. Préambule

Le premier article nous a permis d'estimer l'apport de sels nutritifs par la convection et de mettre en évidence son influence sur tout l'écosystème pélagique hauturier de la MNO, notamment via l'efflorescence printanière de grande ampleur qu'il conditionne. L'influence de ce processus sur les cycles biogéochimiques ne se limite évidemment pas aux sels nutritifs. Le mélange convectif en MNO permet aussi d'exporter la matière organique accumulée en surface vers les zones méso et bathypélagiques (Pujo-Pay et Conan, 2003; Santinelli et al., 2010; Stabholz et al., 2013; Gogou et al., 2014). Les procaryotes (bactéries et archées) étant des acteurs clés dans la reminéralisation de la matière organique dans la colonne d'eau, l'objet de cette partie de la thèse visait à mieux saisir le devenir des procaryotes suite à un évènement de convection et d'appréhender de manière plus globale l'impact de ce processus sur la biogéochimie de l'écosystème pélagique en MNO.

Ce deuxième article explore la dynamique des procaryotes à la station centrale SC (noté SC2400 dans l'article 1 ; Figure II-1) pendant et 5 jours après le mélange convectif de mars 2011 en MNO (notés respectivement SCC et SCS ; campagne CASCADE). Une comparaison avec la station de référence ANTARES (Astronomy with a Neutrino Telescope and Abyss environmental RESearch ; noté ANT) située en dehors de la zone de convection nous a permis d'évaluer les modifications générées par la convection. Dans cette étude, une vue générale du compartiment procaryotique a été appréciée sur toute la colonne d'eau par la combinaison de mesures d'abondance des procaryotes (cytométrie en flux), de diversité procaryotique (bactéries et archées par pyroséquençage), et d'activités procaryotiques (production hétérotrophique procaryotique (PHP) et activités enzymatiques extracellulaires). Cette étude nous a permis de mettre en évidence que le mélange convectif favorisait l'export de groupes taxonomiques typiques de surface jusqu'à 1500 m de profondeur, tels que des *Oceanospirillales*, des *Flavobacteriales*, et des Marine Group II *Euryarchaeota*, tout en permettant un faible transport vers la surface de groupes caractéristiques des eaux profondes, comme les SAR406, les SAR202 et les Marine Group I *Thaumarchaeota*. De plus, nous avons observé que la PHP ainsi que l'abondance bactérienne étaient stimulées au sein de la cellule de convection, alors que les activités extracellulaires diminuaient, suggérant une augmentation de l'utilisation de la matière organique labile durant les épisodes de convection. Des analyses

multivariées directes (Canonical Correspondence Analysis, CCA) ont confirmé l'influence significative de la matière organique, à priori labile, sur les communautés formées lors du mélange convectif. En seulement 5 jours, la rapide stratification de la colonne d'eau a permis un retour des communautés procaryotiques typiques de surface (AW et LIW), alors que la communauté formée pendant la convection restait présente dans les eaux profondes nouvellement formées ($nWMDW_{mar}$).

Dans un second temps, nous nous sommes intéressés au devenir de 3 « écotypes » dominant (SAR11, Marine Group I et Marine Group II) lors de cet épisode de convection et après la restratification de la colonne d'eau (voir article 3, section III.4).

III.2. Article 2: Impact of an open-ocean convection event (0-1500m) on prokaryotic diversity and activity in the NW Mediterranean Sea

T. Severin[a,b], M. Boutrif[c,d], L. Oriol[a,b], J. Caparros[a,b], M. Pujo-Pay[a,b], X. Durrieu de Madron[e], M. Garel[c,d], C. Tamburini[c,d], P. Conan[a,b], and J. F. Ghiglione[a,b*].

[a]Sorbonne Universités, UPMC Univ Paris 06, UMR 7621, Laboratoire d'Océanographie Microbienne, Observatoire Océanologique, F-66650 Banyuls/mer, France

[b]CNRS, UMR 7621, Laboratoire d'Océanographie Microbienne, Observatoire Océanologique, F-66650 Banyuls/mer, France

[c]Aix-Marseille University, Mediterranean Institute of Oceanography (MIO), 13288, Marseille, Cedex 9, France CNRS-INSU/IRD UM 110.

[d]Université du Sud Toulon-Var, Mediterranean Institute of Oceanography (MIO), 83957, La Garde Cedex, France CNRS-INSU/IRD UM 110.

[e]CEFREM, UMR 5110, CNRS-UPVD, F-66860, Perpignan, France

[*]**Corresponding author**:

J.F. Ghiglione, Laboratoire d'Océanographie Microbienne, Observatoire Océanologique, Avenue du Fontaulé, F-66650 Banyuls/mer, France. Tel.: + 33 (0) 4 68 88 73 16. E-mail address: ghiglione@obs-banyuls.fr

Abstract

Open-ocean convection is a fundamental process for thermohaline circulation and biogeochemical cycles that causes spectacular mixing of the water column. Here, we explored the dynamic of water-column stratified prokaryotic (bacteria and archaea) communities during a deep convection event (0-1500m) and the following re-stratification that occurred in winter 2010-2011 in the NW Mediterranean Sea. The convection event resulted in a homogenization of the prokaryotic communities over the entire convective cell, which were composed predominantly of typical surface living operational taxonomic units, such as *Oceanospirillales, Flavobacteriales*, and Marine Group II *Euryarchaeota*. Direct multivariate analysis evidenced that physical turbulence together with exported particulate and dissolved organic matters were the main environmental drivers of the distribution of these communities. The convection event resulted in the stimulation of the prokaryotic abundance (+21%) and heterotrophic production (+43%), and to a decrease in extracellular enzymatic activities (-67%), suggesting an increase in the turnover of the labile organic matter in the convective water column. Five days after the convection, we observed a rapid resilience of the prokaryotic diversity and activities in the surface and intermediate layers, whereas the mixed community formed during the convective event remained present in residual deep mixed water patch.

Keywords: Open-ocean convection, Northwestern Mediterranean Sea, bacteria, archaea, pyrosequencing, heterotrophic prokaryotic production, extracellular enzymatic activities

1. Introduction

Deep open-ocean convection is an essential process for the thermohaline circulation of the global ocean (Marshall and Schott, 1999). In the NW Mediterranean (NWM), this process is responsible for the formation and circulation of the Western Mediterranean Deep Water (WMDW) over the entire western basin (Millot, 1999). Open-ocean convection is an annual event in the Gulf of Lion, triggered by the production of surface dense waters in winter through atmospheric forcing (cooling and evaporation) where the "convection chimney" can reach over 100 km in diameter (Medoc Group, 1970; Send and Marshall, 1995). During the mixing phase, kilometric scale dense water plumes can sink down to large depth (> 1000 m or even to the bottom at 2500 m) with downward currents exceeding 10 $cm.s^{-1}$. This sinking flow is balanced by upward motions of deep waters rich in nutrients (Mertens and Schott, 1998), which eventually can sustain the spring phytoplanktonic bloom occurring in NWM (Severin et al., submitted). Open-ocean convection indirectly participates to the carbone sequestration by stimulating the biological carbon pump, but also via the exportation of particulate organic carbon (POC), of the order of 10 mg $C.m^{-2}.d^{-1}$ at 1000 m deep (Stabholz et al., 2013). Large amount of dissolved organic matter (DOC), of the order of 3000 mg $C.m^{-2}.d^{-1}$ are also exported during such event (Santinelli et al., 2010) (e.g. for a convection area of 100 km² in diameter). Moreover, POC and DOC supply in the deep waters, due to deep open-ocean convection, has the potential to fuel the deep-sea biological activity (Tamburini et al., 2013; Martini et al., accepted for publication). The quantity and the quality of the exported organic matter may have important consequences on the diversity and activity of heterotrophic prokaryotes that are responsible for the mineralization of the organic matter in the water column, but this hypothesis has been poorly documented (Boutrif et al., 2011).

In oligotrophic regions such as the Mediterranean Sea, the functioning and productivity of the pelagic ecosystem largely depends on the activity of heterotrophic prokaryotes (Bacteria and Archaea) which are at the center of the balance between exported and mineralized carbon (Pulido-Villena et al., 2012). In the euphotic zone, prokaryotes are abundant, achieving densities of around 10^6 ml^{-1} and they consume on an average 20–50% of the daily primary production (Ducklow, 1999). Below the deep chlorophyll maximum, the abundance of prokaryotes declined with depth. In the Mediterranean Sea, the depth-dependent decrease of prokaryotic abundance was greater in the bathypelagic layer (>500 m) than in the mesopelagic layer (110-500 m) (Tanaka and Rassoulzadegan, 2002). The exponential decrease with depth was even higher for prokaryotic heterotrophic production than for prokaryote abundance (Tanaka and Rassoulzadegan, 2004). Prokaryote species composition is an important variable

controlling the rates and patterns of organic matter remineralization (Martinez et al., 1996), and variability with depth has also been shown to be marked in open waters (Ghiglione et al., 2012; Karner et al., 2001). In the Mediterranean Sea, a stable vertical zonation of bacterial assemblages was observed at several offshore stations and at different seasons with a clear organization in three layers above, in or just below the chlorophyll maximum and deeper (Moeseneder et al., 2001; Ghiglione et al., 2007, 2008, 2009; Rodríguez-Blanco et al., 2009). Archaeal community appeared also to be highly stratified between the surface, meso- and bathypelagic waters in the Mediterranean Sea (De Corte et al., 2009; Tamburini et al., 2009; Winter et al., 2009).

Few studies deal with the prokaryotic response to deep open-ocean convection (heterotrophic production, activity, diversity), an episodic process strongly disturbing the water column, and particularly crucial for the annual biogeochemical cycle. In the Sargasso Sea, the depth-dependent quality of the organic matter induced by the intermediate convection (~300 m) drive two different bacterial community in the euphotic and in the mesopelagic zones (Morris et al., 2005). In the Southern Adriatic Sea, a two year study observed an increase of prokaryote metabolism (abundance, activity, and productivity) following open-ocean deep convection and dense shelf water cascading episodes (Azzaro et al., 2012). Another study followed the prokaryotic compartment before, during and after a convection episode in the Adriatic Sea (Najdek et al., 2014). An increase of the prokaryotic activity was also observed after the convection but in the euphotic zone only, and the prokaryotic diversity was not significantly different during and after the convective mixing. Recent long-term records from the ANTARES neutrino telescope deployed at 2475 m of water depth in the Eastern Gulf of Lion, have shown major bioluminescence activity events to occur in the deep-sea waters during spring months when the newly formed deep waters sink down to the deep basin (Tamburini et al., 2013). Luminous bacteria have been proposed as the main contributors to the observed deep-sea bioluminescence blooms (Al Ali et al., 2010; Martini et al., 2013; Tamburini et al., 2013). Those bioluminescence events, proposed as a proxy of biological activity, constitute a compelling evidence of the quick response of the deep-sea pelagic ecosystem to seasonal atmospheric forcing leading to dense water formation and propagation. Moreover, Stabholz et al. (2013) showed that open-sea convection can cause significant remobilization of bottom sediments in the deep outer margin and basin, including the sustainment of a several hundred meters thick bottom nepheloid layer. This alteration of the seabed may also impact biogeochemical fluxes and the overall functioning of the deep-sea ecosystem. Surprisingly,

none of these studies concerned the intense NWM convective mixing, certainly because of the sampling difficulties of this area during this period.

In this study we describe the impact of a deep NWM open-ocean convection on the prokaryotic compartment during the winter 2011. Using pyrosequencing technology, we analyzed (i) the community structure of both Bacteria and Archaea over the entire water column during the intense convective mixing, (ii) and its evolution in a rapidly restratified water column. As open-ocean convection is a complex process with strong physical disturbance and active biogeochemical fluxes, we determined (iii) the environmental variables responsible for the prokaryotic community structure, and (iv) their influence on the prokaryotic metabolism (ectoenzymatic activities and production) during and after the deep convection event.

2. Materials and Methods

2.1. Study area and sampling strategy

The CASCADE cruise (Cascading, Surge, Convection, Advection and Downwelling Events) was carried out in the Gulf of Lion from the 04 to 23 March 2011 aboard the R/V *L'Atalante*. At each station, water samples were collected at 10 levels with 12L Niskin bottles mounted on a SBE 32 Carousel water sampler equipped with a Seabird 911Plus conductivity-temperature-depth (CTD) probe. For this study, samples for bacterial diversity analysis were selected from seven depths all over the water column (10, 50, 100, 350, 500, 1000, and 2000 m) at three typical stations of the Northwestern Mediterranean Sea (Fig. 1). The Antares station (noted ANT) is used as a reference away from the convection area and was sampled on the 2 March 2011. The SC station, at the center of the convection area, had been sampled twice the 4 and 9 March 2011 (noted SCC and SCS respectively).

2.2. Chemical and biological analysis

Nutrient concentrations (silicate ± 0.05µM, nitrate ± 0.02µM, nitrite ± 0.01µM and phosphate ± 0.01µM) were estimated from samples immediately filtered on board (0.45µm cellulose acetate filters) and stored in 20 ml polyethylene vials at -20°C until analysis. In the laboratory, samples were analyzed by colorimetry on a Seal-Bran-Luebbe autoanalyzer AA3 HR (Aminot and Kérouel, 2007). Ammonium concentrations (NH_4 ± 2nM) were determined on board by nanomolar fluorometric method (Holmes et al., 1999) on a fluorometer Jasco FP-2020.

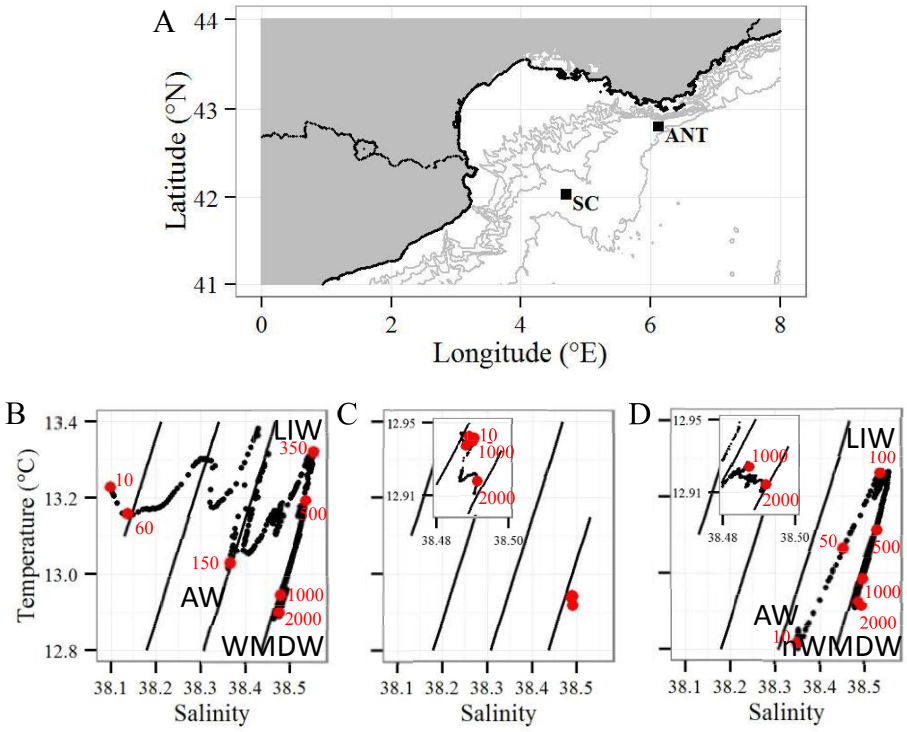

Figure 1: (A) Sampling map of the sequenced stations during the CASCADE cruise leg 1 (1-23 March 2011). (B-D) Potential temperature (°C) - salinity diagrams at the sampled stations, (B) ANT, (C) SCC (with a zoom on top-left) and (D) SCS (with a zoom of the WMDW on top-left). The depths of the studying samples are signaled in red and the water masses AW are annotated

Samples for dissolved organic matter (DOM) were collected from the Niskin bottles in combusted glass bottles. They were immediately filtered on board through 2 precombusted (24 h, 450°C) glass fiber filters (Whatman GF/F, 25 mm). Samples for dissolved organic carbon (DOC), were acidified with orthophosphoric acid (H_3PO_4) and stored into in precombusted glass tubes. At the laboratory, They were immediately analyzed by high temperature catalytic oxidation (HTCO) (Sugimura and Suzuki, 1988; Cauwet, 1994, 1999) on a Shimadzu TOC L analyzer. Samples for dissolved organic nitrogen (DON) and phosphorus (DOP), collected in Teflon vials, were immediately frozen and then analyzed at the laboratory by persulfate wet-oxidation (Pujo-Pay and Raimbault , 1994; Pujo-Pay et al., 1997).

Particulate organic Carbon (POC), nitrogen (PON) and phosphorus (POP) were filtered on precombusted (24 h, 450°C) glass fiber filters (Whatman GF/F, 25 mm). Filters were dried overnight at 50°C, then stored in ashed glass vial in a dessicator. At the laboratory, POC and PON where simultaneously analyzed according to the wet oxidation method (Pujo-Pay and Raimbault, 1994). POC samples were analysed on a CHN Perkin Elmer 2400.

For total chlorophylls a (Chla) and phaeopigments a (Phae; pigment of Chla degradation), 250 ml of seawater were filtered on Whatman GF/F 25mm glass fiber filters, then filters were stored at -80°C. After extraction by 90% acetone, Chla and Phae concentrations were measured by fluorometry on a Turner Design 10-AU fluorometer (Strickland and Parsons, 1997).

2.3. Prokaryotic abundance and activities

For prokaryotic abundance, 1.8 mL of samples were fixed with glutaraldehyde (1% final concentration). Sampled were incubated 15 min in the dark at ambient temperature then store at -80°C until flow cytometric analysis. 1 mL of sub-sample was incubated with SYBR Green I (Invitrogen−Molecular Probes) at 0.025% (v/v) final concentration for 15 min at room temperature in the dark. Counts were performed with a FACS Calibur flow cytometer (Becton Dickinson) equipped with an air-cooled argon laser (488 nm, 15 mW) (Lebaron et al., 2001).

Prokaryotic heterotrophic production (PHP) was measured by ^{3}H-leucine incorporation into proteins (Kirchman, 1993). ^{3}H-leucine (specific activity 155 Ci.mmol^{-1}; Perkin Elmer) was added to samples from surface water (0-150 m) and from meso- and bathypelagic (>150 m) waters, in final concentrations of 20 and 10 nM respectively. Samples were incubated in sterile Falcon vials in the dark at *in situ* temperature for 4 and 8h for surface and meso- or bathypelagic samples respectively. After incubation, samples were filtered onto 25-mm-diameter 0.2-µm polycarbonate filters. Trichloroacetic acid (TCA 5%) was then directly added on filters and incubated 15 min. Filters were stored at -20°C until analysis. At the laboratory, filters were dissolved in 1 mL ethyl acetate, and radioactivity retained on filters was measured as disintegrations per minute using a liquid scintillation counter (Packard 1600). Leucine uptake was converted into prokaryotic production by a factor of 1.55 kg C per mol of incorporated leucine, assuming a dilution factor of 1 since saturating conditions were respected (Kirchman, 1993). PHP (in ngC.L^{-1}.h^{-1}) was obtained by multiplying this actor with the incorporation rate (in pmol.L^{-1}.h^{-1}).

Extracellular enzymatic activities for aminopeptidase, β-glucosidase, lipase and phosphatase were measured by adding to 390 µL of triplicate samples, the substrates L-leucine-7amido-4-methyl coumarin (LL, 200 µM final), MUF-β-D-glucoside (β-Glc, 10 µM final), MUF-palmitate (Lip, 10 µM final) and MUF-phosphate (Pho, 10 µM final), all prepared in methycellosolve, according to Hoppe's protocols (Hoppe, 1983). These analogue substrates concentrations were representative of saturating concentration. This was verified with calibration kinetics during the cruise where a large set of concentrations (from 1 to 250 µM) and times (from 0

to 8h) were tested (data not shown). Incubations were run in the dark at *in situ* temperature during 4 and 8h for surface samples and meso- or bathypelagic samples respectively. Boiled water blanks were run to check for abiotic activity. Reactions were stopped using 50 µL of SDS 20%, ammonium-glycine buffer (pH 10.5), TRIS solution (1M, pH 11) and formaldehyde 30% for aminopeptidase, glucosidase, lipase and phosphatase activities respectively. Samples were stored at -20°C until fluorescence measurement. After an addition of 550 µL of borate buffer (pH=11), release of the product of aminopeptidase activity (MCA) and the others activities (MUF) were followed by measuring the increase of fluorescence at 380, 364 nm (MCA and MUF respectively) excitation wavelengths, and 440, 450 nm (MCA and MUF respectively) emission wavelength, using a microplate spectrofluorometer (1420 Multilabel counter, VICTOR3, Perkin Elmer) calibrated with standards MCA and MUF solution prepared in 0.2 µm-filtered seawater.

2.4. Prokaryotic diversity and pyrosequencing analysis

Samples for prokaryotic diversity were collected with 2 L acid cleaned (HCl) polycarbonate bottles. They were sequentially filtered on board through 2 µm and 0.2 µm (free-living fraction) pore-size polycarbonate filters (47 mm diameter) using a peristaltic pump under low pressure (<100 mbar). Filters were stored à -80°C. DNA extractions were performed as previously described (Ghiglione et al., 2009) using a AllPrep DNA/RNA mini kit (Qiagen).

DNA from the free-living fraction (0.2 µm filters) were analyzed by prokaryote tag-encoded FLX amplicon pyrosequencing (bTEFAP) using Gray926F (5′-AAACTYAAAKGAATTGRCGG-3′) and Gray1392R (5′-ACGGGCGGTGTGTRC-3′), which amplify V6, V7 and V8 regions of the 16S rRNA gene (Sun et al., 2011). A one-step PCR was performed and tag-encoded FLX amplicon pyrosequencing analyses were completed using the Roche 454 FLX instrument with Titanium reagents. Procedures were performed at the Research and Testing Laboratory (Lubbock, TX) based upon RTL protocols.

Sequences were processed and analyzed using the QIIME pipeline (Caporaso et al., 2010). There were denoised using the AmpliconNoise pipeline and chimera checked was done using Perseus (Quince et al., 2011). The resulting clean sequences were clustered using operational taxonomic units (OTUs) at a 97% sequence identity level using the UCLUST algorithm (Edgar, 2010). A representative sequence from each OTU was taxonomically classified using the Ribosomal Database Project (RDP) classifier (Wang et al., 2007) using the Greengenes database. OTUs from Bacteria and Archaea were separated resulting in 2 different OTU tables. To enable comparison between samples, sequences were randomly subsampled to the sample with the fewest sequences for each OTU table (3372 and 167 sequences for Bacteria

and Archaea OTU tables respectively) using NumPy from the Mersenne twister PRNG implemented in QIIME pipeline. All OTU and diversity analyses were performed on the randomly re-sampled OTU tables.

2.5. Diversity and statistical analysis

SPADE (Species Prediction and Diversity Estimation; http://chao.stat.nthu.edu) was used to calculate the non-parametric species richness estimator Chao1 and ACE. Rarefaction curves were generated using PAST (PAleontological STatistics v3.01; http://folk.uio.no/ohammer/past/). Simpson, Shannon and Pielou diversity indexes (which take into account both richness and evenness for the 2 first indexes, and only the evenness for the last index) were calculated using PRIMER 6 software (PRIMER-E, UK).

Similarity matrices of Bray-Curtis were calculated for each OTU table (Bacteria and Archaea) to compare prokaryotic community structures, and were used to build dendrograms by the unweighted-pair group method with arithmetic averages (UPGMA). A similarity profile test (SIMPROF, PRIMER 6) was performed on a null hypothesis that a specific sub-cluster can be recreated by permuting the entry species and samples. The significant branch (SIMPROF, $p < 0.05$) was used as a prerequisite for defining bacterial clusters. One-way analysis of similarity (ANOSIM, PRIMER 6) was performed on the same distance matrix to test the null hypothesis that there was no difference between bacterial communities of different clusters.

To investigate the relationships between prokaryotic community structures and environmental parameters, we used a canonical correspondence analysis (CCA) using the software package CANOCO, version 4.5 for Windows, as previously described (Berdjeb et al., 2011). Environmental parameters were transformed according to their pairwise distributions (Legendre and Legendre, 1983), then spearman rank pairwise correlations between the transformed environmental variables helped to determine their significance. To statistically evaluate the significance of the canonical axes, we used a Monte Carlo permutation full model test with 199 unrestricted permutations. Significant variables were chosen using a forward-selection procedure of 999 permutations, and explanatory variables were added until further addition of variables failed to contribute significantly ($p < 0.05$) to a substantial improvement to the model's explanatory power.

In order to evaluate the relationship between prokaryotic community structures and the physical disturbance, we numerically simulated a vertical homogenization at the reference station ANT from 10 to 1500 m depth. For each sample, 2 factors were determined according to their initial prokaryotic abundance, and the volume of the surface, intermediate and deep

water masses which they belong (see their definition afterwards). Each OTUs was weighted by these factors according to their initial depth at ANT, and added up in a single sample named ANT-M (for ANTARES – Model). This sample was finally subsampled to 3372 virtual reads in order to be compared to the others samples, using NumPy algorithm from the Mersenne twister PRNG. The same protocol was applied on SCC, with factors determined from the initial conditions of SCC. SCC-M (for Convection – Model) was used as a control, to validate our model.

3. Results

3.1. Hydrography

Three different hydrological conditions have been studied according to the temperature and salinity properties of the water column at the sampled stations (Fig. 1). At station ANT (Fig. 1B), 3 water masses were observed: the AW (Atlantic Water) between 0 and ~250 m depth, dispersed in potential temperature (13.10 - 13.40°C) and salinity (38.12 - 38.43); the warmer (13.30°C) and saltier (38.55) LIW (Levantine Intermediate Water) from 250 to ~600 m; and the colder (12.90°C), salty (38.47) and densest (potential density anomaly>29.1 kg.m-3) WMDW (Western Mediterranean Deep Water) situated from 600 m to the bottom (~2500 m). The presence of the 3 typical NW Mediterranean water masses at ANT illustrated that this station was well stratified and not impacted by the convective mixing. Conversely, the convective mixing was well observed at the SC station (SCC) (Fig. 1C) with a homogeneous cold (12.94°C), salty (38.49), and dense (>29.1 $kg.m^{-3}$) water mass, in the upper 1500 m of the water column, indicative of a deep convective mixed layer. The colder (12-91-12.92°C) and saltier (38.49) underneath layer was mostly composed of recent deep waters formed during an episode of bottom-reaching convection that occurred at the same location one month earlier, from late January to early February 2011 (Severin et al., submitted). The SC station, sampled again 5 days after the convection episode (SCS), was characterized by the reappearance of a moderately stratified water column organized in 3 water masses: AW (12.80°C, 38.35) in the upper tens of meters of the water column, LIW (13.25°C, 38.55) between 100 and 500 m deep, and newly-formed WMDW (12.9 1-12.92°C, 38.49) composed of the WMDW below 1000 m deep formed by the convection episode of February (noted $nWMDW_{feb}$), and the WMDW formed by the convection of March (noted $nWMDW_{mar}$).

3.2. Prokaryotic communities structure

Bacterial and archaeal community structures mostly followed the distribution of the corresponding water masses (Fig. 2). At the stratified stations (ANT and SCS), communities of each water mass clustered together and independently of the station, with higher dissimilarities between the surface (AW) and the deep layers (LIW and WMDW) (ANOSIM $R^2 = 0.81$, $p < 0.01$ for Bacteria, and $R^2 = 0.60$, $p < 0.01$ for Archaea). A significant difference was also observed between bacterial and archeal communities of LIW and WMDW, (ANOSIM $R^2 = 0.57$, $p < 0.01$ for bacteria, and $R^2 = 0.91$, $p < 0.01$ for archaea). During the convection event (SCC), the bacterial and archaeal community structures were homogeneous throughout the 1500 m deep mixed water layer, and differ for the deepest sample SCC2000m located below the mixing zone. Samples influenced by the convection were significantly different to the surface samples associated to the AW (ANOSIM $R^2= 0.82$, $p < 0.05$ for Bacteria, and $R^2 = 0.95$, $p < 0.05$ for Archaea), but were closer to them than the deep samples associated to the LIW and WMDW.

Alphaproteobacteria dominated the bacterial diversity (27 to 49% of all the sequenced bacterial OTUs) of all the samples (Fig. 3), in which the SAR11 composed the majority of the OTUs of the *Alphaproteobacteria* class (87% of the *Alphaproteobacteria*, and 24-43% of total bacterial OTUs). At the stratified stations (ANT and SCS), *Rickettsiales*, *Flavobacteriales*, *Oceanospirillales* and *Synechoccocales* represented the most abundant OTUs in the AW with 34-44%, 9-24%, 12-19% and 3-16% of total bacterial OTUs respectively. In the LIW and WMDW, the contribution of these taxonomic classes decreased drastically, with the notable absence of *Synechoccocales*. *Rickettsiales* remained predominant in the LIW and WMDW with 32-42% and 32-36% of the total bacterial community respectively. Some OTUs were undetected at the surface layers but broke out in the deeper water mass (WMDW), such as SAR406 (10-18% and 9-16% in the LIW and WMDW, respectively), Sva0853 from *Deltaproteobacteria* (2-6%, 3-7% in the LIW and WMDW respectively), and SAR202 (2-3%, 5-8% in the LIW and WMDW, respectively). Overall, convective communities were dominated by taxa found in surface stratified waters. For example, *Rickettsiales* (from 25 to 33% of total bacterial OTUs), *Oceanospirillales* (from 16 to 29% of total bacterial OTUs) and *Flavobacteriales* (from 19 to 22% of the total bacterial community) dominated the convective community and were mainly found in surface waters under stratified regime. OTUs overwhelmingly found in deep stratified waters were also found but in lower abundance in convective waters, such as SAR406 (4 to 6% of total bacterial OTUs) and SAR202 (from 0.5 to 1% of total bacterial OTUs). The bacterial diversity at SCC2000m and SCS2000m was slightly different to the corresponding WMDW diversity at ANT2000m with higher abundance

of *Flabobacteriales* (+84%), *Oceanospirillales* (+70%) and *Acidimicrobiales* (+75%) to the expense of SAR406 (-18%), Sva0853 (-50%); SAR202 (-60%) and *Thiohalorhabdales* (-44%).

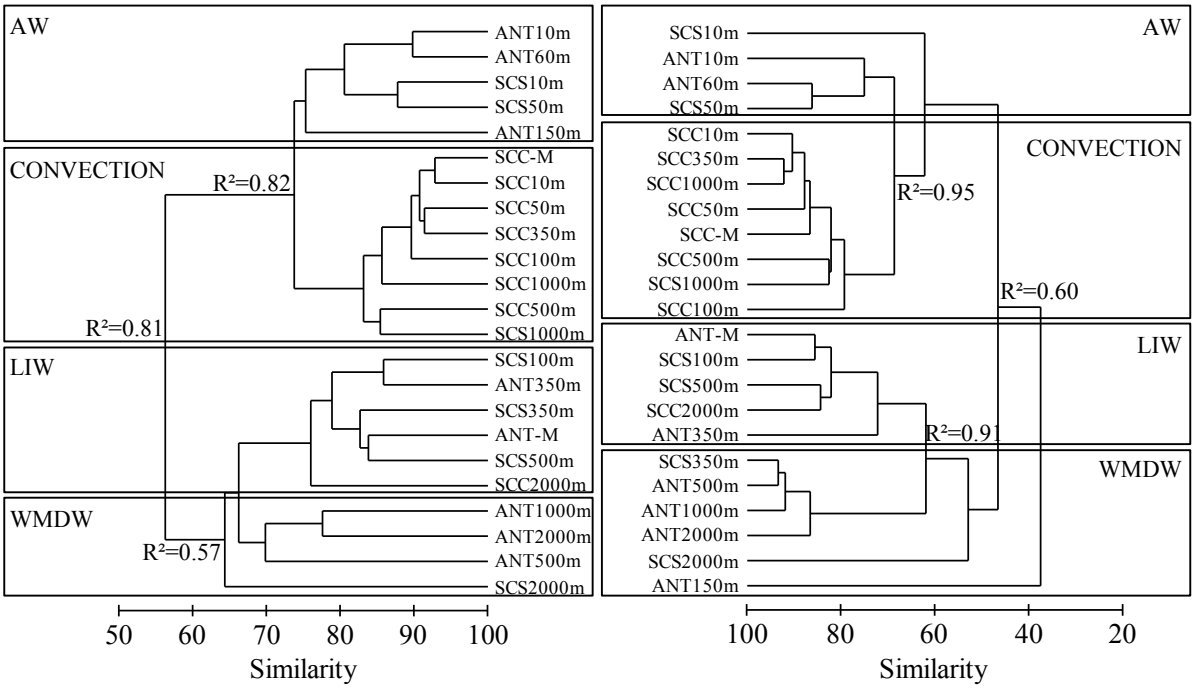

Figure 2: Unweighted-pair group method with arithmetic mean (UPGMA) dendrograms based on Bray-Curtis similarities of bacteria OTU tables (left) and archaea OTU table (right). Results of anosim tests (R) are indicated at each main node. The water masses are indicated by rectangles

The archaeal diversity (Supplementary S1) presented a similar trend than bacterial diversity. At the stratified stations (ANT and SCS), Marine group II *Euryarchaeota* dominated at ~60% the surface AW, with a predominance of the winter ecotype Marine group IIb (50%). In the LIW and WMDW, the contribution of this family decreased drastically to 10%. Marine group I *Thaumarchaeota* which contributed to less than 30% in the surface stratified waters, strongly increased to 88% in the LIW, and to 83% in the WMDW. The archaeal diversity at SCS2000m was also different to the corresponding WMDW diversity at ANT2000m, with higher contribution of Marine group IIb (44%) than at ANT (7%). Convective communities (at SCC) were dominated by the two main surface and deep taxa observed at the stratified stations (ANT and SCS), i.e. Marine group I (50%) and Marine group II (50%).

Table 1: Numbers of OTUs, Chao1, Pielou, Shannon and Simpson diversity indexes at 0.03 level of clustering after 454-tag pyrosequencing for bacteria and Archaea OTU tables

	BACTERIA					ARCHAEA				
Samples	No OTUs	Chao1	Pielou	Shannon	Simpson	No OTUs	Chao1	Pielou	Shannon	Simpson
ANT10m	87	121.7	0.62	2.75	0.88	11		0.77	1.85	0.79
ANT60m	88	110.0	0.61	2.71	0.86	11	12.0	0.76	1.82	0.80
ANT150m	98	104.3	0.64	2.93	0.86	11	19.0	0.60	1.45	0.68
ANT350m	95	98.6	0.74	3.35	0.92	12		0.80	1.98	0.81
ANT500m	90	97.2	0.76	3.41	0.94	8		0.34	0.70	0.28
ANT1000m	114	161.1	0.73	3.44	0.94	9	11.3	0.29	0.64	0.25
ANT2000m	119	145.2	0.73	3.47	0.93	8		0.46	0.96	0.39
SCC10m	95	113.4	0.65	2.96	0.90	12	12.3	0.80	1.98	0.82
SCC50m	95	130.6	0.65	2.95	0.90	11	13.0	0.74	1.78	0.78
SCC100m	97	157.1	0.66	3.02	0.90	15	14.1	0.70	1.90	0.77
SCC350m	103	112.0	0.66	3.08	0.91	13	15.0	0.75	1.92	0.80
SCC500m	94	160.1	0.67	3.03	0.89	14	22.0	0.72	1.91	0.80
SCC1000m	91	130.1	0.64	2.87	0.89	11	15.5	0.73	1.74	0.78
SCC2000m	104	116.5	0.77	3.56	0.95	14	15.5	0.59	1.57	0.64
SCS10m	75	93.3	0.61	2.65	0.86	11	12.0	0.59	1.42	0.59
SCS50m	98	107.0	0.63	2.88	0.87	11	13.0	0.76	1.83	0.79
SCS100m	113	141.2	0.72	3.41	0.93	13	14.1	0.65	1.66	0.71
SCS350m	128	190.2	0.71	3.44	0.92	8	10.0	0.34	0.71	0.29
SCS500m	126	162.3	0.72	3.46	0.92	13	13.7	0.58	1.48	0.61
SCS1000m	98	113.4	0.7	3.20	0.92	18	24.0	0.73	2.11	0.82
SCS2000m	106	119.9	0.76	3.55	0.95	16	24.0	0.76	2.11	0.83
ANT-M	119	154.0	0.73	3.49	0.93	12	16.0	0.60	1.49	0.67
SCC-M	104	138.6	0.64	2.99	0.90	15	17.3	0.71	1.92	0.80

At the stratified stations (ANT and SCS), we found a higher bacterial richness and evenness in the deep WMDW (Chao1 = 142 ± 21, Pielou = 0.74 ± 0.02) than in the surface AW (Chao1 = 107 ± 12, Pielou = 0.62 ± 0.01). As for the WMDW, LIW had an elevated richness and evenness (Chao1 = 138 ± 28, Pielou = 0.73 ± 0.03). Values of the convective bacterial diversity indexes (SCC) were between AW and LIW indexes (Chao1 = 134 ± 21, Pielou = 0.66 ± 0.01). The archaeal richness had the same trend than bacterial diversity indexes at the stratified stations (ANT and SCS): higher richness in the deep waters (LIW and WMDW) than in surface layers (AW). Archaeal evenness had an inverse trend with higher values in the AW (Pielou = 0.70 ± 0.09) than in the LIW (Pielou = 0.54 ± 0.16), and in the WMDW (Pielou = 0.50 ± 0.24). Contrary to the convective bacterial diversity, archaeal diversity in the convective cell presented higher richness (Chao1 = 15 ± 3) and evenness (Pielou = 0.74 ± 0.03) than the other stratified archaeal communities.

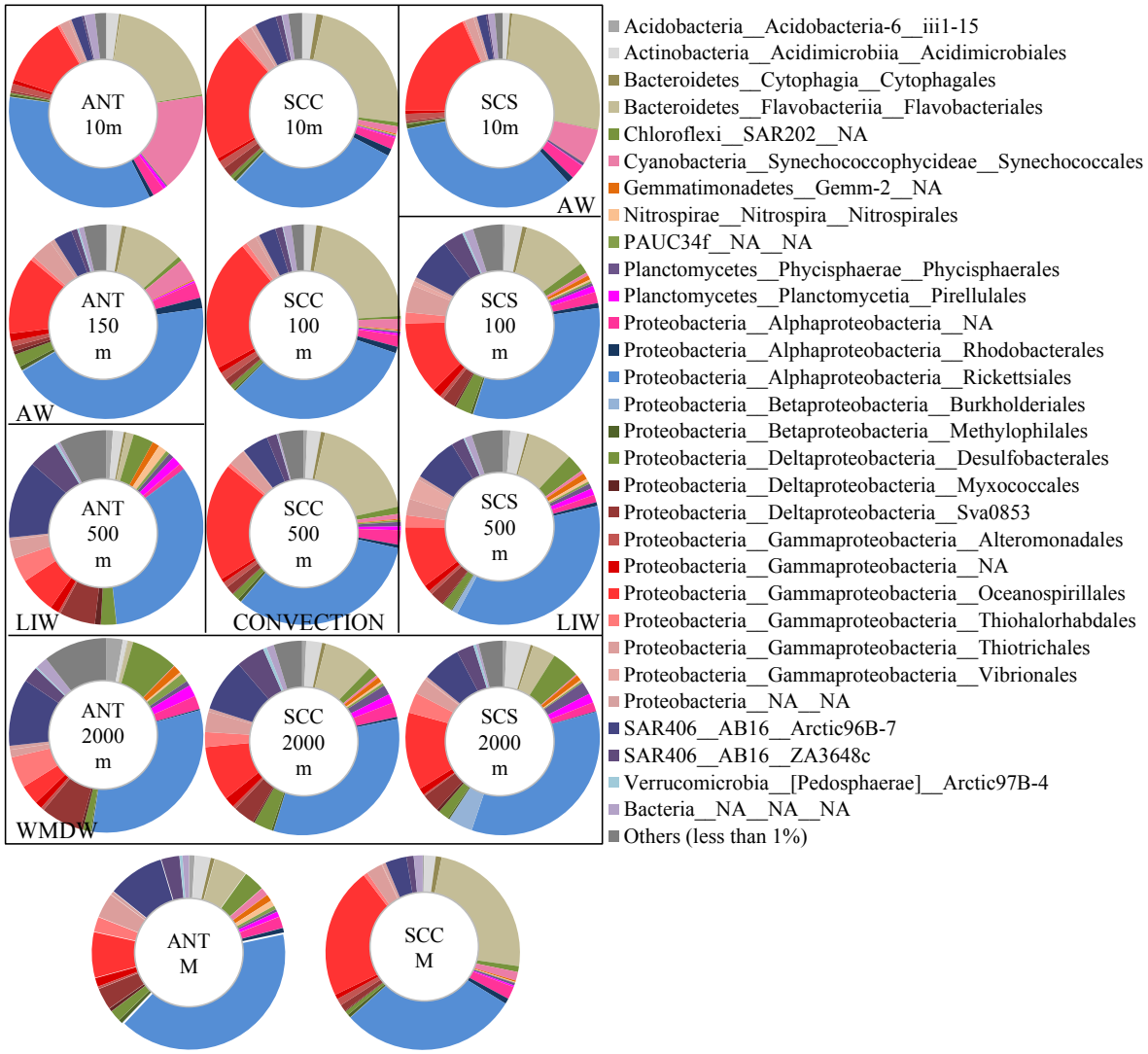

Figure 3: Taxonomic distribution (Phylum_Class_Order) for OTUs that occurred more than 37 times (>1%) from the bacterial OTU table and the model. The remaining sequences are grouped in « other ». Taxonomy not assigned is symbolyzed by NA. The water masses of the samples are noted in black

To investigate the influence of the convection event on the bacterial and archaeal community, we simulated a vertical mixing using the diversity of ANT (noted ANT-M) and SCC (noted SCC-M) from 10 to 1500 m. The bacterial and archaeal community structures of ANT-M was significantly the same that the natural assemblages of LIW (Fig. 2), with quite the same amount of *Rickettsiales* (40%), SAR406 (13%), Sva0853 (4%), SAR202 (4%) (Fig. 3) and Marine group I (85%; S1). SSC-M had a similar bacterial and archaeal community structure than the populations from the convective water mass (Fig. 2, 3 and S1), dominated by Rickettsiales (30%), Oceanospirillales (22%), Flavobacteriales (24%) (Fig. 3), Marine group I

(54%) and Marine group II (40%) (Fig. S1), with the scarce presence of the deep SAR406 (5%) and SAR202 (1%).

3.3. Environmental drivers of prokaryotic communities structure

As the hydrological conditions were very different between the stratified (ANT and SCS) and the convective stations (SCC), we performed canonical correspondence analyses (CCA) at each station for bacterial and archaeal communities separately. We explored the environmental drivers of the bacterial and archaeal community structures at the reference station (ANT), as well as during (SCC) and after (SCS) the convective event (Fig. 4). Prior to the CCAs, Spearman's rank pairwise correlation tests were realized at each station. For the ANT station, strong correlation was found between nitrate (NO_3+NO_2), phosphate (PO_4), silicate ($Si(OH)_4$), salinity and density, with correlation coefficients > 0.90 and $p < 0.01$ (n=7). Nitrate was used as a proxy of these parameters for further multivariate analysis. For the SCC station, we used the chlorophyll *a* (Chla) as a proxy of particulate organic phosphorous (POP) and phaeopigments *a* (Phaeo *a*) ($\rho > 0.90$, $p < 0.01$, n=7). The same approach was used for station SCS ($\rho > 0.90$, $p < 0.01$, n=7), which resulted in the use of NO_3+NO_2 as a proxy of PO_4, Chla, POP and density, and DOP as a proxy of $Si(OH)_4$.

For both communities of Bacteria and Archaea, and at each station, the cumulative percentage of variance of the species-environment relationship indicated that the first and second canonical axes explained more than 50% and 10% of the variance respectively (Table 2). Others axes accounted for less than 10% of the variance each, and were not further considered here. At the ANT station, the first canonical axis, for both Bacteria and Archaea, was highly positively correlated with temperature, DOP, and DOC for bacteria, NOP for archaea, and negatively correlated with NO_3+NO_2 (and PO_4, $Si(OH)_4$, density by correlation) (Fig. 4A, D). The concomitant effect of these parameters explained 89% and 90% (ratio between the total inertia and the sum of all eigenvalues) of the changes in community structure of Bacteria and Archaea, respectively (Table 2). At the SCC station, for both Bacteria and Archaea, the first canonical axis was positively correlated with density, and negatively correlated with PON (and POC for bacterial community, Chla and temperature for archaeal community). DOC contributed to a lesser extent to the first axis of bacterial community (Fig. 4B, E). All these parameters explained 88% and 84% of the changes in community structure of Bacteria and Archaea respectively (Table 2). At the SCS station, the first canonical axis was highly positively correlated with DOP and DON for both Bacteria and Archaea (and with POC for Bacteria), and negatively correlated with NO_3+NO_2 and temperature for Archaea. For

Bacteria, the second canonical axis was positively correlated with DON, and negatively with temperature (Fig. 4C, F). 82% and 88% of the variance was explained by these parameters in the community structure of Bacteria and Archaea, respectively.

Table 2: Results of canonical correspondence analyses (CCAs) for bacteria and Archaea OTU tables at each sampled stations

	BACTERIA			ARCHAEA		
ANTARES						
Axes	1	2		1	2	
Eigenvalues	0.386	0.107		0.549	0.156	
Species-environment correlations	0.976	0.993		0.994	0.965	
Cumulative percentage variance of:						
species data	56.2	71.7		60.8	78.7	
species-environment relation	63.3	80.8		67.7	86.9	
Total inertia			0.687			0.903
Sum of all canonical eigenvalues			0.610			0.811
SCC						
Axes	1	2		1	2	
Eigenvalues	0.128	0.021		0.100	0.044	
Species-environment correlations	0.998	0.977		0.992	0.999	
Cumulative percentage variance of:						
species data	63.4	73.7		43.5	62.6	
species-environment relation	72.5	84.9		51.7	74.4	
Total inertia			0.201			0.231
Sum of all canonical eigenvalues			0.176			0.194
SCC						
Axes	1	2		1	2	
Eigenvalues	0.205	0.073		0.363	0.133	
Species-environment correlations	0.961	0.984		0.989	0.933	
Cumulative percentage variance of:						
species data	52.5	71.3		55.8	76.3	
species-environment relation	63.9	86.8		63.7	87.1	
Total inertia			0.390			0.649
Sum of all canonical eigenvalues			0.321			0.569

3.4. Prokaryotic activities

At the reference stratified station ANT, prokaryotic abundance was elevated in the AW ($8.0\ 10^5$ cells.mL^{-1} at 10 m) and decreased rapidly with depth, to finally stabilized at $5.0\ 10^4$ cells.ml^{-1} around 1000 m and below (Fig. 5A). At the convective mixing station (SCC), the prokaryotic abundance was homogeneous between 10 and 1500 m at $2.0\ 10^5$ cells.mL^{-1} (SD = $0.41\ 10^4$, n=7). Integrated value between 10 to 1500 m was slightly higher at SCC ($1.75\ 10^5$ cells.m^{-3}) than at ANT ($1.38\ 10^5$ cells.m^{-3}). At the re-stratification (SCS), the prokaryotic abundance throughout the water column was similar to that of the reference station.

Overall, prokaryotic heterotrophic production (PHP) followed the same trend as prokaryotic abundance at the 3 sampled stations (Fig. 5B). Elevated production rates were measured in stratified surface waters (26 and 62 $ngC.L^{-1}.h^{-1}$ at ANT and SCS respectively), and progressively decreased to vanish below 500 m depth. PHP was low (~2.5 $ngC.L^{-1}.h^{-1}$) in the convective cell (10-1500m) but the 10-1500 m integrated production rate was higher at the SCC station (33.0 $ngC.m^{-3}.h^{-1}$) than at the ANT station (18.6 $ngC.m^{-3}.h^{-1}$).

Extracellular enzymatic activities were normalized by the prokaryotic abundance in order to evaluate the cell specific response to the environmental modifications. Aminopeptidase (LL), glucosidase (β-Glc), lipase (Lip) and phosphatase (Pho) activities followed all the same trend at the 3 sampled stations (Fig. 5C-F). At the ANT station, activities were low in the surface (2 10^{-13}, 5 10^{-15}, 9 10^{-14}, and 2 10^{-14} $mol.l^{-1}.h^{-1}.cell^{-1}$ for LL, β-Glc, Lip, and Pho respectively), and progressively increases to a maximum activity around 2000 m depth (2 10^{-12}, 3 10^{-14}, 4 10^{-13}, and 9 10^{-14} $mol.l^{-1}.h^{-1}.cell^{-1}$ for LL, β-Glc, Lip, and Pho respectively). At the convective station (SCC), activities were low and homogeneous all over the water column. After restratification (SCS station), activities remained low in the surface (0-100 m) and deep layers (below 1000 m), but increased between 100 and 1000 m (maximum values of 1.5 10^{-12}, 3 10^{-14}, 3 10^{-13} and 8 10^{-14} $mol.l^{-1}.h^{-1}.cell^{-1}$ for LL, β-Glc, Lip, and Pho respectively).

4. Discussion

The CASCADE cruise sampled the last deep convection episode of the year 2011 which mixed 1500 m of the water column (Fig. 1C) in the convection region (Severin et al., submitted). Despite the key role of convection process into the biogeochemical cycles regulation (Santinelli et al., 2010; Turchetto et al., 2012; Stabholz et al., 2013; Gogou et al., 2014), the prokaryotic compartment had never been studied during such intense NWM convective mixing. The combination of pyrosequencing analysis and prokaryotic activities for both bacteria and archaea will improve our knowledge of the ecosystem response to this key process.

4.1 Spatial variability of prokaryotic community structures

At the reference station situated outside of the convection (ANT), bacterial and archaeal diversities were stratified according to the different layers AW, LIW and WMDW. The strong relation-ship existing between prokaryotes and phytoplankton communities (Teeling et al., 2012) resulted in a focus of the prokaryotic diversity attention in the relatively shallow waters of the euphotic zone (Crespo et al., 2013; Ghiglione et al., 2008; Van Wambeke et al., 2002) yet recent works highlighted the different taxonomic compositions between the epi-, meso and

bathypelagic zones (e.g. Agogué et al., 2011 North Atlantic). In the Mediterranean Sea, an increase of cells size was observed with increasing depth (Azzaro et al., 2012). Likewise, the increase with depth of the evenness (from 0.43 at 5 m to 0.59 at 2000 m) and richness (total number of OTUs from 600 at 5 m to 2100 at 2000 m) (Pommier et al., 2010) supported the likely presence of different prokaryotic populations over the water column (Nagata et al., 2010). The pelagic habitat of the Mediterranean was characterized by higher abundance of *Rhizobiales* (from *Alphaproteobacteria* class), *Oceanospirillales* (*Gammaproteobacteria*), *Desulfuromonadales* (*Deltaproteobacteria*), *Actinobacteridae* (*Actinobacteria*), *Dehalococcoidetes* (*Chloroflexi*), *Planctomycetacia* (*Planctomycetes*) (Martín-Cuadrado et al., 2007) and Marine group I *Thaumarchaeota* (Massana et al., 2000). But the different structures were mostly related to the pelagic zones delimited by their light and depth properties, rather than the water masses determined by their temperature and salinity characteristics (Tamburini et al., 2009). In our study, bacteria showed also an evenness and a richness more elevated in the deep LIW and WMDW than in the surface AW. But despite the elevated relative abundance of *Oceanospirillales* and Marine group I *Thaumarchaeota*, the other dominant taxa were SAR11 (from *Alphaproteobacteria* class), Sva0853 (*Deltaproteobacteria*), SAR202 (*Chloroflexi*), and SAR406.

The deep convection process was responsible for a drastic modification of the prokaryotic community structure all over the convective cell. The mixing over the first 1500 m of the water column induced a homogenization of the bacterial and archaeal communities (Fig. 2). Previous studies demonstrated that vertical convective currents were able to rapidly export particles from the surface to the deep oceans estimated to 200 $mg.m^{-2}.d^{-1}$ (Stabholz et al., 2013). Accordingly, OTUs found in the surface water of the stratified reference station were diluted in the convective cell, as depicted by the dominance of *Oceanospirillales* and *Flavobacteriales* during the convection event (Fig. 3). But the convection process is more complex than a single export of surface waters. Upwards currents exist inside the convective cell that balance the upward flow (Send and Marshall, 1995). Some deep bacteria (SAR406, SAR202) and archaea (Marine group I *Thaumarchaeota*) could then be carried from the deep water to the surface of the convection cell, but in weaker relative abundances compared to the exported surface taxa.

Following the early March 2011 deep convection episode, a rapid re-stratification of the water column linked to the horizontal advection of AW and LIW over the convection region occurred within a few days (Fig. 1D). The bacterial and archaeal community assemblages and diversities came back to a stratified distribution in the first 500 m, with similar communities to the AW and LIW water masses not influenced by the open-ocean convection (as for the ANT

station) (Fig. 2-3, Table 1). Below 500 m, the prokaryotic communities differed from the usual WMDW population (Fig. 2-3). The restratification abruptly isolated and trapped a volume of dense mixed water between 500 and 1500 m that eventually spread horizontally around a hydrostatic pressure of ~1000 m (named $nWMDW_{Mar}$; Fig. 1D). The $nWMDW_{Mar}$ contained surface and deep taxa that survived at least 5 days at SCS1000m after the convection event. The deeper communities at SCS2000m differed from the other samples because they were present in denser waters formed during a previous bottom-reaching convection event that took place in late January - early February (named $nWMDW_{Feb}$), and then equilibrated deeper (Severin et al. submitted). At the time of our sampling, this community was composed of more surface taxa than the deep community of our reference convection station outside the convection region (ANT). Compared to the community inside the trapped volume of dense water ($nWMDW_{Mar}$, station SCC), we observed a decline of 56% of the typical surface *Flavobacteriales*, and the appearance of *Burkholderiales* that were not detected neither at the stratified station ANTnor at the convective cell station SCC.

4.2 Environmental drivers of prokaryotic community structure

To evaluate the effect of pure water column mixing on the prokaryotic community distribution along the water column, we tested a simple model. This model takes into account the observed bacterial and archaeal diversity, with a weighted average of the thickness of the corresponding water mass, and then mixed the prokaryotic population. Using the OTU table of the convective station SCS along the first 1500 m, the resulting model clustered with the natural community of the convection (Fig. 2) with also a similar taxonomic distribution (Fig. 3 and S1), thus validating our simulation. However, using the OTU table of the reference stratified station (ANT), the simulated mixed bacterial and archaeal communities did not clustered with the corresponding convective communities but rather with the deep LIW cluster (Fig. 2-3 and S1). This simulation proved that other factors than a simple mixing of the water column were responsible for the resulting composition of the convective prokaryotic communities. For example, Morris et al. (2005) found a clear relation between the microbial communities and the DOC cycle following a convection overturn (Hansell and Carlson, 2001).

Direct multivariate analysis confirmed the significant contributions of biogeochemical variables in the structuration of prokaryotic communities (Fig. 4B and E). The explanatory variables selected in the CCA models explained more than 80% of the vertical distributions of bacterial and archaeal communities before, during and after the convection, probably because of the large set of environmental variables measured in our study. Under stratified conditions

at the reference station ANT and at the re-stratified SCS station, deep WMDW communities were correlated to elevated concentrations of nutrient, intermediate LIW communities to moderate temperature, and surface AW communities to higher dissolved and particulate organic matter concentrations accumulated through phytoplankton activities prior to and after the convective mixing (Fig. 4A and D). Various studies demonstrated the export of particulate organic matter by convective mixing (Hansell and Carlson, 2001; Santinelli et al., 2010; Heimbürger et al., 2013; Gogou et al., 2014). Together with the vertical physical mixing of the water column, the export by settling particulate organic matter supports the transfer and mixture of the bacterial and archaeal assemblages.

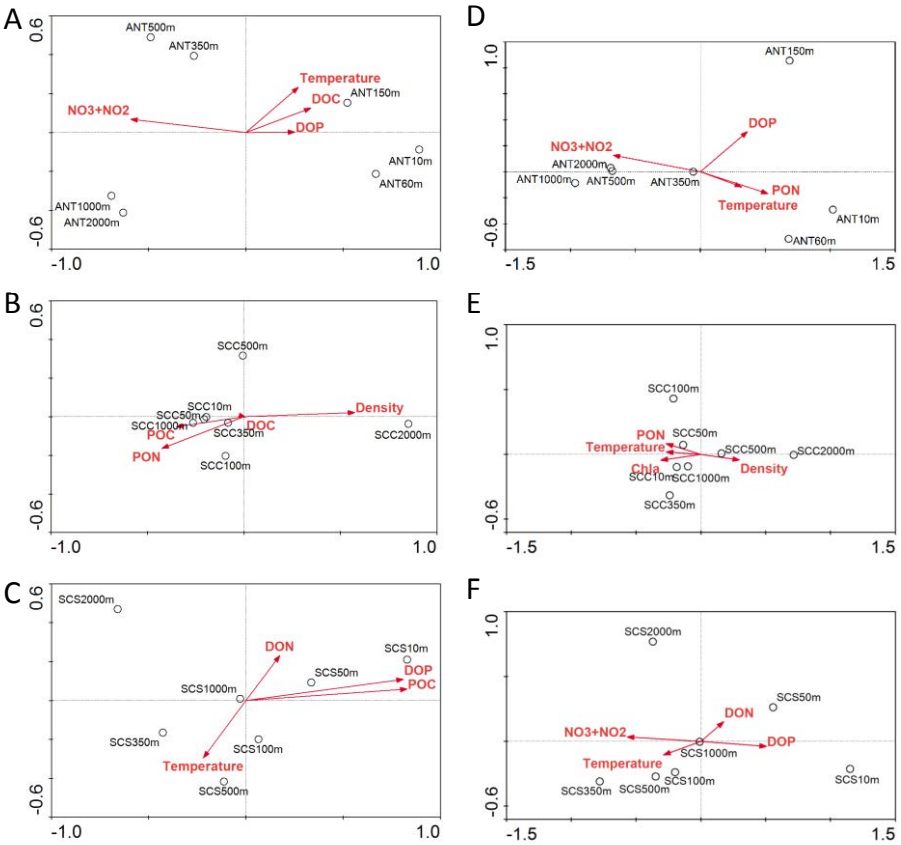

Figure 4: Canonical Correspondence Analysis (CCAs) of (A-C) Bacterial community structure and (D-F) Archaea community structure at each sampled station: (A, D) ANT, (B, E) SCC, (C, F) SCS. The length of the arrows represents degree of correlation with the 2 first presented axis. NO3+NO2: nitrate + nitrite. DOC: dissolved organic carbon. DOP: dissolved organic phosphorus. DON: dissolved organic nitrogen. POC: particulate organic carbon. POP: particulate organic phosphorus. PON: particulate organic nitrogen. Chla: chlorophyll *a*

4.3 Prokaryote activities

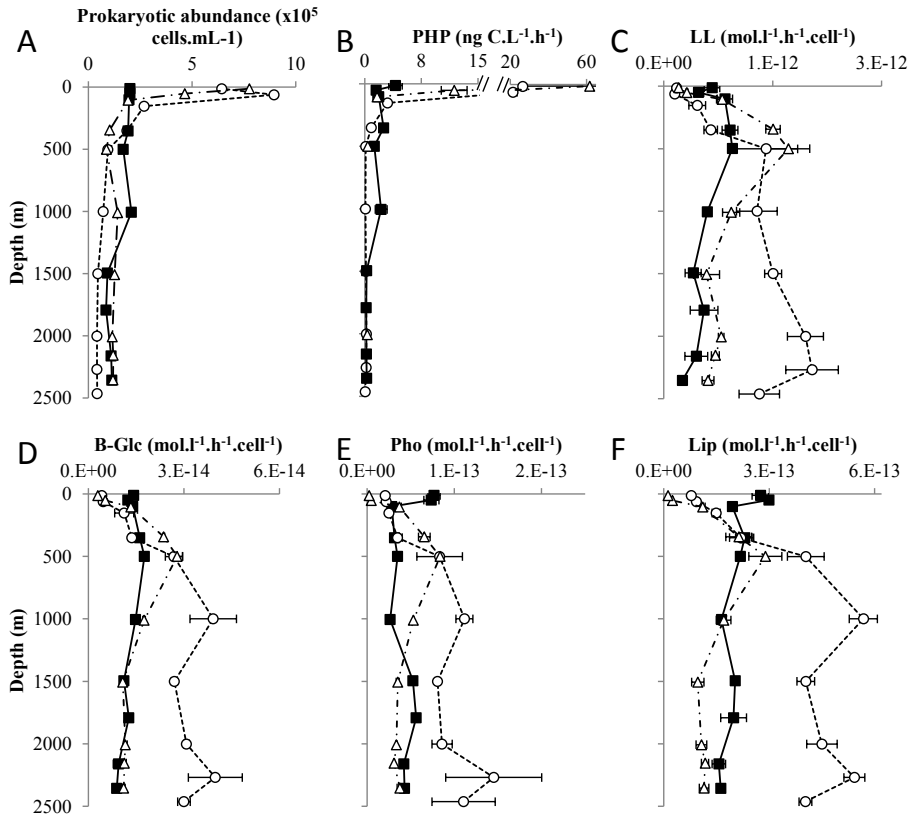

Figure 5: Vertical profils at eatch sampled stations of (A) prokaryotic abundance (B) procaryotic heterotroph production (PHP), (C), aminopeptidase (LL), (D) glucosidase (Glc), (E) lipase (Lip), and (F) phosphatase (Pho) extracellular activities. ANT station is in small dashed lines, SCC in full line and SCS in large dashed lines. For PHP and extracellular activities, the error bars are the standard deviation of the parameter

The transfer of organic matter both in the dissolved and particulate phase further leads to a stimulation of the prokaryotic heterotrophic production (Fig. 5B) despite the strong vertical currents of ± 10 $cm.s^{-1}$ existing in the convective cell that could reached > 10 $cm.s^{-1}$ (Durrieu de Madron et al., 2013; Marshall and Schott, 1999). Even if prokaryote were exported to unusual pressure in a short period of time (Fig. 5A), the mixed convective communities took advantages of the labile organic matter exported down to 1500 m by increasing their biomass and their production rate. Other studies in the Sargasso Sea observed an exportation of labile organic matter in the mesopelagic zone associated to important oxygen utilization rates (Goldberg et al., 2009; Hansell and Carlson, 2001). Mineralization processes were then hypothesized in these convective waters (Morris et al., 2005), but without being able to evidence it. In the stratified period following an open-ocean convection in the Eastern Mediterranean sea (not the intense convection mixing itself), Azzaro et al. (2012) observed in

the deep layer an increase of the PHP rate, the prokaryotic growth efficiency and carbon demand exceeding the POC availability rained down from the euphotic zone. The authors related it to the availability of labile or semi-labile organic matter. In our case, the convective mixing stimulated the prokaryotic production with a doubling of the PHP integrated value between 10 and 1500 m with respect to the reference station. However the following restratified period was not marked by elevated PHP in the deep layers (neither $nWMDW_{feb}$, nor $nWDMW_{mar}$) contrary to Azzaro et al. (2012), suggesting an organic matter depletion in these waters.

Only a small fraction of dissolved organic matter can be directly taken up by bacteria, thus we measured the expression of ectoenzyme activities (Fig. 5). The range of phosphatase (as P provider), aminopeptidase (as N provider) and lipase (as C provider) obtained in our samples was similar that previously described for the NW Mediterranean Sea (van Wambeke et al. 2009). The decrease of the cell-specific extracellular enzymatic activities during the convection event suggested that the exported organic matter was in the form of monomeric molecules, directly assimilable inside the cells. This was not the case during a convection episode in the Adriatic Sea, where exported organic matter was hypothesized to be have a polymeric composition because of an increase of ectoenzyme activities (Azzaro et al., 2012). Five days after the convection event, while the production was null below 100 m, we observed an increase in the cell-specific ectoenzyme activities in the 100-500 m water mass, corresponded to the advected LIW. This is consistent with the fact that LIW are generally depleted in organic matter and dissolved oxygen because of their greater age (Schroeder et al., 2010).

Conclusions

Our results present the first demonstration of the influence of a convection event on the prokaryotic abundance, diversity and activity. Such studies are scarce in the literature because of the difficulty to sample such event, whereas its importance is well known on the oceanic circulation and on the regulation of the global biogeochemical cycles (Send and Marshall, 1995). During the CASCADE cruise, we had the opportunity to follow the dynamic of a convection event until it disappeared, and to compare it with stratified waters outside of the convection zone. Beside the influence of physical variables during the open-ocean convection episode, our study suggested the importance of the exported labile organic matter as a key driver for both the prokaryotic (bacteria and archaeal) diversity and activity. We hypothesized that the exported organic matter was directly accessible to heterotrophic prokaryotes during the convection event, thus resulting in an increase of prokaryotic remineralization over the entire

water column. Further studies are necessary to better characterize the organic matter quality exported during the convection event, in order to better understand these processes.

Despite the large size of the convective event that reached 1500 m depth in our study, we observed a rapid re-stratification of the water column in the first 500 m. The prokaryotic abundance, diversity and activities came back to the prior stratified conditions within only 5 days. Several convective events may occur in the same year, as observed in our study zone in February and March 2011. We observed the preservation of different convective prokaryotic communities entrapped at 2000m in the newly formed bottom water after the January/February bottom-reaching convection episodes ($nWMDW_{Feb}$) and at 1000 m in the deep volume of dense water formed after the March deep convection episode ($nWMDW_{March}$). The lifespan of these community remained to be determined, as for their productivity in water masses which evolved biogeochemical and physically. Moreover, the OTUs observed on a DNA-based may not be active, according to the composition and quality of the exported organic matter (Carlson et al., 2004; Cottrell and Kirchman, 2000; Sarmento and Gasol, 2012; Becker et al., 2014). Investigations on the organic matter quality and on the active fraction (RNA-based) of the prokaryotic diversity should be addressed in further studies to improve our understanding of the ecosystem functioning during open-ocean convection process.

Acknowledgments

We are grateful to the crew and officials of R/V *L'Atalante* and to all the scientific and technical staff involved in the CASCADE cruise for their support during sea operations. This work was funded by the HERMIONE Project (N° 226354) under the European Commission's Seventh Framework Program and the French Program MERMEX under the MISTRALS framework.

References

Agogué, H., Lamy, D., Neal, P.R., Sogin, M.L., Herndl, G.J., 2011. Water mass-specificity of bacterial communities in the North Atlantic revealed by massively parallel sequencing. Mol. Ecol. 20, 258–74. doi:10.1111/j.1365-294X.2010.04932.x

Al Ali, B., Garel, M., Cuny, P., Miquel, J.-C., Toubal, T., Robert, A., Tamburini, C., 2010. Luminous bacteria in the deep-sea waters near the ANTARES underwater neutrino telescope (Mediterranean Sea). Chem. Ecol. 26, 57–72.

Aminot, A., Kérouel, R., 2007. Dosage automatique des nutriments dans les eaux marines : méthodes en flux continu. Ed. Ifremer, Méthodes d'analyse en milieu marin, 188p.

Azzaro, M., La Ferla, R., Maimone, G., Monticelli, L.S., Zaccone, R., Civitarese, G., 2012. Prokaryotic dynamics and heterotrophic metabolism in a deep convection site of Eastern Mediterranean Sea (the Southern Adriatic Pit). Cont. Shelf Res. 44, 106–118. doi:10.1016/j.csr.2011.07.011

Becker, J.W., Berube, P.M., Follett, C.L., Waterbury, J.B., Chisholm, S.W., Delong, E.F., Repeta, D.J., 2014. Closely related phytoplankton species produce similar suites of dissolved organic matter. Front. Microbiol. 5, 111. doi:10.3389/fmicb.2014.00111

Berdjeb, L., Ghiglione, J.-F., Jacquet, S., 2011. Bottom-up versus top-down control of hypo- and epilimnion free-living bacterial community structures in two neighboring freshwater lakes. Appl. Environ. Microbiol. 77, 3591–9. doi:10.1128/AEM.02739-10

Boutrif, M., Garel, M., Cottrell, M.T., Tamburini, C., 2011. Assimilation of marine extracellular polymeric substances by deep-sea prokaryotes in the NW Mediterranean Sea. Environ. Microbiol. Rep. 3, 705–9. doi:10.1111/j.1758-2229.2011.00285.x

Caporaso, J.G., Kuczynski, J., Stombaugh, J., Bittinger, K., Bushman, F.D., Costello, E.K., Fierer, N., Peña, A.G., Goodrich, K., Gordon, J.I., Huttley, G.A., Kelley, S.T., Knights, D., Jeremy, E., Ley, R.E., Lozupone, C.A., Mcdonald, D., Muegge, B.D., Reeder, J., Sevinsky, J.R., Turnbaugh, P.J., Walters, W.A., 2010. QIIME allows analysis of high-throughput community sequencing data. Nat. Methods 7, 335–336. doi:10.1038/nmeth.f.303.QIIME

Carlson, C.A., Giovannoni, S.J., Hansell, D.A., Goldberg, S.J., Parsons, R., Vergin, K., 2004. Interactions among Dissolved Organic Carbon, Microbial Processes, and Community Structure in the Mesopelagic Zone of the Northwestern Sargasso Sea. Limnol. Oceanogr. 49, 1073–1083. doi:10.2307/3597658

Cauwet, G., 1994. HTCO method for dissolved organic carbon analysis in seawater: influence of catalyst on blank estimation. Mar. Chem. 47, 55–64.

Cauwet, G., 1999. Determination of dissolved organic carbon and nitrogen by high temperature combustion, in: Methods of Seawater Analysis. Wiley-VCH Verlag GmbH, pp. 407–420. doi:10.1002/9783527613984.ch15

Cottrell, M.T., Kirchman, D.L., 2000. Natural Assemblages of Marine Proteobacteria and Members of the Cytophaga-Flavobacter Cluster Consuming Low- and High-Molecular-Weight Dissolved Organic Matter. Appl. Environ. Microbiol. 66, 1692–1697. doi:10.1128/AEM.66.4.1692-1697.2000

Crespo, B.G., Pommier, T., Fernández-Gómez, B., Pedrós-Alió, C., 2013. Taxonomic composition of the particle-attached and free-living bacterial assemblages in the Northwest Mediterranean Sea analyzed by pyrosequencing of the 16S rRNA. Microbiologyopen 2, 541–52. doi:10.1002/mbo3.92

De Corte, D., Yokokawa, T., Varela, M.M., Agogué, H., Herndl, G.J., 2009. Spatial distribution of Bacteria and Archaea and amoA gene copy numbers throughout the water column of the Eastern Mediterranean Sea. ISME J. 3, 147–58. doi:10.1038/ismej.2008.94

Ducklow, H., 1999. The bacterial component of the oceanic euphotic zone. FEMS Microbiol. Ecol. 30, 1–10. doi:10.1016/S0168-6496(99)00031-8

Durrieu de Madron, X., Houpert, L., Puig, P., Sanchez-Vidal, a., Testor, P., Bosse, a., Estournel, C., Somot, S., Bourrin, F., Bouin, M.N., Beauverger, M., Beguery, L., Calafat, a., Canals, M., Cassou, C., Coppola, L., Dausse, D., D'Ortenzio, F., Font, J., Heussner, S., Kunesch, S., Lefevre, D., Le Goff, H., Martín, J., Mortier, L., Palanques, a., Raimbault, P., 2013. Interaction of dense shelf water cascading and open-sea convection in the northwestern Mediterranean during winter 2012. Geophys. Res. Lett. 40, 1379–1385. doi:10.1002/grl.50331

Edgar, R.C., 2010. Search and clustering orders of magnitude faster than BLAST. Bioinformatics 26, 2460–1. doi:10.1093/bioinformatics/btq461

Ghiglione, J.-F., Conan, P., Pujo-Pay, M., 2009. Diversity of total and active free-living vs. particle-attached bacteria in the euphotic zone of the NW Mediterranean Sea. FEMS Microbiol. Lett. 299, 9–21. doi:10.1111/j.1574-6968.2009.01694.x

Ghiglione, J.-F., Galand, P.E., Pommier, T., Pedrós-Alió, C., Maas, E.W., Bakker, K., Bertilson, S., Kirchmanj, D.L., Lovejoy, C., Yager, P.L., Murray, A.E., 2012. Pole-to-pole biogeography of surface and deep marine bacterial communities. Proc. Natl. Acad. Sci. U. S. A. 109, 17633–8. doi:10.1073/pnas.1208160109

Ghiglione, J.F., Mevel, G., Pujo-Pay, M., Mousseau, L., Lebaron, P., Goutx, M., 2007. Diel and seasonal variations in abundance, activity, and community structure of particle-attached and free-living bacteria in NW Mediterranean Sea. Microb. Ecol. 54, 217–31. doi:10.1007/s00248-006-9189-7

Ghiglione, J.F., Palacios, C., Marty, J.C., Mével, G., Labrune, C., Conan, P., Pujo-Pay, M., Garcia, N., Goutx, M., 2008. Role of environmental factors for the vertical distribution (0–1000 m) of marine bacterial communities in the NW Mediterranean Sea. Biogeosciences 5, 1751–1764. doi:10.5194/bg-5-1751-2008

Gogou, A., Sanchez-Vidal, A., Durrieu de Madron, X., Stavrakakis, S., Calafat, A.M., Stabholz, M., Psarra, S., Canals, M., Heussner, S., Stavrakaki, I., Papathanassiou, E., 2014. Carbon flux to the deep in three open sites of the Southern European Seas (SES). J. Mar. Syst. 129, 224–233. doi:10.1016/j.jmarsys.2013.05.013

Hansell, D. a, Carlson, C. a, 2001. Biogeochemistry of total organic carbon and nitrogen in the Sargasso Sea: control by convective overturn. Deep Sea Res. Part II Top. Stud. Oceanogr. 48, 1649–1667. doi:10.1016/S0967-0645(00)00153-3

Heimbürger, L.-E., Lavigne, H., Migon, C., D'Ortenzio, F., Estournel, C., Coppola, L., Miquel, J.-C., 2013. Temporal variability of vertical export flux at the DYFAMED time-series station (Northwestern Mediterranean Sea). Prog. Oceanogr. 119, 59–67. doi:10.1016/j.pocean.2013.08.005

Holmes, R.M., Aminot, A., Kérouel, R., Hooker, B. a, Peterson, B.J., 1999. A simple and precise method for measuring ammonium in marine and freshwater ecosystems. Can. J. Fish. Aquat. Sci. 56, 1801–1808. doi:10.1139/f99-128

Hoppe, H., 1983. Significance of exoenzymatic activities in the ecology of brackish water-measurements by means of methylumbelliferyl-substrates. Mar. Ecol. Prog. Ser. 11, 299–308.

Karner, M., DeLong, E., Karl, D., 2001. Archaeal dominance in the mesopelagic zone of the Pacific Ocean. Nature 409, 507–510.

Kirchman, D.L., 1993. Leucine incorporation as a measure of biomass production by heterotrophic bacteria, in: Kemp, P.F., Sherr, B.F., Sherrand, E.B., Cole, J.J. (Eds.), Handbook of Methods in Aquatic Microbial Ecology. pp. 509–512.

Lebaron, P., Servais, P., Agogué, H., Courties, C., Joux, F., 2001. Does the high nucleic acid content of individual bacterial cells allow us to discriminate between active cells and inactive cells in aquatic systems? Appl. Environ. Microbiol. 67, 1775–1782. doi:10.1128/AEM.67.4.1775

Legendre, L., Legendre, P., 1983. Numerical ecology, 3rd ed. Elsevier science B.V.

Marshall, J., Schott, F., 1999. Open ocean convection: Observations, theory, and models. Rev. Geophys. 37, 1–64.

Martín-Cuadrado, A.-B., López-García, P., Alba, J.-C., Moreira, D., Monticelli, L., Strittmatter, A., Gottschalk, G., Rodríguez-Valera, F., 2007. Metagenomics of the deep Mediterranean, a warm bathypelagic habitat. PLoS One 2, e914. doi:10.1371/journal.pone.0000914

Martinez, J., Smith, D., Steward, G., Azam, F., 1996. Variability in ectohydrolytic enzyme activities of pelagic marine bacteria and its significance for substrate processing in the sea. Aquat. Microb. Ecol. 10, 223–230.

Martini, S., Al Ali, B., Garel, M., Nerini, D., Grossi, V., Pacton, M., Casalot, L., Cuny, P., Tamburini, C., 2013. Effects of hydrostatic pressure on growth and luminescence of a moderately-piezophilic luminous bacteria Photobacterium phosphoreum ANT-2200. PLoS One 8, e66580. doi:10.1371/journal.pone.0066580

Martini, S., Nerini, D., Tamburini, C., n.d. Relation between deep bioluminescence and oceanographic variables : a statistical analysis using time-frequency decompositions. Prog. Oceanogr.

Massana, R., DeLong, E.F., Pedrós-Alió, C., 2000. A few cosmopolitan phylotypes dominate planktonic archaeal assemblages in widely different oceanic provinces. Appl. Environ. Microbiol. 66, 1777–1787. doi:10.1128/AEM.66.5.1777-1787.2000.Updated

Medoc Group, 1970. Observation of formation of deep water in the mediterranean sea. Nature 227, 1937–1040.

Mertens, C., Schott, F., 1998. Interannual Variability of Deep-Water Formation in the Northwestern Mediterranean. J. Phys. Oceanogr. 28, 1410–1424. doi:10.1175/1520-0485(1998)028<1410:IVODWF>2.0.CO;2

Millot, C., 1999. Circulation in the Western Mediterranean Sea. J. Mar. Syst. 20, 423–442. doi:10.1016/S0924-7963(98)00078-5

Moeseneder, M.M., Winter, C., Herndl, G.J., 2001. Horizontal and vertical complexity of attached and free-living bacteria of the eastern Mediterranean Sea , determined by 16S rDNA and 16S rRNA fingerprints. Limnol. Oceanogr. 46, 95–107. doi:10.4319/lo.2001.46.1.0095

Morris, R.M., Vergin, K.L., Rappe, M.S., Carlson, C.A., Giovannoni, S.J., 2005. Temporal and spatial response of bacterioplankton lineages to annual convective overturn at the Bermuda Atlantic Time-series Study site. Limnol. Oceanogr. 50, 1687–1696.

Nagata, T., Tamburini, C., Arístegui, J., Baltar, F., Bochdansky, A.B., Fonda-Umani, S., Fukuda, H., Gogou, A., Hansell, D. a., Hansman, R.L., Herndl, G.J., Panagiotopoulos, C., Reinthaler, T., Sohrin, R., Verdugo, P., Yamada, N., Yamashita, Y., Yokokawa, T., Bartlett, D.H., 2010. Emerging concepts on microbial processes in the bathypelagic ocean – ecology, biogeochemistry, and genomics. Deep Sea Res. Part II Top. Stud. Oceanogr. 57, 1519–1536. doi:10.1016/j.dsr2.2010.02.019

Najdek, M., Paliaga, P., Šilović, T., Batistić, M., Garić, R., Supić, N., Ivančić, I., Ljubimir, S., Korlević, M., Jasprica, N., Hrustić, E., Dupčić-Radić, I., Blažina, M., Orlić, S., 2014. Picoplankton community structure before, during and after convection event in the offshore waters of the Southern Adriatic Sea. Biogeosciences 11, 2645–2659. doi:10.5194/bg-11-2645-2014

Pommier, T., Neal, P., Gasol, J., Coll, M., Acinas, S., Pedrós-Alió, C., 2010. Spatial patterns of bacterial richness and evenness in the NW Mediterranean Sea explored by pyrosequencing of the 16S rRNA. Aquat. Microb. Ecol. 61, 221–233. doi:10.3354/ame01484

Pujo-Pay, M., Conan, P., Raimbault, P., 1997. Excretion of dissolved organic nitrogen by phytoplankton assessed by wet oxidation and 1 5 N tracer procedures. Mar. Ecol. Prog. Ser. 153, 99–111.

Pujo-Pay, M., Raimbault, P., 1994. Improvement of the Wet-Oxidation Procedure for Simultaneous Determination of Particulate Organic Nitrogen and Phosphorus Collected on Filters. Mar. Ecol. Prog. Ser. 105, 203–207. doi:10.3354/meps105203

Pulido-Villena, E., Ghiglione, J.-F., Ortega-Retuerta, E., Van Wambeke, F., Zohary, T., 2012. Heterotrophic bacteria in the pelagic realm of the mediterranean sea, in: Stambler, N. (Ed.), Life in the Mediterranean Sea: A Look at Habitat Changes. pp. 227–265.

Quince, C., Lanzen, A., Davenport, R.J., Turnbaugh, P.J., 2011. Removing noise from pyrosequenced amplicons. BMC Bioinformatics 12, 38. doi:10.1186/1471-2105-12-38

Rodríguez-Blanco, A., Ghiglione, J.-F., Catala, P., Casamayor, E.O., Lebaron, P., 2009. Spatial comparison of total vs. active bacterial populations by coupling genetic fingerprinting and clone library analyses in the NW Mediterranean Sea. FEMS Microbiol. Ecol. 67, 30–42. doi:10.1111/j.1574-6941.2008.00591.x

Santinelli, C., Nannicini, L., Seritti, A., 2010. DOC dynamics in the meso and bathypelagic layers of the Mediterranean Sea. Deep Sea Res. Part II Top. Stud. Oceanogr. 57, 1446–1459. doi:10.1016/j.dsr2.2010.02.014

Sarmento, H., Gasol, J., 2012. Use of phytoplankton derived dissolved organic carbon by different types of bacterioplankton. Environ. Microbiol. 14, 2348–2360.

Schroeder, K., Gasparini, G.P., Borghini, M., Cerrati, G., Delfanti, R., 2010. Biogeochemical tracers and fluxes in the Western Mediterranean Sea, spring 2005. J. Mar. Syst. 80, 8–24. doi:10.1016/j.jmarsys.2009.08.002

Send, U., Marshall, J., 1995. Integral effects of deep convection. J. Phys. Oceanogr. 25, 855–872.

Severin, T., Conan, P., Durrieu De Madron, X., Houpert, L., Oliver, M.J., Oriol, L., Caparros, J., Pujo-Pay, M., Submitted. Impact of open-ocean convection on nutrient, phytoplankton biomass and activity. Deep Sea Res. Part I Oceanogr. Res. Pap.

Stabholz, M., Durrieu de Madron, X., Canals, M., Khripounoff, A., Taupier-Letage, I., Testor, P., Heussner, S., Kerhervé, P., Delsaut, N., Houpert, L., Lastras, G., Dennielou, B., 2013. Impact of open-ocean convection on particle fluxes and sediment dynamics in the deep margin of the Gulf of Lions. Biogeosciences 10, 1097–1116. doi:10.5194/bg-10-1097-2013

Strickland, J.D.H., Parsons, T.R., 1997. A Practical Handbook of Seawater Analysis, Internationale Revue der gesamten Hydrobiologie und Hydrographie. Ottawa, Fisheries Research Board of Canada, Bulletin 167.

Sugimura, Y., Suzuki, Y., 1988. A high-temperature catalytic oxidation method for the determination of non-volatile dissolved organic carbon in seawater by direct injection of a liquid sample. Mar. Chem. 24, 105–131. doi:10.1016/0304-4203(88)90043-6

Sun, Y., Wolcott, R., Dowd, S., 2011. Tag-Encoded FLX Amplicon Pyrosequencing for the Elucidation of Microbial and Functional Gene Diversity in Any Environment, in: Kwon, Y.M., Ricke, S.C. (Eds.), High-Throughput Next Generation Sequencing SE - 9, Methods in Molecular Biology. Humana Press, pp. 129–141. doi:10.1007/978-1-61779-089-8_9

Tamburini, C., Canals, M., Durrieu de Madron, X., Houpert, L., Lefèvre, D., Martini, S., D'Ortenzio, F., Robert, A., Testor, P., Aguilar, J.A., Samarai, I. Al, Albert, A., André, M., Anghinolfi, M., Anton, G., Anvar, S., Ardid, M., Jesus, A.C.A., Astraatmadja, T.L., Aubert, J.-J., Baret, B., Basa, S., Bertin, V., Biagi, S., Bigi, A., Bigongiari, C., Bogazzi, C., Bou-Cabo, M., Bouhou, B., Bouwhuis, M.C., Brunner, J., Busto, J., Camarena, F., Capone, A., Cârloganu, C., Carminati, G., Carr, J., Cecchini, S., Charif, Z., Charvis, P., Chiarusi, T., Circella, M., Coniglione, R., Costantini, H., Coyle, P., Curtil, C., Decowski, P., Dekeyser, I., Deschamps, A., Donzaud, C., Dornic, D., Dorosti, H.Q., Drouhin, D., Eberl, T., Emanuele, U., Ernenwein, J.-P., Escoffier, S., Fermani, P., Ferri, M., Flaminio, V., Folger, F., Fritsch, U., Fuda, J.-L., Galatà, S., Gay, P., Giacomelli, G., Giordano, V., Gómez-González, J.-P., Graf, K., Guillard, G., Halladjian, G., Hallewell, G., van Haren, H., Hartman, J., Heijboer, A.J., Hello, Y., Hernández-Rey, J.J., Herold, B., Hößl, J., Hsu, C.-C., de Jong, M., Kadler, M., Kalekin, O., Kappes, A., Katz, U., Kavatsyuk, O., Kooijman, P., Kopper, C., Kouchner, A., Kreykenbohm, I., Kulikovskiy, V., Lahmann, R., Lamare, P., Larosa, G., Lattuada, D., Lim, G., Presti, D. Lo, Loehner, H., Loucatos, S., Mangano, S., Marcelin, M., Margiotta, A., Martinez-Mora, J.A., Meli, A., Montaruli, T., Moscoso, L., Motz, H., Neff, M., Nezri, E.N., Palioselitis, D., Păvălaş, G.E., Payet, K., Payre, P., Petrovic, J., Piattelli, P., Picot-Clemente, N., Popa, V., Pradier, T., Presani, E., Racca, C., Reed, C., Riccobene, G., Richardt, C., Richter, R., Rivière, C., Roensch, K., Rostovtsev, A., Ruiz-Rivas, J., Rujoiu, M., Russo, V.G., Salesa, F., Sánchez-Losa, A., Sapienza, P., Schöck, F., Schuller, J.-P., Schussler, F., Shanidze, R., Simeone, F., Spies, A., Spurio, M., Steijger, J.J.M., Stolarczyk, T., Taiuti, M.G.F., Toscano, S., Vallage, B., Van Elewyck, V., Vannoni, G., Vecchi, M., Vernin, P., Wijnker, G., Wilms, J., de Wolf, E., Yepes, H., Zaborov, D., De Dios Zornoza, J., Zúñiga, J., 2013. Deep-sea bioluminescence blooms after dense water formation at the ocean surface. PLoS One 8, e67523. doi:10.1371/journal.pone.0067523

Tamburini, C., Garel, M., Al Ali, B., Mérigot, B., Kriwy, P., Charrière, B., Budillon, G., 2009. Distribution and activity of Bacteria and Archaea in the different water masses of the Tyrrhenian Sea. Deep Sea Res. Part II Top. Stud. Oceanogr. 56, 700–712. doi:10.1016/j.dsr2.2008.07.021

Tanaka, T., Rassoulzadegan, F., 2002. Full-depth profile (0–2000m) of bacteria, heterotrophic nanoflagellates and ciliates in the NW Mediterranean Sea: vertical partitioning of microbial trophic structures. Deep Sea Res. Part II Top. Stud. … 49, 2093–2107. doi:10.1016/S0967-0645(02)00029-2

Tanaka, T., Rassoulzadegan, F., 2004. Vertical and seasonal variations of bacterial abundance and production in the mesopelagic layer of the NW Mediterranean Sea: bottom-up and top-down controls. Deep Sea Res. Part I Oceanogr. Res. Pap. 51, 531–544. doi:10.1016/j.dsr.2003.12.001

Teeling, H., Fuchs, B.M., Becher, D., Klockow, C., Gardebrecht, A., Bennke, C.M., Kassabgy, M., Huang, S., Mann, A.J., Waldmann, J., Weber, M., Klindworth, A., Otto, A., Lange, J., Bernhardt, J., Reinsch, C., Hecker, M., Peplies, J., Bockelmann, F.D., Callies, U., Gerdts, G., Wichels, A., Wiltshire, K.H., Glöckner, F.O., Schweder, T., Amann, R., 2012. Substrate-controlled succession of marine bacterioplankton populations induced by a phytoplankton bloom. Science 336, 608–11. doi:10.1126/science.1218344

Turchetto, M., Boldrin, a., Langone, L., Miserocchi, S., 2012. Physical and biogeochemical processes controlling particle fluxes variability and carbon export in the Southern Adriatic. Cont. Shelf Res. 44, 72–82. doi:10.1016/j.csr.2011.05.005

Van Wambeke, F., Heussner, S., Diaz, F., Raimbault, P., Conan, P., 2002. Small-scale variability in the coupling/uncoupling of bacteria, phytoplankton and organic carbon fluxes along the continental margin of the Gulf of Lions, Northwestern. J. Mar. Syst. 34, 411–429.

Wang, Q., Garrity, G.M., Tiedje, J.M., Cole, J.R., 2007. Naive Bayesian classifier for rapid assignment of rRNA sequences into the new bacterial taxonomy. Appl. Environ. Microbiol. 73, 5261–7. doi:10.1128/AEM.00062-07

Winter, C., Kerros, M.-E., Weinbauer, M.G., 2009. Seasonal changes of bacterial and archaeal communities in the dark ocean: Evidence from the Mediterranean Sea. Limnol. Oceanogr. 54, 160–170. doi:10.4319/lo.2009.54.1.0160

Supplementary information

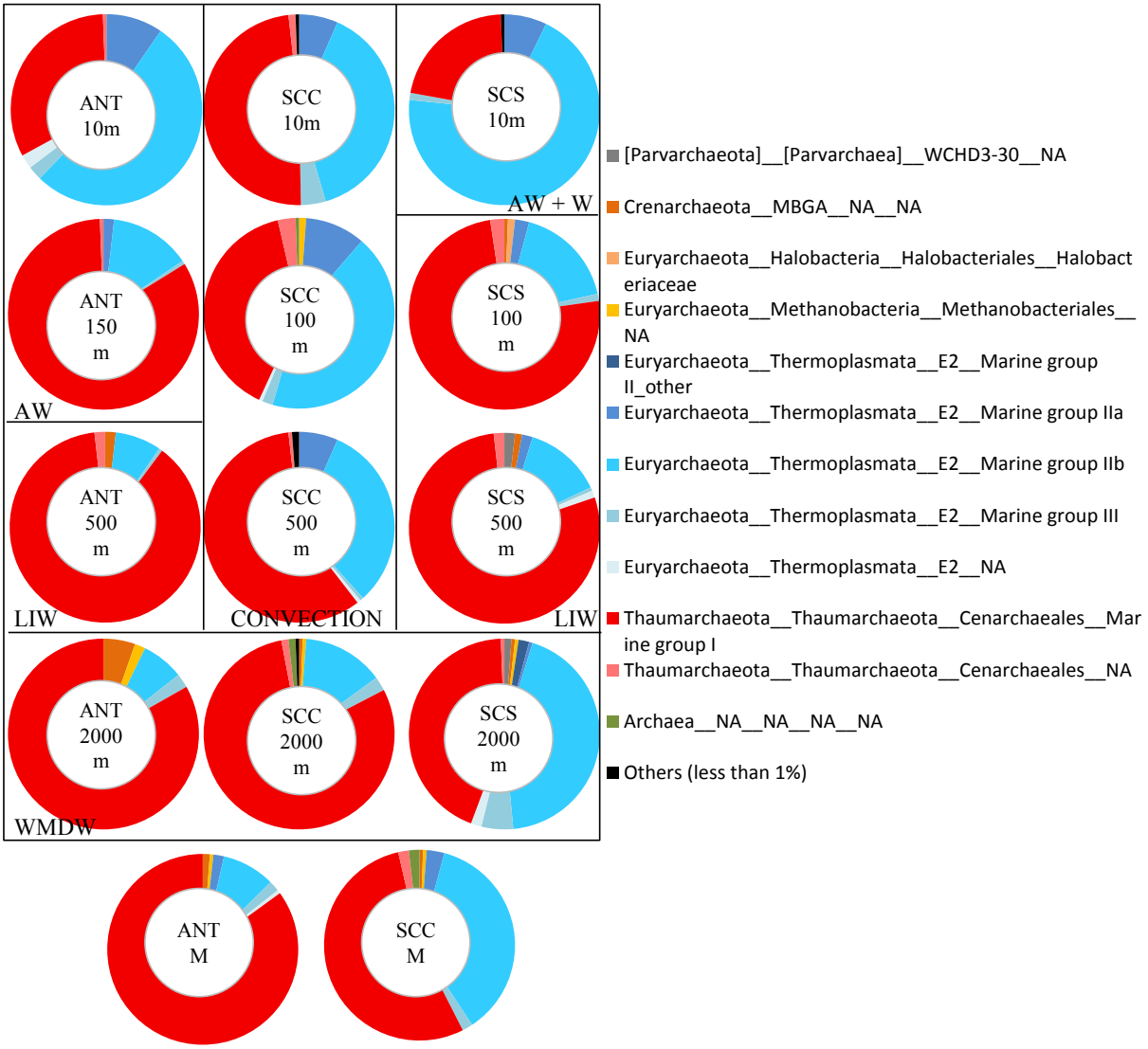

Figure S1: Taxonomic distribution (Phylum_Class_Order_Family) for OTUs that occurred more than 2 times (>1%) from the Archaea OTU table and the model. The remaining sequences are grouped in « other ». Taxonomy not assigned is symbolyzed by NA. The water masses of the samples are noted in black

III.3. Préambule

Dans le 2ème article, les résultats taxonomiques ont mis en évidence l'ubiquisme des SAR11 chez les bactéries dans la colonne d'eau, et des Marine Group I *Thaumarchaeota* (MGI) et Marine Group II *Euryarchaeota* (MGII) chez les archées. L'abondance relative des SAR11 s'élevait à 24-43% de la communauté bactérienne totale, les MGI contribuaient entre 22 et 92% de la communauté archée totale, et les MGII entre 4 et 77% de la communauté archée totale (Figure III-1). Leur distribution verticale était généralement conditionnée par les différentes masses d'eaux. L'omniprésence de ces clades le long de la colonne d'eau suggère une plasticité métabolique et fonctionnelle permettant aux organismes de s'adapter à des milieux environnementaux différents. Cette plasticité est reflétée par la présence de plusieurs écotypes au sein des SAR11 (Vergin et al., 2013), MGI (Massana et al., 2000) et MGII (Galand et al., 2010; Hugoni et al., 2013). La définition actuelle des écotypes consiste en *des groupes écologiques distincts appartenant à des lignées génétiquement cohésives et irréversiblement séparées d'un point de vue de leur évolution, et qui n'ont été inventées qu'une seule fois* (de Queiroz, 2005; Gevers et al., 2005; Cohan and Perry, 2007; Koeppel et al., 2008). D'après Cohan et Perry (2007) et Shapiro et Poltz (2014), un nouvel écotype apparait lorsqu'une *mutation adaptative, innovante et compétitive permet à l'organisme de coloniser une nouvelle niche écologique, empêchant donc toute compétition avec les autres organismes dont il s'est différencié*.

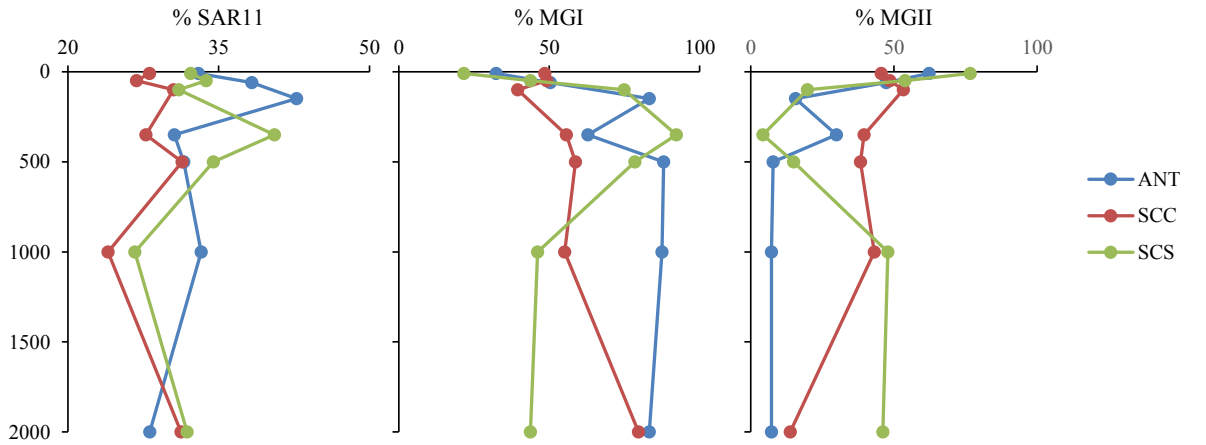

Figure III-1 : Pourcentage de contribution relative des (A) SAR11 à la population bactérienne totale, (B) des Marine Group I et (C) Marine Group II à la population totale d'archées le long de la colonne d'eau, à la station de référence Antares située en dehors de la convection (bleu), à la station centrale SC pendant la convection (SCC, rouge) et après restratification de la colonne d'eau (SCS, vert) lors de la campagne CASCADE.

L'ubiquiste clade des SAR11 est le groupe phylogénétique le plus abondant dans les océans, avec un total qui s'élèverait à 2.4 10^{28} cellules (Morris et al., 2002). La phylogénie de ce clade a montré la présence de plusieurs sous-clades correspondant à des écotypes spécialisés selon les saisons et dans les différents couches de la colonne d'eau (eaux de surface et profondes) (Field et al., 1997; Vergin et al., 2013). MGI et MGII sont les clades des archées les plus répandus dans le milieu marin et la présence de plusieurs écotypes dans chacun de ces clades a été précédemment démontrée (García-Martínez and Rodríguez-Valera, 2000; Massana et al., 2000). Dans le 2ème article, MGI est plus abondant dans les eaux profondes (Figure III-1), ce qui va dans le sens de précédentes études réalisées en Méditerranée (Galand et al., 2010; Hugoni et al., 2013). MGII est généralement dominant dans les eaux de surface (Galand et al., 2010) tout comme dans notre étude. Cependant, la distribution relative de chacun de ces clades a été largement modifiée suite au mélange convectif (Figure III-1), suggérant un réarrangement des écotypes au sein de chacun des clades.

Dans le 3ème article, nous avons voulu tester la validité des écotypes de SAR11, MGI et MGII, en vérifiant que le principe fondamental du concept d'écotype soit respecté : *un écotype d'un groupe taxonomique particulier ne peut coloniser qu'une seule niche écologique* (Shapiro and Polz, 2014). Dans notre étude, le processus de convection a été utilisé comme modèle de turbulence physique homogénéisant toute la colonne d'eau, et donc annihilant momentanément les niches écologiques, ainsi que toute structuration verticale des communautés procaryotes. Les niches écologiques des stations ANT, SCC et SCS ont été définies le long de la colonne d'eau par des outils statistiques robustes (PCA, Principal Correspondence Analysis, puis classification hiérarchique) à partir des variables environnementales physiques et biogéochimiques. A la station de référence ANT, la distribution des écotypes des 3 clades (listés dans le tableau S1 de l'article 3) était en accord avec leurs niches écologiques signalées dans la littérature. Cinq jours après la convection, nous avons pu observer un retour des écotypes dans leurs niches écologiques respectives. La force des associations entre les OTUs, et avec les paramètres environnementaux a été calculée via le coefficient d'information maximal (MIC, Maximal Information Coefficient). Cette approche obéit à la définition de base d'une étude « écologique », définie comme l'étude des interactions des organismes entre eux et avec leur environnement. Les relations ainsi mises en évidence ont permis de confirmer la répartition des écotypes en période stratifiée dans principalement 2 niches écologiques : la niche de surface (0-150 m) et la niche de fond (350-2000 m). Pour les 3 clades, les écotypes de surface étaient fortement associés à la concentration de matière organique, alors que les écotypes de fond étaient associés aux concentrations en sels nutritifs et carbone inorganique dissous (DIC,

Dissolved Inorganic Carbon). La capacité de fixer du bicarbonate est connue pour le clade des MGI (Berg et al., 2007; Tully et al., 2012), mais un tel métabolisme n'a pas été découvert ni chez les SAR11, ni chez les MGII (Martin-Cuadrado et al., 2008; Cameron et al., 2014). Pour finir, la coexistence dans une même niche des subclades SAR11 Ia, IIa et IV, mais aussi de MGIa, MGIb et MGIIb_O, MGIIb_P, MGIIb_Q remet en question leur titre d'« écotype ».

III.4. Article 3: Vertical niche partitioning of marine bacterial (SAR11) and archaeal (Marine group I and II) ecotypes in response to physical turbulence

T. Severin[a,b], P.E. Galand[a,c], L. Oriol[a,b], J. Caparros[a,b], M. Pujo-Pay[a,b], X. Durrieu de Madron[d], P. Conan[a,b], and J.F. Ghiglione[a,b*].

[a]Sorbonne Universités, UPMC Univ Paris 06, UMR 7621, Laboratoire d'Océanographie Microbienne, UMR 8222, LECOB, Observatoire Océanologique, F-66650 Banyuls/mer, France

[b]CNRS, UMR 7621, Laboratoire d'Océanographie Microbienne, Observatoire Océanologique, F-66650 Banyuls/mer, France

[c]CNRS, UMR 8222, LECOB, Observatoire Océanologique, F-66650 Banyuls-sur-Mer,

France.

[d]CEFREM, UMR 5110, CNRS-UPVD, F-66860, Perpignan, France

[*]**Corresponding author**:

J.F. Ghiglione, Laboratoire d'Océanographie Microbienne, Observatoire Océanologique, Avenue du Fontaulé, F-66650 Banyuls/mer, France. Tel.: + 33 (0) 4 68 88 73 16. E-mail address: ghiglione@obs-banyuls.fr

Abstract

The dynamic of SAR11, Marine Group I *Thaumarchaeota* (MGI) and Marine Group II *Euryarchaeota* (MGII) subclades was studied to evaluate their vertical niche partitioning in the open NW Mediterranean Sea. We used the opportunity of an intense convection that temporarily mixed the water column down to 1500m to evaluate the dynamic of these ecotypes in relation to the disturbance of their potential ecological niches. Most of the subclades were assigned to either surface (SAR11 IIa and IV, MGIa and Ib, MGIIa and IIb WHARN) or deep waters (SAR11 Ic, IIb, Vb, MGIc, MGIIb_O, IIb_P and IIb_Q). Multivariate statistical analysis showed clear relationships between surface ecotypes and the concentration of organic matter, whereas deep ecotypes were associated to nutrient and dissolved inorganic carbon concentrations. The convection episode resulted in a strong homogenization of the SAR11, MGI and MGII ecotypes. Interestingly, we observed a rapid return of most of the ecotypes to their respective niches 5 days after the convection episode. The ubiquity of some subclades (SAR11 Ia, IIb, and MGII O, P and Q) call their ecotype affiliation into question. This study give new insights on the dynamic and strength of bacterial and archaeal ecotypes, which are necessary to better understand microbial community ecology in marine ecosystems.

Keywords: ecotype, SAR11, Marine group I *Thaumarchaeota*, Marine group II *Euryarchaeota*, open-ocean convection, Northwestern Mediterranean

1. Introduction

Understanding microbial community ecology is a difficult task because of the enormous number of species and ecological roles played by microorganisms (Yokokawa and Nagata, 2010) and due to our inability to cultivate only a small fraction of the species constituting a community (Epstein, 2013). Moreover, defining microbial species is a challenge and a critical concept which remains controversial (Rosselló-Mora, 2003; de Queiroz, 2005; Polz et al., 2013). In the actual microbial systematic, a species unit may have several ecological functions, a concept which hinder microbial ecologists from identifying the ecological fundamental units within prokaryotic species (Koeppel et al., 2008; Yokokawa and Nagata, 2010; Shapiro and Polz, 2014). The ecotype concept emerged from the need to formally define "ecologically distinct groups belonging to genetically cohesive and irreversibly separate evolutionary lineages, that they were each invented only once" (Koeppel et al., 2008). A new ecotype emerges when an innovative and competitive adaptive mutation allows the organism to colonize a novel ecological niche, limiting any competition with the others organisms from whom it differentiated (Cohan, 2006). Several authors suggested that some ecotypes may be used as marker of specific ecological niches (Ward et al., 2008). This is the case for two marine ecotypes of *Prochlorococcus* sp., one ecotype living in deep water is adapted to weak irradiances, whereas the other 'surface ecotype' is adapted to elevated irradiances and acquired a gene involved in the degradation of organic matter rich in phosphorus (Rocap et al., 2003), which is quasi absent from deep water masses (Robinson et al., 2010).

Microbiologists agreed on the use of phylogeny to identify ecotypes on the basis of microbial subclades (Cohan and Perry, 2007; Koeppel et al., 2008; Shapiro and Polz, 2014). Once subclades are identified, they may be defined as ecotype through their association to a single ecological niche or by their unique ecological function (Cohan and Perry, 2007; Shapiro and Polz, 2014). Few examples exist in marine waters, mainly on the *Cyanobacteria* and SAR11 clade (Rocap et al., 2003; Ward et al., 2006; Carlson et al., 2009; Vergin et al., 2013).

The SAR11 clade is a phylogenetic group that dominates marine bacterial communities representing >25% of the bacteria in the Sargasso Sea (Giovannoni and Rappé, 2000), 35% in the Atlantic ocean (Morris et al., 2002), and ~31% in the Northwestern Mediterranean Sea (Rodríguez-Blanco et al., 2009), for a total of 2.4 10^{28} SAR11 cells estimated in the oceans (Morris et al., 2002). SAR11 has been divided into 10 different subclades (Vergin et al., 2013). Each of these subclades have been defined as ecotypes due to their spatio-temporal niches specialization (Field et al., 1997; Carlson et al., 2009). Three SAR11 ecotypes are encountered

only in deep waters, while three others are specialized in the surface summer niche. One ecotype bloom in surface during the fall, and two other during spring (supplementary Table S1). Moreover, some surface SAR11 from the Atlantic Ocean have the ability to assimilate free dissolved amino acids and dimethylsulfoniopropionate (DMSP) (Malmstrom et al., 2004; Mou et al., 2007), two products present mainly in surface waters due to their marine phytoplankton origin (Kiene and Linn, 2000). But these capacity have not been assigned specifically to one of the surface ecotype.

Archaea defined as extremophile organisms only (Woese, 1987), are now recognized to be widespread in the ocean (Delong, 1992; Fuhrman et al., 1992). Marine group I *Thaumarchaeota* (MGI) and Marine group II *Euryarchaeota* (MGII) are the most abundant archaeal clades in marine environments (Massana et al., 1997, 2000) and account to >40-60% of the prokaryotes communities in California and Mediterranean waters (Fuhrman and Ouverney, 1998). MGI clade is predominant at depths (Massana et al., 2000; Herndl et al., 2005; Teira et al., 2008) and is composed of organisms able to assimilate both dissolved amino acids (Ouverney and Fuhrman, 2000; Teira et al., 2006) and dissolved carbon dioxide (Wuchter et al., 2003; Herndl et al., 2005; Ingalls et al., 2006), and some are capable to oxidize ammonia to nitrite (Francis et al., 2005). The MGII clade predominates in surface waters (Massana et al., 2000; Galand et al., 2010). Some MGII organisms have a proteorhodopsin gene, suggesting that they could use light as an additional energy source (Frigaard et al., 2006; Iverson et al., 2012). Phylogenetic analysis of both MGI and MGII clades revealed the presence of several subclades (Massana et al., 2000), which were assigned to ecotypes because of their specific spatio-temporal distributions (García-Martínez and Rodríguez-Valera, 2000; Galand et al., 2010; Hugoni et al., 2013). Some divergence where found between surface and deep ammonia oxidizer MGI ecotypes based on their ability to acclimate to medium ammonia concentrations in shallow waters and to low ammonia concentrations in deep waters (Sintes et al., 2013), without related them to the pre-defined MGI ecotypes. In general, relationship between the presence of given archaeal subclades and the physico-chemical properties of ecological niches remained to be investigated to validate their potential distinction as ecotypes.

On the basis of the ecological concept defining an ecotype as a subclade of a given phylogenetic group that colonize an ecological niche, this paper aims to conciliate *in situ* physico-chemical observations with the vertical distribution of SAR11, MGI and MGII subclades, the most abundant and widespread bacterial and archaeal clades. We used an intense convection episode that temporarily mixed down the water column to 1500 m as a physical turbulence of a well stratified system, to test if a phylogenetically based subclades separation

corresponded to ecotype definitions. By using 16S rRNA pyrosequencing-based analysis, we compared the distribution of SAR11, MGI and MGII subclades along depth profiles at a reference well-stratified station situated outside of a convective mixing (ANT), at a station convectively mixed down to 1500 m depth (SCC) and at the same station re-stratified 5 days after the convection event (named SCS).

2. Materials and Methods

2.1 Study area and sampling strategy

The CASCADE cruise (Cascading, Surge, Convection, Advection and Downwelling Events) was carried out in the Northwestern Mediterranean Sea from the 04 to 23 March 2011 aboard the R/V *L'Atalante*. At each station, water samples were collected at 10 levels with 12L Niskin bottles mounted on a SBE 32 Carousel water sampler equipped with a Seabird 911Plus CTD profiler. For this study, samples for SAR11, Marine Group I *Thaumarchaeota* (MGI), and Marine Group II *Euryarchaeota* (MGII) ecotypes diversities analysis were selected from seven depths all over the water column (10, 50, 100, 350, 500, 1000, and 2000 m) at three typical stations of the Northwestern Mediterranean Sea. Antares station (Astronomy with a Neutrino Telescope and Abyss environmental RESearch localized at 42°48.200' N - 06°04.500' E, noted ANT) sampled the 2 March 2011, was used as a pre-convection ecosystem reference in this study. The SC station, centered in the MEDOC area at 42°1.900' E - 04°41.800' E (Medoc Group, 1970), had been sampled twice the 4 March (noted SCC for SC in Convection) and the 9 March 2011 (noted SCS for SC Stratified).

2.2 Chemical analysis and statistics

Nutrient concentrations (silicate ± 0.05µM, nitrate ± 0.02µM, nitrite ± 0.01µM and phosphate ± 0.01µM) were estimated from samples immediately filtered on board (0.45µm cellulose acetate filters) and stored in 20 ml polyethylene vials at -20°C until analysis. In the laboratory, samples were analyzed by colorimetry on a Seal-Bran-Luebbe autoanalyzer AA3 HR (Aminot and Kérouel, 2007). Ammonium concentrations (NH_4 ± 2nM) were determined on board by nanomolar fluorometric method (Holmes et al., 1999) on a fluorometer Jasco FP-2020.

Samples for dissolved organic matter (DOM) were collected from the Niskin bottles in combusted glass bottles. They were immediately filtered on board through 2 precombusted (24

h, 450°C) glass fiber filters (Whatman GF/F, 25 mm). Samples for dissolved organic carbon (DOC), were acidified with orthophosphoric acid (H_3PO_4) and stored into in precombusted glass tubes. At the laboratory, they were immediately analyzed by high temperature catalytic oxidation (HTCO) (Sugimura and Suzuki, 1988; Cauwet, 1994, 1999) on a Shimadzu TOC L analyzer. Samples for dissolved organic nitrogen (DON) and phosphorus (DOP), collected in Teflon vials, were immediately frozen and then analyzed at the laboratory by persulfate wet-oxidation (Pujo-Pay and Raimbault , 1994; Pujo-Pay et al., 1997).

Particulate organic Carbon (POC), nitrogen (PON) and phosphorus (POP) were filtered on precombusted (24 h, 450°C) glass fiber filters (Whatman GF/F, 25 mm). Filters were dried overnight at 50°C, then stored in ashed glass vial in a dessicator. At the laboratory, POC and PON where simultaneously analyzed according to the wet oxidation method (Pujo-Pay and Raimbault, 1994). POC samples were analysed on a CHN Perkin Elmer 2400.

For total chlorophylls a (Chla) and phaeopigments a (Phae; pigment of Chla degradation), 250 ml of seawater were filtered on Whatman GF/F 25mm glass fiber filters, then filters were stored at -80°C. After extraction by 90% acetone, Chla and Phae concentrations were measured by fluorometry on a Turner Design 10-AU fluorometer (Strickland and Parsons, 1997).

In order to delimit the environmental groups along the water column at each sampled station, we used a principal correspondence analysis (PCA) followed by a hierarchical cluster analysis (agglomeration method of ward) using the R software. At each station, a spearman rank correlations between the non-transformed environmental parameters (physical and biogeochemical) helped us to choose the significant variables for the PCA. The samples coordinates of the 2 first axes which explained more than 70% of the variance, were extracted to calculate the Euclidian distances and were used to build hierarchical clustering using the agglomeration method of ward.

2.3 Prokaryotic sampling and sequencing

Samples for prokaryotic diversity were collected with 2 L acid cleaned (HCl) polycarbonate bottles. They were sequentially filtered on board through 2 µm and 0.2 µm (free-living fraction) pore-size polycarbonate filters (47 mm diameter) using a peristaltic pump under low pressure (<100 mbar). Filters were stored at -80°C. DNA extractions were performed as previously described (Ghiglione et al., 2009) using an AllPrep DNA/RNA mini kit (Qiagen).

DNA from the free-living fraction (0.2 µm filters) were analyzed by prokaryote tag-encoded FLX amplicon pyrosequencing (bTEFAP) using Gray926F (5′-AAACTYAAAKGAATTGRCGG-3′) and Gray1392R (5′-ACGGGCGGTGTGTRC-3′), which amplify V6, V7 and V8 regions of the 16S rRNA gene (Sun et al., 2011). A one-step PCR was performed and tag-encoded FLX amplicon pyrosequencing analyses were completed using the Roche 454 FLX instrument with Titanium reagents. Procedures were performed at the Research and Testing Laboratory (Lubbock, TX) based upon RTL protocols.

2.4 Sequence analyses

In order to divide our environmental sequences into SAR11, MGI and MGII subclades we used full-length 16S rRNA reference sequences from the Greengenes database. Reference sequences identified at a >97% similarity level as *Rickettsiales*, Marine Group I *Thaumarchaeota*, and Marine Group II *Euryarchaeota* were extracted from Greengenes database. For each taxonomic group, Greengenes sequences were aligned together with previously published full-length 16S rRNA sequences defined as ecotype of SAR11, MGI and MGII with MUSCLE (Edgar, 2004). Aligned sequences were cut to a same length and trees were built in PHYLIP (PHYLogeny Inference Package) (Felsenstein, 1989) with the neighbor-joining method using the Kimura distance estimation (Marine Group I and II, phylogenetic) or in QIIME using FastTree (Price et al., 2009) (*Rickettsiales*). Greengenes sequences were annotated according to their closest reference ecotype sequence (Cohan and Perry, 2007; Cohan, 2006). Our own *Rickettsiales*, MGI and MGII databases were created using the 16S sequences Greengenes sequences newly annotated.

Environmental sequences were processed and analyzed using the QIIME pipeline (Caporaso et al., 2010). There were denoised using the AmpliconNoise pipeline and chimera checked was done using Perseus (Quince et al., 2011). The resulting cleaned sequences were clustered using operational taxonomic units (OTUs) defined at a 97% sequence identity level using the UCLUST algorithm (Edgar, 2010). A representative sequence from each OTU was taxonomically classified using the Ribosomal Database Project (RDP) classifier (Wang et al., 2007) using our own newly designed Greengenes databases. OTUs from Bacteria and Archaea were separated resulting in 2 different OTU tables, and subsampled at 3372 and 167 sequences respectively, using NumPy from the Mersenne twister PRNG implemented in QIIME pipeline. OTUs of SAR11, MGI, and MGII were isolated resulting in 3 different OTU tables. To enable comparison between samples for each OTU table, OTUs were normalized by the total numbers

of sequences in each sample. All OTU and diversity analyses were performed on the normalized OTU tables of SAR11, MGI, and MGII.

2.5 Diversity and statistical analyses

Similarity matrices of Bray-Curtis were calculated for each OTU table to compare ecotypes community structures, and were used to build dendrograms by the unweighted-pair group method with arithmetic averages (UPGMA). A similarity profile test (SIMPROF, PRIMER 6) was performed on a null hypothesis that a specific sub-cluster can be recreated by permuting the entry species and samples. The significant branch (SIMPROF, $p < 0.05$) was used as a prerequisite for defining ecotypes clusters. One-way analysis of similarity (ANOSIM, PRIMER 6) was performed on the same distance matrix to test the null hypothesis that there was no difference between ecotypes communities of different clusters.

To investigate the relationships between ecotypes community structures and environmental parameters, we used a canonical correspondence analysis (CCA) using the software package CANOCO, version 4.5 for Windows, as previously described (Berdjeb et al., 2011). Environmental parameters were transformed according to their pairwise distributions (Legendre and Legendre, 1983), then spearman rank pairwise correlations between the transformed environmental variables helped to determine their significance. To statistically evaluate the significance of the canonical axes, we used a Monte Carlo permutation full model test with 199 unrestricted permutations. Significant variables were chosen using a forward-selection procedure of 999 permutations, and explanatory variables were added until further addition of variables failed to contribute significantly ($p < 0.05$) to a substantial improvement to the model's explanatory power.

To identify possible associations between individual OTUs and the significant environmental parameters determined with the CCA, we calculated the maximal information coefficient (MIC) using the MINE package (Reshef et al., 2011). False discovery rates were calculated from an empirical null distribution with the R package fdrtool (Strimmer, 2008) using the locfdr method (Efron, 2004). An association was considered significant when false discovery rate was < 60%, that was equivalent to MIC >0.55 for SAR11 ecotypes, and to >0 for MGI and MGII ecotypes. The significant MIC matrix was exported to Cytoscape 3.0.2 (Shannon et al., 2003) to visualized the network of association where ecotypes OTUs and environmental parameters are represented as node, connected by lines proportional to the pairwise associations (a strong association will be visualized by a short edge).

Statistical analyses were done using R software (version 3.0.1, http://www.R-project.org).

3. Results

3.1 Physico-chemical characterization of the water column

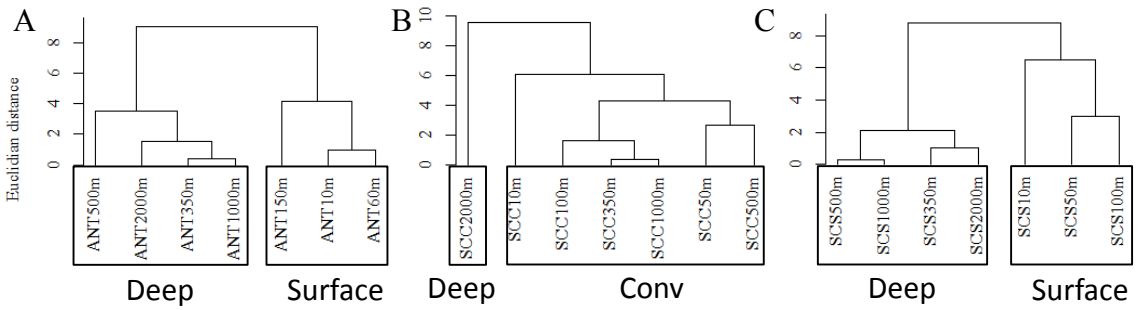

Figure 1: Ecological niches delimitation based on hierarchical clustering of the Euclidean distances between samples coordinates of the 2 first axes from the environmental PCAs analyses. The resulting niches for (A) ANT, (B) SCC and (C) SCS are framed and annotated according to their position in the water column.

Significant physical and biogeochemical parameters were used to delimitate possible environmental groups at each station. At Antares, significant correlations were found between nitrate (NO_3) and silicate ($Si(OH)_4$), and between dissolved inorganic carbon (DIC), salinity, density and phosphate (PO_4), with Spearman correlation coefficients > 0.90 and $p < 0.01$ (n=7). NO_3 was thus used as a proxy of $Si(OH)_4$ and DIC as a proxy of the others parameters for further multivariate analysis. Particulate organic carbon (POC) was used as a proxy of chlorophyll *a* (Chla), particulate organic nitrogen (PON) and phosphorus (POP) ($\rho > 0.90$, $p < 0.01$, n=7). At station SCC, we used Chla as a proxy of POP and phaeopigments *a* (Pheo *a*) ($\rho > 0.90$, $p < 0.01$, n=7). The same approach was used at station SCS ($\rho > 0.90$, $p < 0.01$, n=7), which resulted in the use of NO_3 as a proxy of PO_4, Chla, POP and density. Dissolved organic phosphorus (DOP) was a proxy of $Si(OH)_4$ and DIC a proxy of salinity. Based on Euclidian dissimilarity distance between samples, the surface and deep waters were clearly separated (Fig. 1). At ANT, the surface environmental group was characterized by relatively elevated temperature, dissolved organic matter (elements C, N and P) and particulate organic carbon concentrations (PCA results, supplementary Fig. S6), and was constituted of ANT10m, 60m and 150m samples. The deep group was characterized by elevated concentrations of NO_3 and DIC, and was composed

of ANT350m, 500m, 1000m and 2000m. At SCS, the surface group was characterized by the same physico-chemical parameters than ANT, and was constituted of SCS10m, 50m and 100m. The deep group was composed of SCS350m, 500m, 1000m and 2000m, and characterized by elevated NO_3, DIC and salinity. At SCC, a first group mainly drove by relatively elevated NOP, POC, Chla and temperature, pooled the samples from the convective water masse from 10 to 1000 m (SCC10m, 50m, 100m, 350m, 500m and 1000m). A second group could be distinguished at SCC2000m which correspond to a deep zone not impacted by the convective mixing with more nutrient (NO_3, PO_4, $Si(OH)_4$) and higher density and salinity.

3.2 Vertical distribution of SAR11, MGI and MGII assemblages

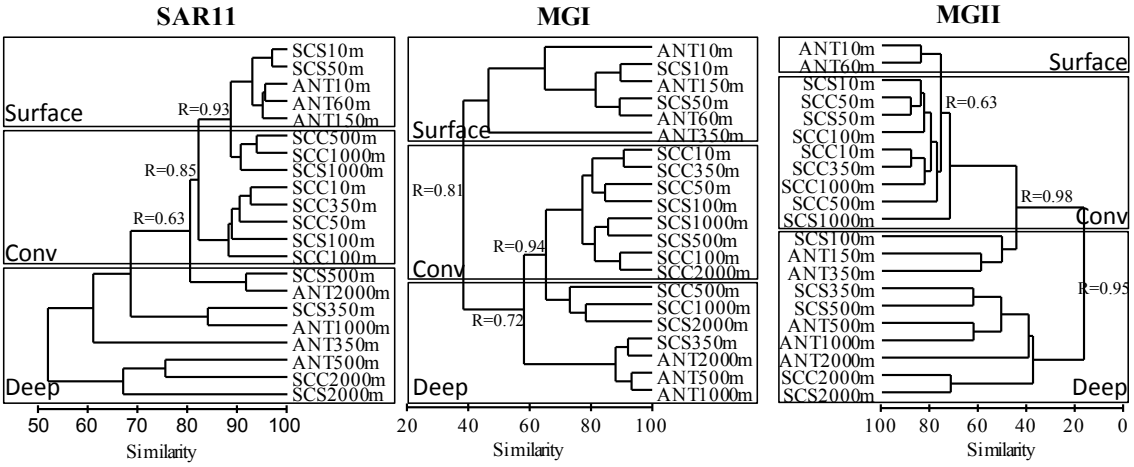

Figure 2: Unweighted-pair group method with arithmetic mean (UPGMA) dendrograms based on Bray-Curtis similarities between samples taken at different depth at ANT, SCC and SCS. Each dendrograms correspond to SAR11 (left), Marine group I (noted MGI) (middle), and marine group II (noted MGII) (right) communities. Results of significant ($p<0.01$) ANOSIM tests (R) are indicated at each main node.

Overall, the community structure of the SAR11, MGI and MGII groups followed the same distribution than the environmental groups defined above (Fig. 2). At the stratified station ANT and SCS, clear differences were found between surface (10 to 50-60m) and deep communities (below 150m). In the same manner, the communities of the three groups were affected by the convection event and formed a cluster of samples in the first 1500 m but dissimilar to the deep sample below the convection at 2000 m, except for MGI.

More specifically, independently of the stratified ANT and SCS stations, SAR11 and MGII (Fig. 2A and C) communities of deep samples grouped in 2 clusters highly differentiated from surface and convective communities (ANOSIM $R=0.63$, $p<0.01$ for SAR11; $R=0.98$, $p<0.01$ for MGII). In the same manner, convective and surface communities were significantly

different (A ANOSIM R= 0.93, $p < 0.05$ for SAR11; R=0.63, $p < 0.05$ for MGII). But some samples did not followed the environmental groups defined above. SAR11 community structure at SCS100 clustered in the deep group, while SCS1000m grouped with the convective community. The MGII communities at ANT150m, SCS10m and 50m were closer to the deep communities than the surface, and SCS1000m MGII community clustered with convective structure like for SAR11 community at SCS1000m.

MGI community structure of deep samples (Fig. 2B) were distributed almost together in 2 clusters highly different from the surface one (ANOSIM R=0.81, $p < 0.01$) which corresponded to the deep environmental group of ANT and SCS stations. Inversely to SAR11 and MGII clades, MGI subclades structures associated to the SCC convective group were grouped together in a deep cluster highly differentiated to the others deep clusters (ANOSIM R=0.94, $p < 0.01$). Some MGI samples assigned to SCS surface and deep environmental groups clustered in the convective group (SCS100m, 500m and 1000m). Surface MGI subclades from the stratified stations (ANT and SCS) had the same structure and grouped together in a well define surface cluster which was associated to the surface environmental group.

3.3 Vertical distribution of SAR11, MGI and MGII subclades

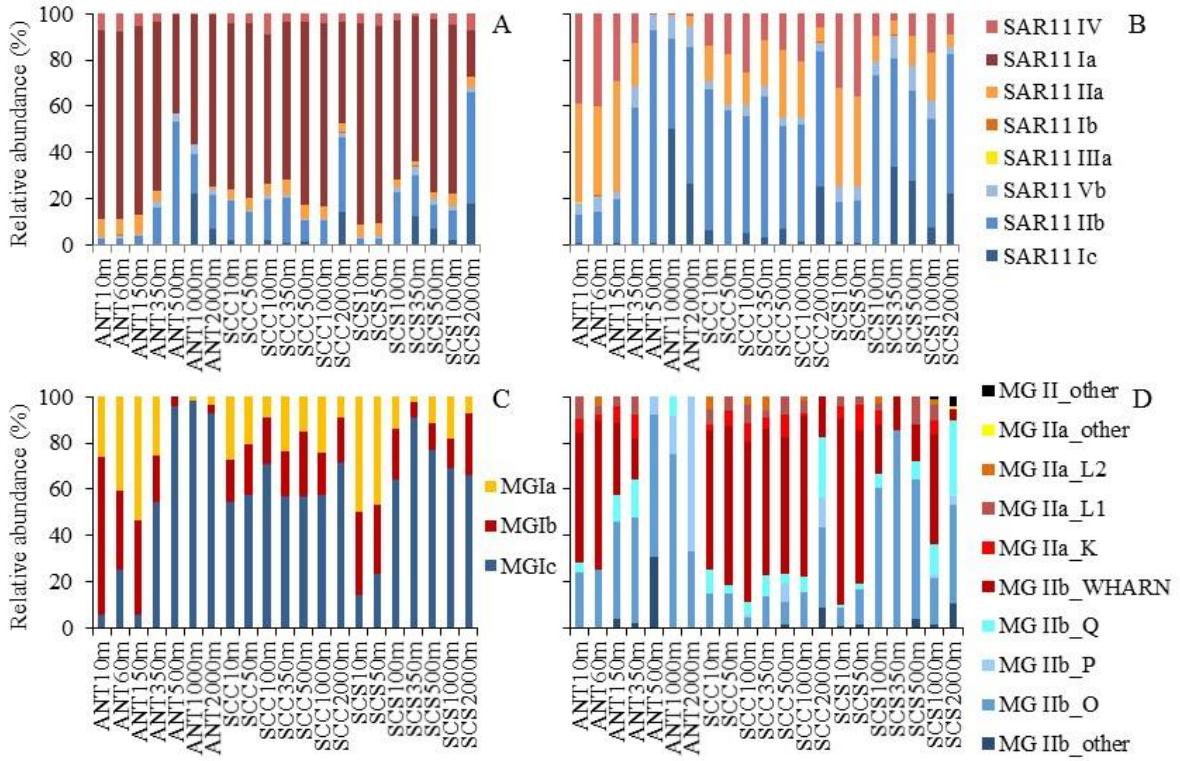

Figure 3: Vertical composition of SAR11 (A), SAR11 without the Ia subclade (B), Marine Group I (C) and Marine Group II (D) subclades according to the three sampled stations.

SAR11, MGI and MGII subclades were determined through phylogenetic trees of the 16S full-length Greengenes sequences (Supp. S2, S3, S4). According to the reference sequences used, 10 SAR11 subclades were identified in the Greengenes database, including a subclade from fresh water (supplementary Table S1). In MGI group, 4 subclades were determined and 11 in MGII clade.

In our study, 8 SAR11 subclades were found, 5 previously defined as surface subclades (Ib, Ia, IIIa and IV), and 3 as deep subclades (Ic, IIb, Vb) (Carlson et al., 2009; Vergin et al., 2013). Three MGI subclades were observed in this study, 2 as surface subclades (Ia and Ib) and one MGIc deep subclade, and 9 MGII subclades, 5 attributed as surface subclade and 4 as deep one (supplementary Table S1).

Overall, the subclades distribution (Fig. 3) followed the same patterns than environmental groups. The SAR11 Ia subclade was present all over the water column with high relative abundance, but was more dominant (>90% of the SAR11 clade) in the surface group of the stratified stations (ANT and SCS). The SAR11 IIIa and IIb subclades were in minority (<1%) and were observed only at ANT10m, ANT60m and SCC2000m.

In the MGI clade, the subclades Ia and Ib dominated the surface environmental group in stratified conditions (ANT and SCS station) at ~39 and 48% of the total MGI community respectively, while the deep MMGIc was dominant at almost 100% in the deep group at ANT and at 76% at SCS.

Five surface MGII subclades were observed (IIb_WHARN, IIa_K, IIa_L1, IIa_L2 and IIa_other), with the MGIIb_WHARN subclade dominant at ~60% in the surface group and the MGIIa subclades contributed to <20% of the total MGII clade. Four MGII subclades were assigned to the deep groups (IIb_O, IIb_P, IIb_Q and IIb_other).

SAR11, MGI and MGII surface subclades dominated the surface group at ~95%, ~70%, 70% of SAR11, MGI and MGII clades respectively at ANT, and at >75%, ~80% and >70% of SAR11, MGI and MGII clades respectively at SCS. Inversely, if we do not take into consideration the ubiquitous subclade SAR11 Ia, deep subclades of the 3 clades were dominant in the deep groups at ANT (~35%, ~80% and ~100% of SAR11, MGI and MGII clades respectively) and at SCS (~35%, ~85%, and ~80% of SAR11, MGI and MGII clades respectively).

Some deep subclades were ubiquitous, SAR11 Vb, SAR11 IIb, MGIc, MGII_O and MGII_P, only the subclades SAR11 Ic and MGII_Q were specific to the deep layer. At SCS, a slight decrease of the deep subclades contribution in the deep layer was observed compared to ANT for the 3 clades.

The convective group was characterized by a dominant contribution of surface subclades for SAR11 (>80% of SAR11 clade) and MGII clades (~80% of MGII clade), while MGI convective group was dominated by the deep MGIc subclade (>50% of MGI clade). For the 3 clades, deep subclades were shallower at SCC and were present in both convective and deep groups.

3.4 Relation between the distributions of SAR11, MGI and MGII subclades and physico-chemical environmental parameters

Pairwise associations between OTUs assigned to specific subclades and environmental parameters were studied using MIC statistics (Fig. 4-6). Environmental parameters which significantly contributed to the communities structures were chosen (Monte Carlo test from the CCA analyses, supplementary Fig. S5), among the non-correlated environmental parameters were chosen (Spearman rank pairwise correlations test).

For the 3 studied clades, ANT (Fig. 4A, 4A, 4A) was characterized by close relationship between OTUs assigned as surface subclades and parameters which defined the surface group, i.e. high organic matter concentrations and relatively elevated temperature. Reciprocally, OTUs assigned as deep subclades were highly associated to elevated concentrations of dissolved inorganic carbon (DIC) and nitrate (NO_3). These associations formed 2 sub-networks corresponding to the surface and deep groups. Nevertheless, some OTUs assigned as deep subclades were highly associated to OTUs and environmental parameters from the surface group for SAR11, MGI and MGII clades. And inversely, some OTUs assigned as surface subclades were highly associated to the deep group. During the convection event (Fig. 4B, 5B, 6B), a single network was observed without a clear discrimination of the convective and deep groups, excepted for MGII clade. A surface versus deep groups differentiation was anew observed at SCS for the 3 clades (Fig. 4C, 5C, 6C), but not well separated by associations more distant between OTUs and parameters from the 2 group.

Networks allowed us to follow some specific OTUs across stations. Some rare OTUs assigned as surface subclades which made strong associations in the surface group at ANT, then associated to OTUs and environmental parameters from the deep group after restratification

(SCS, noted ☻) for MGI and MGII clades. At ANT, OTUs from the surface group which were more relatively abundant there, stayed associated to the surface group at SCS (noted ☺ for the 3 clades). The reciprocal was also observed with deep OTUs at ANT, which at SCS strongly associated in the surface group (noted ■). While some deep OTUs at ANT made associations in the surface group (noted ♦). For SAR11 and MGII subclades assemblages, some rare OTUs were also observed in the groups that there were not supposed to be associated with. Some OTUs assigned as deep subclades were strongly associated to OTUs and variables from the surface group (noted ▲). And inversely some OTUs assigned as surface subclades were related to variable and OTUs from the deep group (noted ☼) at ANT and SCS.

4. Discussion

4.1 Influence of intense convection event and re-stratification on surface and deep environmental groups

Deep open-ocean convection process is a winter physical turbulence which can mix the water column until the seabed (Send and Marshall, 1995), thus destroying the vertical ecological niches classically found in the water column. This process is not unusual in the Northwestern Mediterranean Sea, it happens every winter, with variable intensity (Schott et al., 1996; Durrieu de Madron et al., 2013) and allows the export of particulate and organic matter to deep waters (Gogou et al., 2014; Santinelli et al., 2010). The convection episode of March 2011 mixed the water column down to 1500m depth, on an area of ~1000km² (Severin et al., submitted-b). By this process, a unique water mass was formed from the surface to 1500m, corresponding to a convective environmental group (Fig1C) characterized by relatively elevated dissolved and particulate organic matter and also chlorophyll *a* (Chla) concentrations (see CCAs PCA results in supplementary Fig. S5 and S6). Waters below 1500m were not impacted by the deep mixing, and formed a deep environmental group with higher density and nutrient content. The convective mixing annihilated the prior vertical stratification composed of two separated surface (0-150m) and deep (350-2000m) layers, characterized by either high dissolved organic matter or high nutrient concentrations, respectively (Fig. 1A). Five days after the convective mixing, we observed a freshly re-stratified water column organized in surface (0-100m) and deep environmental groups (350-2000m) (Fig. 1C). The clear identification of these environmental groups allowed us to follow the re-colonization of new environments by the SAR11, Marine Group I *Thaumarchaeota* (MGI) and Marine Group II *Euryarchaeota* (MGII) subclades after the convection event, in comparison to the prior stratified conditions.

4.2 SAR11 ecotypes distribution and dynamic across changes in environments

Over the three taxonomic groups studied here, SAR11 subclades were the most documented in terms of spatio-temporal distributions (see supplementary Table S1; Carlson et al., 2009; Morris et al., 2005; Vergin et al., 2013) and ecological functions (Malmstrom et al., 2004; Mou et al., 2007). These subclades were titled as ecotypes (Field et al., 1997) because of their conformity to the ecotype concept which is a distinction in physiological details allowing a niche specialization of some organisms (Cohan and Perry, 2007; Cohan, 2006).

SAR11 subclades composition across the environmental groups were in accordance with the ecotypes niches specialization previously described (Carlson et al., 2009; Vergin et al., 2013). A significant difference was observed between the surface and the deep structures (Fig. 2A) prior and after the physical turbulence, except for some SAR11 communities at 100 and 1000m that remained close to typical convective samples after the re-stratification. This could indicate that the elapsed time after the convective mixing was too short for the SAR11 community to completely recolonize their environmental groups. Previous studies on SAR11 subclades found that the subclades Ic, IIb and Vb were associated to deep waters while subclades Ia, Ib, IIa, IIIa and IV specialized in surface waters (see supplementary Table S1; Carlson et al., 2009; Vergin et al., 2013). Our data are in accordance with these studies (Fig. 3A) with a maximal contribution of the 3 deep subclades of ~60%, and a contribution of the 5 surface subclades up to 95% in surface niches. The SAR11-Ic deep subclade, IIa and IV surface subclades were strictly assigned to deep and surface layers respectively, except during the intense convective mixing. The intense upward and downward motions existing inside the convective cell (Send and Marshall, 1995) exported to deeper waters the surface subclades while it brought shallower the deep subclades. The absence of subclade Va, normally associated to summer surface waters (Vergin et al., 2013), and the scarce presence of subclades IIIa (autumnal surface waters) and Ib (spring waters) during our winter sampling confirmed their ecotype status by their temporal environment specialization. Inversely, the omnipresence of the subclade Ia, normally assigned to summer surface waters (Carlson et al., 2009) was due to a single OTU similar at 99% to the HTCC1002 strain of *Pelagibacter ubique*. This Ia subclade contributed from 50 to 60% of SAR11 clade in the deep environmental group, and to more than 80% in the surface layer in stratified conditions. Such vertical distribution was in contradiction with the niche specialization of the ecotype concept, as the ubiquitous SAR11 IIb and Vb.

In each of the defined environmental group of this study, we observed a strong relationship between the environmental properties and the prokaryotic communities. This led us to define our environmental groups as ecological niches.

Pairwise associations between OTUs, and also with environmental parameters (Fig. 4) indicated the relationship of each SAR11 subclades with the environmental properties of their ecological niches. Prior to the physical turbulence (Fig. 4A), OTUs defined as surface subclades were mostly related to dissolved organic nitrogen (DON) and particulate organic nitrogen (PON). This is in accordance with the surface SAR11 subclades capacity to assimilate organic matter enriched in nitrogen, like amino acid (Malmstrom et al., 2004, 2005). In the North Atlantic Ocean, surface SAR11 (<100m) were responsible for an amino acid assimilation from 34 to 61% of the total prokaryotes assimilation (Malmstrom et al., 2005). Despite their elevated relative abundance in others oceans, they were surprisingly weakly active on amino acid substrate than the others prokaryotes in the Mediterranean Sea (<30%) (Alonso-Sáez and Gasol, 2007; Alonso-Sáez et al., 2008), and also in the Delaware Bay (~15%) (Elifantz and Malmstrom, 2005). In a same manner, the strong relations between OTUs of surface subclades and particulate organic carbon (POC) confirmed the affinity of surface SAR11 subclades for glucose substrate. Surface SAR11 glucose assimilation was elevated in the North Atlantic (45-57%) (Malmstrom et al., 2005), but not in the Mediterranean (Alonso-Sáez and Gasol, 2007), nor in the Delaware Bay (Elifantz and Malmstrom, 2005). Some OTUs mostly assigned as the deep IIb and a few as IV subclades, were situated in the surface niche prior to the convection event (Fig. 3A-B, 4A). Few of them were related to organic matter, while the majority made strong relations between them in the surface niche without any environmental parameter association. This may suggested that either the weak winter surface mixing (sampling in March) brought some deep subclades, with no visible relation with any of the measured physical parameters, or a special association with a non-identified substrate available in this surface niche. The last hypothesis implied that some organisms from the deep IIb subclade may specialized on a typical surface substrate. SAR11 phylogenetic analysis (Supplementary Fig. S2) showed the presence of several sub-clusters inside the IIb group. This may imply different ecological functions inside the SAR IIb subclade. Surprisingly, none of the SAR11 subclades studied in the literature dealt with depths greater than 300m. Prior to the turbulence, we observed a cohesion in the deep niche of the OTUs assigned as deep subclades, reinforcing the description of SAR11 Ic, IIb and Vb as ecotypes, even if scarce surface subclades were present in the deep niche. A part of the deep OTUs was related to elevated nutrient concentrations (prior to the turbulence, nitrate was used as a proxy of silicate). Some deep OTUs made strong

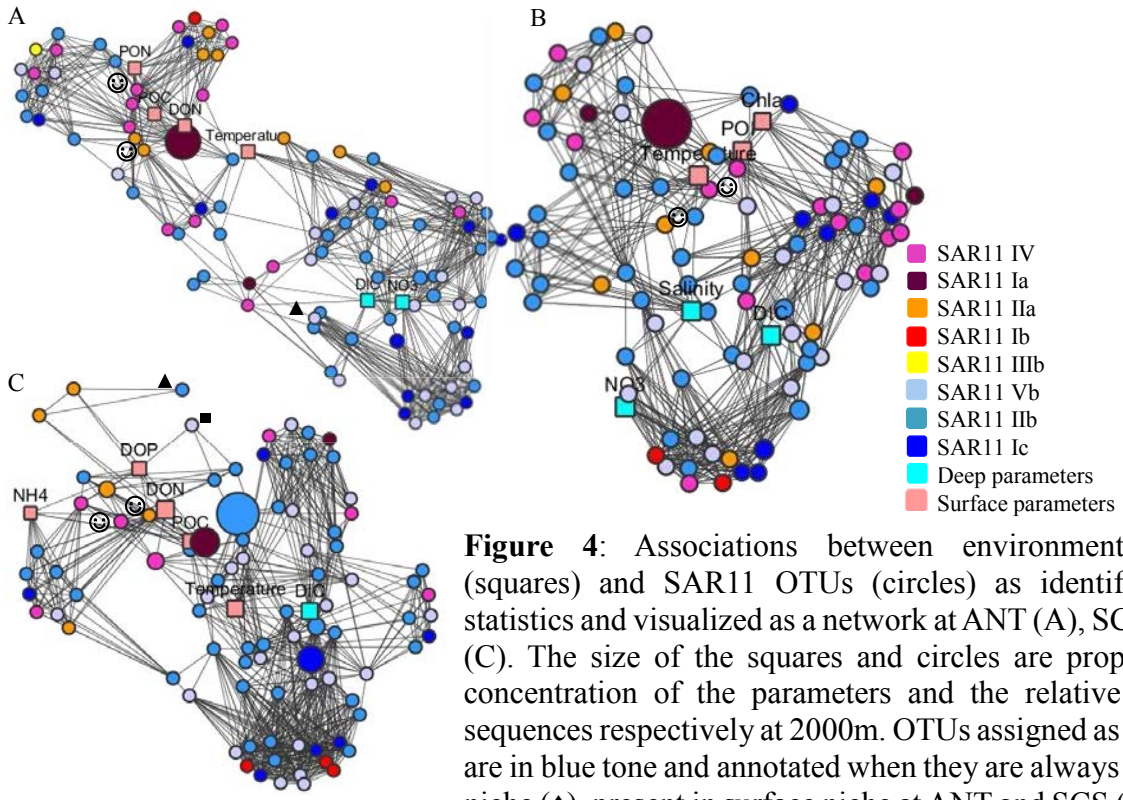

Figure 4: Associations between environmental parameters (squares) and SAR11 OTUs (circles) as identified with MIC statistics and visualized as a network at ANT (A), SCC (B) and SCS (C). The size of the squares and circles are proportional to the concentration of the parameters and the relative abundance of sequences respectively at 2000m. OTUs assigned as deep subclades are in blue tone and annotated when they are always present in deep niche (♦), present in surface niche at ANT and SCS (■), and present in surface niche only at SCS (▲). OTUs assigned as surface subclades are in warm tone and annotated when they are always present in surface niche (☺), and present in deep niche at ANT and SCS (☼).

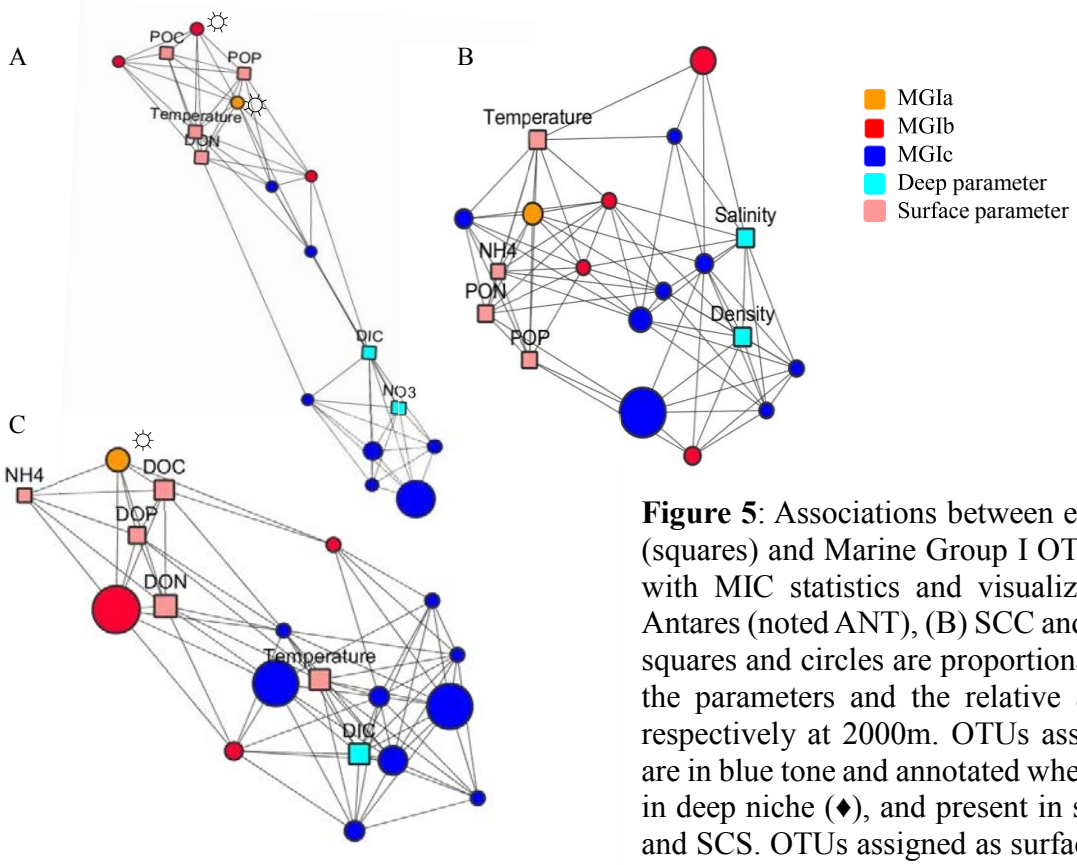

Figure 5: Associations between environmental parameters (squares) and Marine Group I OTUs (circles) as identified with MIC statistics and visualized as a network at (A) Antares (noted ANT), (B) SCC and (C) SCS. The size of the squares and circles are proportional to the concentration of the parameters and the relative abundance of sequences respectively at 2000m. OTUs assigned as deep subclades are in blue tone and annotated when they are always present in deep niche (♦), and present in surface niche (■) at ANT and SCS. OTUs assigned as surface subclades are in warm tone and annotated when they are present in deep niche at ANT and SCS (☼), and present in deep niche only at SCS (☻).

associations with the dissolved inorganic carbon (proxy of nitrate). However, single cell genomic analysis of the SAR11 Ic subclade revealed the absence of autotrophy pathways (Cameron et al., 2014). But the observed associations concerned the subclades IIb and IV, and not the Ic subclade.

The physical turbulence mixed the OTUs assigned as deep or surface subclades, and destabilized the well-defined surface and deep niches (Fig. 4B). Within only five days, OTUs of surface subclades return, or grew back, in their surface niche, strongly related to the surface dissolved organic matter, and most of the deep OTUs returned to the deep niche in relation to high nutrient concentrations. This reinforced again their affiliation as ecotype, even if some rare deep OTUs remained alive in the surface niche. As this study was done during the winter, the weak relative abundance of these deep OTUs in the surface niche may be due to the winter surface mixing (sampling in March). The surface sub-network formed of OTUs assigned as deep subclades present before the turbulence came back in the surface niche. But these OTUs were associated to the DON, suggesting a change in the quality of the organic matter that may be more labile because of the bloom in development following the convection event (Gačić et al., 2002; D'Asaro, 2008; Severin et al., submitted-b).

4.3 Marine Group I subclades

Marine group I *Thaumarchaeota* (MGI) is one of the most widespread archaeal clade in the ocean, accounting for more than 20% of the total prokaryote biomass (Karner et al., 2001). Four MGI subclades had been identified until now: the summer surface MGIa (or I-α), the winter surface MGIb (or I-β), the rare and deep MGIc (or I-γ) and the rare MGId (Massana et al., 2000; Galand et al., 2010; Hugoni et al., 2013). In our study, we did not find the last MGId subclade, and both MGIa and MGIb surface subclade were encountered despite a winter sampling (Fig. 3C).

MGI subclades assemblages were stratified by ecological niches (Fig. 2B), respecting the ecotype concept. Some exceptions were found after the re-stratification, when a group of subclades influenced by the convection remained, as observed with SAR11 subclades. This significant difference was due to a large contribution (>90%) of the surface Ia and Ib subclades in the surface niche, and a dominance of the deep Ic subclade in the deep ecological niche (Fig. 3C). Contrary to a previous study in the Mediterranean Sea (Hugoni et al., 2013), the subclade Ic was not rare below 100m and could reached almost 100% of the total MGI clade. As this previous study was limited to the first 3m of the water column, it could have missed the

abundant deep MGIc subclade. The structure of MGI subclades present in the convective niche was closer to the assemblages of the deep niches than the surface ones (Fig. 2B), contrary to the SAR11. As the entire MGI clade is generally more abundant in deep waters (Galand et al., 2010; Massana et al., 2000), the convective mixing certainly transported more Ic subclade in shallower waters, than it exported the surface Ia and Ib to deep layers. This was corroborated by the important contribution up to 50% of the subclade Ic in the convective niche.

The widespread MGI clade were well distributed in surface and deep ecological niches according to their subclades assignment (Fig. 5). MGI subclades were identified as ammonia oxidizers (Francis et al., 2007; Erguder et al., 2009; Sintes et al., 2013; Smith et al., 2014) and they would have the capacity to produce enough nitrite (NO_2) and nitrate (NO_3) to account for all 'new' nitrogen in the upper ocean (Ingalls et al., 2006; Tully et al., 2012). Our results are in accordance with these function since we observed close relations between the surface MGI OTUs and ammonia (NH_4) and NO_2 after the physical turbulence (NH_4 was used as a NO_2 proxy in this study; Fig. 5C). But prior to the convection, neither NH_4 nor NO_2 were significant explanatory variables, certainly because of their low concentrations at this time. Only NO_3 significantly contributed to the MGI subclades structures (see CCAs results in supplementary Fig. S5). Before and after the physical turbulence, only the deep subclades OTUs from the deep niches were associated to NO_3 and to dissolved inorganic carbon (DIC, used as a proxy of NO_3 at the re-stratified SCS station). Previous studies showed that the members of MGI clade were able to fix bicarbonate, and that it would contribute to 1% of the total global carbon fixation (Berg et al., 2007; Tully et al., 2012). But not all MGI subclades had this capacity (Massana et al., 1997; Murray et al., 1998; Ouverney and Fuhrman, 2000), and that could be limited to deep MGI subclades only. Because of the strong interactions between the organic matter (dissolved and particulate) and OTUs assigned as surface subclades before and after the physical turbulence, some MGI members may be heterotrophs or mixotrophs (Ouverney & Fuhrman, 2000; Ingalls et al., 2006; Martin-Cuadrado et al., 2008). The convective mixing brought to the surface some DIC by the upwards motions, like it brought nutrient. A metabolism change may then be hypothesized since OTUs assigned as surface subclades firstly associated to organic matter prior to the convection event were present in both surface and deep niches after restratification, and had a strong interactions with the DIC (Fig. 5A and C). The MGI mixotrophic metabolism theory was also corroborated by the interactions with both organic matter and DIC of some OTUs assigned as deep and also as surface subclades, which were always present in both surface and deep niches before and after the physical turbulence.

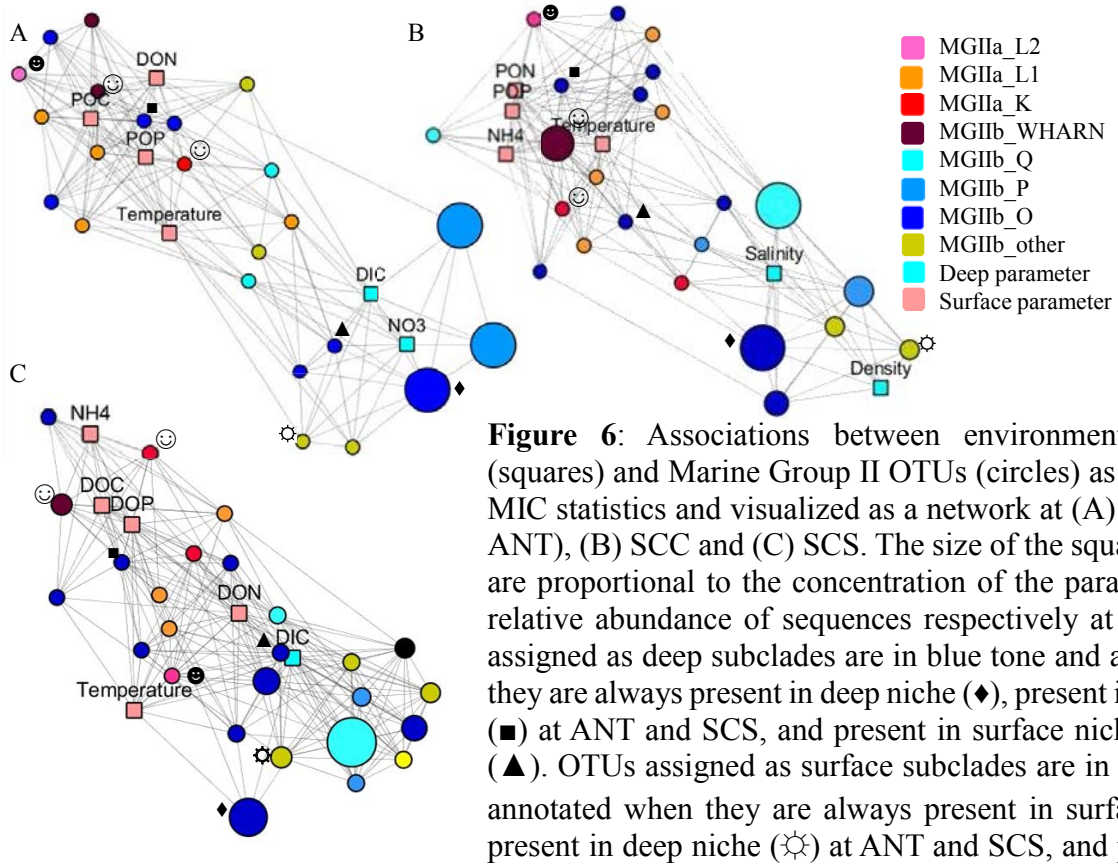

Figure 6: Associations between environmental parameters (squares) and Marine Group II OTUs (circles) as identified with MIC statistics and visualized as a network at (A) Antares (noted ANT), (B) SCC and (C) SCS. The size of the squares and circles are proportional to the concentration of the parameters and the relative abundance of sequences respectively at 2000m. OTUs assigned as deep subclades are in blue tone and annotated when they are always present in deep niche (♦), present in surface niche (■) at ANT and SCS, and present in surface niche only at SCS (▲). OTUs assigned as surface subclades are in warm tone and annotated when they are always present in surface niche (☺), present in deep niche (☼) at ANT and SCS, and present in deep niche only at SCS (☻).

4.4 Marine Group II subclades

Marine Group II *Euryarchaeota* appeared to be the most abundant archaeal group in surface waters of the Mediterranean Sea (Hugoni et al., 2013), and in the Santa Barbara channel (Massana et al., 1997). Since the phylogenetic discovery of several MGII subclades, their ecological functions remained poorly known (Massana et al., 2000; Hugoni et al., 2013). A seasonal distribution of the 2 main subclades led to the conclusion of a niche specialization of MGIIa and MGIIb (Pernthaler & Preston, 2002; Herfort et al., 2007; Galand et al., 2010). While MGIIb was dominant in winter surface waters, MGIIa appeared as a summer surface ecotype. This was corroborated by metagenomic analysis which revealed the presence of a gene light-capturing proteorhodopsins in this summer subclade (Frigaard et al., 2006; Iverson et al., 2012), favoring the use of light as an additional energy source.

In our winter study, both MGIIa and MGIIb were observed (Fig. 3D), with a larger contribution of the winter IIb subclade (>80%). Despite this MGIIb domination, a subclades structuration by ecological niches was observed (Fig. 2C), reinforcing the veracity of a subdivision of MGIIb clade in several sub-subclades, like for the summer MGIIa subclade (Galand et al., 2010; Hugoni et al., 2013). In these studies, MGIIa was divided in 3 clusters: MGIIa_K, MGIIa_L (composed of the L1, L2, L3 groups) presumably heterotroph, and

MGIIa_M dominant from May to August. In previous studies (Galand et al., 2010; Hugoni et al., 2013), MGIIb was divided in 2 clusters, MGIIb_O composed of MGIIb_WHARN, the most abundant winter surface sub-subclade, and the rarest MGIIb_N. In light of our phylogenetic analysis, we proposed 2 new MGIIb sub-subclades: MGIIb_P and MGIIb_Q (Supplementary Fig. S4).

Studies cited above were restricted to the first 3m. Our sampling down to 2000m depth revealed the surface niche specialization of the MGIIa and MGIIb_WHARN, while the ubiquitous MGIIb_O, P and Q were the only MGII representatives in the deep niche prior to the physical turbulence (Fig. 3D). This led to a highly differentiation of the MGII subclades structures between the surface and the deep niches prior to the physical turbulence (Fig. 3D, 6A). Like for SAR11 and MGI clades, OTUs from the surface niche were strongly associated to dissolved and organic matter, while the deep OTUs were related to the NO_3 and DIC in the deep enriched waters. However, the lack of studies on the ecological functions of MGII subclades limited us in the interpretations of such interactions. Certainly that the surface subclades have in general a heterotrophic metabolism, with a focus on protein and lipid degradation as shown by metagenomic analysis (Iverson et al., 2012). While the deep subclades may be autotrophs because of their interactions with DIC. Genes coding for anaerobic respiratory chains were discovered in deep MGII subclades (Martin-Cuadrado et al., 2008), but the measured substrate in our study cannot give any evidence of such metabolism.

After the re-stratification, MGIIa and MGIIb_WHARN subclades were not restrained any more to the surface niche (Fig. 3D), which led to an unclear delimitation of the surface and deep niches. Some OTUs previously situated in the surface niche; remained alive in the deep niche after the re-stratification (Fig. 6). The process behind this phenomena is not well understood. Some authors suggested that the sinking convective water, entrapped the prokaryote community formed during the convective mixing (Azzaro et al., 2012; Severin et al., submitted-a). Thanks to the enrichment through the export of particulate and dissolved organic matter by the convection event (Santinelli et al., 2010; Gogou et al., 2014), the heterotrophic surface subclade would stayed alive despite the more elevated density.

Conclusion

Our results present the first study of ecological niches recolonization by potential ecotypes of SAR11, Marine Group I *Thaumarchaeota* and Marine Group II *Euryarchaeota*. Characterization of a subclade as an ecotype need deep analyses on its ecological functions and

niche specialization, but it is a necessary step to understand their influences on biogeochemical cycles. Our results globally confirmed the ecotype relevance of the SAR11 subclades, except for the SAR11 IIb. The omnipresence of the deep IIb subclade in surface niches, globally independent from the others surface ecotypes and environmental parameters, would indicated a possible division in several sub-subclades with ecological unit adapted to a non-measured surface substrate. By a sampling until 2000m, we highlighted a novel niche specialization for MGIc which was not a rare subclade in deep waters, and for MGIIb subclades which were not restricted to winter surface waters. Interactions of deep MGIIb subclades with dissolved inorganic carbon potentially imply an autotrophic metabolism, but more ecological analyses are necessary to confirm this hypothesis.

The mixotrophy of MGI clades led one subclade to colonize several niches at the same time, which niches already colonized by others subclades from the same group. In such situation, the ecotype concept implying the colonization of a single niche per subclade to avoid any competition is not any more respected. We can then wonder about the legitimacy to call this subclade an ecotype. We also observed the co-existence in the same niche of several subclades from the same clade, for instance SAR11 Ia, IIa and IV were in surface waters, MGIa and Ib were also in surface waters, and MGIIb_O, P and Q were in deep ecological niche. If they were true ecotypes, the co-occurrence of subclades from the same group in a same niche would imply a specialization on a substrate not measured in order to avoid any competition. The need to collect several different environmental data rapidly face to the difficulties in gather several parameters in the same laboratory. An alternative would be a comparison of co-existing subclades by genomic and/or metagenomic analyses, in order to reveal the unit ecological function of each subclade.

Acknowledgments

We are grateful to the crew and officials of R/V *L'Atalante* and to all the scientific and technical staff involved in the CASCADE cruise for their support during sea operations. This work was funded by the HERMIONE Project (N° 226354) under the European Commission's Seventh Framework Program and the French Program MERMEX under the MISTRALS framework.

References

Alonso-Sáez, L., Gasol, J.M., 2007. Seasonal variations in the contributions of different bacterial groups to the uptake of low-molecular-weight compounds in northwestern Mediterranean coastal waters. Appl. Environ. Microbiol. 73, 3528–35. doi:10.1128/AEM.02627-06

Alonso-Sáez, L., Sánchez, O., Gasol, J.M., Balagué, V., Pedrós-Alio, C., 2008. Winter-to-summer changes in the composition and single-cell activity of near-surface Arctic prokaryotes. Environ. Microbiol. 10, 2444–54. doi:10.1111/j.1462-2920.2008.01674.x

Aminot, A., Kérouel, R., 2007. Dosage automatique des nutriments dans les eaux marines : méthodes en flux continu. Ed. Ifremer, Méthodes d'analyse en milieu marin, 188p.

Azzaro, M., La Ferla, R., Maimone, G., Monticelli, L.S., Zaccone, R., Civitarese, G., 2012. Prokaryotic dynamics and heterotrophic metabolism in a deep convection site of Eastern Mediterranean Sea (the Southern Adriatic Pit). Cont. Shelf Res. 44, 106–118. doi:10.1016/j.csr.2011.07.011

Berdjeb, L., Ghiglione, J.-F., Jacquet, S., 2011. Bottom-up versus top-down control of hypo- and epilimnion free-living bacterial community structures in two neighboring freshwater lakes. Appl. Environ. Microbiol. 77, 3591–9. doi:10.1128/AEM.02739-10

Berg, I. a, Kockelkorn, D., Buckel, W., Fuchs, G., 2007. A 3-hydroxypropionate/4-hydroxybutyrate autotrophic carbon dioxide assimilation pathway in Archaea. Science 318, 1782–1786. doi:10.1126/science.1149976

Cameron, T.J., Temperton, B., Swan, B.K., Landry, Z.C., Woyke, T., Delong, E.F., Stepanauskas, R., Giovannoni, S.J., 2014. Single-cell enabled comparative genomics of a deep ocean SAR11 bathytype. ISME J. 8, 1440–1451. doi:10.1038/ismej.2013.243

Caporaso, J.G., Kuczynski, J., Stombaugh, J., Bittinger, K., Bushman, F.D., Costello, E.K., Fierer, N., Peña, A.G., Goodrich, K., Gordon, J.I., Huttley, G.A., Kelley, S.T., Knights, D., Jeremy, E., Ley, R.E., Lozupone, C.A., Mcdonald, D., Muegge, B.D., Reeder, J., Sevinsky, J.R., Turnbaugh, P.J., Walters, W.A., 2010. QIIME allows analysis of high-throughput community sequencing data. Nat. Methods 7, 335–336. doi:10.1038/nmeth.f.303.QIIME

Carlson, C.A., Morris, R., Parsons, R., Treusch, A.H., Giovannoni, S.J., Vergin, K., 2009. Seasonal dynamics of SAR11 populations in the euphotic and mesopelagic zones of the northwestern Sargasso Sea. ISME J. 3, 283–295. doi:10.1038/ismej.2008.117

Cauwet, G., 1994. HTCO method for dissolved organic carbon analysis in seawater: influence of catalyst on blank estimation. Mar. Chem. 47, 55–64.

Cauwet, G., 1999. Determination of dissolved organic carbon and nitrogen by high temperature combustion, in: Methods of Seawater Analysis. Wiley-VCH Verlag GmbH, pp. 407–420. doi:10.1002/9783527613984.ch15

Cohan, F.M., 2006. Towards a conceptual and operational union of bacterial systematics, ecology, and evolution. Philos. Trans. R. Soc. Lond. B. Biol. Sci. 361, 1985–96. doi:10.1098/rstb.2006.1918

Cohan, F.M., Perry, E.B., 2007. A systematics for discovering the fundamental units of bacterial diversity. Curr. Biol. 17, R373–86. doi:10.1016/j.cub.2007.03.032

D'Asaro, E. a., 2008. Convection and the seeding of the North Atlantic bloom. J. Mar. Syst. 69, 233–237. doi:10.1016/j.jmarsys.2005.08.005

De Queiroz, K., 2005. Ernst Mayr and the modern concept of species. Proc. Natl. Acad. Sci. U. S. A. 102 Suppl , 6600–7. doi:10.1073/pnas.0502030102

Delong, E.F., 1992. Archaea in coastal marine environments. Proc. Natl. Acad. Sci. 89, 5685–5689.

Durrieu de Madron, X., Houpert, L., Puig, P., Sanchez-Vidal, a., Testor, P., Bosse, a., Estournel, C., Somot, S., Bourrin, F., Bouin, M.N., Beauverger, M., Beguery, L., Calafat, a., Canals, M., Cassou, C., Coppola, L., Dausse, D., D'Ortenzio, F., Font, J., Heussner, S., Kunesch, S., Lefevre, D., Le Goff, H., Martín, J., Mortier, L., Palanques, a., Raimbault, P., 2013. Interaction of dense shelf water cascading and open-sea convection in the northwestern Mediterranean during winter 2012. Geophys. Res. Lett. 40, 1379–1385. doi:10.1002/grl.50331

Edgar, R.C., 2004. MUSCLE: multiple sequence alignment with high accuracy and high throughput. Nucleic Acids Res. 32, 1792–7. doi:10.1093/nar/gkh340

Edgar, R.C., 2010. Search and clustering orders of magnitude faster than BLAST. Bioinformatics 26, 2460–1. doi:10.1093/bioinformatics/btq461

Efron, B., 2004. Large-Scale Simultaneous Hypothesis Testing. J. Am. Stat. Assoc. 99, 96–104. doi:10.1198/016214504000000089

Elifantz, H., Malmstrom, R., 2005. Assimilation of polysaccharides and glucose by major bacterial groups in the Delaware Estuary. Appl. Environ. Microbiol. 71, 7799–7805. doi:10.1128/AEM.71.12.7799

Epstein, S.S., 2013. The phenomenon of microbial uncultivability. Curr. Opin. Microbiol. 16, 636–42. doi:10.1016/j.mib.2013.08.003

Erguder, T.H., Boon, N., Wittebolle, L., Marzorati, M., Verstraete, W., 2009. Environmental factors shaping the ecological niches of ammonia-oxidizing archaea. FEMS Microbiol. Rev. 33, 855–69. doi:10.1111/j.1574-6976.2009.00179.x

Felsenstein, J., 1989. PHYLIP - Phylogeny Inference Package (Version 3.2). Cladistics 5, 164–166.

Field, K.G., Gordon, D., Wright, T., Rappé, M., Urback, E., Vergin, K., Giovannoni, S.J., 1997. Diversity and depth-specific distribution of SAR11 cluster rRNA genes from marine planktonic bacteria. Appl. Environ. Microbiol. 63, 63–70.

Francis, C. a, Beman, J.M., Kuypers, M.M.M., 2007. New processes and players in the nitrogen cycle: the microbial ecology of anaerobic and archaeal ammonia oxidation. ISME J. 1, 19–27. doi:10.1038/ismej.2007.8

Francis, C.A., Roberts, K.J., Beman, J.M., Santoro, A.E., Oakley, B.B., 2005. Ubiquity and diversity of ammonia-oxidizing archaea in water columns and sediments of the ocean. Proc. Natl. Acad. Sci. U. S. A. 102, 14683–14688. doi:10.1073/pnas.0506625102

Frigaard, N.-U., Martinez, A., Mincer, T.J., DeLong, E.F., 2006. Proteorhodopsin lateral gene transfer between marine planktonic Bacteria and Archaea. Nature 439, 847–850.

Fuhrman, J.A., McCallum, K., Davis, A.A., 1992. Novel major archaebacterial group. Nature 356, 148–149.

Fuhrman, J.A., Ouverney, C.C., 1998. Marine microbial diversity studied via 16S rRNA sequences : cloning results from coastal waters and counting of native archaea with fluorescent single cell probes. Aquat. Ecol. 32, 3–15.

Gačić, M., Civitarese, G., Miserocchi, S., Cardin, V., Crise, A., Mauri, E., 2002. The open-ocean convection in the Southern Adriatic: a controlling mechanism of the spring phytoplankton bloom. Cont. Shelf Res. 22, 1897–1908. doi:10.1016/S0278-4343(02)00050-X

Galand, P.E., Gutiérrez-Provecho, C., Massana, R., Gasol, J.M., Casamayor, E.O., 2010. Inter-annual recurrence of archaeal assemblages in the coastal NW Mediterranean Sea (Blanes Bay Microbial Observatory). Limnol. Oceanogr. 55, 2117–2125. doi:10.4319/lo.2010.55.5.2117

García-Martínez, J., Rodríguez-Valera, F., 2000. Microdiversity of uncultured marine prokaryotes: the SAR11 cluster and the marine Archaea of Group I. Mol. Ecol. 9, 935–48.

Gevers, D., Cohan, F., Lawrence, J., 2005. Re-evaluating prokaryotic species. Nat. Rev. Microbiol. 3, 733–739.

Ghiglione, J.-F., Conan, P., Pujo-Pay, M., 2009. Diversity of total and active free-living vs. particle-attached bacteria in the euphotic zone of the NW Mediterranean Sea. FEMS Microbiol. Lett. 299, 9–21. doi:10.1111/j.1574-6968.2009.01694.x

Giovannoni, S.J., Rappé, M.S., 2000. Evolution, diversity, and molecular ecology of marine prokaryotes, in: Kirchman, D.L. (Ed.), Microbial Ecology of the Oceans. pp. 47–84.

Gogou, A., Sanchez-Vidal, A., Durrieu de Madron, X., Stavrakakis, S., Calafat, A.M., Stabholz, M., Psarra, S., Canals, M., Heussner, S., Stavrakaki, I., Papathanassiou, E., 2014. Carbon flux to the deep in three open sites of the Southern European Seas (SES). J. Mar. Syst. 129, 224–233. doi:10.1016/j.jmarsys.2013.05.013

Herfort, L., Schouten, S., Abbas, B., Veldhuis, M.J.W., Coolen, M.J.L., Wuchter, C., Boon, J.P., Herndl, G.J., Sinninghe Damsté, J.S., 2007. Variations in spatial and temporal distribution of Archaea in the North Sea in relation to environmental variables. FEMS Microbiol. Ecol. 62, 242–57. doi:10.1111/j.1574-6941.2007.00397.x

Herndl, G.J., Reinthaler, T., Teira, E., van Aken, H., Veth, C., Pernthaler, A., Pernthaler, J., 2005. Contribution of Archaea to Total Prokaryotic Production in the Deep Atlantic Ocean. Appl. Environ. Microbiol. 71, 2303–2309. doi:10.1128/AEM.71.5.2303-2309.2005

Holmes, R.M., Aminot, A., Kérouel, R., Hooker, B. a, Peterson, B.J., 1999. A simple and precise method for measuring ammonium in marine and freshwater ecosystems. Can. J. Fish. Aquat. Sci. 56, 1801–1808. doi:10.1139/f99-128

Hugoni, M., Taib, N., Debroas, D., Domaizon, I., Jouan, I., 2013. Structure of the rare archaeal biosphere and seasonal dynamics of active ecotypes in surface coastal waters. PNAS 110, 6004–6009.

Ingalls, A.E., Shah, S.R., Hansman, R.L., Aluwihare, L.I., Santos, G.M., Druffel, E.R.M., Pearson, A., 2006. Quantifying archaeal community autotrophy in the mesopelagic ocean using natural radiocarbon. Proc. Natl. Acad. Sci. U. S. A. 103, 6442–7. doi:10.1073/pnas.0510157103

Iverson, V., Morris, R.M., Frazar, C.D., Berthiaume, C.T., Morales, R.L., Armbrust, E.V., 2012. Untangling genomes from metagenomes: revealing an uncultured class of marine Euryarchaeota. Science (80-.). 335, 587–590. doi:10.1126/science.1212665

Karner, M., DeLong, E., Karl, D., 2001. Archaeal dominance in the mesopelagic zone of the Pacific Ocean. Nature 409, 507–510.

Kiene, R.P., Linn, L.J., 2000. The fate of dissolved dimethylsulfoniopropionate (DMSP) in seawater: tracer studies using 35 S-DMSP. Geochim. Cosmochim. Acta 64, 2797–2810.

Koeppel, A., Perry, E.B., Sikorski, J., Krizanc, D., Warner, A., Ward, D.M., Rooney, A.P., Brambilla, E., Connor, N., Ratcliff, R.M., Nevo, E., Cohan, F.M., 2008. Identifying the fundamental units of bacterial diversity: a paradigm shift to incorporate ecology into bacterial systematics. Proc. Natl. Acad. Sci. U. S. A. 105, 2504–9. doi:10.1073/pnas.0712205105

Legendre, L., Legendre, P., 1983. Numerical ecology, 3rd ed. Elsevier science B.V.

Malmstrom, R.R., Cottrell, M.T., Elifantz, H., Kirchman, D.L., 2005. Biomass production and assimilation of dissolved organic matter by SAR11 bacteria in the Northwest Atlantic Ocean. Appl. Environ. Microbiol. 71, 279–2986. doi:10.1128/AEM.71.6.2979

Malmstrom, R.R., Kiene, R.P., Cottrell, M.T., Kirchman, D.L., 2004. Contribution of SAR11 Bacteria to Dissolved Dimethylsulfoniopropionate and Amino Acid Uptake in the North Atlantic Ocean. Appl. Environ. Microbiol. 70, 4129–4135. doi:10.1128/AEM.70.7.4129

Martin-Cuadrado, A.-B., Rodriguez-Valera, F., Moreira, D., Alba, J.C., Ivars-Martínez, E., Henn, M.R., Talla, E., López-García, P., 2008. Hindsight in the relative abundance, metabolic potential and genome dynamics of uncultivated marine archaea from comparative metagenomic analyses of bathypelagic plankton of different oceanic regions. ISME J. 2, 865–86. doi:10.1038/ismej.2008.40

Massana, R., DeLong, E.F., Pedrós-Alió, C., 2000. A few cosmopolitan phylotypes dominate planktonic archaeal assemblages in widely different oceanic provinces. Appl. Environ. Microbiol. 66, 1777–1787. doi:10.1128/AEM.66.5.1777-1787.2000.Updated

Massana, R., Murray, A.E., Preston, C.M., DeLong, E.F., 1997. Vertical distribution and phylogenetic characterization of marine planktonic Archaea in the Santa Barbara Channel. Appl. Environ. Microbiol. 63, 50–56.

Medoc Group, 1970. Observation of formation of deep water in the mediterranean sea. Nature 227, 1937–1040.

Morris, R., Rappé, M., Connon, S., 2002. SAR11 clade dominates ocean surface bacterioplankton communities. Nature 420, 806–810. doi:10.1038/nature01281.1.

Morris, R.M., Vergin, K.L., Rappe, M.S., Carlson, C.A., Giovannoni, S.J., 2005. Temporal and spatial response of bacterioplankton lineages to annual convective overturn at the Bermuda Atlantic Time-series Study site. Limnol. Oceanogr. 50, 1687–1696.

Mou, X., Hodson, R.E., Moran, M.A., 2007. Bacterioplankton assemblages transforming dissolved organic compounds in coastal seawater. Environ. Microbiol. 9, 2025–37. doi:10.1111/j.1462-2920.2007.01318.x

Murray, A.E., Preston, C.M., Massana, R., Taylor, L.T., Blakis, A., Wu, K., DeLong, E.F., 1998. Seasonal and spatial variability of bacterial and archaeal assemblages in the coastal waters near Anvers Island, Antarctica. Appl. Environ. Microbiol. 64, 2585–2595.

Ouverney, C.C., Fuhrman, J.A., 2000. Marine Planktonic Archaea Take Up Amino Acids. Appl. Environ. Microbiol. 66, 4829–4833. doi:10.1128/AEM.66.11.4829-4833.2000

Pernthaler, A., Preston, C., 2002. Comparison of fluorescently labeled oligonucleotide and polynucleotide probes for the detection of pelagic marine bacteria and archaea. Appl. Environ. Microbiol. 68, 661–667. doi:10.1128/AEM.68.2.661

Polz, M.F., Alm, E.J., Hanage, W.P., 2013. Horizontal gene transfer and the evolution of bacterial and archaeal population structure. Trends Genet. 29, 170–5. doi:10.1016/j.tig.2012.12.006

Price, M.N., Dehal, P.S., Arkin, A.P., 2009. FastTree: computing large minimum evolution trees with profiles instead of a distance matrix. Mol. Biol. Evol. 26, 1641–50. doi:10.1093/molbev/msp077

Pujo-Pay, M., Conan, P., Raimbault, P., 1997. Excretion of dissolved organic nitrogen by phytoplankton assessed by wet oxidation and 1 5 N tracer procedures. Mar. Ecol. Prog. Ser. 153, 99–111.

Pujo-Pay, M., Raimbault, P., 1994. Improvement of the Wet-Oxidation Procedure for Simultaneous Determination of Particulate Organic Nitrogen and Phosphorus Collected on Filters. Mar. Ecol. Prog. Ser. 105, 203–207. doi:10.3354/meps105203

Quince, C., Lanzen, A., Davenport, R.J., Turnbaugh, P.J., 2011. Removing noise from pyrosequenced amplicons. BMC Bioinformatics 12, 38. doi:10.1186/1471-2105-12-38

Reshef, D.N., Reshef, Y. a, Finucane, H.K., Grossman, S.R., McVean, G., Turnbaugh, P.J., Lander, E.S., Mitzenmacher, M., Sabeti, P.C., 2011. Detecting novel associations in large data sets. Science (80-.). 334, 1518–24. doi:10.1126/science.1205438

Robinson, C., Steinberg, D.K., Anderson, T.R., Arístegui, J., Carlson, C. a., Frost, J.R., Ghiglione, J.-F., Hernández-León, S., Jackson, G. a., Koppelmann, R., Quéguiner, B., Ragueneau, O., Rassoulzadegan, F., Robison, B.H., Tamburini, C., Tanaka, T., Wishner, K.F., Zhang, J., 2010. Mesopelagic zone ecology and biogeochemistry – a synthesis. Deep Sea Res. Part II Top. Stud. Oceanogr. 57, 1504–1518. doi:10.1016/j.dsr2.2010.02.018

Rocap, G., Larimer, F.W., Lamerdin, J., Malfatti, S., Chain, P., Ahlgren, N.A., Arellano, A., Coleman, M., Hauser, L., Hess, W.R., Johnson, Z.I., Land, M., Lindell, D., Post, A.F., Regala, W., Shah, M., Shaw, S.L., Steglich, C., Sullivan, M.B., Ting, C.S., Tolonen, A., Webb, E.A., Zinser, E.R., Chisholm, S.W., 2003. Genome divergence in two Prochlorococcus ecotypes reflects oceanic niche differentiation. Nature 424, 1042–1047.

Rodríguez-Blanco, A., Ghiglione, J.-F., Catala, P., Casamayor, E.O., Lebaron, P., 2009. Spatial comparison of total vs. active bacterial populations by coupling genetic fingerprinting and clone library analyses in the NW Mediterranean Sea. FEMS Microbiol. Ecol. 67, 30–42. doi:10.1111/j.1574-6941.2008.00591.x

Rosselló-Mora, R., 2003. Opinion: the species problem, can we achieve a universal concept? Syst. Appl. Microbiol. 26, 323–6. doi:10.1078/072320203322497347

Santinelli, C., Nannicini, L., Seritti, A., 2010. DOC dynamics in the meso and bathypelagic layers of the Mediterranean Sea. Deep Sea Res. Part II Top. Stud. Oceanogr. 57, 1446–1459. doi:10.1016/j.dsr2.2010.02.014

Schott, F., Visbeck, M., Send, U., Fisher, J., Stramma, L., Desaubies, Y., 1996. Observations of deep convection in the Gulf of Lions, northern Mediterranean, during the winter of 1991/92. J. Phys. … 26, 505–524.

Send, U., Marshall, J., 1995. Integral effects of deep convection. J. Phys. Oceanogr. 25, 855–872.

Severin, T., Boutrif, M., Oriol, L., Caparros, J., Pujo-Pay, M., Durrieu De Madron, X., Garel, M., Tamburini, C., Conan, P., Ghiglione, J.-F., Sumitted-a. Impact of an open-sea convection event (0-1500m) on prokaryotic diversity and activity in the NW Mediterranean Sea. Environ. Microbiol.

Severin, T., Conan, P., Durrieu De Madron, X., Houpert, L., Oliver, M.J., Oriol, L., Caparros, J., Pujo-Pay, M., Submitted-b. Impact of open-ocean convection on nutrient, phytoplankton biomass and activity. Deep Sea Res. Part I Oceanogr. Res. Pap.

Shannon, P., Markiel, A., Ozier, O., Baliga, N.S., Wang, J.T., Ramage, D., Amin, N., Schwikowski, B., Ideker, T., 2003. Cytoscape: a software environment for integrated models of biomolecular interaction networks. Genome Res. 13, 2498–504. doi:10.1101/gr.1239303

Shapiro, B.J., Polz, M.F., 2014. Ordering microbial diversity into ecologically and genetically cohesive units. Trends Microbiol. 22, 235–247. doi:http://dx.doi.org/10.1016/j.tim.2014.02.006

Sintes, E., Bergauer, K., De Corte, D., Yokokawa, T., Herndl, G.J., 2013. Archaeal amoA gene diversity points to distinct biogeography of ammonia-oxidizing Crenarchaeota in the ocean. Environ. Microbiol. 15, 1647–58. doi:10.1111/j.1462-2920.2012.02801.x

Smith, J.M., Casciotti, K.L., Chavez, F.P., Francis, C.A., 2014. Differential contributions of archaeal ammonia oxidizer ecotypes to nitrification in coastal surface waters. ISME J.

Strickland, J.D.H., Parsons, T.R., 1997. A Practical Handbook of Seawater Analysis, Internationale Revue der gesamten Hydrobiologie und Hydrographie. Ottawa, Fisheries Research Board of Canada, Bulletin 167.

Strimmer, K., 2008. fdrtool: a versatile R package for estimating local and tail area-based false discovery rates. Bioinformatics 24, 1461–2. doi:10.1093/bioinformatics/btn209

Sugimura, Y., Suzuki, Y., 1988. A high-temperature catalytic oxidation method for the determination of non-volatile dissolved organic carbon in seawater by direct injection of a liquid sample. Mar. Chem. 24, 105–131. doi:10.1016/0304-4203(88)90043-6

Sun, Y., Wolcott, R., Dowd, S., 2011. Tag-Encoded FLX Amplicon Pyrosequencing for the Elucidation of Microbial and Functional Gene Diversity in Any Environment, in: Kwon, Y.M., Ricke, S.C. (Eds.), High-Throughput Next Generation Sequencing SE - 9, Methods in Molecular Biology. Humana Press, pp. 129–141. doi:10.1007/978-1-61779-089-8_9

Teira, E., Aken, H. Van, Veth, C., Herndl, G., 2006. Archaeal uptake of enantiomeric amino acids in the meso-and bathypelagic waters of the North Atlantic. Limnol. Oceanogr. 51, 60–69.

Teira, E., Gasol, J.M., Aranguren-Gassis, M., Fernández, A., González, J., Lekunberri, I., Alvarez-Salgado, X.A., 2008. Linkages between bacterioplankton community composition, heterotrophic

carbon cycling and environmental conditions in a highly dynamic coastal ecosystem. Environ. Microbiol. 10, 906–17. doi:10.1111/j.1462-2920.2007.01509.x

Tully, B.J., Nelson, W.C., Heidelberg, J.F., 2012. Metagenomic analysis of a complex marine planktonic thaumarchaeal community from the Gulf of Maine. Environ. Microbiol. 14, 254–67. doi:10.1111/j.1462-2920.2011.02628.x

Vergin, K.L., Beszteri, B., Monier, A., Thrash, J.C., Temperton, B., Treusch, A.H., Kilpert, F., Worden, A.Z., Giovannoni, S.J., 2013. High-resolution SAR11 ecotype dynamics at the Bermuda Atlantic Time-series Study site by phylogenetic placement of pyrosequences. ISME J. 7, 1322–32. doi:10.1038/ismej.2013.32

Wang, Q., Garrity, G.M., Tiedje, J.M., Cole, J.R., 2007. Naive Bayesian classifier for rapid assignment of rRNA sequences into the new bacterial taxonomy. Appl. Environ. Microbiol. 73, 5261–7. doi:10.1128/AEM.00062-07

Ward, D.M., Bateson, M.M., Ferris, M.J., Kühl, M., Wieland, A., Koeppel, A., Cohan, F.M., 2006. Cyanobacterial ecotypes in the microbial mat community of Mushroom Spring (Yellowstone National Park, Wyoming) as species-like units linking microbial community composition, structure and function. Philos. Trans. R. Soc. Lond. B. Biol. Sci. 361, 1997–2008. doi:10.1098/rstb.2006.1919

Ward, D.M., Cohan, F.M., Bhaya, D., Heidelberg, J.F., Kühl, M., Grossman, A., 2008. Genomics, environmental genomics and the issue of microbial species. Heredity (Edinb). 100, 207–19. doi:10.1038/sj.hdy.6801011

Woese, C.R., 1987. Bacterial Evolution. Microb. Rev. 51, 221–271.

Wuchter, C., Schouten, S., Boschker, H.T.S., Sinninghe Damsté, J.S., 2003. Bicarbonate uptake by marine Crenarchaeota. FEMS Microbiol. Lett. 219, 203–207. doi:http://dx.doi.org/10.1016/S0378-1097(03)00060-0

Yokokawa, T., Nagata, T., 2010. Linking bacterial community structure to carbon fluxes in marine environments. J. Oceanogr. 66, 1–12.

Supplementary information

Table S1: Characteristics of each SAR11, Marine Group I and II ecotypes

Subclade	Niche	Season	Water origin	Reference
SAR11 Ia	Surface	Summer	Sea water	Carlson et al. 2009
SAR11 Ib	Surface + deep	Spring	Sea water	Carlson et al. 2009
SAR11 Ic	Deep	All year	Sea water	Vergin et al., 2013
SAR11 IIa	Surface	Spring	Sea water	Vergin et al., 2013
SAR11 IIb	Deep	All year	Sea water	Vergin et al., 2013
SAR11 IIIa	Surface	Fall	Sea water	Vergin et al., 2013
SAR11 IIIb	Surface		Fresh water	Carlson et al. 2009
SAR11 IV	Surface	Summer	Sea water	Vergin et al., 2013
SAR11 Va	Surface	Summer	Sea water	Vergin et al., 2013
SAR11 Vb	Deep	All year	Sea water	Vergin et al., 2013
MGIa	Surface	Summer	Sea water	Massana et al., 2000
MGIb	Surface	Winter	Sea water	Massana et al., 2000
MGIc	Deep	All year	Sea water	Massana et al., 2000
MGId			Sea water	Hugoni et al., 2012
MGIIa_K	Surface	Summer	Sea water	Galand et al., 2010
MGIIa_L1	Surface	Summer	Sea water	Galand et al., 2010
MGIIa_L2 (formerly L3 et M)	Surface	Summer	Sea water	Galand et al., 2010
MGIIa_L3 (formerly L2)	Surface	Summer	Sea water	Galand et al., 2010
MGIIa_other	Surface		Sea water	This study
MGIIb_WHARN	Surface	Winter	Sea water	Galand et al., 2010
MGIIb_O	Ubiquitous	All year	Sea water	Galand et al., 2010
MGIIb_P	Ubiquitous	All year	Sea water	This study and Galand et al., 2010
MGIIb_Q	Ubiquitous	All year	Sea water	This study and Galand et al., 2010
MGIIb_N	Surface	All year	Sea water	Galand et al., 2010
MGIIb_N	Deep		Sea water	This study and Galand et al., 2010

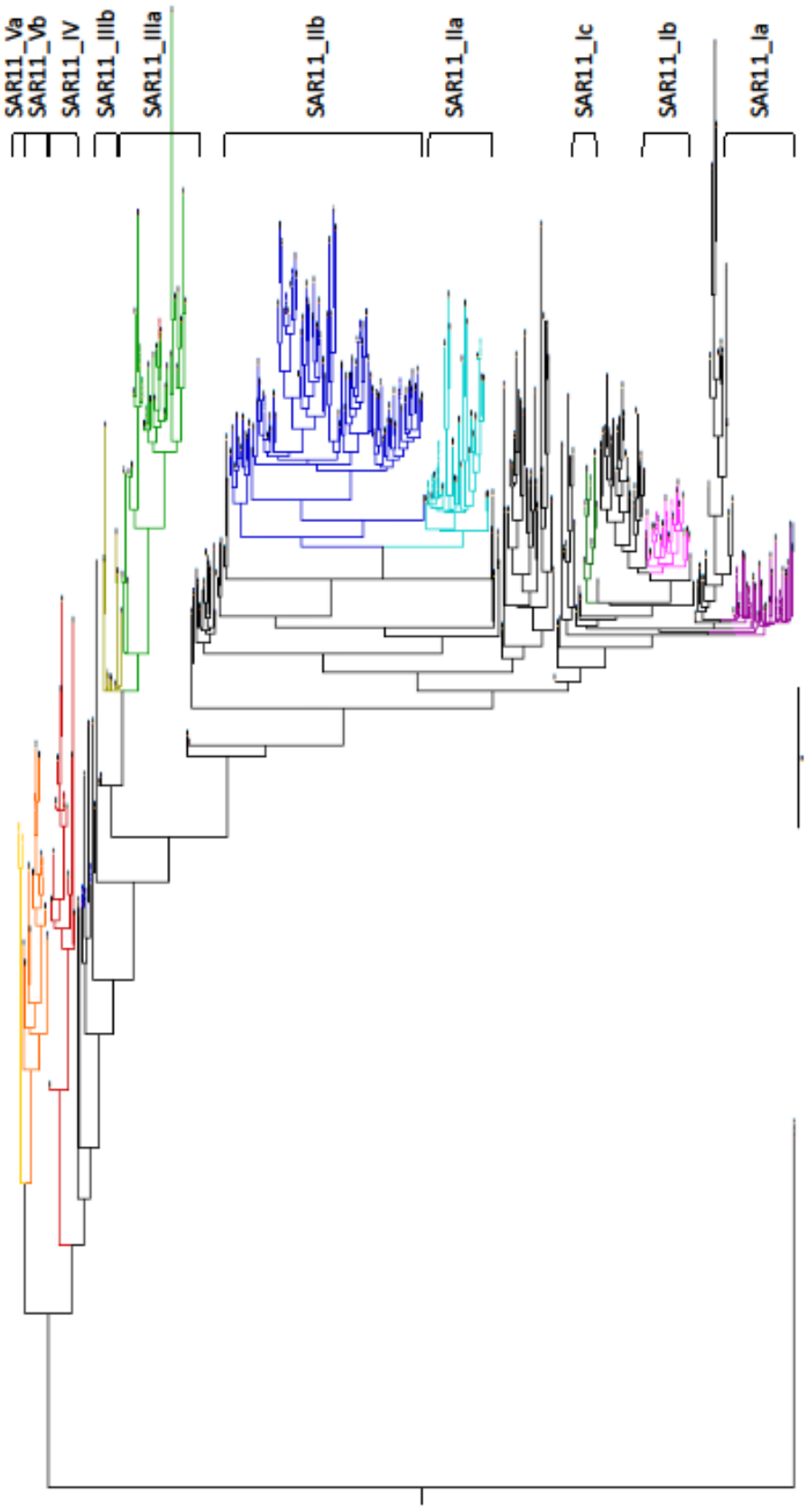

Figure S2: Phylogenetic tree of the SAR11 full length 16S rRNA sequences from the Greengenes database. Reference sequences retrieved from published papersare in bold.

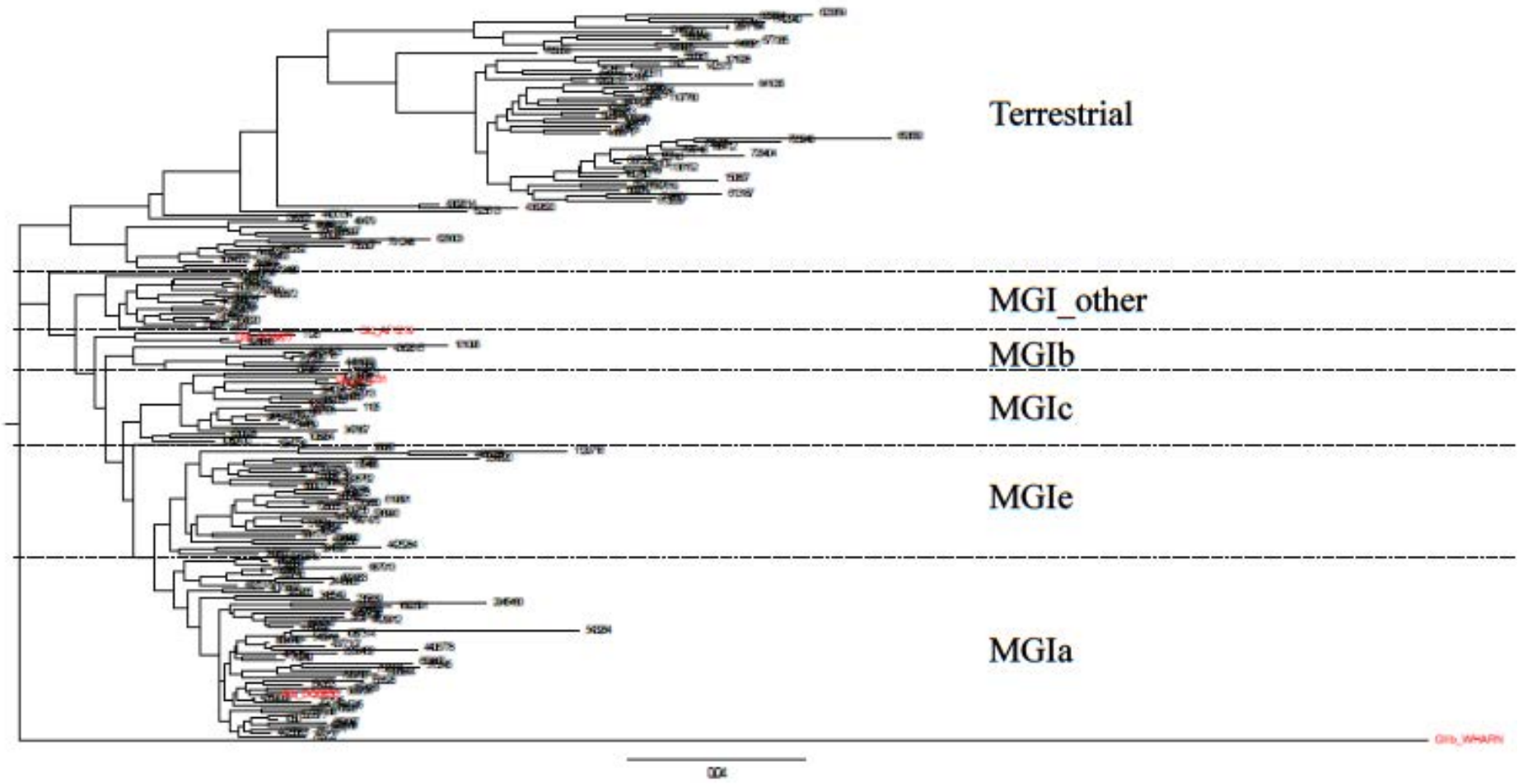

Figure S3: Phylogenetic tree of the Marine group I *Thaumarchaeota* full length 16S rRNA sequences from the Greengenes database. Reference sequences retrieved published sequences are in red.

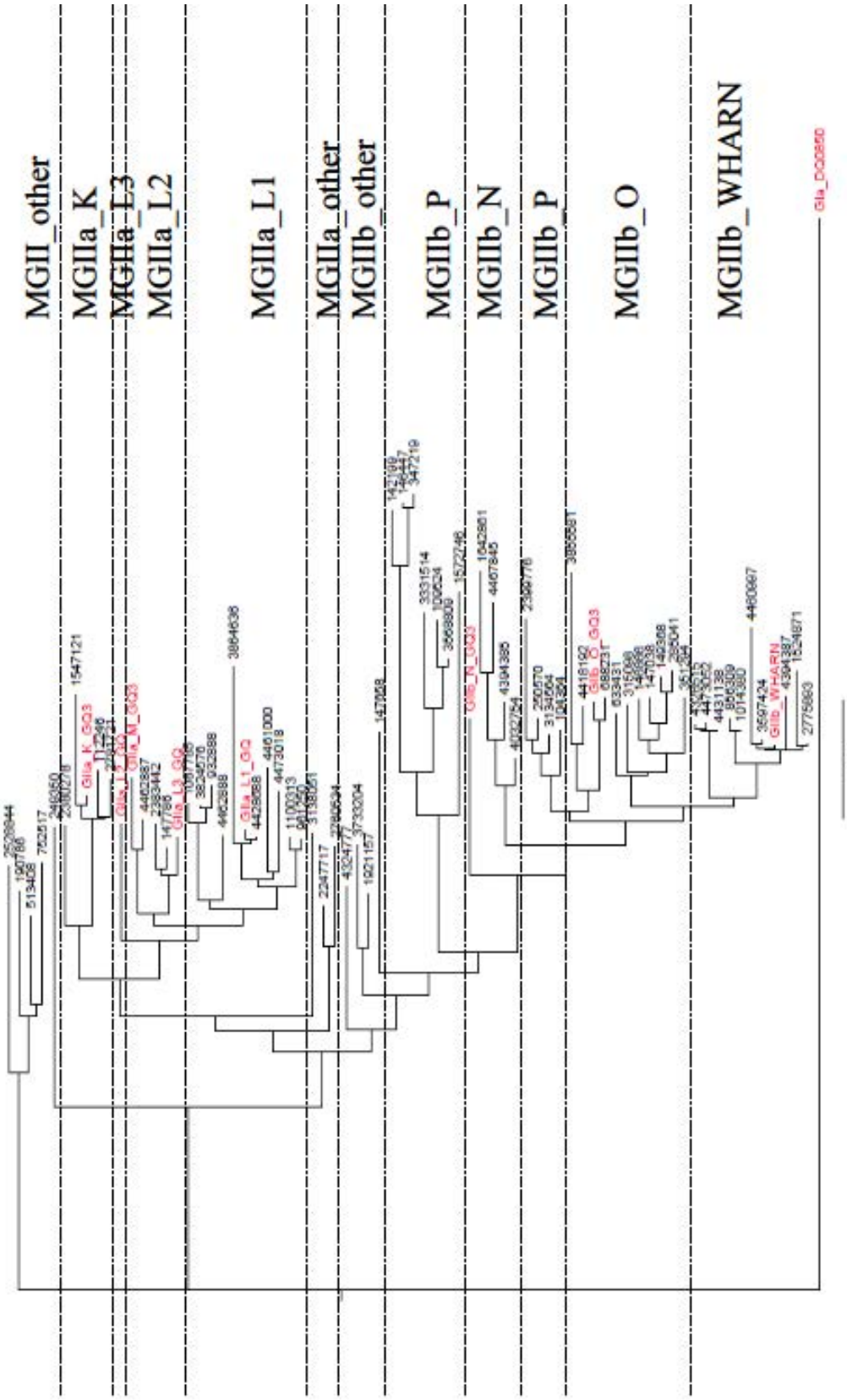

Figure S4: Phylogenetic tree of the Marine group II *Euryarchaeota* full length 16S rRNA sequences from the Greengenes database. Reference sequences retrieved from published papers are in red.

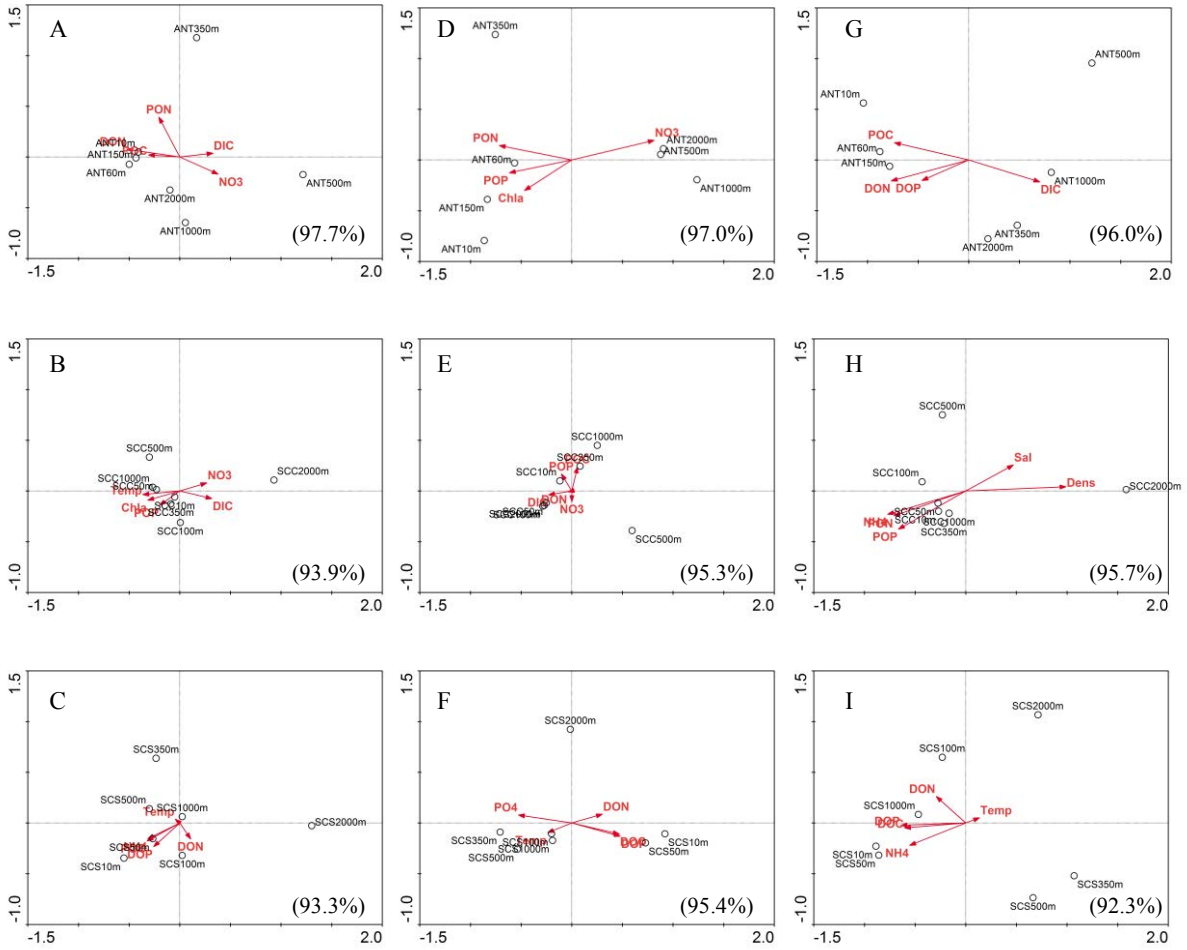

Figure S5: Canonical correspondence analysis (CCAs) of SAR11 subclades structure (A-C), Marine Group I subclades structure(D-F), and Marine Group II subclades structures (G-I) at each sampled station: ANT(A, D, G) , SCC (B, E, H) and SCS (C, F, I) . The lenght of the arrows represents the degree of correlation with the 2 first presented axis. NO3: nitrate, PO4: phosphate, DIC: dissolved inorganic carbon, DOC: dissolved organic carbon, DON: dissolved organic nitrogen, DOP: dissolved organic phosphorus, POC: particulate organic carbon, PON: particulate organic nitrogen, POP: particulate organic phosphorus, Chla: chlorophylla, Sal: salinity, Temp: temperature, Dens: density. The percentage explained by the model (r=ratio between the sum of all canonical eigenvalues and the total inertia x 100) are given in brackets.

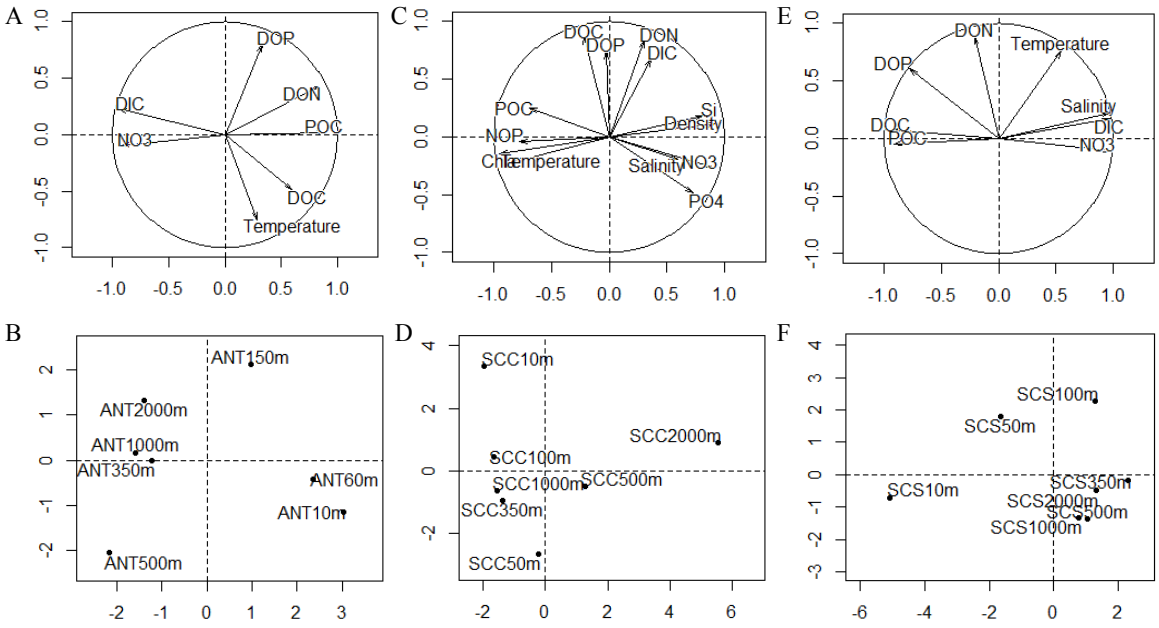

Figure S6: Principal Correspondance Analyses (PCA) of non-correlated environmental parameters selected accordinf to the Monte Carlos test of CCA analyses at ANT (A, B), SCC (C, D) and SCS (E, F) stations. Contributions of environmental parameters (A, C, D) and samples distributions (B, D, F) are indicated for each station.

Chapitre IV
DISCUSSION GÉNÉRALE ET PERSPECTIVES

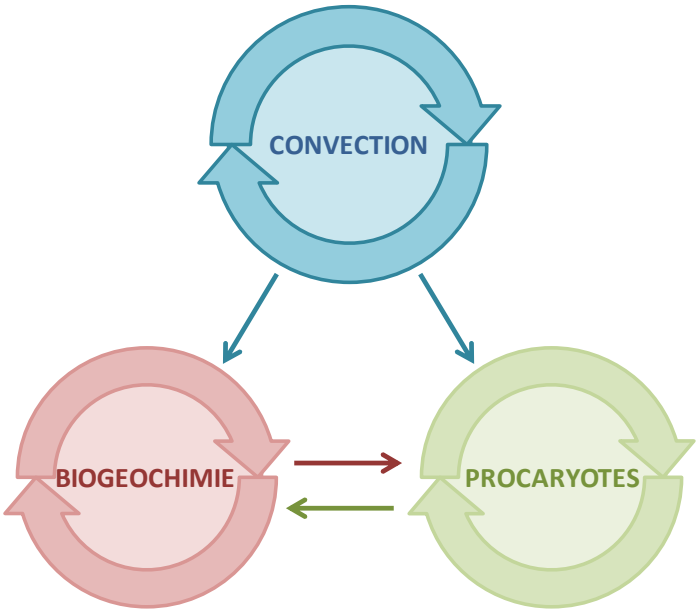

IV. DISCUSSION GÉNÉRALE ET PERSPECTIVES

En se basant sur les résultats de la campagne CASCADE exposés dans les chapitres précédents, ce dernier chapitre a pour objectif de discuter et d'envisager des perspectives réalistes autour des 3 questions fondamentales qui ont été abordées dans cette thèse :

- Quels sont les impacts d'un évènement de convection en MNO sur les stocks et la stœchiométrie biogéochimique ?
- Quels sont les impacts d'un évènement de convection en MNO sur la diversité et l'activité des procaryotes ?
- Quels sont les impacts d'un évènement de convection en MNO sur les écotypes de SAR11, Marine Group I et Marine Group II ?

IV.1. Impact de la convection sur la biogéochimie de la MNO

IV.1.1. Discussion : les sels nutritifs

Les principes physiques régissant le processus de convection sont assez bien décrits en Méditerranée (Medoc Group, 1970; Send and Marshall, 1995; Mertens and Schott, 1998; Durrieu de Madron et al., 2013). Pourtant, le phénomène d'enrichissement en sels nutritifs de la couche de surface par la remontée des eaux profondes et l'exportation de matière organique vers les profondeurs n'ont pas encore été correctement échantillonnés. L'originalité du 1er article réside dans les premières mesures directes du stock de sels nutritifs réalisées durant un évènement de convection atteignant 1500 m de profondeur dans le golfe du Lion, ainsi que dans le suivi stœchiométrique du devenir de ces sels nutritifs jusqu'à 12 jours après ce mélange intensif pendant la phase de restratification.

En comparaison avec des études précédentes réalisées lors des mélanges convectifs en mer Adriatique et dans la région de Rhodes (Gačić et al., 2002; Santinelli et al., 2012; Yılmaz and Tuğrul, 1998), l'apport de nitrate en MNO était 2 à 3 fois supérieur et 4 fois supérieur pour les phosphates. Cette différence est certainement due au gradient d'oligotrophie croissant caractérisant le passage du bassin occidental vers le bassin oriental (Pujo-Pay et al., 2011).

L'étendue de la zone de convection étant le facteur conditionnant la quantité de sels nutritifs apportés, dans la mesure où la profondeur de mélange atteint la nutricline (avec un maximum en fin d'été d'~200 m de profondeur en MNO ; Conan et al., 1999; Diaz et al., 2000), on estime que l'épisode de convection de février 2011 étendu sur 17 000 km² (cf. section II.2) a pu apporter 17 fois plus de nitrate, phosphate et silicate que l'épisode secondaire de mars 2011

étendu sur seulement 1 000 km². Cependant d'autres facteurs tels que la durée du mélange convectif ou la vitesse de remontée des eaux profondes pourraient affiner ou complètement contredire nos estimations. Nos résultats soulèvent donc un certain nombre de questions :

- Les estimations des apports en sels nutritifs par le premier mélange de l'hiver 2011 s'approchent-elles de la réalité ? Peuvent-elles surestimées ou sous-estimées ?
- Existe-il d'autres processus physiques ou biologiques non observés durant la campagne CASCADE qui pourraient interférer avec les estimations des apports en sels nutritifs par le mélange convectif de février réalisées dans cette étude ?

IV.1.2. Perspectives : les sels nutritifs

Les questions posées ci-dessus pourront trouver des réponses grâce aux campagnes DeWEX. Les analyses et le traitement des échantillons récoltés sont actuellement en cours, mais nous pouvons d'ores et déjà présenter quelques résultats majeurs.

Les campagnes DeWEX 2013 s'inscrivent dans un dispositif d'observation intense de l'année 2012-2013, visant à caractériser finement le rôle de la convection profonde au large sur la distribution des propriétés biogéochimiques des masses d'eau et leur impact sur la structure de l'écosystème lors du bloom printanier. Précédée par une étude préliminaire (CASCADE), le projet DeWEX consiste en une ambitieuse expérience alliant approches de terrain sous forme de plusieurs campagnes océanographiques (MOOSE-GE, DoWEX et DeWEX), l'utilisation de nouvelles plateformes autonomes (flotteurs Bio-Argo et profileurs PROVOR équipés de capteur de fluorescence, d'O_2 et de nitrate, gliders et lignes de mouillages), ainsi qu'un énorme effort de modélisation couplée physique et biogéochimie pour ainsi recouvrir toute la Méditerranée Nord Occidentale depuis juillet 2012 jusqu'à septembre 2013 (Figure IV-1). Ce projet s'implémente dans le workpackage 1 du projet MerMEX, composante biogéochimique du programme MISTRALS. En ce qui me concerne plus directement, l'expérience que j'ai acquise au cours du projet CASCADE m'a permis de participer à l'organisation des 2 campagnes océanographiques DeWEX-2013, campagnes durant lesquelles j'ai embarquée.

Lors du 1er leg de DeWEX-2013 (1-22 février 2013 ; Figure IV-1), une attention particulière a été portée à l'événement de convection profonde afin de déterminer avec précision les apports en nutriments (sels nutritifs, carbone inorganique dissous) et les exports en matière organique (MO). Le 2ème leg (4-26 avril 2013 ; Figure IV-1) avait pour objectif de caractériser l'efflorescence printanière récurrente en MNO qui suit le phénomène de convection profonde, un processus de grande importance pour les bilans de matière à l'échelle du bassin occidental

en termes de productions primaire et secondaire (D'ortenzio and Ribera d'Alcalà, 2009). L'utilisation d'un système de prélèvement ultrapropre d'eau de surface en continu pour des mesures de variables physiques, biologiques et chimiques, a permis d'augmenter considérablement la résolution du réseau de stations de prélèvements et d'obtenir une vision synoptique à haute résolution de l'ensemble de la MNO. A cela s'ajoute une modélisation couplée physique / biogéochimie (modèles SYMPHONIE / ECO3M-S) particulièrement bien adaptée qui devrait permettre pour la première fois de fermer le bilan hydrologique et biogéochimique dans une région convective avec des échanges importants avec le plateau.

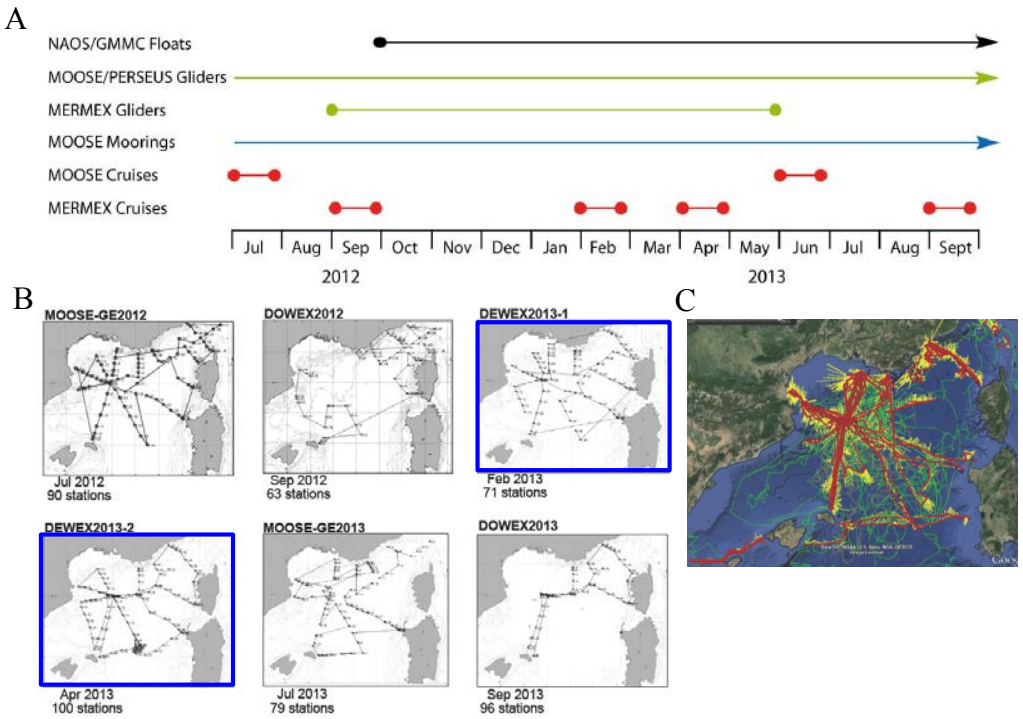

Figure IV-1 *:* (A) Place des campagnes DeWEX-2013 dans le contexte programmatique MerMeX-MOOSE, représentant la couverture temporelle de l'année 2012-2013. (B) Plans d'échantillonnages des campagnes MOOSE, DoWEX et DeWEX-2013 (encadrées en bleues) en MNO. (C) Couverture spatiale par les plateformes autonomes (flotteurs Bio-Argo, gliders).

L'évènement de convection échantillonné durant le leg 1 de la campagne DeWEX était le premier mélange convectif de l'hiver 2012-2013. L'enfoncement de la couche de mélange a débuté vers le 20 janvier 2013 (données de la ligne de mouillage LION transmis par X. Durrieu de Madron) pour atteindre le fond marin le 12 février à la bouée LION. Le mélange convectif concernait plus de 25 000 km² et s'étendait jusqu'en mer Ligure (Figure IV-2). La diminution des forçages atmosphériques a entrainé une remontée de la profondeur de la couche de mélange à partir du 27 février, pour atteindre la surface vers le 6 mars. Un second évènement de mélange, tel que celui échantillonné durant la campagne CASCADE, a eu lieu du ~9 au 20 mars 2013

(Figure IV-2). D'après les images satellites, le bloom printanier a commencé à partir du 22 mars et s'est développé jusqu'à la mi-avril. Il a donc été bien échantillonné durant le leg 2 de la campagne DeWEX-2013 (4-26 avril 2013).

L'échantillonnage du compartiment biogéochimique durant le leg 1 de la campagne DeWEX permettra d'estimer les apports en sel nutritifs par le premier épisode profond de l'hiver 2013. Nous pourrons ainsi confronter ces résultats avec les estimations faites dans le 1er article, et établir si ces dernières étaient cohérentes. Les moyens techniques utilisés pour caractériser les écosystèmes pélagiques entre la période de convection profonde (leg 1 DeWEX-2013) et le bloom printanier (leg 2 DeWEX-2013), tels que les gliders, les flotteurs Bio-Argo, et les lignes de mouillages), combinés aux images satellites, permettront d'identifier des structures physiques et biologiques particulières susceptibles de diminuer ou d'augmenter les stocks de sels nutritifs.

Un premier traitement des images satellites a permis de mettre en évidence un léger développement phytoplanctonique vers le 8 mars (Figure IV-2), un processus biologique pouvant potentiellement consommer les sels nutritifs apportés par le 1er épisode de convection. Les données de température et de salinité de la ligne de mouillage LION ont révélé un évènement secondaire de convection susceptible de réapprovisionner la couche de surface en nutriments, aussi observable via les images satellites (Figure IV-2). D'autres structures physiques identifiables par les lignes de mouillage et les gliders sont aussi susceptibles de modifier les stocks en sels nutritifs. Par exemple, les tourbillons cycloniques provoquent une remontée des eaux profondes riches en sels nutritifs et peuvent donc réapprovisionner la couche de surface. Inversement, les tourbillons anticycloniques participent à la séquestration du carbone en favorisant la plongée des eaux de surface.

IV.1.3. Discussion : export de matière organique

Les évènements secondaires de convection comme celui que nous avons échantillonné au cours de la campagne CASCADE sont rarement pris en compte dans les bilans biogéochimiques en raison de leur faible importance sur les bilans hydrologiques de la Méditerranée (étendue spatiale et temporelle relativement faible, faible volume d'eau dense formé, et profondeur de mélange généralement inférieure à celle de l'épisode convectif du début de l'hiver). Les analyses satellitaires du premier article ont pourtant mis en évidence un développement phytoplanctonique non négligeable entre l'épisode de convection de février

2011 atteignant le fond marin, et celui de mars de la même année atteignant 1500 m de profondeur. Le phytoplancton a bénéficié de l'apport massif de sels nutritifs par la convection de février et de la stratification momentanée de la colonne d'eau induite par la diminution des forçages atmosphériques. Nous avons pu mettre en évidence dans le 1er article que le phytoplancton fraichement développé était exporté à 1500 m, entrainant certainement un flux de carbone organique non négligeable et assimilable par les organismes profonds. Contrairement à l'épisode de février beaucoup plus intense, la remise en suspension du sédiment était moindre en mars puisque le mélange convectif n'atteignait pas le fond marin (Puig et al., 2013), introduisant beaucoup moins de MO réfractaire dans la colonne d'eau (cf. section I.3.3). Les images satellitales de l'année 2013 (Figure IV-2) nous montrent que cette succession d'évènements n'est pas un phénomène propre à l'année 2011. Une convection intense est en effet régulièrement observée au début de l'hiver (janvier - février), suivi d'une période de stratification momentanée permettant au phytoplancton de se développer. En fin d'hiver (mi-mars), un nouveau mélange convectif moins profond et sur une étendue plus restreinte avorte le début de bloom observé. On peut alors formuler les questions suivantes:

- Quelle-est l'importance du flux de carbone généré par l'évènement secondaire de fin d'hiver ? Est-il est plus important que l'intense mélange de début d'hiver atteignant le fond marin ?
- La MO exportée par l'évènement secondaire de convection est-elle différente de celle exportée par le mélange convectif de début d'hiver ?

Les processus secondaires de convection semblent donc mette en évidence un certain découplage entre la physique et la biogéochimie. Comme les scientifiques se sont principalement intéressés aux épisodes de convection intenses susceptibles de former large volume d'eaux profondes, nous en savons relativement peu sur les évènements de convection intermédiaires (~200-300 m de profondeur) qui à priori peuvent se succéder durant la fin de l'hiver et le début du printemps. Tout comme l'évènement secondaire de mars 2011, une période de stabilisation de la colonne d'eau entre chaque épisode intermédiaire pourrait permettant un développement phytoplanctonique puisque la nutricline aurait été atteinte. Ces petits évènements de convection ne seraient pas d'une grande importance en ce qui concerne les bilans hydrologiques de la Méditerranée, mais pourraient significativement influencer les flux de carbone. Ce qui nous amène à poser la question suivante :

Qu'elle est l'influence sur les flux de carbones des épisodes intermédiaires de convection successifs ?

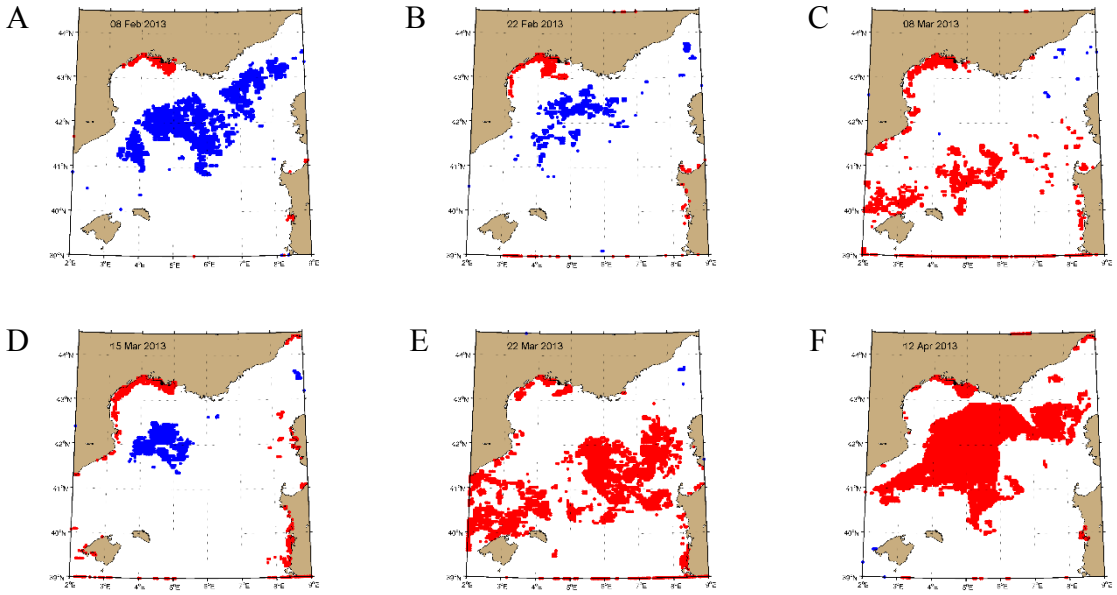

Figure IV-2 : Données du satellite MODIS-aqua indiquant l'aire de convection (bleu, chlorophylle a < 0.12 mg.m-3) et l'aire de l'efflorescence phytoplanctonique (rouge, chlorophylle a > 1 mg.m-3). Les données satellitaires sont moyennées sur 8 jours le (A) 8 février, (B) 22 février, (C) 8 mars, (D) 15 mars, (E) 22 mars, et (F) le 12 avril 2013.

D'autre part, nous avons aussi mis en évidence dans le 1er article un conditionnement de l'efflorescence printanière fortement lié au dernier épisode de convection de l'hiver. Deux études réalisées en MNO ont observé que la quantité de carbone organique particulaire (COP) exportée vers les zones méso- et bathypélagiques étaient plus importantes lors du bloom phytoplanctonique (~40 $mgC.m^{-2}.d^{-1}$), avec néanmoins un export non négligeable lors de l'intense mélange convectif (~10 $mgC.m^{-2}.d^{-1}$) (Stabholz et al., 2013; Gogou et al., 2014). Cependant le COP présent dans les couches profondes durant un épisode de convection serait composé à la fois de MO disponible d'origine phytoplanctonique, et de MO plus réfractaire issue de la resuspension du sédiment (Stabholz et al., 2013). Par contre, le COP exporté durant l'efflorescence serait exclusivement issu de la sédimentation de cellules phytoplanctoniques, donc plus labile et assimilable par les organismes profonds. Des conclusions similaires ont été émises pour le carbone organique dissous (COD) (Santinelli et al., 2010), mais aucun indice rendant compte de la qualité de cette MO dissoute (MOD) n'a encore été calculé en MNO. La question reste entière concernant :

Est-ce que l'export de MO est plus important et de meilleure qualité lors du mélange convectif secondaire ou bien lors du bloom printanier ?

IV.1.4. Perspectives : export de matière organique

Lors de la campagne DeWEX, des données sur les stocks de matière organique dissoute (MOD) et particulaire (MOP) pour les éléments carbone, azote et phosphore, ainsi que sur la MOD chromophorique (MODc) et fluorescente (MODf) ont été récoltées lors du 1er mélange convectif de l'hiver 2012-2013 (leg 1, février 2013), et durant l'efflorescence printanière de 2013 en MNO (leg 2, avril 2013). La MODc, actuellement en cours de traitement, pourra nous fournir des indices sur la qualité et la disponibilité de la MOD exportée. En effet, les données de MODc combinées à celles de la MODf peuvent par exemple donner des informations sur le degré d'aromaticité de la MOD, la taille moléculaire de la MOD, la présence de composés plus ou moins réfractaires, d'acides humiques ou la présence de produits autochtones de faibles poids moléculaires. Toutes les informations déductibles de la MODc et MODf sont répertoriées dans le Tableau IV-1.

Une comparaison des stocks et flux de MO entre le 1er mélange convectif de l'hiver 2013 (leg 1 DeWEX) et le mélange secondaire de l'hiver 2011 (CASCADE) permettrait de déterminer quel type d'épisode convectif participe le plus au flux de carbone (primaire ou secondaire ?). Une comparaison des indices de qualité issus des analyses de la DOMc et DOMf durant le leg 1 de la campagne DeWEX et la campagne CASCADE pourra nous éclaircir sur la qualité de la MO exportée par le 1er mélange convectif de l'hiver et par un évènement secondaire. De même, une comparaison des stocks, des flux et de la qualité de la MO entre l'épisode profond de convection (leg 1 DeWEX) et l'efflorescence printanière (Leg 2 DeWEX) permettra de déterminer quel processus participe le plus au flux de carbone et quelle est la qualité de ce carbone.

En ce qui concerne l'influence de la succession d'épisodes intermédiaires de convection sur les flux de carbone, les campagnes DeWEX-2013 ne pourront pas directement répondre à cette question puisque le 1er leg a échantillonné un évènement profond de convection. Cependant, le déploiement prévu sur 10 ans des flotteurs Bio-Argo, des profileurs PROVOR équipés de capteurs biogéochimiques ainsi que des gliders permettront de suivre sur plusieurs années ce genre d'évènements de convection intermédiaires, et d'évaluer leur importance biogéochimique.

Tableau IV-1 : Résumé et description des propriétés spectroscopiques de la MOD (MODc noté CDOM et MODf noté fDOM). Abs pour paramètres dérivés des spectres d'absorption, Fluo pour paramètres dérivés des spectres de fluorescence, EEM pour les paramètres dérivés des matrices de fluorescence Excitation-Émission. Tableau tiré de Catalan Garcia (2013) et les références ci-inclus.

Parameter	Abs or Fluo	Description	Interpretation
Specific ultra-violet absorbance at 254 nm (SUVA254; L mg^{-1} m^{-1})	Abs	Ratio of the absorbance coefficient at 254nm and the DOC concentration in mg L^{-1}	Informs on the aromaticity of DOM, with values generally ranging between 1 and 6 L mg^{-1} m^{-1}
A350 (m^{-1})	Abs	Absorption coefficient at 350 nm	Indicator of chromophoric dissolved organic matter (CDOM) concentration
S_R	Abs	Slope ratio of $S_{275-295}$ to $S_{350-400}$	Inversely correlated to molecular weight and described to increase upon irradiation
Fluorescence Index (FI)	Fluo	Ratio of the emission intensities at 470/520 nm for an excitation of 370 nm	Indicator of terrestrial-plant derived (low FI ~ 1.2) or microbial-algal derived (high FI ~1.4) origin
Humification Index (HIX)	Fluo	Peak area under the emission spectra 435–480 nm divided by 300–345 nm, at an excitation of 254 nm	Higher values correspond to a higher degree of humification
Biological Index (BIX)	Fluo	Ratio of the emission intensities at 380/430nm for an excitation of 310 nm	Indicator of recent biological activity or recently produced DOM
Peak A (or α')	Fluo-EEM	250Ex – 450Em	Humic substances and recent materials
Peak C (or α)	Fluo-EEM	350Ex – 450Em	Humic substances from terrestrial sources
Peak M (or β)	Fluo-EEM	310Ex – 400Em	Autochthonous production, low molecular weight
Peak T (or δ)	Fluo-EEM	280 Ex – 330Em	Protein-like material (resembling the aminoacid Tryptophan signal)
Peak B (or γ)	Fluo-EEM	270 Ex – 300Em	Protein-like material (resembling the aminoacid Tryrosine signal)

IV.2. Impact de la convection sur la diversité et les activités des procaryotes marins en MNO

IV.2.1. Discussion : influence de la MO exportée sur les communautés convectives

En Méditerranée, la distribution verticale des communautés procaryotiques est généralement organisée selon les paramètres environnementaux de chacune des masses d'eau (cf. section I.4.1 ; La Ferla et Azzaro, 2001; Ghiglione et al., 2007, 2009; Galand et al., 2010; Díez-Vives et al., 2014). Des taxa différents caractérisent les eaux de surface et de fond (Acinas et al., 1997; Ghiglione et al., 2012). Cette structuration des communautés selon les masses d'eaux a été mise en évidence dans une zone extérieure à la convection (station Antares – ANT) dans le 2ème article, avec en surface une dominance des SAR11, *Flavobacteriales*, *Oceanospirillales*, *Synechoccocales* et des Marine Group II *Euryarchaeota*. Dans les eaux profondes (LIW et WMDW), les SAR11 restaient dominant, confortant leur plasticité fonctionnelle et l'existence de plusieurs écotypes adaptés à des environnements contrastés

(Carlson et al., 2009; Vergin et al., 2013). Les 3 autres taxa de surface étaient présents dans les eaux profondes mais en quantité beaucoup moins importante. Certains groupes taxonomiques tels que les SAR406, SAR202, les Deltaproteobactéries Sva0853, et les Marine Group I *Thaumarchaeota* caractérisaient par leur présence unique les LIW et WMDW.

Nous avons observé que l'assemblage procaryotique au sein de la cellule de convection (10 - 1500 m) avait une structure proche des communautés de surface en période stratifiée. Néanmoins, la présence sporadique des SAR406, SAR202 et Sva0853 due à la remontée d'eau profonde nous a permis de différencier significativement les communautés issues du mélange convectif de celles des eaux de surface stratifiées. Les analyses multivariées directes (canonical correspondance analysis) ont permis de montrer que l'homogénéisation de la colonne d'eau par le mélange physique n'était pas le seul facteur conditionnant cet assemblage de procaryotes. La MO exportée ainsi que la chlorophylle *a* contribuaient significativement à cette structuration. De plus, la diminution des activités enzymatiques extracellulaires indiquerait que cette MO exportée était sous forme monomérique labile ou semi-labile, donc directement assimilable par les procaryotes. Cette MO labile ou semi-labile favoriserait la production de biomasse par une augmentation de l'abondance des procaryotes de 21% entre 10 m et 1000 m, ainsi que la production hétérotrophe (+43%) malgré les intenses courants existant au sein de la cellule de convection (Send and Marshall, 1995). Une étude récente réalisée en mer Adriatique n'a pas observé cette tendance durant le mélange vertical (Najdek et al., 2014). Ces auteurs ont observés que l'abondance et la production hétérotrophique procaryotique diminuaient au sein de la cellule de convection, et n'étaient stimulées que plus tard par le bloom phytoplanctonique qui a suivi le mélange convectif. Pour expliquer les différences obtenues entre cette étude et nos observations, nous pouvons émettre l'hypothèse que l'absence de développement phytoplanctonique précédent le mélange convectif dans l'étude de Najdek et al. (2014) est à l'origine de l'absence d'activité au sein de la cellule de convection observée dans leur étude. En effet, la MO labile faisant alors défaut au développement des procaryotes, leur métabolisme était potentiellement dormant au moment de leur export. Les données de la littérature relatives à l'impact des phénomènes de convection sur l'activité et la diversité des procaryotes sont rares et l'étude récente de Nadjek et al. (2014) nous amène à nous poser la question suivante :

Lors de la campagne DeWEX (leg1) réalisée dans la même zone d'échantillonnage que notre étude (CASCADE), notre équipe a pu échantillonner le premier mélange convectif de l'hiver 2013, qui ne faisait pas suite à un développement phytoplanctonique précoce comme on a pu l'observer dans l'article 2. Cette situation s'approche des conditions d'échantillonnages de l'étude de Najdek et al. (2014). Sans développement phytoplanctonique précédent le mélange

convectif, observera-t-on une activité procaryotique plus faible pendant ce mélange convectif primaire par rapport à l'épisode secondaire de fin d'hiver échantillonné lors de la campagne CASCADE ?

D'autre part, nous avons mis en évidence dans le 2ème article que la communauté formée lors du mélange convectif était biologiquement active (augmentation de la production hétérotrophe procaryotique intégrée de 43% entre 10 et 1500 m). Cependant, nous ne savons pas quels taxa en particuliers sont responsables de cette activité. Par exemple, le clade des SAR11 est le plus abondant dans notre étude. Il est aussi le groupe phylogénétique prépondérant dans tous les océans du monde (Morris et al., 2002). Néanmoins une faible activité est souvent conférée à ce groupe (Alonso-Sáez and Gasol, 2007; Rodríguez-Blanco et al., 2009) en raison de leur petit génome (Giovannoni et al., 2005). Sachant que tous les groupes taxonomiques n'ont pas la même activité :

? Quels sont les groupes taxonomiques présents au sein de la cellule de convection qui participent le plus à la reminéralisation de la MO exportée ?

IV.2.2. Perspectives : influence de la MO exportée sur les communautés convectives

Comme nous l'avons évoqué ci-dessus, une comparaison des activités hétérotrophiques réalisées lors du premier mélange convectif de l'hiver 2013 (campagne DeWEX) avec celles réalisées lors de l'épisode secondaire échantillonnée pendant la campagne CASCADE pourra nous éclairer sur la différence de résultats obtenus avec notre étude (mélange secondaire) et celle de la mer Adriatique (mélange primaire ; Najdek et al., 2014). Cette comparaison permettrait de répondre à la première question posée dans cette partie.

La deuxième question aborde une interrogation plus large de la relation entre diversité/fonction des procaryotes. Cette question est récurrente en écologie microbienne et reste d'actualité. Malgré l'émergence des outils moléculaires qui ont permis de mieux décrire la taxonomie et la diversité des espèces présentes dans une communauté, leur inventaire ne permet pas de savoir si les espèces présentes sont métaboliquement actives ou non, et quelles fonctions elles remplissent au sein de la communauté.

Une première réponse peut être donnée en décrivant les communautés à partir de l'expression de leur ARNr16S. En effet, différents auteurs ont montré que le taux de croissance bactérien est corrélé au contenu cellulaire en ARNr (Delong et al., 1989; Poulsen et al., 1993). Par conséquent, l'information de l'activité d'une cellule peut être obtenue en utilisant l'information donnée par les transcrits de l'ARNr 16S (Casamayor et al., 2001). Même si

l'abondance des procaryotes en mer est élevée, seule une faible proportion est métaboliquement active (Del Giorgio and Bouvier, 2002; Sherr et al., 1999). Par conséquent, on peut observer des différences nettes entre les communautés totales (comprenant des populations actives, dormantes, sénescentes et mortes) et les populations actives. Pour répondre à la question de l'activité potentielle des communautés procaryotes influencées par le phénomène de convection, des analyses de la diversité de l'ADNr et de l'ARNr 16S permettraient de faire la différence entre les organismes présents dans la cellule de convection, de ceux métaboliquement actifs, identifiant ainsi les taxa potentiellement investis dans la reminéralisation de la MO exportée.

Une seconde réponse peut être apportée par l'utilisation de la technique de DNA-Stable Isotope Probing (SIP) (Radajewski et al., 2000) afin de suivre l'assimilation de la MO issue du phytoplancton par les procaryotes de la communauté convective. Dans l'article 4 (voir ANNEXES A), j'ai participé à la mise au point et à l'utilisation de cette technique qui a été employée pour la première fois en milieu marin. Si la technique de comparaison de la diversité via l'ADNr 16S et l'ARNr 16S nous permet d'identifier les taxa actifs, elle ne permet pas de déterminer les fonctions remplies par ces communautés actives. Ici, l'objectif serait d'identifier les procaryotes capables d'assimiler la MO exportée. La technique de DNA-SIP est applicable à tout type de substrat carboné qui peut être marqué par un isotope stable du carbone, le ^{13}C (voir article de synthèse de Sauret et Ghiglione, 2013) et donc d'identifier plus précisément la relation diversité/fonction des procaryotes (cf. section I.4.1). Dans notre cas, l'approche expérimentale (Figure IV-3) consisterait à marquer isotopiquement des cellules phytoplanctoniques en utilisant un milieu contenant du bicarbonate marqué au carbone 13 (^{13}C). De cette manière, les cellules et la MO qui les composent serait marquée au ^{13}C. Afin de simuler les conséquences des forts courants présents au sein de la cellule de convection, différents traitements seraient appliqués aux cultures pour récupérer (i) l'exsudat phytoplanctonique (noté E), c'est-à-dire une MO labile naturellement excrétée par les cellules, (ii) le lysat phytoplanctonique (noté L) composé de débris cellulaires et du contenu intracellulaire, un mélange de MOD et MOP plus ou moins labile, et (iii) le lysat filtré (noté LF) composé uniquement du contenu intracellulaire, donc de la MOD plus ou moins labile. Des incubations combinant une population naturelle de procaryotes marins bathypélagiques et les substrats marqués au ^{13}C seraient ensuite réalisées. De cette manière, les procaryotes capables d'assimiler le substrat seraient discernés du reste de la communauté par le marquage de leur ADN au ^{13}C. Un gradient de chlorure de césium (ClCs) permettra de séparer les 2 types d'ADN, l'ADN marqué au ^{13}C (noté ^{13}ADN) d'une densité de 1.72 $g.ml^{-1}$ et celui non marqué des procaryotes

n'ayant pas assimilé le ^{13}C-substrat, contenant donc exclusivement du ^{12}C (noté ^{12}ADN) d'une densité de 1.71 g.ml^{-1}.

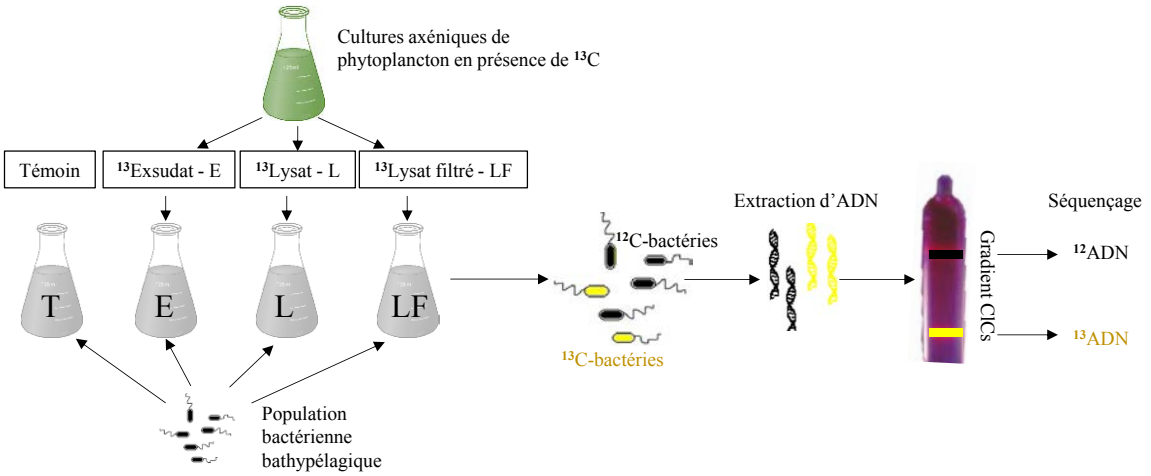

Figure IV-3 : Principe générale de l'expérience de SIP couplée à des substrats phytoplanctoniques.

Une expérience préliminaire sur l'exsudat, le lysat et le lysat filtré de cultures de *Chaetoceros* sp ont permis de mettre en évidence l'assimilation de ces 3 substrats par différentes communautés. Malheureusement, l'expérience que nous avons réalisée ne nous a pas permis de mettre en évidence de différence significative entre les fractions ^{12}ADN et ^{13}ADN pour chacun des substrats (Figure IV-4). Cette absence de différence semble être due à un mauvais marquage des substrats phytoplanctoniques. Les cellules phytoplanctoniques n'auraient pas incorporé le bicarbonate marqué au ^{13}C, certainement présent en quantité insuffisante dans le milieu. Néanmoins, cette approche reste très prometteuse et originale. L'approche expérimentale de DNA-SIP utilisant des cultures phytoplanctoniques axéniques marquées au ^{13}C devra être améliorée afin d'identifier les procaryotes responsables de la minéralisation de la MO exportée lors des épisodes convectifs, et de déterminer la quantité de MO non minéralisée restant disponible pour les organismes benthiques, ou pour séquestration dans les sédiments marins.

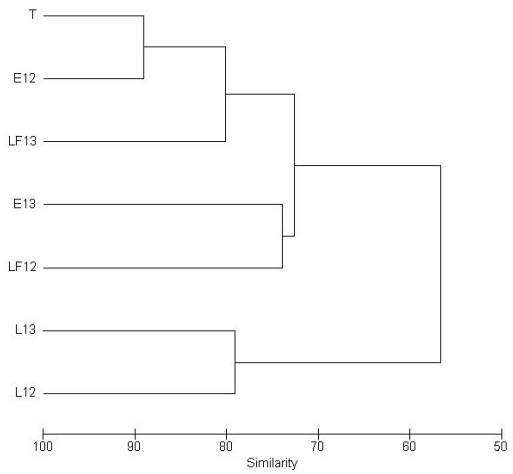

Figure IV-4 : Dendrogramme UPGMA (Unweighted-Pair Group Method with Arithmetic mean) basé sur une matrice de similarité des analyses bactériennes de T-RFLP. T pour Témoin, E pour Exsudat, L pour Lysat, LF pour Lysat Filtré. Les annotations 12 et 13 réfèrent aux fractions d'ADN ^{12}C et ^{13}C récupérées après le gradient de ClCs pour chacune des incubations.

IV.2.3. Discussion : devenir des communautés dans les nouvelles WMDW

Dans notre étude, les assemblages procaryotiques des AW et LIW post mélange convectif (station SCS) retrouvaient une structuration typique des couches de surface stratifiées (station ANT), se différenciant donc significativement de la population formée par le mélange convectif. Cependant, nous avons vu dans le 2ème article que l'organisation des communautés bactériennes et archées formées durant la convection restaient intactes à 1000 m de profondeur après l'arrêt de la convection et restratification de la colonne d'eau. Il semblerait que les nouvelles eaux profondes formées par la convection de mars (nommées $nWMDW_{mar}$, cf. I.1.2) aient piégé une partie de la MO exportée par le mélange convectif en s'équilibrant à sa pression hydrostatique. Cela permettrait à l'assemblage procaryotique convectif de perdurer 5 jours après la convection dans ces $nWMDW_{mar}$ (Figure IV-5). Un tel assemblage doit avoir des répercussions sur les stocks biogéochimiques des masses d'eaux profondes, ainsi que sur la consommation d'O_2.

Mais quel est la durée de vie de cet assemblage de procaryotes ?

Restent-ils actifs dans cette masse d'eau piégée malgré des conditions physiques et environnementales différentes susceptibles d'évoluer ?

IV.2.1. Perspectives : devenir des communautés dans les nouvelles WMDW

Un suivi temporel sur plusieurs mois après le mélange convectif, permettrait de répondre à ces questions et de suivre l'évolution de la diversité et de l'activité des procaryotes *in situ*.

Des incubations en laboratoire de l'eau dense en plein mélange convectif permettrait également de déterminer différentes variables comme le taux de respiration, ou de minéralisation pour ainsi mieux appréhender les cycles biogéochimiques pendant et post-convection et alimenter les modèles biogéochimiques portant sur le processus de convection. Nous pouvons toutefois émettre certaines hypothèses grâce à la communauté de procaryotes présente à 2000 m de profondeur à la station SC de l'article 2. En effet, la convection de mars n'a atteint que 1500 m de profondeur, laissant intacte les communautés sous-jacentes. Un mélange profond atteignant le fond marin avait par contre eu lieu le mois précédent (février 2011), remodelant ainsi la communauté de 2000 m de la même manière que celle de 1000 m a été modifiée par le mélange convectif de mars 2011. Les dendrogrammes UPGMA (Fig. 2 de l'article 2) ainsi que les camemberts taxonomiques (Fig. 3 et S1 de l'article 2) nous confirment que les communautés procaryotiques présentes à 2000 m pendant la convection (station SCC) et après restratification (station SCS) sont légèrement différentes de celles à 2000 m hors convection (station ANT). On peut donc supposer que la durée de vie de cet assemblage est d'au moins un mois après le mélange profond du mois de février et que sur cette période l'advection est suffisamment faible pour toujours être en présence de la même masse d'eau profonde formée en février 2011.

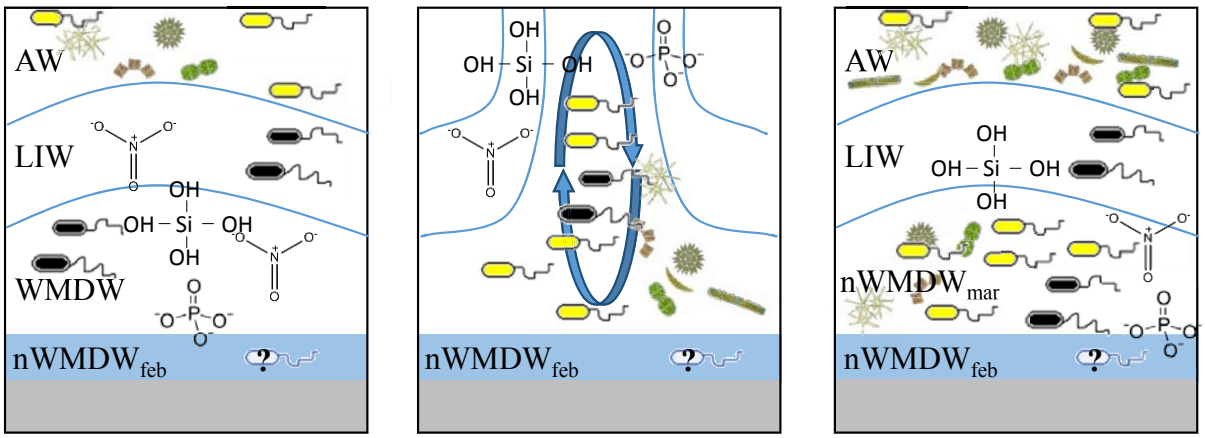

Figure IV-5 : Schémas conceptuels des évènements qui se sont succédé durant l'hiver 2011. A gauche, période pré-convection (entre février et mars) avec un développement phytoplanctonique en surface (organismes verts), des communautés procaryotiques différentes en surface (en jaune) et au fond (en noir), des LIW et WMDW riches en sels nutritifs, et les nouvelles WMDW au fond formées par le mélange convectif de février (notés nWMDW$_{feb}$). Au milieu, mélange convectif de mars 2011 qui exporte le phytoplancton dans les couches profondes, apporte en surface des sels nutritifs et conditionne une communauté convective issue du mélange de procaryotes de surface et de fond. A droite, restratification de la colonne d'eau 5 jours après la convection de mars avec un développement phytoplanctonique en surface, et une nouvelle masse d'eau profonde formée par la convection de mars (noté nWMDW$_{mar}$) ayant piégée de la MO exportée par la convection (symbolisée par des cellules phytoplanctoniques), et un assemblage procaryotique particulier formé pendant le mélange convectif.

IV.2.2. Discussion : écotypes de SAR11, Marine Group I et Marine Group II

La classification systématique actuelle des espèces procaryotiques échouant dans l'identification d'une unité fondamentale écologique (Cohan, 2006), le concept d'écotype est apparu avec pour objectif d'identifier phylogénétiquement au sein d'une espèce des sous-groupes ayant une/des fonction(s) écologique(s) unique(s) (Turesson, 1922). Un nouvel écotype est identifié *lorsqu'une mutation adaptative innovante et compétitive permet à l'organisme de coloniser une nouvelle niche écologique, empêchant donc toute compétition avec les autres organismes dont il s'est différencié* (Cohan and Perry, 2007; Shapiro and Polz, 2014). Comme seul un écotype d'une espèce peut être spécialiste d'une niche écologique, cela suggère que certains écotypes puissent être utilisés comme marqueurs de niches particulières, comme pour les écotypes de surface et de fond de *Prochlorococcus* (Rocap et al., 2003).

Dans le 3ème article, nous avons utilisé le processus de convection comme un modèle physique turbulent annihilant momentanément les niches écologiques définies selon leur propriété physico-chimiques (campagne CASCADE). La restratification de la colonne d'eau 5 jours plus tard nous a permis d'observer la recolonisation des niches par les supposés écotypes que nous avons nommés subclades dans le 3ème article. Cela nous a permis de tester la validité des écotypes de SAR11, Marine Group I (MGI) et Marine Group II (MGII) en se basant sur le concept fondamental qu'un seul écotype au sein d'un taxa ne peut coloniser qu'une seule niche. Dans le 2ème article, les 3 clades étudiés étaient omniprésents sur toute la colonne d'eau (Figure III-1), confirmant leur plasticité, et leur organisation en plusieurs écotypes (García-Martínez et Rodríguez-Valera, 2000; Carlson et al., 2009; Galand et al., 2010; Hugoni et al., 2013; Vergin et al., 2013).

La distribution verticale des subclades de SAR11 (5 de surface et 3 de fond), MGI (2 de surface et 1 de fond) et MGII (5 de surface et 4 de fond) semble en accord avec leur niche respective en dehors de la convection (station ANT), ainsi qu'après le mélange convectif (station SCS) malgré quelques exceptions. En effet, comme dans l'article 2, les assemblages de subclades formés lors du mélange convectif ont été maintenus à 1000 m de profondeur pour les 3 clades étudiés, ainsi qu'à 100 m pour les subclades de SAR11, 100 et 500 m pour les subclades de MGI et 10 et 50 m pour les subclades de MGII.

? La recolonisation des niches écologiques par les différents subclades était donc incomplète, mais comment ces subclades peuvent-ils survivre 5 jours dans une niche qui ne peut normalement pas subvenir à leurs besoins métaboliques ?

Les analyses statistiques identifiant la force des associations entre les OTUs et avec les paramètres environnementaux ont permis de conforter la répartition des subclades entre 2 niches écologiques en dehors de la convection: la niche de surface (10-150 m) et la niche de fond (350-2000 m). Cependant, une certaine plasticité fonctionnelle au niveau des subclades a été mise en évidence aussi bien avant la convection qu'après. En ce qui concerne le clade des SAR11, des OTUs correspondant aux subclades de fond IIb et Vb formaient un sous-assemblage parmi les subclades de surface hors convection. Ce sous-assemblage était retrouvé après le mélange convectif avec une forte association à l'ammonium (NH_4) et à l'azote organique dissous (NOD). Ces paramètres biogéochimiques étaient en concentrations relativement élevées dans les couches de surface en raison de l'activité phytoplanctonique. La possibilité de coloniser 2 sortes de niches (surface et fond) est contraire au concept d'écotype, ce qui remet en question leur qualification d'écotype. De plus, les analyses phylogénétiques du clade des SAR11 (Fig. supplémentaire S2 de l'article 3) indique la présence de plusieurs clusters au sein des SAR11 IIb.

Aux vues des analyses phylogénétiques et des associations avec les paramètres environnementaux, le subclade SAR11 IIb pourrait-il être composé de plusieurs écotypes ?

La présence de 2 métabolismes distincts en fonction de la profondeur a été confirmée pour le clade des MGI (Ingalls et al., 2006). L'association forte entre les subclades de surface (MGIa et MGIb) et la MO en condition stratifiée confirme leur hétérotrophie. L'autotrophie du subclade de fond MGIc est confortée par ses associations avec le carbone inorganique dissous. Cependant le métabolisme mixotrophe des subclades de surface et de fond (Martin-Cuadrado et al., 2008) conduit certains subclades à coloniser à la fois les niches de surface et de fond. Le concept d'écotype énonce l'apparition d'une fonction unique permettant à l'organisme de coloniser une nouvelle niche écologique.

Dans ce cas, comment expliquer le maintien du subclade de surface MGIb dans la niche de fond où réside déjà le subclade de fond MGIc ?

De la même manière, comment expliquer la co-occurrence des subclades SAR11 Ia, Ib, IIa, IIIa, IV, ou MGIa, MGIb, et MGIIb_WHARN, K, L1, L2 dans la même niche de surface ?

Comment les subclades SAR11 Ia, MGIc et MGIIb_O peuvent-ils être présents sur toute la colonne d'eau ?

IV.2.3. Perspectives : écotypes de SAR11, Marine Group I et Marine Group II

En ce qui concerne la survie des subclades de SAR11, MGI et MGII dans des niches qui ne peuvent normalement pas subvenir à leurs besoins métaboliques, nous avons vu dans la section IV.2.1 que les propriétés chimiques de la $nWMDW_{mar}$ pouvaient avoir été modifiées par le piégeage d'une partie de la MO exportée par la convection (Figure IV-5). Cela pourrait expliquer la survie des subclades de surface dans les couches profondes. De la même manière, les nutriments (sels nutritifs et carbone inorganique dissous) apportés en surface par la convection, peuvent permettre le maintien dans la couche de surface des subclades de fond caractérisés par un métabolisme autotrophe. Une nouvelle analyse de la diversité de ces 3 clades sur un laps de temps plus long après épuisement des nutriments et de la MO dans chacune des couches, permettrait de vérifier que ce sont bien ces substrats qui les maintenaient en vie dans des niches non adéquates. Une comparaison de leur diversité entre le leg1 de DeWEX et le leg 2 (2 mois d'intervalle) devrait permettre de tester cette hypothèse. D'autre part, il est prévu d'étudier les fractions totales (ADNr16S) et métaboliquement actives (ARNr16S) pour les échantillons de la campagne DeWEX. Ces informations nous permettront de vérifier à quel point ces écotypes sont actifs dans les différentes niches écologiques, ce qui nous donnera une idée de leur état physiologique au sein de chaque niche.

Le subclade SAR11 IIb nécessite une étude plus poussée afin de déterminer la présence ou non de plusieurs écotypes. A ce niveau de résolution, seules des analyses métagénomiques portant sur des représentants de chacun de ses sous-structures, associées à des analyses écologiques élucideraient la présence ou non de plusieurs écotypes au sein du subclade SAR11 IIb.

Le subclade de surface MGIb présent dans la niche de fond, la coexistence dans la même niche des différents subclades de SAR11, MGI et MGII, ainsi que les omniprésents SAR11 Ia, MGIc et MGIIb_O manifestent tous le même paradoxe : ils sont présents dans des niches écologiques déjà colonisées par d'autres subclades du même clade. Pour être en accord avec le concept d'écotype, la coexistence de plusieurs subclades du même clade n'est possible que si chacun de ces subclades possèdent une capacité unique à dégrader un substrat non mesuré dans cette étude, empêchant ainsi toute compétition avec les autres subclades. Des analyses métagénomiques permettraient de vérifier la présence d'une fonction unique qui spécialiserait chaque subclade au sein d'un clade sur un substrat particulier (Cohan and Perry, 2007). Si de telles fonctions sont découvertes, nous pourrons alors qualifier ces subclades d'écotypes. Dans le cas contraire, l'absence d'une fonction unique chez ces subclades serait contraire au concept d'écotype.

De manière générale, le 3ème article nous aura démontré que la diversité taxonomique obtenue via des analyses du gène codant pour l'ARN 16S atteint rapidement ses limites dans l'étude écologique des écotypes. Les outils statistiques nous permettent néanmoins d'identifier des assemblages taxonomiques particuliers et de déterminer leur relation ainsi que les relations qu'ils entretiennent avec leur environnement. Mais les études écologiques de la relation entre la diversité et la fonction nécessitent des outils particuliers. Des approches expérimentales telles que la technique du SIP pourraient apporter des éléments de réponse, mais seul un substrat à la fois pourrait être testé pour toute une communauté naturelle. Des analyses métagénomiques sur plusieurs subclades du même groupe taxonomique permettraient de déterminer plus finement le rôle fonctionnel de chacun d'entre eux, et potentiellement de les qualifier d'écotype si une fonction unique peut leur être attribuée.

Les résultats obtenus et discutés tout au long de cette thèse nous ont permis d'identifier les processus physiques et biogéochimiques liés à la convection qui influencent notamment le compartiment procaryotique (Figure IV-6) :

1 Le processus de convection impact la biogéochimie de la colonne d'eau via l'apport de nutriments en surface (sels nutritifs et carbone inorganique dissous), ainsi que via l'export de MO plus ou moins labile.

2 Le processus de convection impact le compartiment procaryotique via le mélange physique exportant les communautés de surface vers le fond, et apportant les communautés de fond vers la surface.

3 Les stocks biogéochimiques modifiées pendant et après la convection influencent le compartiment procaryotique via l'export de MO permettant la sélection de certains taxons procaryotiques.

4 Les procaryotes sélectionnés par les effets physiques et biogéochimiques de la convection influencent à leur tour les stocks biogéochimiques en consommant la MO exportée et piégée dans la masse d'eau convective, et en synthétisant des sels nutritifs. Le métabolisme spécifique de certains groupes (notamment les écotypes), influence certainement d'autres substrats non mesurés dans notre étude.

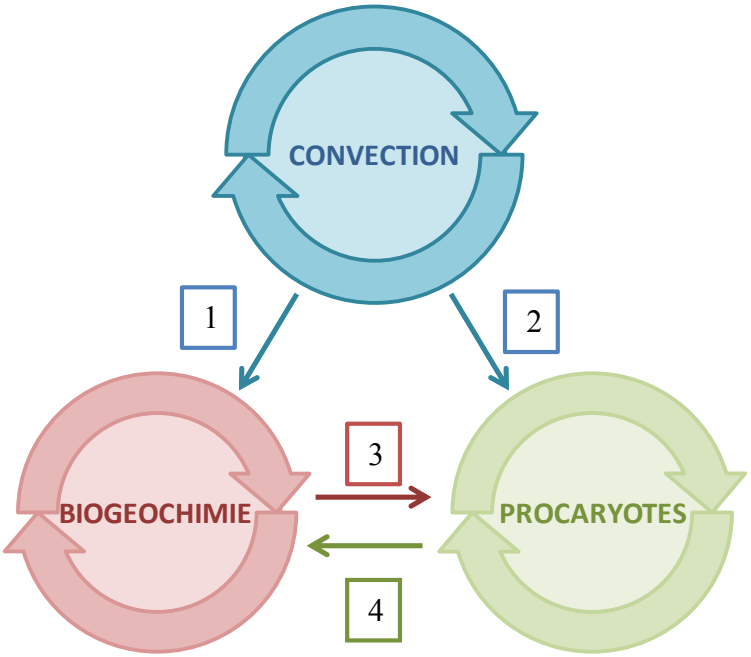

Figure IV-6 : Schéma conceptuel de mon manuscrit de thèse résolu.

RÉFÉRENCES

RÉFÉRENCES

Acinas, S.G., Rodriguez-Valera, F., Pedrós-Alió, C., 1997. Spatial and temporal variation in marine bacterioplankton diversity as shown by RFLP fingerprinting of PCR amplified 16S rDNA. FEMS Microbiol. Ecol. 24, 27–40.

Alonso-Sáez, L., Gasol, J.M., 2007. Seasonal variations in the contributions of different bacterial groups to the uptake of low-molecular-weight compounds in northwestern Mediterranean coastal waters. Appl. Environ. Microbiol. 73, 3528–35. doi:10.1128/AEM.02627-06

Anderson, L.A., Sarmiento, J.L., 1994. Redfiel ratios of remineralization determined by nutrient data analysis. Global Biogeochem. Cycles 8, 65–80.

Anderson, T.R., Hessen, D.O., Elser, J.J., Urabe, J., 2005. Metabolic stoichiometry and the fate of excess carbon and nutrients in consumers. Am. Nat. 165, 1–15. doi:10.1086/426598

Arrigo, K.R., 2005. Marine microorganisms and global nutrient cycles. Nature 437, 349–355.

Azam, F., Fenchel, T., Field, J.G., Meyer-Reil, L.A., Thingstad, F., 1983. The ecological role of water-column microbes in the sea. Mar. Ecol. Prog. Ser. 10, 257–263.

Azam, F., Malfatti, F., 2007. Microbial structuring of marine ecosystems. Nat. Rev. Microbiol. 5, 782–91. doi:10.1038/nrmicro1747

Azzaro, M., La Ferla, R., Maimone, G., Monticelli, L.S., Zaccone, R., Civitarese, G., 2012. Prokaryotic dynamics and heterotrophic metabolism in a deep convection site of Eastern Mediterranean Sea (the Southern Adriatic Pit). Cont. Shelf Res. 44, 106–118. doi:10.1016/j.csr.2011.07.011

Backhaus, J., Wehde, H., 1999. "Phyto-convection": the role of oceanic convection in primary production. Mar. Ecol. Prog. Ser. 189, 77–92.

Backhaus, J.O., Hegseth, E.N., Irigoien, X., Hatten, K., Logemann, K., 2003. Convection and primary production in winter. Mar. Ecol. Prog. Ser. 251, 1–14.

Banse, K., 1994. Uptake of inorganic carbon and nitrate by marine plankton and the Redfield Ratio. Global Biogeochem. Cycles 8, 81–84. doi:10.1029/93GB02865

Becker, J.W., Berube, P.M., Follett, C.L., Waterbury, J.B., Chisholm, S.W., Delong, E.F., Repeta, D.J., 2014. Closely related phytoplankton species produce similar suites of dissolved organic matter. Front. Microbiol. 5, 111. doi:10.3389/fmicb.2014.00111

Behrenfeld, M.J., 2010. Abandoning Sverdrup's Critical Depth Hypothesis on phytoplankton blooms. Ecology 91, 977–89.

Benner, R., 2002. Chemical Composition and Reactivity, in: Hansell, D.A., Carlson, C.A. (Eds.), Biogeochemistry of Marine Dissolved Organic Matter. pp. 59–90.

Berg, I. a, Kockelkorn, D., Buckel, W., Fuchs, G., 2007. A 3-hydroxypropionate/4-hydroxybutyrate autotrophic carbon dioxide assimilation pathway in Archaea. Science 318, 1782–1786. doi:10.1126/science.1149976

Bethoux, J.P., Durieu de Madron, X., Nyffeler, F., Tailliez, D., 2002. Deep water in the western Mediterranean: peculiar 1999 and 2000 characteristics, shelf formation hypothesis, variability

since 1970 and geochemical inferences. J. Mar. Syst. 33-34, 117–131. doi:10.1016/S0924-7963(02)00055-6

Béthoux, J.P., Gentili, B., Morin, P., Nicolas, E., Pierre, C., Ruiz-Pino, D., 1999. The Mediterranean Sea: a miniature ocean for climatic and environmental studies and a key for the climatic functioning of the North Atlantic. Prog. Oceanogr. 44, 131–146. doi:10.1016/S0079-6611(99)00023-3

Béthoux, J.P., Gentili, B., Tailliez, D., 1998a. Warming and freshwater budget change in the Mediterranean since the 1940s, their possible relation to the greenhouse effect. Geophys. Res. Lett. 25, 1023–1026.

Béthoux, J.P., Morin, P., Chaumery, C., Connan, O., Gentili, B., Ruiz-Pino, D., 1998b. Nutrients in the Mediterranean Sea, mass balance and statistical analysis of concentrations with respect to environmental change. Mar. Chem. 63, 155–169.

Béthoux, J.P., Morin, P., Ruiz-Pino, D.P., 2002. Temporal trends in nutrient ratios: chemical evidence of Mediterranean ecosystem changes driven by human activity. Deep Sea Res. Part II Top. Stud. Oceanogr. 49, 2007–2016. doi:10.1016/S0967-0645(02)00024-3

Boutrif, M., Garel, M., Cottrell, M.T., Tamburini, C., 2011. Assimilation of marine extracellular polymeric substances by deep-sea prokaryotes in the NW Mediterranean Sea. Environ. Microbiol. Rep. 3, 705–9. doi:10.1111/j.1758-2229.2011.00285.x

Brochier-Armanet, C., Boussau, B., 2008. Mesophilic Crenarchaeota: proposal for a third archaeal phylum, the Thaumarchaeota. Nat. Rev. Microbiol. 6, 245–252. doi:10.1038/nrmicro1852

Brzezinski, M.A., 1985. The Si:C:N ratio of marine diatoms: interspecific variability and the effect of some environmental variables. J. Phycol. 21, 347–357. doi:10.1111/j.0022-3646.1985.00347.x

Cameron, T.J., Temperton, B., Swan, B.K., Landry, Z.C., Woyke, T., Delong, E.F., Stepanauskas, R., Giovannoni, S.J., 2014. Single-cell enabled comparative genomics of a deep ocean SAR11 bathytype. ISME J. 8, 1440–1451. doi:10.1038/ismej.2013.243

Canals, M., Puig, P., de Madron, X.D., Heussner, S., Palanques, A., Fabres, J., 2006. Flushing submarine canyons. Nature 444, 354–7. doi:10.1038/nature05271

Carlson, C.A., 2002. Production and Removal Processes, in: Hansell, D.A., Carlson, C.A. (Eds.), Biogeochemistry of Marine Dissolved Organic Matter. pp. 139–151.

Carlson, C.A., Giovannoni, S.J., Hansell, D.A., Goldberg, S.J., Parsons, R., Vergin, K., 2004. Interactions among Dissolved Organic Carbon, Microbial Processes, and Community Structure in the Mesopelagic Zone of the Northwestern Sargasso Sea. Limnol. Oceanogr. 49, 1073–1083. doi:10.2307/3597658

Carlson, C.A., Morris, R., Parsons, R., Treusch, A.H., Giovannoni, S.J., Vergin, K., 2009. Seasonal dynamics of SAR11 populations in the euphotic and mesopelagic zones of the northwestern Sargasso Sea. ISME J. 3, 283–295. doi:10.1038/ismej.2008.117

Casamayor, E.O., Muyzer, G., Pedrós-Alió, C., 2001. Composition and temporal dynamics of planktonic archaeal assemblages from anaerobic sulfurous environments studied by 16S rDNA denaturing gradient gel electrophoresis and sequencing. Aquat. Microb. Ecol. 25, 237–246. doi:10.3354/ame025237

Catalan Garcia, N., 2013. Sources, transformations and controls of dissolved organic matter (DOM) in a Mediterranean catchment. University of Barcelona.

Cauwet, G., 2002. DOM in the Coastal Zone BT, in: Biogeochemistry of Marine Dissolved Organic Matter. Academic Press, San Diego, pp. 579–609. doi:http://dx.doi.org/10.1016/B978-012323841-2/50014-2

Cohan, F.M., 2006. Towards a conceptual and operational union of bacterial systematics, ecology, and evolution. Philos. Trans. R. Soc. Lond. B. Biol. Sci. 361, 1985–96. doi:10.1098/rstb.2006.1918

Cohan, F.M., Perry, E.B., 2007. A systematics for discovering the fundamental units of bacterial diversity. Curr. Biol. 17, R373–86. doi:10.1016/j.cub.2007.03.032

Conan, P., Turley, C., Stutt, E., Pujo-Pay, M., Van Wambeke, F., 1999. Relationship between phytoplankton efficiency and the proportion of bacterial production to primary production in the Mediterranean Sea. Aquat. Microb. Ecol. 17, 131–144. doi:10.3354/ame017131

Cottrell, M.T., Kirchman, D.L., 2000. Natural Assemblages of Marine Proteobacteria and Members of the Cytophaga-Flavobacter Cluster Consuming Low- and High-Molecular-Weight Dissolved Organic Matter. Appl. Environ. Microbiol. 66, 1692–1697. doi:10.1128/AEM.66.4.1692-1697.2000

D'ortenzio, F., Ribera d'Alcalà, M., 2009. On the trophic regimes of the Mediterranean Sea: a satellite analysis. Biogeosciences 6, 1–10.

De Queiroz, K., 2005. Ernst Mayr and the modern concept of species. Proc. Natl. Acad. Sci. U. S. A. 102 Suppl , 6600–7. doi:10.1073/pnas.0502030102

Del Giorgio, P.A., Bouvier, T.C., 2002. Linking the physiologic and phylogenetic successions in free-living bacterial communities along an estuarine salinity gradient. Limnol. Oceanogr. 47, 471–486. doi:10.4319/lo.2002.47.2.0471

Delong, E.F., Wickham, G.S., Pace, N.R., 1989. Phylogenetc Stains: Ribosomal RNA-Based Probes for the Identification of Single Cells. Science. 243, 1360–1363.

Diaz, F., Raimbault, P., Conan, P., 2000. Small-scale study of primary productivity during spring in a Mediterranean coastal area (Gulf of Lions). Cont. Shelf Res. 20, 975–996. doi:10.1016/S0278-4343(00)00006-6

Díez-Vives, C., Gasol, J.M., Acinas, S.G., 2014. Spatial and temporal variability among marine Bacteroidetes populations in the NW Mediterranean Sea. Syst. Appl. Microbiol. 37, 68–78. doi:http://dx.doi.org/10.1016/j.syapm.2013.08.006

Durrieu de Madron, X., Houpert, L., Puig, P., Sanchez-Vidal, a., Testor, P., Bosse, a., Estournel, C., Somot, S., Bourrin, F., Bouin, M.N., Beauverger, M., Beguery, L., Calafat, a., Canals, M., Cassou, C., Coppola, L., Dausse, D., D'Ortenzio, F., Font, J., Heussner, S., Kunesch, S., Lefevre, D., Le Goff, H., Martín, J., Mortier, L., Palanques, a., Raimbault, P., 2013. Interaction of dense shelf water cascading and open-sea convection in the northwestern Mediterranean during winter 2012. Geophys. Res. Lett. 40, 1379–1385. doi:10.1002/grl.50331

Durrieu de Madron, X., Zervakis, V., Theocharis, a., Georgopoulos, D., 2005. Comments on "Cascades of dense water around the world ocean". Prog. Oceanogr. 64, 83–90. doi:10.1016/j.pocean.2004.08.004

Field, K.G., Gordon, D., Wright, T., Rappé, M., Urback, E., Vergin, K., Giovannoni, S.J., 1997. Diversity and depth-specific distribution of SAR11 cluster rRNA genes from marine planktonic bacteria. Appl. Environ. Microbiol. 63, 63–70.

Francis, C.A., Roberts, K.J., Beman, J.M., Santoro, A.E., Oakley, B.B., 2005. Ubiquity and diversity of ammonia-oxidizing archaea in water columns and sediments of the ocean. Proc. Natl. Acad. Sci. U. S. A. 102, 14683–14688. doi:10.1073/pnas.0506625102

Frigaard, N.-U., Martinez, A., Mincer, T.J., DeLong, E.F., 2006. Proteorhodopsin lateral gene transfer between marine planktonic Bacteria and Archaea. Nature 439, 847–850.

Gačić, M., Civitarese, G., Miserocchi, S., Cardin, V., Crise, A., Mauri, E., 2002. The open-ocean convection in the Southern Adriatic: a controlling mechanism of the spring phytoplankton bloom. Cont. Shelf Res. 22, 1897–1908. doi:10.1016/S0278-4343(02)00050-X

Galand, P.E., Gutiérrez-Provecho, C., Massana, R., Gasol, J.M., Casamayor, E.O., 2010. Inter-annual recurrence of archaeal assemblages in the coastal NW Mediterranean Sea (Blanes Bay Microbial Observatory). Limnol. Oceanogr. 55, 2117–2125. doi:10.4319/lo.2010.55.5.2117

García-Martínez, J., Rodríguez-Valera, F., 2000. Microdiversity of uncultured marine prokaryotes: the SAR11 cluster and the marine Archaea of Group I. Mol. Ecol. 9, 935–48.

Geider, R., La Roche, J., 2002. Redfield revisited: variability of C:N:P in marine microalgae and its biochemical basis. Eur. J. Phycol. 37, 1–17. doi:10.1017/S0967026201003456

Gevers, D., Cohan, F., Lawrence, J., 2005. Re-evaluating prokaryotic species. Nat. Rev. Microbiol. 3, 733–739.

Ghiglione, J.-F., Conan, P., Pujo-Pay, M., 2009. Diversity of total and active free-living vs. particle-attached bacteria in the euphotic zone of the NW Mediterranean Sea. FEMS Microbiol. Lett. 299, 9–21. doi:10.1111/j.1574-6968.2009.01694.x

Ghiglione, J.-F., Galand, P.E., Pommier, T., Pedrós-Alió, C., Maas, E.W., Bakker, K., Bertilson, S., Kirchmanj, D.L., Lovejoy, C., Yager, P.L., Murray, A.E., 2012. Pole-to-pole biogeography of surface and deep marine bacterial communities. Proc. Natl. Acad. Sci. U. S. A. 109, 17633–8. doi:10.1073/pnas.1208160109

Ghiglione, J.F., Mevel, G., Pujo-Pay, M., Mousseau, L., Lebaron, P., Goutx, M., 2007. Diel and seasonal variations in abundance, activity, and community structure of particle-attached and free-living bacteria in NW Mediterranean Sea. Microb. Ecol. 54, 217–31. doi:10.1007/s00248-006-9189-7

Giovannoni, S.J., Tripp, H.J., Givan, S., Podar, M., Vergin, K.L., Baptista, D., Bibbs, L., Eads, J., Richardson, T.H., Noordewier, M., Rappé, M.S., Short, J.M., Carrington, J.C., Mathur, E.J., 2005. Genome Streamlining in a Cosmopolitan Oceanic Bacterium. Science (80-.). 309, 1242–1245. doi:10.1126/science.1114057

Glöckner, F.O., Fuchs, B.M., Amann, R., 1999. Bacterioplankton Compositions of Lakes and Oceans: a First Comparison Based on Fluorescence In Situ Hybridization. Appl. Environ. Microbiol. 65, 3721–3726.

Gogou, A., Sanchez-Vidal, A., Durrieu de Madron, X., Stavrakakis, S., Calafat, A.M., Stabholz, M., Psarra, S., Canals, M., Heussner, S., Stavrakaki, I., Papathanassiou, E., 2014. Carbon flux to the

deep in three open sites of the Southern European Seas (SES). J. Mar. Syst. 129, 224–233. doi:10.1016/j.jmarsys.2013.05.013

Goldberg, S.J., Carlson, C. a., Hansell, D. a., Nelson, N.B., Siegel, D. a., 2009. Temporal dynamics of dissolved combined neutral sugars and the quality of dissolved organic matter in the Northwestern Sargasso Sea. Deep Sea Res. Part I Oceanogr. Res. Pap. 56, 672–685. doi:10.1016/j.dsr.2008.12.013

Hansell, D. a, Carlson, C. a, 2001. Biogeochemistry of total organic carbon and nitrogen in the Sargasso Sea: control by convective overturn. Deep Sea Res. Part II Top. Stud. Oceanogr. 48, 1649–1667. doi:10.1016/S0967-0645(00)00153-3

Heimbürger, L.-E., Lavigne, H., Migon, C., D'Ortenzio, F., Estournel, C., Coppola, L., Miquel, J.-C., 2013. Temporal variability of vertical export flux at the DYFAMED time-series station (Northwestern Mediterranean Sea). Prog. Oceanogr. 119, 59–67. doi:10.1016/j.pocean.2013.08.005

Herndl, G.J., Reinthaler, T., Teira, E., van Aken, H., Veth, C., Pernthaler, A., Pernthaler, J., 2005. Contribution of Archaea to Total Prokaryotic Production in the Deep Atlantic Ocean. Appl. Environ. Microbiol. 71, 2303–2309. doi:10.1128/AEM.71.5.2303-2309.2005

Houpert, L., 2013. Contribution to the study of transfer processes from the surface to the deep ocean in the Mediterranean sea using in situ measurements. Université de Perpignan via Domitia.

Hugoni, M., Taib, N., Debroas, D., Domaizon, I., Jouan, I., 2013. Structure of the rare archaeal biosphere and seasonal dynamics of active ecotypes in surface coastal waters. PNAS 110, 6004–6009.

Ingalls, A.E., Shah, S.R., Hansman, R.L., Aluwihare, L.I., Santos, G.M., Druffel, E.R.M., Pearson, A., 2006. Quantifying archaeal community autotrophy in the mesopelagic ocean using natural radiocarbon. Proc. Natl. Acad. Sci. U. S. A. 103, 6442–7. doi:10.1073/pnas.0510157103

IPCC, 2007. Climate Change 2007. The physical science basis.

Jickells, T.D., 1998. Nutrient Biogeochemistry of the Coastal Zone. Science (80-.). 281, 217–222.

Killworth, P.D., 1983. Deep convection in the World Ocean. Rev. Geophys. 21, 1–26. doi:10.1029/RG021i001p00001

Kirchman, D., K'nees, E., Hodson, R., 1985. Leucine incorporation and its potential as a measure of protein synthesis by bacteria in natural aquatic systems. Appl. Environ. Microbiol. 49, 599–607.

Kirchman, D.L., Dittel, A.I., Malmstrom, R.R., Cottrell, M.T., 2005. Biogeography of Major Bacterial Groups in the Delaware Estuary. Limnol. Oceanogr. 50, 1697–1706. doi:10.2307/3597712

Koeppel, A., Perry, E.B., Sikorski, J., Krizanc, D., Warner, A., Ward, D.M., Rooney, A.P., Brambilla, E., Connor, N., Ratcliff, R.M., Nevo, E., Cohan, F.M., 2008. Identifying the fundamental units of bacterial diversity: a paradigm shift to incorporate ecology into bacterial systematics. Proc. Natl. Acad. Sci. U. S. A. 105, 2504–9. doi:10.1073/pnas.0712205105

Krom, M., Herut, B., Mantoura, R., 2004. Nutrient budget for the Eastern Mediterranean: Implications for phosphorus limitation. Limnol. Oceanogr. 49, 1582–1592.

Krom, M.D., 2011. Insights on nitrogen balance in the Eastern Mediterranean Sea. Environ. Microbiol. 13, 851–853. doi:10.1111/j.1462-2920.2010.02404.x

La Ferla, R., Azzaro, M., 2001. Microbial respiration in the Levantine Sea: evolution of the oxidative processes in relation to the main Mediterranean water masses. Deep Sea Res. Part I Oceanogr. Res. Pap. 48, 2147–2159. doi:10.1016/S0967-0637(01)00009-7

La Violette, P.E., 1994. Overview of the Major Forcings and Water Masses of the Western Mediterranean Sea 46, 1–11.

Landa, M., Cottrell, M., Kirchman, D., Blain, S., Obernosterer, I., 2013. Changes in bacterial diversity in response to dissolved organic matter supply in a continuous culture experiment. Aquat. Microb. Ecol. 69, 157–168. doi:10.3354/ame01632

Landa, M., Cottrell, M.T., Kirchman, D.L., Kaiser, K., Medeiros, P.M., Tremblay, L., Batailler, N., Caparros, J., Catala, P., Escoubeyrou, K., Oriol, L., Blain, S., Obernosterer, I., 2014. Phylogenetic and structural response of heterotrophic bacteria to dissolved organic matter of different chemical composition in a continuous culture study. Environ. Microbiol. 16, 1668–1681. doi:10.1111/1462-2920.12242

Lavigne, H., D'Ortenzio, F., Migon, C., Claustre, H., Testor, P., d'Alcalà, M.R., Lavezza, R., Houpert, L., Prieur, L., 2013. Enhancing the comprehension of mixed layer depth control on the Mediterranean phytoplankton phenology. J. Geophys. Res. Ocean. 118, 3416–3430. doi:10.1002/jgrc.20251

Letunic, I., Bork, P., 2007. Interactive Tree Of Life (iTOL): an online tool for phylogenetic tree display and annotation. Bioinformatics 23, 127–8. doi:10.1093/bioinformatics/btl529

Letunic, I., Bork, P., 2011. Interactive Tree Of Life v2: online annotation and display of phylogenetic trees made easy. Nucleic Acids Res. 39, W475–8. doi:10.1093/nar/gkr201

Ludwig, W., Dumont, E., Meybeck, M., Heussner, S., 2009. River discharges of water and nutrients to the Mediterranean and Black Sea: Major drivers for ecosystem changes during past and future decades? Prog. Oceanogr. 80, 199–217. doi:10.1016/j.pocean.2009.02.001

Marshall, J., Schott, F., 1999. Open ocean convection: Observations, theory, and models. Rev. Geophys. 37, 1–64.

Martin-Cuadrado, A.-B., Rodriguez-Valera, F., Moreira, D., Alba, J.C., Ivars-Martínez, E., Henn, M.R., Talla, E., López-García, P., 2008. Hindsight in the relative abundance, metabolic potential and genome dynamics of uncultivated marine archaea from comparative metagenomic analyses of bathypelagic plankton of different oceanic regions. ISME J. 2, 865–86. doi:10.1038/ismej.2008.40

Marty, J., Chiavérini, J., 2002. Seasonal and interannual variations in phytoplankton production at DYFAMED time-series station, northwestern Mediterranean Sea. Deep Sea Res. Part II Top. Stud. Oceanogr. 49, 2017–2030.

Marty, J., Chiavérini, J., Pizay, M., Avril, B., 2002. Seasonal and interannual dynamics of nutrients and phytoplankton pigments in the western Mediterranean Sea at the DYFAMED time-series station (1991–1999). Deep Sea Res. Part II Top. Stud. Oceanogr. 49, 1965–1985.

Marty, J.C., Chiavérini, J., 2010. Hydrological changes in the Ligurian Sea (NW Mediterranean, DYFAMED site) during 1995–2007 and biogeochemical consequences. Biogeosciences 7, 2117–2128. doi:10.5194/bg-7-2117-2010

Massana, R., DeLong, E.F., Pedrós-Alió, C., 2000. A few cosmopolitan phylotypes dominate planktonic archaeal assemblages in widely different oceanic provinces. Appl. Environ. Microbiol. 66, 1777–1787. doi:10.1128/AEM.66.5.1777-1787.2000.Updated

Mauritzen, C., 1996. Production of dense overflow waters feeding the North Atlantic across the Greenland-Scotland Ridge. Part 1: Evidence for a revised circulation scheme. Deep Sea Res. Part I Oceanogr. Res. Pap. 43, 769–806.

Medoc Group, 1970. Observation of formation of deep water in the mediterranean sea. Nature 227, 1937–1040.

Meredith, M.P., 2005. Rapid climate change in the ocean west of the Antarctic Peninsula during the second half of the 20th century. Geophys. Res. Lett. 32, L19604. doi:10.1029/2005GL024042

Mermex group, 2011. Marine ecosystems' responses to climatic and anthropogenic forcings in the Mediterranean. Prog. Oceanogr. 91, 97–166. doi:10.1016/j.pocean.2011.02.003

Mertens, C., Schott, F., 1998. Interannual Variability of Deep-Water Formation in the Northwestern Mediterranean. J. Phys. Oceanogr. 28, 1410–1424. doi:10.1175/1520-0485(1998)028<1410:IVODWF>2.0.CO;2

Millot, C., 1999. Circulation in the Western Mediterranean Sea. J. Mar. Syst. 20, 423–442. doi:10.1016/S0924-7963(98)00078-5

Millot, C., Candela, J., Fuda, J.-L., Tber, Y., 2006. Large warming and salinification of the Mediterranean outflow due to changes in its composition. Deep Sea Res. Part I Oceanogr. Res. Pap. 53, 656–666. doi:10.1016/j.dsr.2005.12.017

Millot, C., Taupier-Letage, I., 2005. Circulation in the Mediterranean Sea, in: Saliot, A. (Ed.), The Mediterranean Sea. Springer Berlin Heidelberg, pp. 29–66.

Moncheva, S., Gotsis-Skretas, O., Pagou, K., Krastev, A., 2001. Phytoplankton Blooms in Black Sea and Mediterranean Coastal Ecosystems Subjected to Anthropogenic Eutrophication: Similarities and Differences. Estuar. Coast. Shelf Sci. 53, 281–295.

Morris, R., Rappé, M., Connon, S., 2002. SAR11 clade dominates ocean surface bacterioplankton communities. Nature 420, 806–810. doi:10.1038/nature01281.1.

Morris, R.M., Vergin, K.L., Rappe, M.S., Carlson, C.A., Giovannoni, S.J., 2005. Temporal and spatial response of bacterioplankton lineages to annual convective overturn at the Bermuda Atlantic Time-series Study site. Limnol. Oceanogr. 50, 1687–1696.

Moutin, T., Raimbault, P., Golterman, H.L., Coste, B., 1998. The input of nutrients by the Rhône river into the Mediterranean Sea: recent observations and comparison with earlier data. Hydrologica 373/374, 237–246.

Nagata, T., 2008. Organic Matter–Bacteria Interactions in Seawater, in: Microbial Ecology of the Oceans. John Wiley & Sons, Inc., pp. 207–241. doi:10.1002/9780470281840.ch7

Najdek, M., Paliaga, P., Šilović, T., Batistić, M., Garić, R., Supić, N., Ivančić, I., Ljubimir, S., Korlević, M., Jasprica, N., Hrustić, E., Dupčić-Radić, I., Blažina, M., Orlić, S., 2014. Picoplankton community structure before, during and after convection event in the offshore waters of the Southern Adriatic Sea. Biogeosciences 11, 2645–2659. doi:10.5194/bg-11-2645-2014

Officer, C.B., Ryther, J.H.., 1980. The possible importance of silicon in marine eutrophication. Mar. Ecol. Prog. Ser. 3, 83–91.

Orsi, A.H., Johnson, G.C., Bullister, J.L., 1999. Circulation, mixing, and production of Antarctic Bottom Water. Prog. Oceanogr. 43, 55–109. doi:10.1016/S0079-6611(99)00004-X

Ouverney, C.C., Fuhrman, J.A., 2000. Marine Planktonic Archaea Take Up Amino Acids. Appl. Environ. Microbiol. 66, 4829–4833. doi:10.1128/AEM.66.11.4829-4833.2000

Pomeroy, L., 1974. The ocean's food web, a changing paradigm. Bioscience.

Pomeroy, L.R., LeB. Williams, P.J., Azam, F., Hobbie, J.E., 2007. The microbial loop. Oceanography 20, 28–33. doi:http://dx.doi.org/10.5670/oceanog.2007.45.

Poulsen, L., Ballard, G., Stahl, D., 1993. Use of rRNA fluorescence in situ hybridization for measuring the activity of single cells in young and established biofilms. Appl. Environ. Microbiol. 59, 1354–1360.

Puig, P., Madron, X.D. De, Salat, J., Schroeder, K., Martín, J., Karageorgis, A.P., Palanques, A., Roullier, F., Lopez-Jurado, J.L., Emelianov, M., Moutin, T., Houpert, L., 2013. Thick bottom nepheloid layers in the western Mediterranean generated by deep dense shelf water cascading. Prog. Oceanogr. 111, 1–23. doi:10.1016/j.pocean.2012.10.003

Pujo-Pay, M., Conan, P., 2003. Seasonal variability and export of dissolved organic nitrogen in the northwestern Mediterranean Sea. J. Geophys. Res. 108, 3188. doi:10.1029/2000JC000368

Pujo-Pay, M., Conan, P., Oriol, L., Cornet-Barthaux, V., Falco, C., Ghiglione, J.-F., Goyet, C., Moutin, T., Prieur, L., 2011. Integrated survey of elemental stoichiometry (C, N, P) from the western to eastern Mediterranean Sea. Biogeosciences 8, 883–899. doi:10.5194/bg-8-883-2011

Pulido-Villena, E., Ghiglione, J.-F., Ortega-Retuerta, E., Van Wambeke, F., Zohary, T., 2012. Heterotrophic bacteria in the pelagic realm of the mediterranean sea, in: Stambler, N. (Ed.), Life in the Mediterranean Sea: A Look at Habitat Changes. pp. 227–265.

Pusceddu, A., Mea, M., Gambi, C., Bianchelli, S., Sanchez-Vidal, A., Calafat, A., Heussner, S., Durrieu De Madron, X., Avril, J., Thomsen, L., García, R., Danovaro, R., 2010. Ecosystem effects of dense water formation on deep Mediterranean Sea ecosystems: an overview. Adv. Oceanogr. Limnol. 1, 67–83.

Radajewski, S., Ineson, P., Parekh, N.R., Murrell, J.C., 2000. Stable-isotope probing as a tool in microbial ecology. Nature 403, 646–9. doi:10.1038/35001054

Ramirez-Romero, E., Macias, D., Garcia, C., Bruno, M., 2014. Biogeochemical patterns in the Atlantic Inflow through the Strait of Gibraltar. Deep Sea Res. Part I Oceanogr. Res. Pap. 85, 88–100.

Redfield, A., 1934. On the proportions of organic derivatives in sea water and their relation to the composition of plankton, in: Daniel, R.J. (Ed.), James Johnstone Memorial Volum. University press of Liverpool, pp. 176–192.

Redfield, A.C., Ketchum, B.H., Richards, F.A., 1963. The influence of organisms on the composition of sea water, in: The Sea. Wiley Interscience, Hoboken, N. J., Hills, M. N., pp. 26–77.

Reid, P.C., Fischer, A.C., Lewis-Brown, E., Meredith, M.P., Sparrow, M., Andersson, A.J., Antia, A., Bates, N.R., Bathmann, U., Beaugrand, G., Brix, H., Dye, S., Edwards, M., Furevik, T., Gangstø, R., Hátún, H., Hopcroft, R.R., Kendall, M., Kasten, S., Keeling, R., Le Quéré, C., Mackenzie, F.T., Malin, G., Mauritzen, C., Olafsson, J., Paull, C., Rignot, E., Shimada, K., Vogt, M., Wallace, C., Wang, Z., Washington, R., 2009. Chapter 1. Impacts of the oceans on climate change., Advances in marine biology. doi:10.1016/S0065-2881(09)56001-4

Repeta, D.J., Quan, T.M., Aluwihare, L.I., Accardi, A.M., 2002. Chemical characterization of high molecular weight dissolved organic matter in fresh and marine waters. Geochim. Cosmochim. Acta.

Ridame, C., Guieu, C., 2002. Saharan input of phosphate to the oligotrophic water of the ope ocean western Mediterranean Sea. Limnol. Oceanogr. 47, 856–869.

Rocap, G., Larimer, F.W., Lamerdin, J., Malfatti, S., Chain, P., Ahlgren, N.A., Arellano, A., Coleman, M., Hauser, L., Hess, W.R., Johnson, Z.I., Land, M., Lindell, D., Post, A.F., Regala, W., Shah, M., Shaw, S.L., Steglich, C., Sullivan, M.B., Ting, C.S., Tolonen, A., Webb, E.A., Zinser, E.R., Chisholm, S.W., 2003. Genome divergence in two Prochlorococcus ecotypes reflects oceanic niche differentiation. Nature 424, 1042–1047.

Rodríguez-Blanco, A., Ghiglione, J.-F., Catala, P., Casamayor, E.O., Lebaron, P., 2009. Spatial comparison of total vs. active bacterial populations by coupling genetic fingerprinting and clone library analyses in the NW Mediterranean Sea. FEMS Microbiol. Ecol. 67, 30–42. doi:10.1111/j.1574-6941.2008.00591.x

Roether, W., Manca, B.B., Klein, B., Bregant, D., Georgopoulos, D., Beitzel, V., Kovacevic, V., Luchetta, A., 1995. Recent Changes in Eastern Mediterranean Deep Waters. Science (80-.). 1995, 1995–1997.

Sachs, J.P., Repeta, D.J., 1999. Oligotrophy and Nitrogen Fixation During Eastern Mediterranean Sapropel Events. Science (80-.). 286, 2485–2488. doi:10.1126/science.286.5449.2485

Santinelli, C., Hansell, D. a., Ribera d'Alcalà, M., 2013. Influence of stratification on marine dissolved organic carbon (DOC) dynamics: The Mediterranean Sea case. Prog. Oceanogr. 119, 68–77. doi:10.1016/j.pocean.2013.06.001

Santinelli, C., Ibello, V., Lavezza, R., Civitarese, G., Seritti, a., 2012. New insights into C, N and P stoichiometry in the Mediterranean Sea: The Adriatic Sea case. Cont. Shelf Res. 44, 83–93. doi:10.1016/j.csr.2012.02.015

Santinelli, C., Nannicini, L., Seritti, A., 2010. DOC dynamics in the meso and bathypelagic layers of the Mediterranean Sea. Deep Sea Res. Part II Top. Stud. Oceanogr. 57, 1446–1459. doi:10.1016/j.dsr2.2010.02.014

Sarmento, H., Gasol, J., 2012. Use of phytoplankton derived dissolved organic carbon by different types of bacterioplankton. Environ. Microbiol. 14, 2348–2360.

Sauret, C., Ghiglione, J.-F., 2013. Monitoring of Oil-Degrading Bacteria by Stable Isotope Probing, in: Férard, J.-F., Blaise, C. (Eds.), Encyclopedia of Aquatic Ecotoxicology. Springer Netherlands, pp. 751–766. doi:10.1007/978-94-007-5704-2_69

Schröder, K., Gasparini, G.P., Tangherlini, M., Astraldi, M., 2006. Deep and intermediate water in the western Mediterranean under the influence of the Eastern Mediterranean Transient. Geophys. Res. Lett. 33, L21607. doi:10.1029/2006GL027121

Schroeder, K., Ribotti, a., Borghini, M., Sorgente, R., Perilli, a., Gasparini, G.P., 2008. An extensive western Mediterranean deep water renewal between 2004 and 2006. Geophys. Res. Lett. 35, L18605. doi:10.1029/2008GL035146

Selje, N., Simon, M., Brinkhoff, T., 2004. A newly discovered Roseobacter cluster in temperate and polar oceans. Nature 427, 445–448.

Send, U., Marshall, J., 1995. Integral effects of deep convection. J. Phys. Oceanogr. 25, 855–872.

Shapiro, B.J., Polz, M.F., 2014. Ordering microbial diversity into ecologically and genetically cohesive units. Trends Microbiol. 22, 235–247. doi:http://dx.doi.org/10.1016/j.tim.2014.02.006

Sherr, E., Sherr, B., Sigmon, C., 1999. Activity of marine bacteria under incubated and in situ conditions. Aquat. Ecol. 20, 213–223.

Spang, A., Hatzenpichler, R., 2010. Distinct gene set in two different lineages of ammonia-oxidizing archaea supports the phylum Thaumarchaeota. Trends Microbiol. 18, 331–340. doi:10.1016/j.tim.2010.06.003

Stabholz, M., Durrieu de Madron, X., Canals, M., Khripounoff, A., Taupier-Letage, I., Testor, P., Heussner, S., Kerhervé, P., Delsaut, N., Houpert, L., Lastras, G., Dennielou, B., 2013. Impact of open-ocean convection on particle fluxes and sediment dynamics in the deep margin of the Gulf of Lions. Biogeosciences 10, 1097–1116. doi:10.5194/bg-10-1097-2013

Sterner, R.W., Andersen, T., Elser, J.J., Hessen, D.O., Hood, J.M., McCauley, E., Urabe, J., 2008. Scale-dependent carbon:nitrogen:phosphorus seston stoichiometry in marine and freshwaters. Limnol. Oceanogr. 53, 1169–1180. doi:10.4319/lo.2008.53.3.1169

Tamburini, C., Canals, M., Durrieu de Madron, X., Houpert, L., Lefèvre, D., Martini, S., D'Ortenzio, F., Robert, A., Testor, P., Aguilar, J.A., Samarai, I. Al, Albert, A., André, M., Anghinolfi, M., Anton, G., Anvar, S., Ardid, M., Jesus, A.C.A., Astraatmadja, T.L., Aubert, J.-J., Baret, B., Basa, S., Bertin, V., Biagi, S., Bigi, A., Bigongiari, C., Bogazzi, C., Bou-Cabo, M., Bouhou, B., Bouwhuis, M.C., Brunner, J., Busto, J., Camarena, F., Capone, A., Cârloganu, C., Carminati, G., Carr, J., Cecchini, S., Charif, Z., Charvis, P., Chiarusi, T., Circella, M., Coniglione, R., Costantini, H., Coyle, P., Curtil, C., Decowski, P., Dekeyser, I., Deschamps, A., Donzaud, C., Dornic, D., Dorosti, H.Q., Drouhin, D., Eberl, T., Emanuele, U., Ernenwein, J.-P., Escoffier, S., Fermani, P., Ferri, M., Flaminio, V., Folger, F., Fritsch, U., Fuda, J.-L., Galatà, S., Gay, P., Giacomelli, G., Giordano, V., Gómez-González, J.-P., Graf, K., Guillard, G., Halladjian, G., Hallewell, G., van Haren, H., Hartman, J., Heijboer, A.J., Hello, Y., Hernández-Rey, J.J., Herold, B., Hößl, J., Hsu, C.-C., de Jong, M., Kadler, M., Kalekin, O., Kappes, A., Katz, U., Kavatsyuk, O., Kooijman, P., Kopper, C., Kouchner, A., Kreykenbohm, I., Kulikovskiy, V., Lahmann, R., Lamare, P., Larosa, G., Lattuada, D., Lim, G., Presti, D. Lo, Loehner, H., Loucatos, S., Mangano, S., Marcelin, M., Margiotta, A., Martinez-Mora, J.A., Meli, A., Montaruli, T., Moscoso, L., Motz, H., Neff, M., Nezri, E.N., Palioselitis, D., Păvălaş, G.E., Payet, K., Payre, P., Petrovic, J., Piattelli, P., Picot-Clemente, N., Popa, V., Pradier, T., Presani, E., Racca, C., Reed, C., Riccobene, G., Richardt, C., Richter, R., Rivière, C., Roensch, K., Rostovtsev, A., Ruiz-Rivas, J., Rujoiu, M., Russo, V.G., Salesa, F., Sánchez-Losa, A., Sapienza, P., Schöck, F., Schuller, J.-P., Schussler, F., Shanidze, R., Simeone, F., Spies, A., Spurio, M., Steijger, J.J.M., Stolarczyk, T., Taiuti, M.G.F., Toscano, S., Vallage, B., Van Elewyck, V., Vannoni, G., Vecchi, M., Vernin, P., Wijnker, G., Wilms, J., de Wolf, E., Yepes, H., Zaborov, D., De Dios Zornoza, J., Zúñiga, J., 2013. Deep-sea

bioluminescence blooms after dense water formation at the ocean surface. PLoS One 8, e67523. doi:10.1371/journal.pone.0067523

Teira, E., Aken, H. Van, Veth, C., Herndl, G., 2006. Archaeal uptake of enantiomeric amino acids in the meso-and bathypelagic waters of the North Atlantic. Limnol. Oceanogr. 51, 60–69.

Testor, P., Gascard, J.-C., 2006. Post-convection spreading phase in the Northwestern Mediterranean Sea. Deep Sea Res. Part I Oceanogr. Res. Pap. 53, 869–893. doi:10.1016/j.dsr.2006.02.004

Thetis Group, 1994. Open-ocean deep convection explored in the Mediterranean. EOS Trans. 75, 217–224.

Tully, B.J., Nelson, W.C., Heidelberg, J.F., 2012. Metagenomic analysis of a complex marine planktonic thaumarchaeal community from the Gulf of Maine. Environ. Microbiol. 14, 254–67. doi:10.1111/j.1462-2920.2011.02628.x

Turesson, G., 1922. The species and the variety as ecological units. Hereditas 3, 100–113.

Vergin, K.L., Beszteri, B., Monier, A., Thrash, J.C., Temperton, B., Treusch, A.H., Kilpert, F., Worden, A.Z., Giovannoni, S.J., 2013. High-resolution SAR11 ecotype dynamics at the Bermuda Atlantic Time-series Study site by phylogenetic placement of pyrosequences. ISME J. 7, 1322–32. doi:10.1038/ismej.2013.32

Vilibić, I., Matijević, S., Šepić, J., Kušpilić, G., 2012. Changes in the Adriatic oceanographic properties induced by the Eastern Mediterranean Transient. Biogeosciences 9, 2085–2097. doi:10.5194/bg-9-2085-2012

Whitman, W.B., Coleman, D.C., Wiebe, W.J., 1998. Prokaryotes: The unseen majority. Proc. Natl. Acad. Sci. 95, 6578–6583.

Woese, C.R., 1987. Bacterial Evolution. Microb. Rev. 51, 221–271.

Wuchter, C., Schouten, S., Boschker, H.T.S., Sinninghe Damsté, J.S., 2003. Bicarbonate uptake by marine Crenarchaeota. FEMS Microbiol. Lett. 219, 203–207. doi:http://dx.doi.org/10.1016/S0378-1097(03)00060-0

Yılmaz, A., Tuğrul, S., 1998. The effect of cold-and warm-core eddies on the distribution and stoichiometry of dissolved nutrients in the northeastern Mediterranean. J. Mar. Syst. 16, 253–268.

Yogev, T., Rahav, E., Bar-Zeev, E., Man-Aharonovich, D., Stambler, N., Kress, N., Béjà, O., Mulholland, M.R., Herut, B., Berman-Frank, I., 2011. Is dinitrogen fixation significant in the Levantine Basin, East Mediterranean Sea? Environ. Microbiol. 13, 854–871. doi:10.1111/j.1462-2920.2010.02402.x

Yokokawa, T., Nagata, T., 2010. Linking bacterial community structure to carbon fluxes in marine environments. J. Oceanogr. 66, 1–12.

Yunev, O.A., Carstensen, J., Moncheva, S., Khaliulin, A., Aertebjerg, G., Nixon, S., 2007. Nutrient and phytoplankton trends on the western Black Sea shelf in response to cultural eutrophication and climate changes. Estuar. Coast. Shelf Sci. 74, 63–76.

Zavatarelli, M., Mellor, G.L., 1995. A numerical study of the mediterranean sea. Am. Meteorol. Soc. 25, 1384–1414.

Zunino, P., Schroeder, K., Plaza, F., Serra, M., Castro, C., Moya, F., Salat, J., 2012. Extreme Western Intermediate Water formation in winter 2010. J. Mar. Syst. doi:10.1016/j.jmarsys.2012.05.010

ANNEXES

A. Papier accepté dans Environmental Pollution

'Rare biosphere' bacteria as key phenanthrene degraders in coastal seawaters

Running title: Rare biosphere bacteria as dominant PAH-degraders

List of authors: Caroline Sauret[1,2], Tatiana Severin[1,2], Gilles Vétion[1,2], Catherine Guigue[3], Madeleine Goutx[3], Mireille Pujo-Pay[1,2], Pascal Conan[1,2], Sonja K Fagervold[1,4], Jean-François Ghiglione[1,2]

(1) University Pierre et Marie Curie (UPMC) 06, Unité Mixte de Recherche (UMR) 7621, Laboratoire d'Océanographie Microbienne (LOMIC), UMR 8222, Laboratoire d'Ecogéochimie des Environments Benthiques (LECOB), Observatoire Océanologique, F 66650 Banyuls/mer, France;
(2) CNRS, UMR 7621, LOMIC, Observatoire Océanologique, F-66650, Banyuls/mer, France;
(3) Aix-Marseille University, Mediterranean Institute of Oceanography (M I O), 13288, Marseille, Cedex 9, France ; Université du Sud Toulon-Var, 83957, La Garde Cedex, France; CNRS-INSU/IRD UM 110 (4) CNRS, UMR 8222, LECOB, Observatoire Océanologique, F-66650 Banyuls/Mer, France

Subject Category: microbial ecology and functional diversity of natural habitats

Correspondence: JF Ghiglione, Laboratoire d'Océanographie Microbienne, University of Paris 6, Avenue Fontaulé, F-66650 Banyuls sur mer, France.
E-mail : ghiglione@obs-banyuls.fr

Abstract

The vast majority of microbial species is present at extremely low abundances and form the so-called 'rare biosphere' whose role in ecosystem functioning remains largely unknown. By coupling DNA-SIP and pyrosequencing approaches, we present independent lines of evidence that members of the bacterial rare biosphere may function as a 'seed bank' to support the environment to withstand pollution events. We identified *Cycloclasticu*s sp. as a keystone degrader of polycyclic aromatic hydrocarbons (PAH) despite being a member of the 'rare biosphere' in NW Mediterranean seawaters with various pollution histories. We discovered novel PAH-degrading bacteria (*Oceanibaculum sp. and Sneathiella sp.*) and we identified other groups already known to possess this function (*Alteromonas sp., Paracoccus sp.*). Together with *Cycloclasticus* sp., these groups contributed to potential *in situ* phenanthrene degradation at a rate of up to 0.5 mg l^{-1} day^{-1}, sufficient to account for a considerable part of PAH degradation in marine waters. Further, we characterized the PAH-tolerant bacterial community, which were much more diverse in chronically polluted site by comparison to unpolluted marine references. PAH-tolerant bacteria were also members of the rare biosphere, such as *Glaciecola* sp. that drastically increased in abundance after phenanthrene addition but without being able to degrade it. Collectively, these data show the complex interactions between PAH-degraders and PAH-tolerant bacteria that coexist in seawaters and gives new insight for the understanding of the functional ecology of marine bacteria in polluted waters.

Keywords: rare biosphere / keystone species / PAH-degraders / PAH-tolerant bacteria / DNA-SIP pyrosequencing

Introduction

Polycyclic aromatic hydrocarbons (PAHs) are recognized as high-priority pollutants in the environment and are a significant concern to human health since, together with their toxic and mutagenic properties, they are the most potent carcinogens known (Djomo et al. 1995). An estimated 9.10^5 metric tons of PAHs are released to global oceans annually, the majority of which is derived from anthropogenic sources, mainly from urban runoff and accidental releases of petroleum (Kennish 1992). Coastal areas close to oil refinery discharges contain particularly elevated PAH concentrations (Le Dréau et al. 1997).

Taxonomically diverse marine bacteria able to utilize low-molecular-weight PAHs, such as naphthalene, phenanthrene and fluorene as sources of carbon and energy have been isolated and characterized. For example, bacteria belonging to the genera *Pseudomonas* (García-Valdés et al. 1988), *Vibrio* (Hedlund and Staley 2001), *Thalassospira* (Zhao et al. 2010), *Cycloclasticus* (Dyksterhouse et al. 1995), *Flavobacterium* (Shiraris et al. 1983), *Sphingomonas* (Zylstra et al. 1997), *Oleispira* (Yakimov et al. 2003), *Galaecimonas* (Rodriguez-Blanco et al. 2010b), *Marinobacter* (Grimaud et al. 2012), *Oceanibaculum* (Dong et al. 2010) and *Mycobacterium* (Khan et al. 2002) have been isolated from oil contaminated marine environments. However, isolation of pure cultures, which is typically accomplished by enrichment methods, is not necessarily an indication of the importance of PAH degraders *in situ* and fails to describe the complex interactions with other microorganisms and with their abiotic environment, i.e. the ecology of PAH degraders.

Several culture-independent studies of oil-impacted marine environments have shown that oil pollution leads to a decrease of the number of bacterial operational taxonomic units (OTUs), with fewer dominant groups and radical shifts in the bacterial community structure (Kasai et al., 2002; Rodríguez-Blanco et al., 2010a; Röling et al., 2002). For example, *Cycloclasticus* spp. appeared to be strongly augmented in PAH-contaminated marine environments (Geiselbrecht et al. 1998; Röling et al. 2002), sometimes enriched by 5 orders of magnitude after oil contamination (Kasai et al. 2002). Because such bacteria use hydrocarbons almost exclusively as a carbon source, it is generally thought that these hydrocarbonoclastic organisms are normally present in very small numbers, growing and multiplying rapidly to become dominant after PAH addition. With the development of new pyrosequencing technologies we can now test this hypothesis, since it allows the study of very low-abundant bacteria (<0.1-1% of the total diversity), also referred to as the 'rare biosphere' (Sogin et al. 2006).

Most culture-independent studies for *in situ* taxonomic characterization of marine microorganisms lack the ability to establish a causal relationship to function within the

community. Description of changes in bacterial diversity after PAH addition failed to distinguish between PAH-degraders and other tolerant, dormant, senescent or dead cells (Rodríguez-Blanco et al. 2010a). Recently, the use of DNA stable-isotope probing (DNA-SIP) for the study of contaminated sites has considerably facilitated the direct identification of PAH-degrading bacterial communities. To date, most of these studies were performed in soil environments (Martin et al. 2012; Cébron et al. 2011; Jones et al. 2011; Singleton et al. 2011). Only one study focused on PAH-degraders using DNA-SIP in seawaters, revealing *Rhodobacteraceae* as dominant naphthalene degrader in Tampa Bay, Florida (Gutierrez et al. 2011).

The aim of this study was to identify the functional communities actively assimilating PAH in coastal waters and to determine their geographical distribution in NW Mediterranean seawaters in relation to the pollution history of the sites. Using phenanthrene as model PAH compound, we examined changes in the seawater PAH-exposed bacteria as a function of the dose and time of exposure to the tracer. The composition of the phenanthrene-degrading and phenanthrene-tolerant bacterial communities were monitored by a combination of molecular methods, including capillary electrophoresis single strand conformation polymorphism (CE-SSCP) and 454 FLX pyrosequencing technology coupled with DNA-SIP with uniformly labeled ^{13}C-phenanthrene.

Materials and methods

Sampling sites

Seawaters were sampled from the North Western Mediterranean Sea (France) in one chronically polluted site in the Fos-sur-Mer gulf (F site) and two nearshore observation stations of the Service d'Observation en Milieu LITtoral (SOMLIT; http://www.domino.u-bordeaux.fr/somlit_national/) as marine references in the bays of Marseille (M site) and Banyuls sur mer (B site). Samples were collected with 9 l Nalgene® bottles, previously washed with 1 M hydrochloric acid (HCl) and ultrapure water, rinsed three times with the respective sample before filling with seawater at ~0.2 m below the surface and placed in the dark after the sample collection. Seawater was processed in the laboratory within 2h of sampling.

Microcosm setup and incubation conditions

Incubations were performed in 500ml precombusted and sterilized glass Erlenmeyer flasks closed with Teflon-lined caps. Three experiments were run in parallel with a total of 27 flasks

per site. In the first experiment, flasks were filled with 250 ml of 2.0 µm pre-filtered seawater (47mm, PC Nucleopore) amended with nutrient solution (0.11 mg l^{-1} NH_4Cl and 0.06 mg l^{-1} Na_2HPO_4) after addition of unlabeled ^{12}C- phenanthrene solubilized in dichloromethane (CH_2Cl_2) and evaporation of CH_2Cl_2 leading to final ^{12}C-phenanthrene concentrations of 0.1, 1 or 10 mg l^{-1}, respectively. The incubation flasks were maintained under agitation (300 rpm) in the dark at *in situ* temperature during 0, 3, 7, 14 days. The turnover of phenanthrene was measured for all ^{12}C-phenanthrene incubations conditions. In addition two controls were analyzed only after 0 and 14 days, one with no phenanthrene but CH_2Cl_2 and 2.0 µm pre-filtered seawater, and one as an abiotic control filled with phenanthrene and with 0.2 µm pore-size pore-size filtered (47mm, PC nucleopore) and autoclaved seawater (16 flasks). In the second experiment, the effect of the addition of 1 mg l^{-1} of ^{12}C-phenanthrene on bacterial community structure was investigated at all incubation times as well as for a control without phenanthrene but CH_2Cl_2 added at 3, 7 and 14 days (7 flasks). In a third experiment, seawater incubations were performed with 1 mg l^{-1} of uniformly labeled $^{13}C_{14}$-phenanthrene (99% atom ^{13}C, Sigma-Aldrich) where the turnover of phenanthrene and the bacterial diversity was measured after 0 and 7 days (4 flasks).

PAH extraction and quantification

PAHs were extracted from sacrificed 250 ml seawater microcosms by liquid–liquid extraction with 20ml of CH_2Cl_2 together with pyrene as internal standard to assess the recovery of analytical procedure and to perform quantitation accuracy. The organic phase was collected and evaporated on a rotary evaporation (Speed Vac concentrator, Fisher, France). Extracts were resuspended in ultrapure toluene solvent and analyzed by gas chromatograph-mass spectrometer (GC-MS) (Varian, 2100T). The GC-MS was equipped with a capillary column (VF-5ms, Varian) and operated at ionization energy of 70 eV for a m/z range of 40-650, using helium as carrier gas at a flow rate of 1 ml min^{-1}. The injector temperature was 300°C. The initial column temperature was held 1min at 60°C, then ramped at 5 °C min^{-1} to a final temperature of 200°C which was held for 16 min. Phenanthrene and pyrene were quantified according to an external calibration performed with standard solutions. The simultaneous quantification of phenanthrene and pyrene provided an extraction yield that was always under 80% of recuperation. The quantification in abiotic controls allowed the estimation of the physical disappearance of phenanthrene during the incubation time of the experiment.

In addition, the quantification of 17 individual PAH concentrations (including phenanthrene) from seawaters was performed according to Guigue et al. (2011).

Nucleic acid extraction and CsCl gradient fractionation

Bacterial cells from 250 ml sacrificed flasks were concentrated onto 0.22 µm-pore-size filters (47 mm, PC Nuclepore) and stored in 2 ml Eppendorf tubes at -80°C. Chromosomal DNA was obtained using a phenol-chloroform extraction, as previously described (Ghiglione et al. 1999). Separation between ^{12}C- and ^{13}C-DNA was performed by isopycnic ultracentrifugation on a CsCl gradient. Gradients were precisely adjusted to a density of 1.715 g ml^{-1} in 4.9 ml OptiSeal™ polyallomer centrifuge tubes (Beckman Coulter) after loading of 2µg of total extracted DNA. Ultracentrifugation was carried out at 44,500 rpm (180,000 g_{av}) for 40 h at 20°C in a Vti 65.2 vertical rotor using an Optima LE-80K Ultracentifuge (Beckman Coulter). Gradient fractionation was adapted from Lueders et al. (2004) using a peristaltic pump to collect fractions of ~200 µL in a 96-well microtiter plate and DNA in each fraction was then quantified by Quant-iT™ Picogreen® dsDNA kit (Invitrogen). The fractions containing heavy or light DNA were purified with the Geneclean Turbokit (MPbio) according to manufacturer instructions.

Molecular fingerprinting and pyrosequencing

For community analysis of phenantrene amended microcosms using CE-SSCP, DNA was used as a template for PCR amplification of the variable V3 region of the 16S rRNA gene with primer w49 and w34, as previously described (Abboudi et al., 2008). CE-SSCP was performed using the ABI 310 Genetic Analyzer (Applied Biosystems) according to Ghiglione et al. (2009).

DNA from each sampling site and the corresponding heavy and light DNA fractions were analyzed by bacterial tag-encoded FLX amplicon pyrosequencing (Roche 454 FLX) at the Research and Testing Laboratory (Lubbock, TX) using RTL protocols (www.researchandtesting.com) with Gray28F and Gray519r primers, as previously described (Ortegua-Retuerta et al., 2013). Sequences were processed and analyzed using the Qiime software (Caporaso et al., 2010). Briefly, samples were denoised using the AmpliconNoise program and checked for chimeric sequences using Perseus (Quince et al., 2011). The resulting clean sequences were clustered using operational taxonomic units (OTUs) at a 97% sequence identity level using the UCLUST algorithm (Edgar, 2010). A representative sequence from each OTU was taxonomically classified using the Ribosomal Database Project (RDP) classifier (Wang et al., 2007) using the Greengenes training set. To normalize the number of tags sequenced between samples, tags were randomly resampled to the sample with the fewest tags (3,715 tags) using Daisychopper v. 0.6 (Gilbert et al., 2009). This step was performed on

operational taxonomic unit (OTU) files clustered at a distance of 0.03 (Ghiglione and Murray, 2012). All OTU and diversity analyses were performed on the re-sampled datasets.

We used SPADE (Species Prediction and Diversity Estimation; http://chao.stat.nthu.edu) to calculate the non-parametric species richness estimator Chao1. PAST (PAleontological STatistics v 1.19; http://folk.uio.no/ohammer/past/) was used to generate rarefaction curves. Both Simpson and Shannon diversity indexes were calculated using PRIMER 6 software (PRIMER-E, UK). Bacterial community structures, either as number and area of the peaks in the CE-SSCP profiles or presence and abundance of OTU in the pyrosequencing data, were compared using ordination of Bray–Curtis similarities and used to build dendrograms by the unweighted-pair group method with arithmetic averages (UPGMA).

Results

Rate and extent of phenanthrene degradation

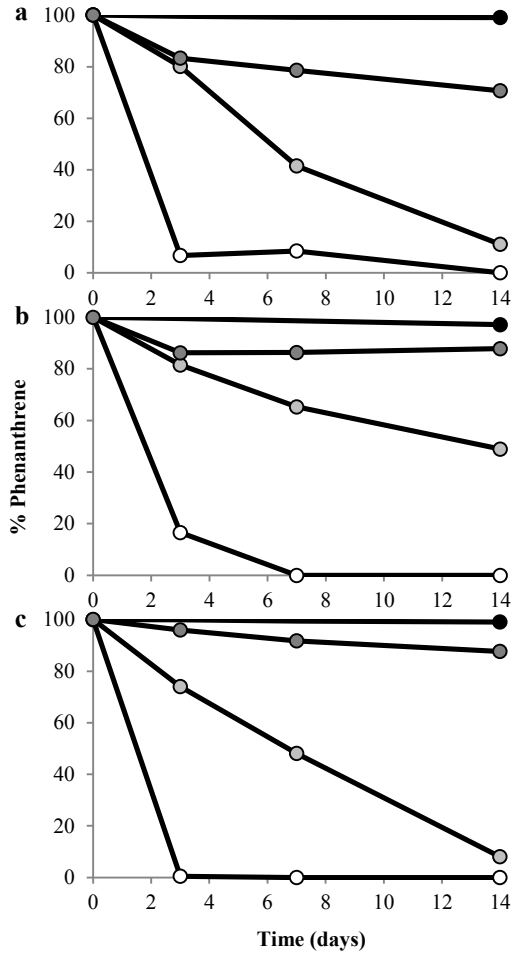

Figure 1 Percentage of phenanthrene remaining during the course of the experiment with Fos-sur-mer (a), Marseille (b) and Banyuls-sur-mer (c) seawaters incubated with 0.1 (white circle), 1 (light grey circle) and 10 (dark grey circle) mg l^{-1} phenanthrene and for an abiotic control with 1 mg l^{-1} phenanthrene (black circle).

Seawaters used in this study represented a gradient of *in situ* PAH concentrations from 30.5, 14.2 and 5.0 ng l^{-1}, including 2.9, 1.0 and 0.6 ng l^{-1} of phenanthrene in the bays of Fos-sur-mer

(F), Marseille (M) and Banyuls-sur-mer (B), respectively. Dose- and time-response relationships for bacterial degradation of phenanthrene were investigated in sacrificed microcosms containing 250 mL seawater amended with 0.1, 1 or 10 mg l^{-1} of phenanthrene and incubated during 0, 3, 7 and 14 days, in comparison to an abiotic control amended with 1 mg l^{-1} phenanthrene. While almost no phenanthrene degradation was found in the abiotic control, it was completely degraded in all sites after 3 days of incubation in the microcosms amended with 0.1 mg l^{-1} phenanthrene (Figure 1). Rate and extent of phenanthrene degradation were comparable between F, M and B sites but always lower in microcosms with 1 mg l^{-1} compared to 10 mg l^{-1} of added phenanthrene. For example, phenanthrene degradation rates in F, M and B sites after 7 days of incubation ranged from 0.06 to 0.10 mg l^{-1} day^{-1} and from 0.12 to 0.30 mg l^{-1} day^{-1} in incubations with 1 and 10 mg l^{-1} of phenanthrene, respectively. Phenanthrene degradation rates were maximal during the first 3 days, with up to 0.56 mg l^{-1} day^{-1} in the chronically polluted F site contaminated with 10 mg l^{-1} of phenanthrene. The incubations with 1 mg l^{-1} phenanthrene, where around half of the substrate was degraded in 7 days, were chosen for further molecular analysis.

Effect of phenanthrene on the overall community structure

Hierarchical clustering analysis based on CE-SSCP profiles of PCR amplified 16S rRNA genes showed a clear influence of the addition of 1 mg l^{-1} phenanthrene on bacterial community structure in all sampling sites (Figure 2). During the 14 days of incubation, control samples without phenanthrene always clustered closer to the initial *in situ* sample than to the cluster of samples exposed to phenanthrene, except for sample from M after 3 days of incubation with phenanthrene that clustered with its control counterpart. After a rapid change within 3 days resulting in the formation of the 2 clusters composed of control without phenanthrene vs. phenanthrene-added samples, little influence of incubation time was generally found on the bacterial community structure in all the sampled sites.

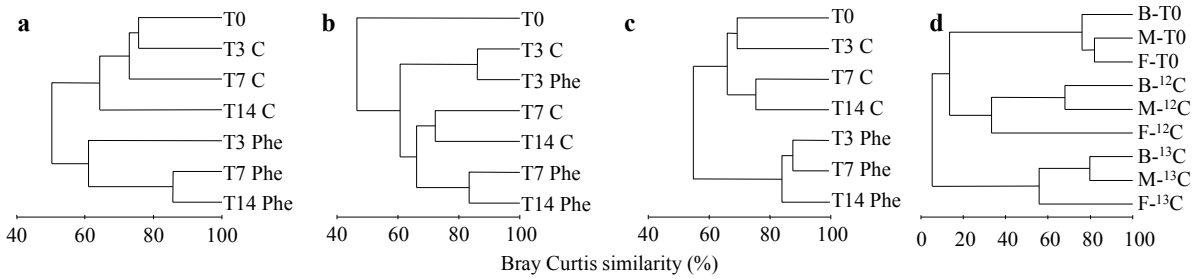

Figure 2 UPGMA dendrogram based on Bray–Curtis dissimilarities between CE-SSCP profiles from Fos-sur-mer (a), Marseille (b) and Banyuls-sur-mer (c) seawaters incubated with 1 mg l^{-1} phenanthrene (Phe) or with no phenanthrene added (C). Dendrogram from SIP experiment (d) with seawaters originated from Fos-sur-mer (F), Marseille (M) and Banyuls-sur-mer (B) at the initial incubation time (T0) and for the heavy (^{13}C) and light (^{12}C) fractions recovered after 7 days of incubation with 1 mg l^{-1} of ^{13}C-labeled phenanthrene.

Identification of labeled and unlabeled community components

To specifically identify phenanthrene-degrading or phenanthrene-tolerant bacteria, uniformly labeled $^{13}C_{14}$-phenanthrene was added to seawaters from different origins and the labeled and unlabeled bacterial communities were analyzed by pyrosequencing. After removing low quality sequences, a total of 93,122 reads were obtained for the nine samples analyzed, with a minimum of 3,715 sequences per sample (Table 1). Tags had a mean length of ~400 nucleotides after primer trimming. All subsequent results were calculated from a re-sampling to the lowest abundant number of sequences (3,715) and 0.03 distance-clustered data set that represented a total of 1,205 unique OTUs for the nine samples. The original *in situ* samples were composed of 177, 150 and 380 OTUs with richness estimated to 336, 358 and 947 OTUs by using Chao1 estimator in F, M and B sites, respectively. The number of OTUs in the ^{12}C-DNA fractions represented 76 and 44% of the number of OTUs found in the original M and B sites respectively, but 124% in the F site. All diversity indicators showed a very low richness and eveness in the ^{13}C-DNA fractions with only 27, 50 and 14 OTUs recovered in F, M and B sites, respectively (Table 1 and Supplementary Figure 1).

Table 1 Bacterioplankton diversity estimates over seawaters originated from Fos-sur-mer (F), Marseille (M) and Banyuls-sur-mer (B) at the initial incubation time (T0) and for the heavy (^{13}C) and light (^{12}C) fractions recovered after 7 days of incubation with 1 mg l^{-1} of ^{13}C-labeled phenanthrene. Number of OTUs and diversity indices were calculated on the 3715 resampled sequences per sample.

Sample ID	No. of reads	No. of OTUs	Chao1	Shannon (H')	Simpson (l)	Pielou (J)
F-T0	9849	177	336	2,07	0,58	0,40
F-^{12}C	3715	220	426	3,41	0,93	0,63
F-^{13}C	9816	27	38	0,97	0,54	0,30
M-T0	10355	150	358	2,17	0,68	0,43
M-^{12}C	9521	114	190	1,12	0,35	0,23
M-^{13}C	12876	50	97	0,62	0,21	0,16
B-T0	5563	380	947	3,01	0,78	0,51
B-^{12}C	11996	166	302	1,83	0,55	0,36
B-^{13}C	19431	14	50	0,08	0,02	0,03

Alphaproteobacteria dominated the *in situ* bacterial diversity of all the original *in situ* sampling sites (Figure 3). *Pelagibacter* composed the majority of the OTUs belonging to the major Alphaproteobacteria group and represented respectively 72, 64 and 65% of the total communities in F, M and B, respectively. Gammaproteobacteria accounted for 6, 4 and 3% and Flavobacteria represented 7, 6 and 2% in F, M and B, respectively. Other groups always represented less than 5% of the total community of each sites.

Clear differences were found in the taxonomic composition of the ^{12}C- and ^{13}C-DNA fractions recovered from the SIP incubations but also in relation to their sampling origin. The taxonomic composition of the unlabeled ^{12}C-DNA differed between the chronically polluted site (F) and the two other sites (B and M). *Glaciecola* sp. (Gammaproteobacteria) represented 80 and 76% of the unlabeled ^{12}C-DNA fractions from M and B sites respectively, but only 20% in the F site (Figure 3). *Pelagibacter* sp. was found at only 3, 8 and 2% in F, M and B sites, respectively. Other groups represented less than 2% in M and B sites, whereas the F site presented higher eveness (Table 1). The F community was also composed of undetermined *Microbacteriaceae* (13%), undetermined Gammaproteobacteria (11%), undetermined *Rhodobacteraceae* (11%), *Neptunibacter* sp. (8%) and other groups representing less than 2%.

The ^{13}C-labeled DNA fractions of all sites were dominated by the Gammaprotebacterium *Cycloclasticus* sp., representing 57, 89, and 99% of the bacterial community in F, M and B, respectively (Figure 3). The eveness of the F site community was again higher than of the M and B sites (Table 1). *Paracoccus* sp. and *Oceanibaculum* sp. represented respectively 4.7 and 2.3% of the heavy DNA from M site and *Sneathiella* sp. and *Alteromonas* sp. represented respectively 37.6 and 2.6% of the heavy DNA from F site. Other groups represented less than 0.5% of the ^{13}C-enriched DNA fractions. It is noticeable that none of the dominant ^{13}C-labeled OTUs were detected in the initial samples and represented less than 5% of the corresponding ^{12}C-labeled OTUs.

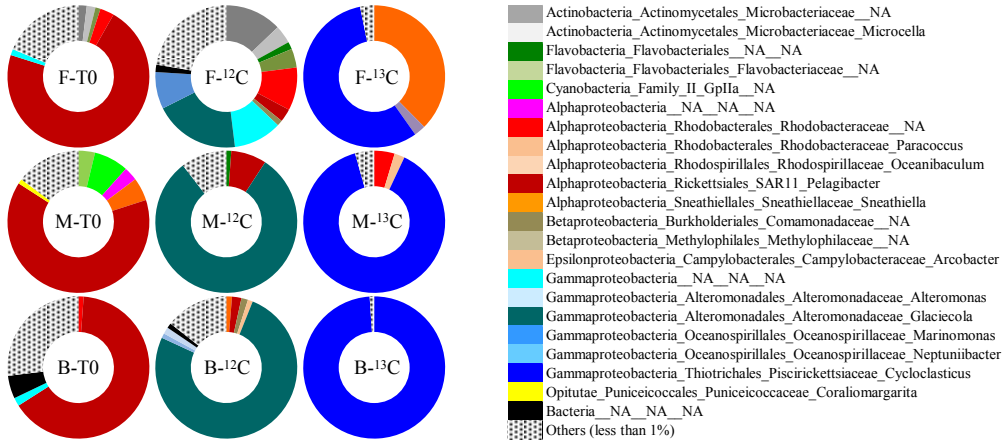

Figure 3 Taxonomic distribution (Class_Order_Familly_Genus) for OTUs that occurred more than 37 times (>1% of the 3715 resampled sequences per sample) in seawaters originated from Fos-sur-mer (F), Marseille (M) and Banyuls-sur-mer (B) at the initial incubation time (T0) and for the heavy (^{13}C) and light (^{12}C) fractions recovered after 7 days of incubation with 1 mg l^{-1} of ^{13}C-labeled phenanthrene. The remaining tag sequences are grouped in 'others'. Taxonomy not assigned, NA.

Discussion

Identification of key phenanthrene degraders in marine environments

The main phenanthrene degrader identified in our study belongs to the Gammaproteobacterial *Cycloclasticus* sp., with 99.8% sequence similarity to known sequences. This result is in accordance with several studies showing the presence of this genera in various PAH polluted environments (Geiselbrecht et al. 1996; Kasai et al. 2002; McKew et al. 2007), accounting for up to 25% of the total bacterial community in severely oil-polluted waters (Maruyama et al. 2003; Harayama et al. 2004). However, these studies made no evidence of its functional role in PAH degradation. By coupling DNA-SIP with pyrosequencing, we could estimate that *Cycloclasticus* sp. accounted from 57 to 99% of the active phenanthrene degraders one week after 1 mg l^{-1} phenanthrene addition in our samples. This concentration was 50 times lower than what was used by Gutierrez et al. (2011) for ^{13}C-labeled naphthalene in seawater. Almost half of the added phenanthrene was degraded after 7 days of incubations in all sampling sites, and for example *Cycloclasticus* sp. alone in B (at 99% of the phenanthrene-degraders) was responsible for the degradation of more than 0.07 mg l^{-1} day^{-1} of phenanthrene. Teira et al. (2007) also observed a quick response of bacteria belonging to the genus *Cycloclasticus* after PAH addition to Atlantic coastal waters, reaching a maximum contribution (~11%) to the total community in about 3 days, as recorded by fluorescent in situ hybridization (FISH). The dominant representation of *Cycloclasticus* sp. suggests that they have a competitive advantage

compared to other bacteria in the field sample (i.e. specialization) by degrading phenanthrene. It was demonstrated that this genus degrades C_{1-2} alkyl aromatic hydrocarbons more efficiently than some other PAH-degrading bacteria such as *Marinobacter*, *Pseudomonas* and *Sphingomonas* (Kasai et al. 2002), a capacity that could explain its systematic dominance in PAH-contaminated sites. These observations suggest that *Cycloclasticus* is an important group in the natural elimination of low-molecular-weight PAHs. Thus, we propose that the presence of *Cycloclasticus* sp. can be used as a proxy for PAH pollution in NW Mediterranean seawaters. This genus was not detectable out of the 3,715 sequences analyzed in each of our initial sampling sites, indicating that the sequences belonging to *Cycloclasticus* sp. were part of the 'rare biosphere' *in situ*. Members of this genus were classified as hydrocarbonoclastic bacteria, which use hydrocarbons almost exclusively as carbon source (Kasai et al. 2002). To our knowledge, this study presents the first observation of the emergence of hydrocarbonoclastic bacteria out of the rare biosphere to become dominant in relation to their active use of PAH. This was also the case for the other phenanthrene-degraders identified in our study. Sequences belonging to *Alteromonas* sp., *Paracoccus* sp., *Oceanibaculum* sp. and *Sneathiella* sp. were only found in the heavy ^{13}C fraction, but not in the initial *in situ* samples. This observation demonstrate that the 'seed bank' theory is particularly well adapted to PAH-degrading bacteria (Pedrós-Alió 2006). Indeed, we have identified members of the PAH-degrading community belonging to the "seed bank". We hypothesize that these are opportunistic species that grow and become the 'core species' involved in PAH degradation in our conditions. Members of the *Alteromonas* and *Paracoccus* genera have already been isolated and characterized as PAH-degraders under culture conditions (Harwati et al. 2007, Radwan et al. 2010). Thus, their presence in the phenanthrene-degrading bacterial communities was not surprising. *Oceanibaculum* has been found in a PAH-polluted hydrothermal field sediment (Dong et al. 2010) and *Sneathiella* has been identified in an oil reservoir in the North sea (Bødtker et al. 2009) but, until now, these bacteria have never been recognized as PAH-degraders. These results reinforce the power of the DNA-SIP coupled with new pyrosequencing technologies to identify new members of a functional community *in situ*, i.e. the phenanthrene-degrader community.

Phenanthrene-tolerant bacteria

In all the sampling sites, a rapid shift of the bacterial community was observed after 3 days between communities incubated with phenanthrene or not, and the selected communities remained very similar during the course of the experiment. Dominant members of the *in situ*

natural community remained generally detectable after phenanthrene addition but represented a much lower percentage of the community in the light ^{12}C-fraction, and none of dominant members *in situ* were detected in the heavy ^{13}C-fraction. For example, bacteria belonging to the genus *Pelagibacter* represented more than 64% of the natural bacterial communities but less than 8% in the light ^{12}C-fractions and remained undetected in the ^{13}C-fraction. Castle et al. (2006) observed the disappearance of entire phyla, i.e. Alphaproteobacteria and Bacteroidetes that became undetectable by FISH after 3 days of the naphthalene exposure. This result was put into perspective by Teira et al. (2007), proposing that such discrepancy may be related to the specificity of the probes used in FISH-based analysis, or to the difference in naphthalene concentration used. Labbé et al. (2007) also found that the abundance of Alphaproteobacteria were double the amount in pristine than in hydrocarbon-contaminated Alpine soils.

In our experiment, *Glaciecola* sp., a Gammaproteobacterium belonging to the *Alteromonadaceae* family, was predominant (from 20 to 80%) in the light ^{12}C-fractions of all sampling sites. This genus has been found in oil contaminated seawaters (Prabagaran et al. 2007; Brakstad et al. 2008). It is then tempting to allocate the function of hydrocarbon-degradation to this genus because of their dominance in the bacterial community selected after oil contamination. In our study, we found very few sequences (less than 20) belonging to *Glaciecola* sp. in the *in situ* communities and they were undetectable in the heavy ^{13}C-fractions from all sampling sites. To our knowledge, this is the first demonstration of the selection of a genera belonging to the 'rare biosphere' that become dominant after PAH addition but without being directly involved in the degradation of PAH. Further studies are needed to understand the physiological mechanisms of tolerance of *Glaciecola* sp. to PAH toxicity that made this bacterium a serious competitor for the nutrient resources in relation to the hydrocarbon-degrading bacteria. The rapid change in bacterial community generally observed after PAH addition may be explained by inhibitory effects of toxic PAH compounds and /or competition between PAH-degraders and PAH-tolerant bacteria. However, this needs to be further elucidated. Little attention has been paid to the light ^{12}C-fractions in previous papers using DNA-SIP, probably because of the time and financial constraints of cloning and sequencing approaches generally used to describe the functional diversity associated with the heavy ^{13}C-fractions. New capabilities offered by pyrosequencing approaches coupled with DNA-SIP may help to better understand the diversity of bacteria exhibiting a tolerance to toxic contaminant and their ecological role in the response of bacterial community to oil pollution.

Influence of seawater origin in the bacterial response to PAH addition

In a recent study, we illustrate the influence of the pollution history on the response of autochthonous bacteria to crude oil addition (Sauret et al. 2012). The present work goes a step further in examining the influence of the pollution history on the functional diversity of PAH degraders. Our chronically-polluted sampling site (F) in the Gulf of Fos-sur-mer is situated in the route of oil cargo ships and is surrounded by a petrochemical complex, which includes several chemical, petroleum and steel-work plants. PAH concentration of 5.6 ng l^{-1} at station F were only 2 times more than at station M (31 km apart) and 6 times more than at station S (181 km apart from station F), the two last station being selected as marine references by comparison to the other anthropogenically impacted sites in this area (Guigue et al. 2011). These values were comparable to previous concentrations measured in other Mediterranean coastal seawaters, showing a moderate contamination compared to other marine areas such as the Chesapeake Bay, the Los Angeles and Leghorn harbors (Guigue et al. 2011 and references therein). In our study, the maximal degradation rates of phenanthrene were 0.56, 0.46 and 0.14 mg l^{-1} day^{-1} in F, M and B sites respectively (after 3 days of incubation with 10 mg l^{-1} phenanthrene), with each site hosting different bacterial communities. Bacterial diversity in site B was similar to previously observed diversity in NW Mediterranean Sea with the same pyrosequencing approach (Pommier et al. 2010), whereas lower diversity was found in sites F and M, as depicted by various diversity estimators. Inversely, the diversity of phenanthrene degraders was lower in B than in F and M sites. Even though *Cycloclasticus* sp. dominated the diversity of the phenanthrene-degraders in all sites, this genus represented 99% and 89% of the phenanthrene-degraders in the B and M marine references sites. In the chronically polluted site, *Cycloclasticus* sp. competed mainly with *Sneathiella* sp. for the use of phenanthrene, representing 57 and 38% of the phenanthrene-degraders in the F site, respectively. *Sneathiella* sp. was only found as phenanthrene-degrader in the chronically polluted site, but not in the marine references. Other competitors representing less than 5% of the phenanthrene-degraders existed in the M and F sites, such as *Oceanibaculum, Paracoccus, Atleromonas*. Each of them was site-specific, suggesting an influence of the seawater origin on the composition of *Cycloclasticus* sp. competitors for the use of phenanthrene as carbon source.

Interestingly, a much wider diversity of phenanthrene-tolerant bacteria was found in the chronically-polluted site than in the marine references sites. Richness estimators in the chronically-polluted site were higher in the ^{12}C fraction than in the natural sampling site, probably because of a more even distribution of the phenanthrene-tolerant bacterial diversity. To our knowledge, these results give the first evidence of the influence of the recurrence of pollution on the capacity of the marine planktonic bacterial community to withstand PAH

pollution. *Glaciecola* sp. appeared to be the most cosmopolitan phenanthrene-tolerant bacteria in NW Mediterranean seawaters as this group dominated the light fraction of the marine references B and M. Despite the fact that the chronically polluted site presented the lowest diversity *in situ* compared to other marine references, it comprised a remarkable phylogenetic diversity of phenanthrene tolerant bacteria, including Actinobacteria, Flavobacteria, Opitutae, alpha-, beta- and gamma-Proteobacteria. These results offer a clear example of bacterial community adaptation to recurrent PAH contamination and a significant contribution in understanding the ecology of PAH-tolerant and PAH-degrading bacteria in marine coastal seawaters.

Concluding remarks

In the past few years, microbial diversity surveys using high-throughput sequencing of 16S rRNA gene amplicons revealed that most of the microbial communities in the environment is typically composed of abundant taxa, which are considered to carry out the major ecosystem functions, and very low abundant taxa in a dormant or senescent state, which are referred to as the 'rare biosphere' (Sogin et al., 2006). However, we are only starting to learn what different ecological roles these rare microorganisms may have. In this study, we present geographically independent lines of evidence that members of the rare biosphere may function as a 'seed bank' and develop rapidly a predominant role in the ecosystem cleaning after a PAH pollution, including the obligate oil-degrading marine bacteria *Cycloclasticus* sp. as a keystone phenanthrene-degrader in chronically polluted site or marine references in the NW Mediterranean seas. We also characterized opportunists with unknown functions, but with a tolerance to PAH pollution, that could emerge from the 'rare biosphere' and may compete with PAH-degraders for other resources, including nutrients that may rapidly become a limiting factor for bioremediation of organic pollutants in seawaters. The understanding of the ecological significance of how naturally occurring microorganisms respond to anthropogenic compounds can make bioremediation technologies more robust. By coupling DNA-SIP and pyrosequencing approaches, our findings are a major step in understanding the ecology of PAH-degrading and PAH-tolerant bacteria in marine waters.

Acknowledgements

We are grateful to the captain and crew of the R/V Antédon II and R/V Thethys II, as well as to the Service d'Observation of the Mediterranean Institute of Oceanography (M.I.O) managed

by P. Raimbault and to the Service d'Observation of the Oceanographic Observatory of Banyuls sur mer, and especially M.P.A. Guigui to their excellent cooperation. This study was part of the 'IBISCUS' project, funded by the Continental and Coastal Ecosphere (EC2CO) program from the Centre National de la Recherche Scientifique (CNRS) and Institut des Sciences de l'Univers (INSU).

References

Abboudi M, Jeffrey W, Ghiglione JF, Pujo-Pay M, Oriol L, Sempere R et al. (2008). Effects of photochemical transformations of dissolved organic matter on bacterial metabolism and diversity in three contrasting coastal sites in the northwestern Mediterranean Sea during summer. *Microb Ecol* **55**: 344-357.

Bødtker G, Lysnes K, Torsvik T, Bjørnestad EØ, Sunde E. (2009). Microbial analysis of backflowed injection water from a nitrate-treated North Sea oil reservoir. *J Ind Microbiol Biotechnol* **36**: 439-450.

Brakstad OG, Nonstad I, Faksness L-G, Brandvik PJ. (2008). Responses of microbial communities in Arctic sea ice after contamination by crude petroleum oil. *Microb Ecol* **55**: 540-552.

Caporaso JG, Kuczynski J, Stombaugh J, Bittinger K, Bushman FD, Costello EK et al. (2010). QIIME allows analysis of high-throughput community sequencing data. *Nat Methods* **7**: 335-336.

Castle DM, Montgomery MT, Kirchman DL. (2006). Effects of naphthalene on microbial community composition in the Delaware estuary. *FEMS Microbiol Ecol* **56**: 55-63.

Cebron A, Louvel B, Faure P, France-Lanord C, Chen Y, Murrell JC, Leyval C. (2011). Root exudates modify bacterial diversity of phenanthrene degraders in PAH-polluted soil but not phenanthrene degradation rates. *Environ Microbiol* **13**: 722–736.

Djomo JE, Ferrier V, Gauthier L, Zoll-Moreux C, Marty J. (1995). Amphibian micronucleus test in vivo: evaluation of the genotoxicity of some major polycyclic aromatic hydrocarbons found in a crude oil. *Mutagenesis* **10**: 223-226.

Dong C, Lai Q, Chen L, Sun F, Shao Z, Yu Z. (2010). *Oceanibaculum pacificum* sp. nov., isolated from hydrothermal field sediment of the south-west Pacific Ocean. *Int J Syst Evol Microbiol* **60**: 219-222.

Dyksterhouse SE, Gray JP, Herwig RP, Lara JC, Staley JT. (1995). *Cycloclasticus pugetii* gen. nov., sp. nov., an aromatic hydrocarbon-degrading bacterium from marine sediments. *Int J Syst Bacteriol* **45**: 116-123.

Edgar RC. (2010). Search and clustering orders of magnitude faster than BLAST. *Bioinformatics* **26**: 2460-2461.

García-Valdés E, Cozar E, Rotger R, Lalucat J, Ursing J. (1988). New naphthalene-degrading marine *Pseudomonas* strains. *Appl Environ Microbiol* **54**:2478-2485.

Geiselbrecht AD, Hedlund BP, Tichi MA, Staley JT. (1998). Isolation of marine polycyclic aromatic hydrocarbon (PAH)-degrading *Cycloclasticus* strains from the Gulf of Mexico and comparison of their PAH degradation ability with that of Puget Sound *Cycloclasticus* strains. *Appl Environ Microbiol* **64**: 4703–4710.

Geiselbrecht AD, Herwig RP, Deming JW, Staley J. (1996). Enumeration and phylogenetic analysis of polycyclic aromatic hydrocarbon-degrading marine bacteria from Puget sound sediments. *Appl Environ Microbiol* **62**: 3344-3349.

Ghiglione JF, Conan P, Pujo-Pay M. (2009). Diversity of total and active free-living vs. particle-attached bacteria in the euphotic zone of the NW Mediterranean Sea. *FEMS Microbiol Lett* **299**: 9-21.

Ghiglione JF, Murray A. (2012). Pronounced summer to winter differences and higher wintertime richness in coastal Antarctic marine bacterioplankton. *Environ Microbiol* **14**: 617-629.

Ghiglione JF, Philippot L, Normand P, Lensi R, Potier P. (1999). Disruption of narG, the gene encoding the catalytic subunit of respiratory nitrate reductase, also affects nitrite respiration in Pseudomonas fluorescens YT101. *J Bacteriol* **181**: 5099-5102.

Gilbert JA, Field D, Swift P, Newbold L, Oliver A, Smyth T et al. (2009). The seasonal structure of microbial communities in the Western English Channel. *Environ Microbiol* **11**: 3132-3139.

Grimaud R, Ghiglione JF, Cagnon C, Lauga B, Vaysse PJ, Rodriguez-Blanco A, Mangenot S, Cruveiller S, Barbe V, Duran R, Wu LF, Talla E, Bonin P, Michotey V. (2012). Genome sequence of the marine bacterium *Marinobacter hydrocarbonoclasticus* SP17 which forms biofilms on hydrophobic organic compounds. *J Bacteriol* **194**:3539-3540.

Guigue C, Tedetti M, Giorgi S, Goutx M. (2011) Occurrence and distribution of hydrocarbons in the surface microlayer and subsurface water from the urban coastal marine area off Marseilles, Northwestern Mediterranean Sea. *Mar Poll Bull* **62**: 2741-2752

Gutierrez T, Singleton DR, Aitken MD, Semple KT. (2011). Stable isotope probing of an algal bloom to identify uncultivated members of the *Rhodobacteraceae* associated with low-molecular-weight polycyclic aromatic hydrocarbon degradation. *Appl Environ Microbiol* **77**: 7856-7860.

Harayama S, Kasai Y, Hara A. (2004). Microbial communities in oil-contaminated seawater. *Curr Opin Biotechnol* **15**: 205-214.

Harwati TU, Kasai Y, Kodama Y, Susilaningsih D, Watanabe K. (2007). Characterization of diverse hydrocarbon-degrading bacteria isolated from Indonesian seawater. *Microbes Environ* **22**: 412-415.

Hedlund BP, and J.T. Staley. (2001). *Vibrio cyclotrophicus* sp. nov., a polycyclic aromatic hydrocarbon (PAH) degrading marine bacterium. *Int J Syst Evol Microbiol* **51**: 61-66

Jones MD, Singleton DR, Sun W, Aitken MD. (2011). Multiple DNA extractions coupled with stable-isotope probing of anthracene-degrading bacteria in contaminated soil. *Appl Environ Microbiol* **77**: 2984-2991.

Kasai Y, Kishira H, Harayama S. (2002). Bacteria belonging to the genus *Cycloclasticus* play a primary role in the degradation of aromatic hydrocarbons released in a marine environment. *Appl Environ Microbiol* **68**: 5625-5633.

Khan AA, Kim SJ, Paine DD, Cerniglia CE. (2002) Classification of a polycyclic aromatic hydrocarbon-metabolizing bacterium, *Mycobacterium* sp. strain PYR-1, as *Mycobacterium vanbaalenii* sp. nov. *Int J Syst Evol Microbiol* **52**: 1997-2002.

Kennish MJ. (1992). Ecology of estuaries: anthropogenic effects, vol. 1. CRC PressI Llc.

Labbé D, Margesin R, Schinner F, Whyte LG, Greer CW. (2007). Comparative phylogenetic analysis of microbial communities in pristine and hydrocarbon-contaminated Alpine soils. *FEMS Microbiol Ecol* **59**:466-475.

Le Dréau Y, Jacquot F, Doumenq P, Guiliano M, Bertrand JC, Mille G. (1997). Hydrocarbon balance of a site which had been highly and chronically contaminated by petroleum wastes of a refinery (from 1956 to 1992). *Mar Poll Bull* **34**: 456-468.

Lueders T, Manefield M, Friedrich MW. (2004). Enhanced sensitivity of DNA- and rRNA-based stable isotope probing by fractionation and quantitative analysis of isopycnic centrifugation gradients. *Environ Microbiol* **6**: 73-78.

Martin F, Torelli S, Le Paslier D, Barbance A, Martin-Laurent F, Bru D, Geremia R, Blake G, Jouanneau Y. (2012). Betaproteobacteria dominance and diversity shifts in the bacterial community of a PAH-contaminated soil exposed to phenanthrene. *Environ Pollut* **162**: 345-53.

Maruyama A, Ishiwata H, Kitamura K, Sunamura M, Fujita T, Matsuo M et al. (2003). Dynamics of microbial populations and strong selection for *Cycloclasticus pugetii* following the Nakhodka oil spill. *Microb Ecol* **46**: 442-453.

McKew BA, Coulon F, Osborn AM, Timmis KN, McGenity TJ. (2007). Determining the identity and roles of oil-metabolizing marine bacteria from the Thames estuary, UK. *Environ Microbiol* **9**: 165-176.

Ortega-Retuerta E, Joux F, Jeffrey W, Ghiglione JF. (2013). Spatial variability of particle-attached and free-living bacterial diversity in surface waters from the Mackenzie River to the Beaufort Sea (Canadian Arctic). *Biogeosciences* **10**: 2747-2759.

Pedrós-Alió C. (2006). Marine microbial diversity: can it be determined? *Trends Microbiol* **14**: 257-263.

Pommier T, Neal PR, Gasol JM, Coll M, Acinas SG, Pedrós-Alió C. (2010). Spatial patterns of bacterial richness and evenness in the NW Mediterranean Sea explored by pyrosequencing of the 16S rRNA. *Aquat Microb Ecol* **61**:221–234

Prabagaran SR, Manorama R, Delille D, Shivaji S. (2007). Predominance of *Roseobacter*, *Sulfitobacter, Glaciecola* and *Psychrobacter* in seawater collected off Ushuaia, Argentina, sub-Antarctica. *FEMS Microbiol Ecol* **59**: 342–355.

Quince C, Lanzen A, Davenport RJ, Turnbaugh PJ. (2011). Removing noise from pyrosequenced amplicons. *BMC Bioinformatics* **12**: 38.

Radwan S, Mahmoud H, Khanafer M, Al-Habib A, Al-Hasan R. (2010). Identities of epilithic hydrocarbon-utilizing diazotrophic bacteria from the Arabian Gulf coasts, and their potential for oil bioremediation without nitrogen supplementation. *Microb Ecol* **60**: 354-363.

Rodríguez-Blanco A, Antoine V, Pelletier E, Delille D, Ghiglione JF. (2010a). Effects of temperature and fertilization on total vs. active bacterial communities exposed to crude and diesel oil pollution in NW Mediterranean Sea. *Env poll* **158**: 663–673.

Rodríguez-Blanco A, Vetion G, Escande M-L, Delille D, Ghiglione JF. (2010b). *Gallaecimonas pentaromativorans* gen. nov., sp. nov., a bacterium carrying 16S rRNA gene heterogeneity and able to degrade high-molecular-mass polycyclic aromatic hydrocarbons. *Int J Syst Evol Microbiol* **60**: 504-509.

Röling WF, Milner MG, Jones DM, Lee K, Daniel F, Swannell RJ et al. (2002). Robust hydrocarbon degradation and dynamics of bacterial communities during nutrient-enhanced oil spill bioremediation. *Appl Environ Microbiol* **68**: 5537-5548.

Sauret C, Christaki U, Moutsaki P, Hatzianestis I, Gogou A, Ghiglione JF. (2012). Influence of pollution history on the response of coastal bacterial and nanoeukaryote communities to crude oil and biostimulation assays. *Mar Env Res* **79**: 70-78.

Shiraris MP, Cooney JJ. (1983). Replica plating method for estimating phenanthrene-utilizing and phenanthrene-cometabolizing microorganisms. *Appl Environ Microbiol* **45**:706-710.

Singleton DR, Richardson SD, Aitken MD. (2011). Pyrosequence analysis of bacterial communities in aerobic bioreactors treating polycyclic aromatic hydrocarbon-contaminated soil. *Biodegradation* **22**: 1061-1073.

Sogin ML, Morrison HG, Huber JA, Mark Welch D, Huse SM, Neal PR, Arrieta JM, Herndl GJ. (2006) Microbial diversity in the deep sea and the underexplored "rare biosphere", *Proc Natl Acad Sci USA* **103**: 12115-12120.

Teira E, Lekunberri I, Gasol JM, Nieto-Cid M, Álvarez-Salgado XA, Figueiras FG. (2007). Dynamics of the hydrocarbon-degrading *Cycloclasticus* bacteria during mesocosm-simulated oil spills. *Environ Microbiol* **9**: 2551-2562.

Wang Q, Garrity GM, Tiedje JM, Cole JR. (2007). Naive Bayesian classifier for rapid assignment of rRNA sequences into the new bacterial taxonomy. *Appl Environ Microbiol* **73**: 5261-5267.

Yakimov MM, Giuliano L, Gentile G, Crisafi E, Chernikova TN, Abraham WR, Lunsdorf H, Timmis KN, Golyshin PN. (2003) Oleispira antarctica gen. nov., sp. nov., a novel hydrocarbonoclastic marine bacterium isolated from Antarctic coastal sea water. *Int J Syst Evol Microbiol* **53**:779-785.

Zhao BS, Wang H, Li RR, Mao XW. (2010) *Thalassospira xianhensis* sp. nov., a polycyclic aromatic hydrocarbon-degrading marine bacterium. *Int J Syst Evol Microbiol* **60**: 1125–1129.

Zylstra GJ, Kim E, Goyal AK. (1997). Comparative molecular analysis of genes for polycyclic aromatic hydrocarbon degradation. *Genet Eng* **19**:257-269.

Supplementary information is available at ISMEJ's website

Supplementary Figure 1 Rarefaction curves over the 3715 resampled sequences per sample from Fos-sur-mer (F), Marseille (M) and Banyuls-sur-mer (B) at the initial incubation time (T0) and for the heavy (^{13}C) and light (^{12}C) fractions recovered after 7 days of incubation with 1 mg l^{-1} of ^{13}C-labeled phenanthrene.

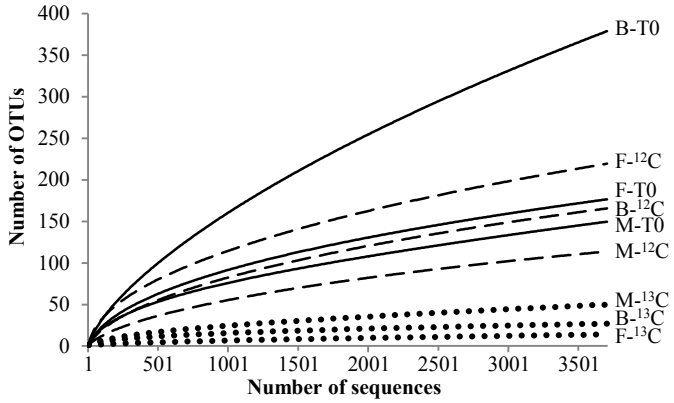

Supplementary Figure 1 Rarefaction curves over the 3715 resampled

B. Communications scientifiques

Posters

T. Severin, J. F. Ghiglione, L. Oriol, J. Caparros, X. Durrieu De Madron, M. Higueras, M. Pujo-Pay. Impact of cascading event on biogeochemical cycles and microbial biomass. Présenté au Worshop Hermione, Carvoerio, Septembre 2012.

T. Severin, P. Conan, X. Durrieu De Madron, L. Houpert, M. Oliver, L. Oriol, J. Caparros, J. F. Ghiglione, M. Pujo-Pay. Impact of open-ocean convection on nutrient and phytoplankton biomass and activity. Présenté au congrès CIESM, Marseille, octobre 2013.

Oraux

T. Severin, P. Conan, X. Durrieu De Madron, L. Oriol, J. Caparros, J. F. Ghiglione, M. Pujo-Pay. Impact of winter offshore convection on phytoplankton biomass and activity. Workshop International Biodiversity and functioning of marine ecosystems, Banyuls sur Mer, juin 2012.

T. Severin, J. F. Ghiglione. Utilisation de couplage DNA-SIP / Pyroséquençage en écotoxicologie microbienne marine. Présenté aux Journées d'écotoxicologie microbienne - AFEM, Banyuls sur Mer, mai 2014.

IMPACT OF CASCADING EVENT ON BIOGEOCHEMICAL CYCLES AND MICROBIAL BIOMASS

Tatiana Severin[1],
Pascal Conan[1], Jean-François Ghiglione[1], Louise Oriol[1], Jocelyne Caparros[1], Xavier Durrieu de Madron[2],Marina Higueras[2], Mireille Pujo-Pay[1]
[1]CNRS-UPMC, UMR 7621, Laboratoire d'Océanographie Microbienne, Observatoire Océanologique, 66650 Banyuls/mer, France
[2]CNRS-CEFREM, UMR 5110, Université de Perpignan, 2 avenue Paul Alduy, 66860 Perpignan Cedex, France

INTRODUCTION

Winter dense water diving (cascading, convection) is an essential process for the control of thermohaline circulation, for deep and intermediate waters renewal, and for the activity of epi- and meso-pelagic and benthic ecosystems (Gascard, 1978; Ivanov et al., 2004), but its impacts on biogeochemical cycles, phytoplankton and bacteria are still misunderstood. A fundamental question concerns the impact of the climate change on the frequency and the intensity of this process. The aim of the CASCADE cruise (Cascading, Surge, Convection, Advection and Downwelling Events, 1-23March 2011) was to have a complete study of cascading process (hydrological, hydrodynamical, sedimentological and biogeochemical) in the Gulf of Lion (GoL) and to propose a realistic matter budget exported to the slope and deep basin by this mechanism. In this work, we focus on a E-SE storm (12/03-13/03) which triggered a downwelling, followed by cascading of dense water through the canyon of Cap de Creus. **The aim of our team is to propose a qualitative and quantitative budget of nutrients, dissolved and particulate organic matter during this event, and their impacts on phytoplankton and bacterial biomass and activity.**

MATERIALS AND METHODS

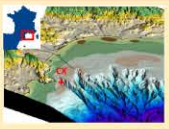

Figure 1: location of the CX station sampled during the Cascade cruise at the exit of the GoL.

Sampling strategies :

Eulerian time series at the head of the canyon Cap de Creus at 300m depth (stations CX; Fig.1) and profiles of the entire water column to follow the nutrient concentrations (NO_3+NO_2, PO_4, $Si(OH)_4$), dissolved (DOM) and particulate (POM) organic matter concentrations (for N, P, C), chlorophyll a concentration (Chla), and bacterial biomass.

RESULTS

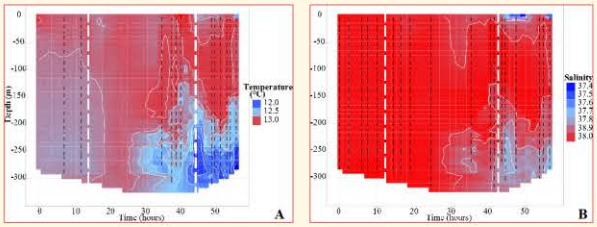

Figure 2 : Profiles along the time of the temperature (**A**) and the salinity (**B**) at CX. Area between the dashed lines corresponds to the period of the E-SE storm.

Decrease of the temperature and the salinity during the storm→ **downwelling**
Apparition of cooler waters at the end of the storm → **cascading**

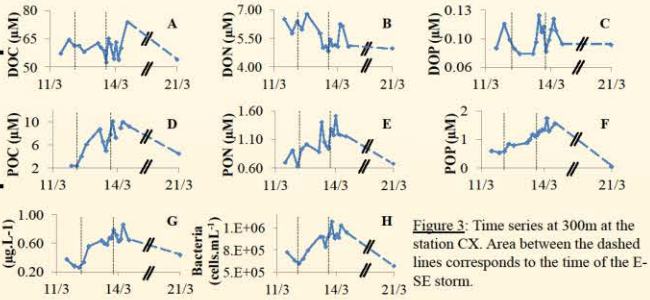

Figure 3: Time series at 300m at the station CX. Area between the dashed lines corresponds to the time of the E-SE storm.

DOM exportation at the end of the storm
Decrease of DON and DOP budget at +8d → **mineralization**

Increase of the POM, Chla and bacteria at the end of the storm → **exportation**
Return to low concentrations at +8d, more marked for POP → **mineralization, with a bigger contribution of attached bacteria**

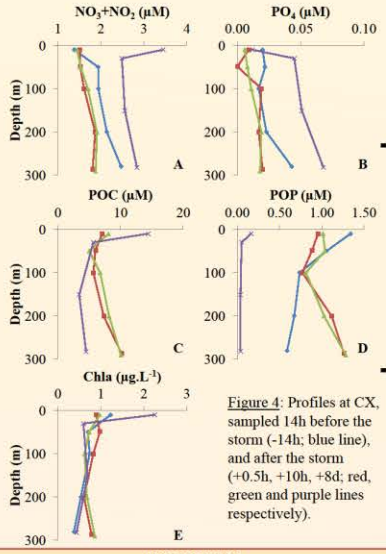

Figure 4: Profiles at CX, sampled 14h before the storm (-14h; blue line), and after the storm (+0.5h, +10h, +8d; red, green and purple lines respectively).

Nutrients homogenization over the entire water column at +0.5h and +10h →**nutrients input in the surface layer**
Increase of the stocks at +8d after the storm → **mineralization**
N:P ratio increase at +8d (data not shown) →**PO_4 consumption**

POM, Chla and bacteria (not shown) **exportation** at +0.5h and +10h
POC and Chla accumulation in the surface layer at +8d → **bloom**
POP depletion on the entire water column at +8d→**mineralisation with a higher contribution of attached bacteria**

DISCUSSION AND CONCLUSION

The downwelling and cascading events triggered by the E-SE storm in March 2011 (Fig. 2), set a rapid **exportation of fresh DOM, POM, surface Chla and bacteria through the canyon**, allowing a real draining of the continental shelf to the deep ecosystems in few hours (Fig. 3 and 4). This matter is an important resource for benthic and deep pelagic ecosystems (Danovaro et al., 1999; Nagata et al., 2010). Concomitantly to the OM export, the homogenization of the water column introduced a large quantity of nutrients in the surface layer (Fig. 4). Height days after the storm, despite a PO_4 depletion a **phytoplanktonic bloom** is observed (Fig. 4). **It is hypothesized that the OM exported is consumed and mineralized by bacteria, with a major contribution of the attached fraction compared to the free one. Phosphorus appears as a key element in the control of this scheme.**

REFERENCES

Danovaro et al. (1999) Benthic response to particulate fluxes in different trophic environments: a comparison between the Gulf of Lions–Catalan Sea (western-Mediterranean) and the Cretan Sea (eastern-Mediterranean). Progress in Oceanopgraphy, 44: 287-312.
Gascard (1978) Mediterranean deep water formation baroclinic instability and oceanic eddies. Oceanologica acta, 1: 315-330.
Ivanov et al. (2004) Cascades of dense water aroud the world ocean. Progress in oceanography, 60(1): 47-98.
Nagata et al. (2010) Emerging concepts on microbial processes in the bathypelagic ocean – ecology, biogeochemistry, and genomics. Deep Sea Research II, 57: 1519–1536

5607

IMPACT OF OPEN OCEAN CONVECTION ON NUTRIENT AND PHYTOPLANKTON BIOMASS AND ACTIVITY

Tatiana Severin[1], P. Conan[1], X. Durrieu de Madron[2], L. Houpert[2], M. Oliver[3], L. Oriol[1], J. Caparros[1], J. F. Ghiglione[1], M. Pujo-Pay[1]

1-CNRS-UPMC, UMR 7621, Laboratoire d'Océanographie Microbienne, Observatoire Océanologique, 66650 Banyuls/mer, France

2-CNRS-CEFREM, UMR 5110, Université de Perpignan, 2 avenue Paul Alduy, 66860 Perpignan Cedex, France

3-Marine Sciences Department, University of Delaware, Lewes, DE 19958, USA

Tatiana.severin@obs-banyuls.fr

Introduction

Open ocean convection is an important process for the global ocean. While sinking dense water exports dissolved and particulate organic matter to the deep layer, upward motions transport nutrients to the surface layer. The convection process is closely related to the recurrent and intense spring bloom observed in the Northwestern Mediterranean Sea, but this link has never been quantify yet. Our aim is to propose a **quantitative nutrient budget during an open ocean convection episode in the Gulf of Lion, to follow the nutrient stoichiometry, and its impact on phytoplankton.**

From convection…

Nutrient input close to deep concentration

Healthy phytoplankton exported down to ~1000m (Chl:Phae>2)

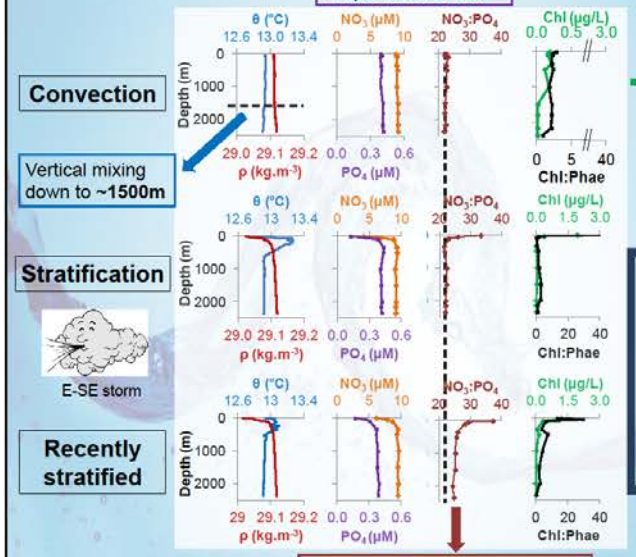

N:P increased (500-2400m)
→ **mineralization ?**
OM exported by convection?

Fig.1: Profiles at the LION site sampled the 4, 9 and 16 March 2011 (top, middle and bottom panels)

… to phytoplanktonic bloom…

1. Advection of the AW and LIW trigger the bloom → inoculum

2. Autochtonous development thanks to nutrient input by the convection

3. Physical **concentration of phytoplankton** maintained alive in the convective cell → inoculum

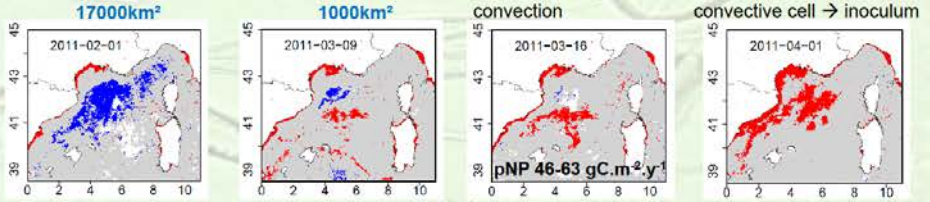

convection sampled

Fig.2: MODIS satellite data averaged on 8 days of the convection area (blue; Chl < 0.12 mg.m-3) and the bloom area (red; Chl > 1 mg.m-3)

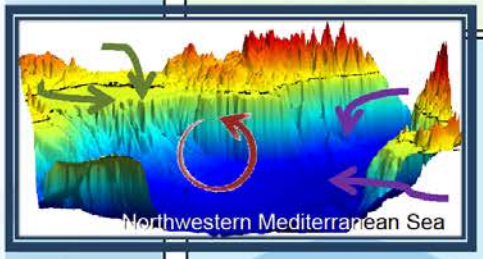

… and nutrient budgets

	$Si(OH)_4$	NO_3	PO_4
Rivers	3.8×10^9 mol/yr	5.9×10^9 mol/yr	1.8×10^8 mol/yr
From Eastern basin		142×10^9 mol/yr	4.4×10^8 mol/yr
Small convection	7.0×10^8 mol/**EPISODE**	8.0×10^8 mol/**EPISODE**	0.36×10^8 mol/**EPISODE**
Extended convection	1.2×10^{10} mol/**EPISODE**	1.4×10^{10} mol/**EPISODE**	6.1×10^8 mol/**EPISODE**

Table 1: Nutrient budgets in the Northwestern Mediterranean Sea

Assumptions:

1-Any mixing below the nutricline bring the same nutrient concentrations (Fig. 1)

2-Nutrient budget depends on the convection area (Fig. 2)

Main conclusions

Our study showed that the nutrient input by a single intermediate convective mixing is comparable to the rivers discharge per year (Table 1). If we consider that any mixing below the nutricline bring the same concentrations of nutrient (Fig 1), we estimated that the bigger convection of February brought much more nutrient that the one of March, and also the rivers discharge per year. Phytoplankton exported by the convection could be maintained alive thanks to the downward and upward motions existing in the convective cell. The stratification will concentrate them into the euphotic layer, participating to the intense spring bloom (Fig. 2).

Résumé

Les épisodes de convection en milieu hauturier sont des processus physiques hivernaux récurrents, mais irréguliers, ayant un fort pouvoir perturbateur sur l'écosystème pélagique. Les principaux objectifs de ma thèse ont été d'étudier l'influence d'épisodes de convection en Méditerranée Nord Occidentale sur les cycles biogéochimiques (distribution et bilan des sels nutritifs) et d'évaluer leurs impacts sur le compartiment microbien (abondance, activité et diversité). Ces travaux reposent sur mon implication active dans les campagnes océanographiques CASCADE (mars 2011) et DeWEX (février et avril 2013) qui s'inscrivent dans le cadre du chantier Méditerranée Mistrals (WP3 et WP1 respectivement du programme MermEX).

Nous avons estimé que les apports en sels nutritifs lors d'un seul phénomène de convection de "moyenne envergure" étaient équivalents aux apports annuels des rivières et des dépôts atmosphériques à l'échelle du golfe du Lion, et pourraient soutenir une production primaire nouvelle de l'ordre de 46 à 63 g $C.m^{-2}.a^{-1}$ (i.e. l'ordre de grandeur de la production nouvelle annuelle de la zone). Une approche satellitale nous a permis de suivre l'évolution de plusieurs épisodes de convection et de mettre en évidence un étroit couplage entre ce type de forçage physique et le développement de blooms phytoplanctoniques en Méditerranée Nord Occidentale.

Pour aborder le rôle des microorganismes dans la régulation des cycles biogéochimiques en réponse à ces épisodes de convection, nous avons identifié l'influence relative des forçages physico-chimiques sur les changements de diversité des communautés microbiennes (bactéries et archées identifiées par pyroséquençage), ceci en relation avec leur activité de reminéralisation de la matière organique. Nous avons également utilisé les épisodes de convection pour évaluer la pertinence écologique des écotypes de SAR11, Marine group I et Marine group II, les 3 groupes taxonomiques les plus répandus et abondants en Méditerranée et dans tous les océans du monde.

Ces travaux ont permis de proposer des scénarii cohérents de l'évolution potentielle des écosystèmes pélagiques en Méditerranée Nord Occidentale dans un contexte de changement climatique global. En effet, mon étude est une contribution à la compréhension de la réponse potentielle des écosystèmes pélagiques à la modification attendue de la fréquence et/ou de l'intensité des processus de convection.

Mots-clés : Convection, Méditerranée Nord-Occidentale, biogéochimie, Bacteria, Archaea, écotype

Abstract

Open-ocean convection episodes are recurrent winter physical processes, but irregular in intensity, with a strong disruptive effect on the pelagic ecosystem. My principal thesis objectives were to study the influence of the Northwestern Mediterranean convection on the biogeochemical cycles (nutrient distribution and assessment), and to evaluate their impacts on the microbial compartment (abundance, activity and diversity). This work was based on my active participation to the oceanographic cruises CASCADE (March 2011) and DeWEX (February and April 2013), which are incorporated in the framework of Mistral Mediterranean project (respectively in the WP3 and WP1 of MermEX program).

We estimated that the nutrient supply by a single convection episode of "average-scale" was equivalent to the annual riverine discharges and atmospheric deposition in the golf of Lion. This could sustain a new primary production from 46 to 63 g $C.m^{-2}.a^{-1}$ (i.e. the annual new primary production rate of this area). A remote sensing approach allowed us to follow open-ocean convection episodes evolution, and to highlight the close relationship between this kind of physical forcing and the phytoplanktonic bloom development in the Northwestern Mediterranean.

During the study of the impact of convection episodes on the role of microorganisms in the biogeochemical cycles regulation, we determined the influence of physical parameters and environmental factors on the modification of the microbial community diversity (pyrosequencing of Bacteria and Archaea), in relation with organic matter mineralization. Besides, we used convection mixing as a model to evaluate the ecological pertinence of SAR11, Marine group I and Marine Group II ecotypes, 3 taxonomic groups the most widespread and abundant in Mediterranean and in all the oceans.

In a climate change context, my works allowed us to propose different coherent scenarios of the potential evolution of the Northwestern Mediterranean pelagic ecosystems. My study contribute to the understanding of the pelagic ecosystem evolution with the predictable modifications in frequency and/or intensity of open-ocean convection processes.

Key words: Convection, Northwestern Mediterranean, biogeochemistry, Bacteria, Archaea, ecotype